DISSERTATION

INITIATION AND REGULATION OF FE ECONOMY IN ARABIDOPSIS THALIANA CHLOROPLASTS

Submitted by

Gretchen Elizabeth Kroh

Department of Biology

In partial fulfillment of the requirements

For the Degree of Doctor of Philosophy

Colorado State University

Fort Collins, Colorado

Summer 2020

Doctoral Committee:

Advisor: Marinus Pilon

Anireddy Reddy
Daniel Bush
Patricia Bedinger
Cristiana Argueso

Copyright by Gretchen Elizabeth Kroh 2020

All Rights Reserved

ABSTRACT

INITIATION AND REGULATION OF FE ECONOMY IN ARABIDOPSIS THALIANA CHLOROPLASTS

Iron (Fe) is biologically important for all organisms because of its role as a protein cofactor which provides redox and catalytic functions. Fe cofactors come in 3 different forms (Fe-S clusters, heme, and non-heme Fe). Plants have a stronger requirement for Fe than non-photosynthetic organisms because the chloroplast has a high demand for Fe. Plants are commonly Fe deficient because soil Fe is typically found in the non-bioavailable, ferric (Fe^{3+}) form, which limits plant growth in natural and agricultural settings. When grown on soils where Fe availability is low, plants can increase Fe uptake and use Fe more efficiently. The leaf response to Fe limitation in the model plant, *Arabidopsis thaliana,* is the topic of my dissertation.

As a major contribution to a larger study, I first characterized the transcriptional response for specific leaf genes to Fe deficiency in the leaf and found that transcripts for abundant chloroplast Fe proteins were down-regulated, suggesting an Fe economy response. Specifically, photosynthetic electron transport and chloroplast Fe-S assembly were targeted for down-regulation.

Fe deficiency affects photosynthesis and chloroplast Fe protein expression. I characterized a photosynthesis mutant and found that the regulation of Fe protein expression is maintained, suggesting that loss of electron transport does not trigger down-regulation of Fe protein expression.

By using RNA-seq, I analyzed genome-wide transcriptomic changes to identify co-regulated transcripts early in the Fe economy response, including candidate transcription factors. The transcriptional responses in wild type Fe limited plants and a chloroplast Fe-S

assembly mutant were independent of each other, suggesting that Fe-S assembly does not generate a signal to regulate chloroplast Fe proteins.

The novel insights provided in this dissertation form a foundation for understanding how photosynthetic organisms cope with Fe limitation. From an applied perspective, the results of this dissertation open new avenues to minimize effects of Fe deficiency in agricultural settings.

ACKNOWLEDGEMENTS

I have been fortunate to have been surrounded by people who have encouraged me to pursue my passions and helped me develop as a scientist. First, I'd like to thank my advisor, Dr. Marinus (Rien) Pilon, for investing his time in me before ever meeting me in person and before knowing if I would join his lab for graduate school. Throughout my time in his lab, Rien has continually provided me opportunities and support needed to become an independent scientist and has encouraged me to gain experience in my interests outside of the lab. I would also like to thank Rien and Dr. Elizabeth (Lianne) Pilon-Smits for creating a lab environment that promotes support, community, and respect among lab members, which has been essential to developing research projects and navigating graduate school. In that vein, I would like to thank all of the members of the Pilon and Pilon-Smits lab who have trained me in lab techniques and who have helped me through graduate school, especially Zack Guignardi, Alyssa Cochran, Leonardo Lima, Michela Schiavon, and Laura Hantzis. Your enthusiasm for your projects and career goals made the lab environment a great place to work. I also like to thank my committee members, Dr. Cristiana Argueso, Dr. Anireddy Reddy, Dr. Patricia Bedinger, and Dr. Daniel Bush for their advice on projects and support throughout my graduate degree. To the undergraduate students who collaborated on my projects: Michaela Koretko-Stephens, Karen Bacalia, Chase Alsup, and Tyler Hempstead- your help in the lab and enthusiasm for your projects was indispensable. To the people who have made my time at CSU some of the best years of my life, especially Ashley Larson, Alyx Shigenaga, Nate Williams, Jessica Warren, Aly Albertson, and Andrew Felton- thank you for always pushing me to try new pursuits and to take time to enjoy life in Colorado. Finally, I'd like to thank my mom and dad who have always encouraged me to pursue subjects that I am passionate about and have supported me in my academic and non-academic endeavors. I cannot express my gratitude for your love and support which made my choice to pursue science possible.

TABLE OF CONTENTS

ABSTRACT …….....ii

ACKNOWLEDGEMENTS …….....iv

CHAPTER 1: INTRODUCTION: REGULATION OF IRON HOMEOSTASIS AND USE IN CHLOROPLASTS …….....1

1 FIGURES AND TABLES ……....31

LITERATURE CITED...…….....38

CHAPTER 2: A PROGRAM FOR IRON ECONOMY DURING DEFICIENCY IN ARABIDOPSIS ROSETTES TARGETS SPECIFIC FE PROTEINS.....….....61

2 FIGURES AND TABLES.……..86

LITERATURE CITED…….…….....92

CHAPTER 3: MICRONUTRIENT HOMEOSTASIS AND CHLOROPLAST IRON PROTEIN EXPRESSION IS LARGELY MAINTAINED IN A CHLOROPLAST COPPER TRANSPORTER MUTANT…….....102

3 FIGURES AND TABLES 117

LITERATURE CITED….....123

CHAPTER 4: IRON DEFICIENCY AND LOSS OF THE CHLOROPLAST IRON-SULFUR CLUSTER ASSEMBLY PROTEIN SUFB TRIGGER OPPOSITE TRANSCRIPTIONAL RESPONSES IN *ARABIDOPSIS* LEAVES…….....131

4 FIGURES AND TABLES.....161

LITERATURE CITED 175

CHAPTER 5: ADDITIONAL OBSERVATIONS ON PLASTID FE DEFICIENCY…..……186

5 FIGURES AND TABLES……..…….201

LITERATURE CITED…….…….....217

CHAPTER 6: SUMMARIZING DISCUSSION……..……219

LITERATURE CITED…….....……....227

APPENDIX: SUPPLEMENTARY FIGURES AND TABLES……231

LITERATURE CITED…….248

CHAPTER 1: REGULATION OF IRON HOMEOSTASIS AND USE IN CHLOROPLASTS[1]

1.1 SUMMARY: Iron (Fe) is essential for life because of its role in protein cofactors. Photosynthesis, in particular photosynthetic electron transport, has a very high demand for Fe cofactors. Fe is commonly limiting in the environment, and therefore photosynthetic organisms must acclimate to Fe availability and avoid stress associated with Fe deficiency. In plants, adjustment of metabolism, of Fe utilization, and gene expression, is especially important in the chloroplasts during Fe limitation. In this review, we discuss Fe use, Fe transport, and mechanisms of acclimation to Fe limitation in green lineages with a focus on the photosynthetic electron transport chain. We compare Fe homeostasis in Cyanobacteria, the evolutionary ancestors of chloroplasts, with Fe homeostasis in green algae, and in land plants in order to provide a deeper understanding of how chloroplasts and photosynthesis may cope with Fe limitation.

1.2 INTRODUCTION

In the early, anoxic, reducing environment of Earth, life was built on iron (Fe). In the low oxygen environment, the bioavailable form of Fe, Fe^{2+}, was abundant and readily reacted with sulfur (S) to form pyrite (Fe_2S). Early life began to incorporate pyrite into biochemistry for catalytic functions such as electron transport (Wacey *et al.,* 2011). The evolution of the oxygenic photosynthetic electron transport chain was especially dependent on Fe (Fischer *et al.,* 2016). After oxygenic photosynthesis evolved, atmospheric oxygen levels began to increase from 0.001% to modern levels of 21% (Lyons *et al.,* 2014). The oldest fossils of cyanobacteria - the earliest important contributor to photosynthesis - are dated to 2.7 BYA (reviewed in Lyons *et al.,* 2014). The rise in oxygen in the Earth's atmosphere is estimated to have begun about 2.4 billion

[1] Submitted to International Journal of Molecular Sciences, Authors: Gretchen E. Kroh and Marinus Pilon (Under Review)

years ago (BYA) (Figure 1-1). However, modern oxygen levels are a result of land plant evolution 420-400 million years ago (Lenton *et al.,* 2016) (Figure 1-1). The rise of oxygenic photosynthesis resulted in geological shifts where the poorly bioavailable, oxidized Fe^{3+} now accumulates (Fischer *et al.,* 2016). Today, Fe is the fourth most abundant element in the earth's crust (Frey and Reed, 2012) but is not readily bioavailable.

While cyanobacteria are considered to be the earliest photosynthetic organisms, endosymbiosis of a cyanobacterial cell allowed expansion of photosynthesis to a eukaryotic lineage, giving rise to algae and land plants (Raven and Allen, 2003). The predominance of oxidized Fe presents a major problem for most organisms, but even more so for modern photosynthetic organisms, as the photosynthetic electron transport chain has an exceptionally high demand for Fe, requiring an estimated 28 Fe atoms per chain (Merchant and Sawaya, 2005) and the chloroplast requires 60-80% of total Fe in leaves (Shikanai *et al.,* 2003).

Two potential stresses are anticipated with the high need of Fe in the chloroplast: first, the low bioavailability of Fe easily leads to deficiency; second, all Fe must be tightly managed because excess free Fe can be toxic. Fe deficiency results in a lack of activity in Fe requiring pathways, such as photosynthetic electron transport, cofactor assembly, sulfur and nitrogen metabolism, which compromises an organisms' growth (Crichton, 2016). Free Fe in the presence of oxygen can lead to the accumulation of harmful hydroxyl radicals (OH^-) and hydrogen peroxide via Fenton and Haber-Weiss reactions, which disrupt membrane integrity and protein structure (Halliwell and Gutteridge, 1984). The effects of Fe toxicity are also hypothesized to be present in severe Fe deficiency: during severe Fe deficiency, reactive oxygen species (ROS) are found to accumulate in plant leaves and must be detoxified by ROS scavenging molecules (Tripathi *et al.,* 2018). The accumulation of ROS may also arise from the decrease in photosynthetic electron transport in response to Fe deficiency (Ramirez *et al.,* 2013). In stress conditions when electron transport is impaired, the organism must adapt to scavenge harmful ROS that may result from excess excitation of photosystems (Sharma *et al.,*

2012). An efficient mechanism to acclimate to Fe toxicity is to induce Fe sequestration. During Fe deficiency, mechanisms to increase Fe uptake and economize Fe for most important cellular functions must be employed. Thus, Fe deficiency, while more common in nature than Fe excess, may also be have a greater detriment on an organisms' health.

The strong requirement for Fe in photosynthesis has led to the evolution of mechanisms in photosynthetic organisms to minimize stress from Fe deficiency. When Fe is limiting, photosynthetic organisms can respond by (1) increasing Fe uptake; (2) remodeling metabolism; (3) increasing efficiency of Fe utilization; (4) remobilization of stored Fe. For example, several cyanobacteria and the unicellular eukaryotic algae, such as *Chlamydomonas reinhardtii*, can increase Fe uptake on the cell membrane (Eckhardt and Buckhout, 1998; Terzulli and Kosman, 2010). Land plants must regulate increased Fe uptake at the root epidermis, and also mediate Fe transport into the xylem from the pericycle for Fe translocation to shoots (for reviews see Kim and Guerinot, 2007; Kobayashi and Nishizawa, 2012;Thomine and Vert, 2013; Connorton *et al.,* 2017).

It is essential that photosynthetic organisms respond to changes in Fe status to maintain photosynthesis and chloroplast integrity without aberrant production of ROS resulting from the presence of free Fe atoms and decreased photosynthetic performance. As cyanobacteria are closely related to the earliest ancestors of chloroplasts, their responses to Fe deficiency may provide insight on chloroplast Fe homeostasis and regulation. As Chlamydomonas is a distant relative of land plants, the response of this organism may also provide an understanding of how mechanisms of acclimation to Fe deficiency have evolved. Similarities in Fe deficiency responses across green lineages (photosynthetic organisms) has given insight into the evolution of the regulation of Fe homeostasis required for photosynthesis. What we continue to learn may also inform research on the regulation of plant Fe sensing and regulation. Here, we will review mechanisms of acclimation to Fe deficiency across green lineages, by comparing Fe metabolism of chloroplasts in land plants with Chlamydomonas and cyanobacteria.

1.3 CHLOROPLAST FE USE

The majority of chloroplast proteins are encoded in the nucleus, translated on cytoplasmic 80S ribosomes and imported into the organelle before maturation and assembly (Waters and Langdale 2009). The chloroplast genome encodes a set of proteins that function in photosynthesis or chloroplast gene expression (Barkan, 2011). Both plant development and the environment affect chloroplast function, and therefore the expression and maturation of plastid-encoded and nucleus-encoded chloroplast proteins must be coordinated to respond to developmental and environmental cues (Waters and Langdale 2009). Micronutrient availability (including Fe) is one important environmental variable. Due to its very low bioavailability, and the high photosynthetic requirement (Merchant and Sawaya 2005) Fe is one of the main nutrients limiting plant productivity.

Fe is required for biological processes because of its role as a protein cofactor. Fe cofactors exist in three main forms (heme, non-heme, and Fe-S clusters) to allow proteins to carry out functions such as catalysis, electron transport, and ROS scavenging (Crichton, 2016). Fe is the most common metal cofactor and Fe cofactors provide a range of redox potentials for different protein functions. The photosynthetic electron transport chain requires all three forms of Fe cofactors. The highest demand is for Fe-S clusters, with Photosystem I (PSI) subunits requiring three 4Fe-4S clusters, each Rieske subunit of the Cyt-b_6f complex requiring a 2Fe-2S cluster and, Ferredoxin (FD) requiring a 2Fe-2S cluster (Fukuyama *et al.,* 1980; Hurt and Hauska*,* 1981; Ben-Shem *et al.,* 2003). The Cyt-b_6f complex also contains multiple heme cofactors for electron transport and exists as a dimer, for a total of 12 Fe atoms spanning the subunits (Merchant and Sawaya 2005). Photosystem II (PSII) requires one non-heme Fe cofactor, but, unlike Fe in the rest of the photosynthetic electron transport chain, it is unlikely that this cofactor is involved in electron transport (Shevela *et al.,* 2012). PSII also contains a cytochrome heme cofactor that has a photoprotective role (Merchant and Sawaya 2005).

Fe cofactor assembly in plastids

Relatively little is known about the maturation of non-heme iron proteins in plants. In contrast, the synthesis and assembly of heme and Fe-S clusters is understood in greater detail. In plants, the synthesis pathway of heme and siroheme is localized in plastids. Siroheme, heme, and chlorophyll synthesis all branch off from the plastid tetrapyrrole pathway (Figure 1-2a; Moulin and Smith, 2005; Tanaka *et al.,* 2011). The tetrapyrrole pathway begins with 3 enzymatic steps whereby glutamate is used to form aminolevulinic acid (ALA), the tetrapyrrole precursor (Czarnecki *et al.,* 2011). ALA is reported to be maintained in two separate pools for heme and chlorophyll biosynthesis (Czarnecki *et al.,* 2011) and heme synthesis is directly linked to the amount of ALA present (Kumar and Soll, 2000). Eight molecules of ALA are used to form uroporphyrinogen III which has the basic the tetrapyrrole conjugated ring structure. The pathway branches at uroporphyrinogen III to form on one hand siroheme, which requires the 2Fe-2S enzyme SirB (Raux-Deery *et al.,* 2005), or on the other hand protoporphyrinogen IX (PPOX), the common precursor for chlorophyll and heme production (Lermontova *et al.,* 1997). Fe insertion into PPOX by Ferrochelatase leads to heme formation while Mg-ion insertion leads to functional chlorophyll (Moulin and Smith, 2005). CCS5/HCH164, a thioredoxin, and CCDA, a thylakoid thiol disulfide transporter, are proteins that are required for the correct insertion of heme into plastid cytochromes (Page *et al.,* 2004; Gabilly *et al.,* 2010). It is notable that several enzymes of heme and chlorophyll metabolism are Fe-S cluster-dependent enzymes (Figure 1-2a).

Fundamental mechanisms of Fe-S cluster synthesis were first uncovered in nitrogen fixing bacteria that utilize the *nif* operon (Zheng *et al.,* 1993; 1998). It became apparent that housekeeping Fe-S proteins in bacteria requires another operon called *isc* (Zheng *et al.,* 1998), while a third bacterial Fe-S system – functioning under oxidative or low sulfur stress conditions - is encoded in the *suf* operon (Takahashi and Tokumoto, 2002; Outten *et al.,* 2003). Fe-S cluster assembly by either the *nif/isc* or *suf* systems can be divided into 3 steps: mobilization of S from

cysteine (Cys) by a Cys desulfurase, assembly of S with Fe on scaffolds to form an Fe-S cluster, and transfer to and insertion into apoproteins (for reviews see Frazzon *et al.,* 2002; Johnson *et al.,* 2005; Lill and Muhlenhoff, 2008). The first discovered Cys desulfurase was NifS (in the *nif* cluster), and later IscS and SufS were found to have the same function in the *isc* and *suf* operons (for a review see Mihara and Esaki, 2002).

Homologues of the bacterial *nif*, *isc* and *suf* genes have been discovered in other organisms including yeast and plants (for reviews see Lill and Muhlenhoff 2008; Balk and Pilon, 2011). In plants there are two major Fe-S cluster biosynthesis machineries, one in mitochondria and one in plastids (Balk and Pilon, 2011). However, in analogy to other eukaryotes (Lill and Muhlenhoff, 2005) the mitochondrial machinery is linked with a cytosolic Fe-S assembly system (Kushnir *et al.,* 2001; Bernard *et al.,* 2009; Schaedler *et al.,* 2014). The mitochondrial machinery is homologous to that encoded by the bacterial *isc* operons, while several of the genes encoding the plastid machinery resemble bacterial *suf* operons (Figure 1-2b; Balk and Pilon, 2011; Dong *et al.,* 2017).

Evidence for a plastid Fe-S cluster assembly system was obtained when FD maturation was observed after *in vitro* import into isolated chloroplasts, which have their own Fe-S biosynthetic machinery (Li *et al.,* 1990; Pilon *et al.,* 1992). Fe-S cluster assembly for FD in isolated chloroplasts used cysteine as the sulfur donor and further required light or ATP and NADPH (Takahashi *et al.,* 1986, 1991a,b). However, the Fe source for plastid Fe-S cofactor formation is unclear (Balk and Schaedler, 2014).

CpNifS/SUFS (called SUFS from hereon) is the only plastid stroma protein with Cys-desulfurase activity (Pilon-Smits *et al.,* 2002; Leon *et al.,* 2003). Arabidopsis SUFS is constitutively expressed in all major plant tissues at about equal levels (Pilon-Smits *et al.,* 2002). Stromal fractions can mediate Fe-S cluster insertion into apoferredoxin *in vitro*, but this activity is lost when SUFS was depleted (Ye *et al.,* 2005). Inducible RNAi knockdown mutant mutants of SUFS led to a gradual loss of all plastidic Fe-S proteins, causing chlorosis, thylakoid

degradation and a severe impairment of photosynthesis, and eventually death; thus, SUFS is required for all Fe-S formation in plastids (Van Hoewyk *et al.,* 2007). SUFS is a type-II Cys desulfurase, which in bacteria is activated by SufE. Plants have three nuclear encoded, plastid-targeted SufE-like proteins. SUFE1 forms a complex with SUFS *in vitro* and stimulates Cys desulfurase activity 40-60 fold (Ye *et al.,* 2006). Homozygous *sufe1* knockout mutants are not viable (Xu and Moller 2006). Next to a SUFE-domain found in both prokaryotes and eukaryotes, the mature SUFE1 protein in plants has a BolA-like domain that is unique to higher plants and that may play a role in regulation via interaction with monothiol glutaredoxins, perhaps in response to redox status (Couturier *et al.,* 2014). There are two additional SUFE proteins in plants: SUFE2 functions in Fe-S assembly in pollen and SUFE3 plays a role in plastid NAD synthesis and carries a 4Fe-4S cluster required for this activity (Murthy *et al.,* 2007).

In the bacterial *suf* system a complex of SufB, C and D forms an Fe-S assembly scaffold with ATPase activity (Outten *et al.,* 2003). Homologues of SufB, C and D are also present in plastids where they form a complex (Figure 1-2b; Moller *et al.,* 2001; Xu *et al.,* 2004; 2005; Ahn *et al.,* 2005; Nagane *et al.,* 2010; Hu *et al.,* 2017a). Arabidopsis SUFB, SUFC and SUFD are known to be essential proteins, and inducible RNAi knockdown mutant of the *sufbcd* scaffold proteins had lower accumulation of Fe-S requiring photosynthetic proteins, suggesting that the SUFBCD complex is required for the synthesis of all photosynthetic Fe-S clusters (Hu *et al.,* 2017a). Other components of the plastid Fe-S machinery are the potential transfer proteins NFU1-3 (Leon *et al.,* 2003, Yabe *et al.,* 2004), CpIscA/SUFA, hereon called SUFA, (Abdel-Ghany *et al.,* 2005) and HCF101 (Lezhneva *et al.,* 2004; Schwenkert *et al.,* 2009). Mutational loss of NFU2 or HCF101 results in defects in the maturation of specific subsets of Fe-S cluster proteins (Touraine *et al.,* 2004; 2019; Yabe *et al.,* 2004; Schwenkert *et al.,* 2009). However, for a *sufa* loss-of-function mutant, no phenotype was described in mutant plants grown on regular soil (Abdel-Ghany *et al.,* 2005; Yabe and Nakai, 2006). Furthermore, two monothiol GRX proteins (GRXS14/GRXS16) could serve as Fe-S scaffolds or transfer proteins, based on *in*

vitro studies, but no strong phenotypes for loss of function mutants have been reported (Bandyopadhyay *et al.,* 2008). Finally, a plastid and mitochondrial dual localized protein called AtNEET has capacity to bind an Fe-S center. Loss-of-function mutations in AtNEET affect chloroplast biogenesis, ROS homeostasis and plant Fe metabolism, but did not seem to affect expression of the Cyt-b_6f Rieske protein (Nechushtai *et al.,* 2012, Zandalinas *et al.,* 2019).

1.4 CHLOROPLAST FE TRANSPORT AND STORAGE

In photosynthetic plant cells, chloroplast Fe uptake systems are induced in the light, suggesting a link between Fe requirement and photosynthetic capacity (Gonzalez-Vallejo *et al.,* 2000; Feng *et al.,* 2006; Bughio *et al.,* 1997). Fe uptake in isolated pea chloroplasts was reported to be dependent on the pH gradient across the inner membrane which is maintained in the light (Shingles *et al.,* 2002). Further, in mature chloroplasts, Fe homeostasis has been closely tied to circadian rhythm (Salome *et al.,* 2013) and light-dark cycles through the Time for Coffee clock regulator (TIC) (Duc *et al.,* 2009). Circadian rhythms in etiolated seedlings (which have undeveloped, non-photosynthetic, chloroplasts) were unresponsive to low Fe suggesting that as the chloroplast develops as a sink for Fe, a signal is produced to modulate the circadian clock based on Fe status. Here we will briefly discuss Fe transport systems. For comprehensive reviews on Fe transport, see Lopez-Millan *et al.* (2016) and Vigani *et al.* (2019).

Chloroplast Fe uptake

Because Cyanobacteria are related to the evolutionary ancestors of chloroplasts, Fe uptake mechanisms in Cyanobacteria may be related to chloroplast Fe uptake. Generally, photosynthetic organisms employ two types of mechanisms for extracellular Fe uptake. In one mechanism, the organism produces siderophores, Fe chelating molecules, which are secreted extracellularly to chelate Fe, and then the siderophore-Fe complex is taken up by the organism. In the second mechanism, Fe is reduced from Fe^{3+} to Fe^{2+} by a membrane bound reductase

enzyme, and then is taken up by a transmembrane Fe uptake protein. Cyanobacteria can employ both strategies, depending on the species (Hopkinson and Morel, 2009; Kranzler *et al.,* 2011; Kranzler *et al.,* 2013; Figure 1-3a). For example, *Anabaena* PCC 7120 secretes a siderophore and takes up the Fe siderophore complex by using a tonB dependent transporter (Lammers and Sandersloehr, 1982; Nicolaisen *et al.,* 2008). *Synechocystis* PCC 6803 binds Fe^{3+} by FutA on the inner membrane surface. There is convincing evidence that reduction of FutA bound Fe^{3+} results in Fe^{2+} release from FutA, which is then transported through the inner membrane by the Fe uptake protein FeoB (Kranzler *et al.,* 2013). However, there is also evidence for non-reduction-based uptake of Fe^{3+} by the FutABC uptake system in *Synechocystis* PCC 6803, in which Fe^{3+} is transported through the FutB transmembrane uptake protein while bound to FutA on either side of the membrane (Kranzler *et al.* 2013).

In higher plants, at both the leaf and chloroplast membranes, Fe is reduced before uptake (Figure 1-3c). *Arabidopsis* FRO6 functions to reduce Fe for import into the leaf cell (Mukherjee *et al.,* 2006) and FRO7 reduces Fe for import from the cytoplasm into the chloroplast (Feng *et al.,* 2006; Jeong *et al.,* 2008). Expression of both FRO6 and FRO7 is positively correlated with the differentiation of leaf cells as chloroplasts mature (Feng *et al.,* 2006). Additionally, FRO6 expression is driven by light-responsive elements in its promoter (Feng *et al.,* 2006). FRO7 is especially linked with photosynthetic need, as *Arabidopsis* knockout mutants exhibited stunted growth, low electron transport, and decreases in the accumulation of Cyt-b_6f, when grown on agar without sucrose (Jeong *et al.,* 2008). However, increasing Fe supply to *fro7* could recover this phenotype, suggesting that there is either an alternative chloroplast reductase enzyme, or an alternative, currently unknown, Fe uptake pathway that does not require reduction.

While the chloroplast seems to employ FRO7 to acquire Fe, it is unclear if the reductase activity for Fe is tied to a specific Fe transporter or if Fe reduced via FRO7 can be taken up by multiple Fe importers. Likely, there are multiple high- and low-affinity transport systems to

modulate Fe movement into or out of the chloroplast based on chloroplast Fe need (Solti *et al.,* 2014). The most viable candidate chloroplast Fe importer is the inner membrane localized, PIC1 (Figure 1-3c). *PIC1* shares sequence similarity with an iron importer, *sll1656*, from *Synechocystis* PCC 6803, and both *sll1565* and *PIC1* complemented a yeast Fe uptake deficient mutant, suggesting a role for Fe import (Duy *et al.,* 2007). *Arabidopsis pic1* knockout mutants had severely underdeveloped chloroplasts along with decreased photosynthetic efficiency and increased plastid Fe storage, as an increased expression of the stromal storage molecule, Ferritin (FER), was observed. FER expression is presumably induced by ROS accumulation as a consequence of breakdown of photosynthetic proteins (Duy *et al.,* 2007). PIC1 was originally characterized as a subunit of the chloroplast protein importer (TIC21) (Teng *et al.,* 2006), but all expressed chloroplast proteins in *pic1* were processed to their mature form, indicating that they were imported into the chloroplast (Duy *et al.,* 2007). Therefore, Duy *et al.,* (2011) propose that PIC1 may closely associate with a TIC protein on the inner chloroplast membrane to coordinate Fe import and Fe cofactor assembly with protein maturation.

A second candidate protein that may mediate chloroplast Fe uptake is NAP14, a non-intrinsic ABC transporter, which shares sequence similarity with the cyanobacterial FutC Fe uptake system (Shimoni-Shor *et al.,* 2010; Figure 1-3c). *Arabidopsis* NAP14 knockout mutants share the severely undeveloped chloroplast phenotype of PIC1 but also exhibit decreases in FER and FRO7 transcripts suggesting an overall lowered Fe content in chloroplasts. Could NAP14 work with FRO7 in uptake of Fe into the chloroplast? While NAP14 clearly is important for chloroplast Fe, the orientation of NAP14 as a possible transporter is unknown—i.e. it could be either an Fe importer or Fe exporter or not involved in Fe uptake.

The unicellular algae, Chlamydomonas, differs in its Fe uptake compared to Cyanobacteria and land plants (Figure 1-3b). Chlamydomonas employs an oxidation strategy similar to yeast, where Fe^{2+} is oxidized by a multicopper ferroxidase (FOX1) and then taken up by a ferric Fe permease yeast homologue (FTR1) (Terzulli and Kosman 2010).

Fe export

Fe export from the chloroplast is equally important as Fe uptake both to ensure that the chloroplast is not overloaded with Fe which can lead to production of free radicals by Fenton Reactions and to export Fe from the chloroplast during senescence. Export from chloroplasts in *Arabidopsis* is thought to be mediated by two Yellow Stripe Like proteins (YSL4 and YSL6). The double mutant, *ysl4/6* over accumulated Fe in the chloroplast and induced FER expression (Divol *et al.,* 2013). However, localization of YSL4/6 has been a matter of debate based on the method used. In immunolocalization experiments, fluorescently tagged antibodies for YSL4/6 were localized to the chloroplast (Divol *et al.,* 2013), while YSL4/6-GFP fusion proteins localized to the tonoplast (Conte *et al.,* 2013; Figure 1-3c). Both a proposed function as a chloroplast Fe exporter or as a tonoplast Fe importer could explain the accumulation of Fe in the chloroplast. Clearly, the loss of a chloroplast Fe exporter would result in higher levels of Fe remaining in the chloroplast. However, the loss of a tonoplast Fe importer could also lead to increases in chloroplast Fe, as less Fe can be distributed into the tonoplast it may be sequestered instead by FER in the chloroplast. Regardless of the location of YSL4/6, it does appear to have a role in modulating intercellular Fe.

Fe sequestration

Available Fe pools are modulated by the Fe chelators, nicotianamine (NA) and citrate. Once inside the chloroplast, Fe was found predominately bound to citrate over NA (Muller *et al.,* 2019). A possible chelate transporter, *Arabidopsis* MAR1 has been localized to the chloroplast inner envelope. MAR1 was discovered as a chloroplast importer of antibiotics but more likely evolved to function in Fe uptake, as its expression has been linked to Fe status (Conte *et al.,* 2009). Most likely, MAR1 functions to couple import of Fe chelators with that of Fe so that once inside the chloroplast (Figure 1-3c), Fe is chelated to avoid Fenton reactions. However, the specific chelator that may be imported by MAR1 is unknown.

Ferritin (FER) is the major Fe storage molecule located in the chloroplast and is vital to modulating the amount of free Fe in the chloroplast for use (Ravet *et al.,* 2009; Figure 1-3c). *Arabidopsis* has 4 ferritin genes: FER1, FER2, and FER3 are major leaf Ferritins, while FER4 is localized to the seed. Ferritins are found in bacteria and animals as well as across green lineages (Proudhon *et al.,* 1996). Ferritin proteins complexes make a shell-like structure that holds Fe^{3+} bound to organic phosphate (Briat et al, 2010). One Ferritin shell is composed of 24 FER molecules (Briat et al., 2010) and ferritin from legumes was found to hold at least 1000 Fe atoms (Lonnerdal 2009). The major function of FER in plastids is to scavenge free Fe to eliminate the threat of ROS production (Figure 1-4; Ravet *et al.,* 2009). FER is especially important for chloroplast protection during Fe toxicity, where its expression is stabilized to strengthen Fe storage. FER triple mutants (*fer1/fer2/fer3*) could not survive at high levels of Fe due to an increase in ROS production (Ravet *et al.,* 2009). The function of FER in Fe homeostasis will be further discussed in the following sections.

1.5 ACCLIMATION TO LOW FE

During Fe deficiency a photosynthetic organism must acclimate both locally and systemically to alter growth and metabolism. The systemic response to low Fe becomes more complex as the number of cells and structures in the organism increases. For example, unicellular cyanobacteria will have one overall response as the organism will sense Fe and respond in the single cell. Filamentous cyanobacteria, such as *Anabaena variabilis,* that have specialized cells for different metabolic functions, such as nitrogen fixation, may sense Fe locally in photosynthetic cells but will have to respond systemically to acclimate other cells to the deficiency in photosynthetic output (Adams and Duggan, 1999). In contrast, the unicellular eukaryotic alga, Chlamydomonas will have local responses in different cellular compartments, and these responses will need to be coordinated by signaling between organelles and nucleus (Glaesener *et al.,* 2013). In land plants, not only do responses need to be coordinated in each

cell, but also between different organs. For instance, plants induce root Fe uptake based on shoot Fe needs. Therefore, in land plants, there are distinct but coordinated local responses to Fe deficiency in leaves, vasculature, roots, and reproductive structures (Lopez-Millan *et al.,* 2013; Kobayashi, 2019).

In green organisms, photosynthesis is a major target for regulation under low Fe availability. During Fe deficiency, photosynthetic organisms become chlorotic as they decrease activity of the chlorophyll biosynthesis pathway which requires Fe for Chlorophyllide A Oxygenase (CAO) and Mg Proto IX Monomethyl Ester Cyclase (MgCY/CRD) (Tanaka *et al.,* 2011). In plants, chlorosis begins in the young leaves with developing chloroplasts, reflecting an inability to remobilize Fe from mature tissue to developing leaves. Photosynthetic electron transport activity when measured by chlorophyll fluorescence is specifically inhibited downstream of PSII as indicated by a lower ϕPSII parameter (Larbi *et al.,* 2006; Lopez-Millan *et al.,* 2013; Hantzis *et al*., 2018). Comparatively, cellular respiration rates are much less affected in a mild Fe deficiency in Arabidopsis (Hantzis *et al.,* 2018), suggesting that chloroplast metabolism, as opposed to that of the mitochondria, is a major target of the Fe deficiency response.

The regulated response to Fe deficiency depends greatly on the severity of the iron deficiency, developmental stage of the organism, and the light environment. Severity of Fe deficiency can be determined by the length of Fe deficiency or the fold change in available Fe (Glaesener *et al.,* 2013). A more severe Fe deficiency can lead to irreversible damage to photosynthetic electron transport chain and secondary stress responses (Glaesener *et al.,* 2013; Rodriguez-Celma *et al.,* 2013). Symptoms of less severe Fe deficiency in Arabidopsis can be recovered by resupplying plants with sufficient levels of Fe (Hantzis *et al.,* 2018). In addition, higher light environments may result in Fe deficiency becoming severe earlier than in low light environments because of the high Fe requirement to maintain integrity of the photosynthetic electron transport chain.

Increase Fe Uptake

The increase in Fe uptake in response to Fe deficiency in photosynthetic organisms has been well documented and up-regulation of uptake systems are common markers of Fe deficiency (Robinson *et al.,* 1999; Vert *et al.,* 2002; Singh *et al.,* 2003; Chen *et al.,* 2008; Chappell and Webb, 2010). Cyanobacteria are known to increase Fe uptake by up-regulating FutA (Singh *et al.,* 2003; Chappell and Webb, 2010; Figure 1-3a), while Chlamydomonas increases Fe^{3+} uptake by up-regulation of FOX1 and FTR1 expression (Chen *et al.,* 2008; Terzulli and Kosman 2009; Figure 1-3b).

In plants, Fe uptake at the root has been thoroughly studied (Jeong *et al.,* 2017; Kobayashi, 2019). In short, dicots and monocots other than grasses employ the Fe uptake strategy I. The strategy I plant *Arabidopsis* acidifies the rhizosphere by the proton pump, AHA2; reduces the poorly bioavailable Fe^{3+} to Fe^{2+} via the Fe Reductase Oxidase 2 (FRO2) enzyme; and finally, takes up Fe^{2+} from the soil through Iron Regulated Transporter 1 (IRT1) (Kobayashi, 2019). Grasses employ the root uptake strategy II where they release phytosiderophores (PS) into the soil, which chelate Fe^{3+} and then uptake the entire PS-Fe^{3+} complex. Expression of proteins required for both strategies is up-regulated in response to Fe deficiency (Kobayashi, 2019).

Metabolic remodeling

Plants remodel metabolism locally, in both the shoots and roots to respond to Fe deficiency. In the roots, C metabolism, ROS metabolism and N metabolism have all been found to be targets of metabolic remodeling in response to Fe deficiency (Lubberding *et al.,* 1988; Thimm *et al.,* 2001, Zheng *et al.,* 2009; Lopez-Millan *et al.,* 2013). Leaf metabolic remodeling coordinates down-regulation of photosynthetic output with photoprotective mechanisms (Rodriguez-Celma *et al.,* 2013). Early in the Fe deficiency response, gene expression of mRNAs that encode enzymes in the tetrapyrrole pathway are down-regulated. The targeted mRNAs

include *HEMA1* which encodes for an enzyme needed for ALA synthesis in the tetrapyrrole pathway, and *CHLP, PORB,* and *GUN5* which are all required for chlorophyll production (Rodriquez-Celma *et al.,* 2013; Figure 1-3c). Additionally, mRNA encoding the Fe responsive protein, Conserved in Green Lineage and Diatoms 27 (CGLD27) is up-regulated and is predicted to function in quenching of ROS that results from photooxidative damage (Rodriguez-Celma *et al.,* 2013). Other ROS scavenging molecules in the leaves, such as the Fe requiring ascorbate peroxidase, are down-regulated during Fe deficiency (Hantzis *et al.,* 2018), suggesting that specific ROS reduction systems are employed for photoprotection. In addition, N metabolism has been found to be altered in leaves, with decreased expression of nitrate reductase, which requires Fe (Tejada-Jimenez *et al.,* 2019), and altered amino acid accumulation (Borlotti *et al.,* 2012). During Fe deficiency, the alterations to N metabolism could represent adjustments to altered chlorophyll and chloroplast protein biosynthesis, which require N assimilation (Tanaka and Tanaka, 2006). Overall, metabolic remodeling in response to Fe deficiency suggests the plant decreases chlorophyll synthesis and increases mechanisms to protect from ROS.

The metabolic remodeling on low Fe in Chlamydomonas depends on the growth requirements of the organism, as Chlamydomonas can grow both photoautotrophically and photoheterotrphically (Urzica *et al.,* 2012a). When grown photoautotrophically, carbon assimilation by means of photosynthesis is maintained on low Fe. When grown photoheterotrophically, in which cells are supplied with light for energy production and an organic carbon source, Fe deficiency results in a similar response as seen in plants with a maintenance of respiration and strong decreases to photosynthetic electron transport (Glaesener *et al.,* 2012). In both growth conditions, the ascorbate concentration was reported to increase 10 fold in the cell during Fe deficiency (Urzica *et al.,* 2012a). Chlamydomonas also increased xanthophyll cycle pigments during Fe deficiency (Terauchi *et al.,* 2010). These

changes to metabolism in chloroplasts of Fe deficient Chlamydomonas suggest a need to increase photoprotective mechanisms and defenses against ROS.

Regulation of Fe Utilization

A second major acclimation to Fe deficiency in photosynthetic organisms is Fe economy, or changes in Fe utilization to prioritize specific Fe requiring proteins and pathways over others when Fe limited (Glaesener *et al.,* 2013). Fe economy is commonly studied by comparing proteomic and transcriptomic changes in response to Fe limitation. Photosynthetic organisms share overall similarities in Fe economy strategies and, specifically, photosynthesis, Fe-S cluster assembly, and Fe sequestration are targeted for down-regulation (Xu *et al.,* 2005; Rodriguez-Celma *et al.,* 2013; Lopez-Millan, 2013; Hantzis *et al.,* 2018; Figure 1-3). Prioritized pathways include respiration and ROS scavenging (Thimm *et al.,* 2001; Lopez-Millan *et al.*, 2013; Hantzis *et al.,* 2018). Within each of these pathways, specific proteins are down-regulated, up-regulated, or maintained to produce the response to Fe deficiency, and these specific molecular responses are detailed in the remainder of this section.

The down-regulation of photosynthetic electron transport in response to Fe deficiency is conserved across green lineages. Interestingly, several cyanobacteria, Chlamydomonas, and land plants all down-regulate Ferredoxin (FD) and the cytochrome-b_6f complex (Cyt-b_6f) proteins after Fe deficiency, presumably to economize Fe for use in other cellular functions (Thimm *et al.,* 2001; Georg *et al.,* 2017; Teraughi *et al.,* 2010; Lopez-Millan, 2013; Rodriguez-Celma *et al.,* 2013; Hantzis *et al.,* 2018; For iron need of photosynthetic proteins see Figure 1-d). In *Synechocystis* PCC 6803 and Arabidopsis, down-regulation of these photosynthetic proteins is ordered to first down-regulate FD and then Cyt-b_6f (Georg *et al.,* 2017; Hantsiz *et al.,* 2018). Down-regulation of *Arabidopsis* FD2 is especially drastic. *A*fter a week of mild Fe deficiency in *Arabidopsis,* FD accumulated to only 8% of its original levels (Hantzis *et al.,* 2018).

Only in the most severe cases of Fe deficiency are Photosystem I and II (PSI and PSII) subunits down-regulated in plants (Terauchi *et al.,* 2010; Rodriquez Celma *et al.,* 2013; Laganowsky *et al.,* 2009; Andaluz *et al.,* 2006; Hantzis *et al.,* 2018). In plants, whether PSI or PSII is more affected by Fe deficiency seems to depend on the growth conditions and severity of Fe starvation. In Fe deficient *Arabidopsis* seedlings, Rodriguez Celma *et al.* (2013) found strong down-regulation of PSI subunits, and Light Harvesting Complexes (LHCs). A proteomics approach analyzing thylakoid membranes of 6 week old hydroponically grown *Arabidopsis* plants after one week of Fe deficiency found that accumulation of all LHCI proteins was decreased, along with a strong decrease in only two PSI subunits, PSAD and PSAC (Laganowsky *et al.,* 2009). PSII subunits and chloroplast ATP synthase were more stable throughout Fe deficiency (Laganowsky *et al.,* 2009). Both PSII and PSI decreased in Fe deficient spinach thylakoids. However, the ratio between the two photosystems did not differ from that of control plants suggesting an overall decrease in the number of intact photosystems to modulate electron transport (Timperio *et al.,* 2007).

The response to down-regulate PSI subunits late in the Fe deficiency response is conserved across green lineages. Cyanobacteria also show a late down-regulation of PSI subunits in the Fe deficiency response (Georg *et al.,* 2017). However, early in the Fe deficiency response in Cyanobacteria PSI ultrastructure remodeling has been observed. *Synechococcus* PCC 7942 and *Synechocystis* PCC 6803, normally rely on a trimeric PSI, but Fe deficiency resulted in accumulation of PSI monomers which decreased electron flow (Ivanov *et al.,* 2006). PSI reduction is also not observed in Chlamydomonas until severe Fe starvation. During Fe limitation, mild changes to PSI function were observed but were attributed to decreased PSI association with LHCs (Moseley *et al.,* 2002). It is not until severe Fe starvation that PSI subunits were down-regulated (Glaesener *et al.,* 2012, Yadavalli *et al.,* 2012).

Chloroplast Fe-S assembly is a second major target of Fe deficiency (Figure 1-3a, c). Regulation of the Suf Fe-S assembly in response to Fe limitation is dependent on the organism.

In land plants, the SUFB subunit of the SUFBCD Fe-S assembly scaffold was found to be an early down-regulated target of Fe deficiency (Xu *et al.,* 2005; Sivitz *et al.,* 2012; Rodriguez-Celma *et al.,* 2013; Liang *et al.,* 2015; Hantzis *et al.,* 2018). While SUFB was the only plant SUF component to be down-regulated at both the transcript and protein level, Fe-S transfer molecules of the SUF pathway (AtNEET, SUFA, NFU, and HCF101) decreased in protein accumulation while transcript levels were maintained (Pan *et al.,* 2015; Hantzis *et al.,* 2018, Zandalinas *et al.,* 2019). Further, a loss of SufA and IscA components of the Cyanobacteria, *Synechococcus* PCC 7002, Fe-S assembly led to induction of Fe deficiency responses (Balasubramanian et al., 2006).

Perhaps unsurprisingly, Fe sequestration is generally down-regulated in Fe deficiency to increase Fe availability (Figure 1-3a,b,c). In plants, it is well known that the chloroplast Fe storage ferritin molecules (FER) are down-regulated quickly after low Fe is induced (Buckhout *et al.,* 2009; Waters *et al.,* 2012; Briat *et al.,* 2015). Conversely, other photosynthetic organisms, Chlamydomonas and cyanobacteria, *FER* expression is induced in response to low Fe perhaps to link Fe status and oxidative stress responses (Long *et al.,* 2008; Busch *et al.,* 2008). Chlamydomonas FER expression was correlated with PSI degradation and may be important for sequestering free Fe as PSI is degraded in severe Fe deficiency (Busch *et al.,* 2008). While knockout mutants of FER in plants only presented a phenotype under Fe toxicity (Ravet *et al.,* 2009), knockout mutants of bacterioferritin in the cyanobacterium *Synechocystis* PCC 6803 resulted in an Fe deficiency response under normal Fe conditions (Keren *et al.,* 2004). Cyanobacterial bacterioferritin is required for buffering Fe stores and a second class of FER (MrgA) is required for modulating release from the bacterioferrtin in Fe deficiency to avoid oxidative damage (Shcolnick *et al.,* 2009), which may be a consequence of Fe deficiency depending on the severity of Fe limitation.

Fe sequestration is also regulated by increasing availability of vacuolar Fe during deficiency (Figure 1-3b,c). In Arabidopsis and in Chlamydomonas, in response to Fe deficiency,

Vacuolar Iron Transporter 1 (VIT1) responsible for vacuolar Fe loading is down-regulated, while NRAMP4, a vacuolar Fe exporter, is up-regulated, suggesting less Fe is sequestered into the vacuole (Zheng *et al.,* 2009, Buckhout *et al.,* 2009; Urzica *et al.* 2012b). The decrease in sequestration must be tightly regulated to avoid toxic side effects of free Fe. Thus, in Rice, MAR1, YSL15, and YSL2, which are proposed to transport nicocianamine-metal complexes across membranes were also up-regulated in shoots in response to Fe deficiency, perhaps to bind free Fe released as Fe requiring proteins are degraded (Zheng *et al.,* 2009).

The decreases in photosynthetic electron transport and Fe sequestration in response to low Fe supply may make the chloroplast more vulnerable to damage caused by ROS. In *Arabidopsis,* only 33% of mRNA encoding ROS scavenging proteins were regulated during low Fe, and of these, about half were down-regulated (Thi Tuyet Le *et al.,* 2019). Stromal Ascorbate Peroxidase (*sAPX*) and Fe Superoxide Dismutase (*FeSOD*) in the chloroplast were also down-regulated during low Fe in *Arabidopsis* (Thimm *et al.,* 2001; Waters *et al.,* 2012; Stein and Waters, 2012; Hantzis *et al.,* 2018), while others, like catalase, were maintained or slightly up-regulated (Thimm *et al.,* 2001; Hantzis *et al.,* 2018; Figure 1-3c). Interestingly, FeSOD is up-regulated by low copper (Cu) availability (Yamasaki and Shikanai, 2009). A known consequence of Fe deficiency is an increase in uptake of Cu (Waters *et al.* 2012; Thomine and Vert 2013). Thus, the decreased expression of FeSOD during Fe deficiency may be regulated indirectly, in response to increased levels of Cu. Conversely, Chlamydomonas FeSOD is maintained during Fe deficiency and it is possible that the required Fe cofactor for this protein is recycled from Fe released by as Fe requiring photosynthetic proteins are degraded (Page *et al.,* 2012). Chlamydomonas also induced expression of MnSOD during low Fe, which is further regulated by free Fe and H2O2 (Figure 1-3b). MnSOD is otherwise not expressed and seems to be regulated by Fe status (Page *et al.,* 2012).

Compensatory responses to Fe deficiency

An interesting Fe deficiency response of some Cyanobacteria and algae is the ability to replace or protect proteins that are affected by Fe deficiency (Figure 1-3a,b). Specifically, these organisms can replace Ferredoxins with Flavodoxin, a non-Fe requiring protein when Fe limited, which may allow them to maintain photosynthesis in Fe limited conditions (Reviewed in Lodeyro *et al.,* 2012). This compensatory mechanism has been lost in land plants (Pierella Karlusich *et al.,* 2014). Interestingly, the insertion of bacterial flavodoxin into tobacco enhanced tolerance to Fe deficiency by preventing loss of photosynthetic components (Tognetti *et al.,* 2007). In addition, cyanobacteria can protect PSI by expressing the protective protein, IsiA (Figure 1-3a), during Fe deficiency. It is thought that IsiA associates with PSI to increase efficiency of electron transport to PSI to avoid oxidative damage (Ma *et al.,* 2017).

1.6 REGULATING RESPONSES TO LOW FE

Both local and systemic responses to Fe deficiency must be tightly regulated to coordinate Fe uptake with Fe needs during deficiency. To quickly adjust Fe homeostasis to changes in Fe status, regulation is both transcriptional and post transcriptional (Kobayashi 2019). While green lineages share similarities in their Fe economy responses, similarities in regulatory mechanisms of responses to Fe deficiency are largely specific to each organism. Further, in eukaryotic photosynthetic organisms, regulation of Fe deficiency is more complex, as the organism must coordinate Fe needs of organelles through retrograde signaling. For a list of *Arabidopsis* Fe homeostasis proteins see Table 1.

Transcriptional regulation

In the cyanobacteria strains, *Anabaena* PCC 7120 and *Synechococcus* PCC 7942, the regulation of Fe uptake is mediated by the transcription factor FUR (reviewed in Gonzalez *et al*.,

2018). FUR can act both as a transcriptional repressor and activator but during Fe sufficiency binds Fe and acts to repress Fe related gene expression (Gonzalez *et al.,* 2018; Figure 1-3a).

Chlamydomonas regulation of Fe uptake is transcriptionally dependent on Fe Responsive Elements (FeRE) in the promoters of genes that encode key components of the Fe uptake machinery (FOX1, and FTR1) (Deng and Eriksson, 2007; Fei *et al.,* 2009; Figure 1-3b). The expression of the Fe uptake protein, FTR1, was both positively and negatively regulated by separate FeRE promoter elements (Fei *et al.,* 2010).

In plants, the regulation of the root Fe uptake response in which Fe is reduced by FRO2 and then taken up through IRT1, is positively regulated by a cascade of Basic Helix Loop Helix (bHLH) transcription factors. Of the 133 bHLH transcription factors in *Arabidopsis,* 16 have a known role in Fe homeostasis (Brumbarova *et al.,* 2015; Connorton *et al.,* 2017; Kobayashi, 2019; Gao *et al.,* 2019). Some of these bHLH transcription factors that are known to regulate root responses have also been found to be expressed in the shoots including bHLH104, Popeye (PYE), bHLH100/101, IAA-Leucine Resistant 3 (ILR3), and the recently identified, Upstream Regulator Of IRT1 (Long *et al.,* 2010; Sivitz *et al.,* 2012; Rodriguez-Celma *et al.,* 2013; Khan *et al.,* 2018; Kim *et al.,* 2019; Figure 1-3c). Interestingly, ILR3 and bHLH104 may be central to chloroplast regulated Fe changes. In the leaf, an ILR3 over expressor repressed the Cyt-b_6f and PSI expression while a bHLH104 over expressing line maintained normal levels of PSI subunits and Cyt*f* (Li *et al.,* 2019). Additionally, ILR3 and bHLH104 work antagonistically to repress and enhance the expression of AtNEET which is thought to transfer Fe-S clusters. ILR3 also interacts with PYE to negatively regulate expression of the chloroplast Fe storage molecule, ferritin (Tissot *et al.,* 2019). Thus, ILR3 may be at the center of plastid transcriptional regulation of Fe homeostasis.

Ethylene Response Factor (ERF) family transcription factors have more recently been associated with the strategy I root Fe uptake response, and regulation of plastid Fe deficiency responses to Fe deficiency (Moran Lautner *et al.,* 2014; Kastoori Ramamurthy *et al.,* 2018;

Balparda *et al.,* 2020). The root specific bHLH FER-Like Fe Deficiency Induced Transcription Factor (FIT) is stabilized by two Ethylene Response Transcription Factors (ERF), Ethylene Insensitive 1 and 3 (EIN1, EIN3; Lingam *et al.,* 2011). In terms of plastid regulation, ERF transcription factors may be necessary for retrograde signaling for Fe deficiency (Balparda *et al.,* 2020). The PAP/SAL1 retrograde signaling pathway consist of the metabolite, 3'-phosphoadenosine 5'-phosphate (PAP), which inhibits 5'-3' exoribonucleases (XRNs), and the SAL1 enzyme that regulates PAP levels by dephosphorylation (Estavillo *et al.,* 2011). Knockout mutants of SAL1 and PAP targeted XRNs had higher accumulation of shoot and root Fe and higher expression of the FER molecules compared to WT, suggesting higher plastid Fe accumulation. Additionally, the *sal1* and *xrn* knockout mutants had increased expression of the ERF1 transcription factor mRNA, compared to WT, which is typically degraded by exoribonucleases 4 (XRN4) in the PAP/SAL1 pathway. Thus, the ERF family may negatively regulate systemic Fe deficiency responses along with the PAP/SAL1 retrograde signaling pathway.

Post-transcriptional regulation

The cyanobacterial Fe responsive FUR transcription factor is regulated post transcriptionally by small RNAs and the ftsH1/ftsH3 protease complex (Gonzalez *et al.,* 2018). Additionally, regulation of photosynthetic proteins in response to Fe deficiency in cyanobacteria is mediated by a small RNA, IsaR (Georg *et al.,* 2017; Figure 1-3a). IsaR directly inhibits translation of photosynthetic proteins and prevents expression of SufBCD transcripts. The post transcriptional regulation of FD may be central to the cyanobacterium response to Fe. The cyanobacterium *Synechocystis* sp. PCC 6803 Ferredoxin homologue, FdC2, contains an extended C terminus and truncated mutant versions of FdC2 inhibited the response to low Fe because the mutant could not up-regulate the IsiA antenna that is critical for PSI protection during Fe deficiency responses (Schorsch *et al.,* 2018; Figure 1-3a). The FdC2 protein is

conserved in green linages (Schorsch *et al.,* 2018), suggesting that FdC2 may regulate Fe deficiency in other photosynthetic organisms.

Post-translational regulation

In Chlamydomonas, the Fe uptake machinery at the cell membrane is positively regulated post-translationally via the MAPK phosphorylation pathway (Fei *et al.,* 2017; Figure 1-3b). In relation to photosynthetic regulation, key is the N-terminal processing of LHCa3 which has been found to stabilize LHC1 and protect the cell from loss of PSI function in Fe deficiency (Naumann *et al.,* 2005).

In plants, post-translational regulation of root and shoot Fe deficiency responses are regulated by E3 ubiquitin ligases, Brutus (BTS) and Brutus Like (BTSL) (Long *et al.,* 2010; Tissot *et al.,* 2019; Rodriguez-Celma *et al.,* 2019; Figure 1-3c). In *Arabidopsis,* BTSL specifically regulates the turnover of the bHLH transcription factors, PYE and ILR3 (Long *et al.,* 2010; Tissot *et al.,* 2019), Thus, while translational regulation is required to ramp up the systemic Fe deficiency response, ubiquitin ligases are required for attenuating and coordinating the response.

Recent evidence suggests that post-translational regulation by protein phosphorylation is necessary in the root Fe deficiency response in plants. Phosphorylation of the newly identified bHLH transcription factor Upstream Regulator of IRT1 (URI) was required to regulate bHLH038/039 and bHLH100/101 to up-regulate the root uptake response, but not for down-regulation of plastid localized ferritin molecules and sAPX (Kim *et al.,* 2019). Therefore, while phosphorylated URI may be vital in regulation of Fe uptake, it may not play a direct regulatory role in chloroplast Fe economy and metabolic remodeling.

The chloroplast Fe-S cluster assembly machinery is integrally tied to regulation of photosynthesis in response to Fe deficiency. For instance, the response to down-regulate SUFB of the SUF Fe-S cluster assembly may be one way in which photosynthetic electron transport

proteins are post-translationally regulated since Fe-S clusters are required for photosynthetic proteins. In *Arabidopsis* RNAi inducible knockdown mutant lines of SUFB, all photosynthetic electron transport Fe-S proteins including FD were lost (Hu *et al.,* 2017a). The decrease in FD seems specific to the loss of SUFBCD scaffold proteins as FD was stable in *Arabidopsis* RNAi inducible knockdown mutant SUFS lines unless SUFS was knocked down during the seedling stage (Van Hoewyk *et al.,* 2007). However, clearly the photosynthetic response to Fe deficiency is not solely regulated by loss of Fe-S clusters as photosystems are maintained during mild deficiency and SUFB is not. Additionally, the putative Fe-S transfer protein, AtNEET, seems to regulate intracellular Fe. AtNEET dominant negative mutants over-accumulated Fe in the chloroplast, had chlorosis, and induced the root Fe uptake system (Zandalinas *et al.,* 2019) suggesting that intracellular Fe-S homeostasis is key in regulating both local and long distance Fe deficiency responses.

Fe sensing

For regulation to occur, Fe status of the organism must be initially sensed and a signal transduced to the nucleus. Again, Fe will be sensed at both the local and systemic levels, but a master Fe sensor should link local response throughout the organism. A master Fe sensor must be able to bind Fe to sense cellular Fe stores and bind DNA to induce transcriptional changes. A well-described example of an Fe sensing system is the yeast monothiol glutaredoxin (Gxs3/4) and Aft1/Aft2 sensing system (Yamaguchi-Iwai *et al.,* 1996; Rutherford *et al.,* 2001; Blaiseau *et al.,* 2001). When yeast is Fe sufficient, Gxs3/4 bind an Fe-S cluster which allows the complex to bind the Fe transcription factors Aft1/Aft2 (Kumanovics *et al.,* 2008). When Fe is limiting, the Fe-S cluster disassociates, thus freeing Aft1/Aft2 to induce transcriptional responses to Fe deficiency (Poor *et al.,* 2014).

In eukaryotic photosynthetic organisms, a master Fe sensor has yet to be discovered, but there is evidence for Fe sensing components in cyanobacteria. FUR, the Fe uptake

transcription factor can both bind Fe and represses transcription (Reviewed in Gonzales *et al.,* 2018; Figure 1-3a). Additionally, the cyanobacterial ferredoxin homologue, FdC2, is predicted to bind an Fe-S cluster and regulate expression of IsiA (Schorsch *et al.,* 2018). However, the direct function of FdC2 in regulation of Fe deficiency is unclear but the Fe binding ability along with changes in expression of the PSI protective protein, IsiA, makes it a strong candidate for Fe sensing.

In plants, potential candidate Fe sensors that are expressed at the root and shoot have been identified. The ubiquitin ligases, Brutus and Brutus-like (BTS/BTSL), that negatively regulate bHLH transcription factors in the Fe deficiency response, are also proposed to be local Fe sensors. BTS/BTSL and its rice orthologue (HRZ), become destabilized when they are bound to Fe (Kobayashi *et al.,* 2013). During Fe replete conditions, BTS/HRZ, bind Fe and are inactivated. When Fe becomes limiting, BTS/HRZ cannot bind Fe, and are activated to degrade transcription factors necessary for regulating the Fe deficiency response (Kobayashi *et al.,* 2013). However, no evidence exists of BTS/HRS initiating transcriptional responses or linking the response of shoot and root Fe deficiency. Instead, the negative regulation by an Fe sensing molecule serves as a quick attenuation of the Fe deficiency response to protect against overaccumulation of Fe as the plant is attempting to increase Fe uptake.

How might chloroplast Fe homeostasis be integrated into an Fe signaling mechanism? In the past, enzymes within the tetrapyrrole synthesis pathway have been suggested as a viable candidates for chloroplast Fe sensing in plants because the tetrapyrrole pathway is known to have a component of retrograde signaling and is required for chlorophyll synthesis (Cottage *et al.,* 2010). Genome Uncoupled (GUN) mutants are defective in communication between chloroplast and nucleus resulting in mis expression of nuclear encoded photosynthesis transcripts even when chloroplast development is inhibited (Susek *et al.,* 1993). Three of these GUN mutations are traced to proteins in the heme synthesis pathway, including the major plastid signaling molecule GUN1 (Larkin 2016). While the tetrapyrrole pathway provides a

simple mechanism for Fe sensing and signaling based on chloroplast Fe status, GUN1 levels are unaffected during Fe deficiency (Salome, 2013). Additionally, heme synthesis components and heme containing proteins seem to be less sensitive to Fe status compared to Fe-S requiring proteins (Salome *et al.,* 2013; Hantzis *et al.,* 2018). It is also possible that the chlorophyll branch of the tetrapyrrole pathway could be responsible for Fe status signaling. Mg-protoporphyrin IX, an intermediate in the chlorophyll biosynthesis pathway accumulates during Norflourazon (an inhibitor of synthesis of carotenoid synthesis which is required to prevent bleaching of chlorophyll) treatment which uncouples plastid development from nuclear gene expression suggesting an interruption in retrograde signaling (Zhang *et al.,* 2011).

The SUF Fe-S cluster assembly pathway may be a more viable candidate for Fe sensing. The SUF pathway has been linked with Fe homeostasis in other organisms, such as *E. coli* and the cyanobacterium *Synechococcus* sp. PCC 7002, which specifically induce suf Fe-S assembly in response to oxidative stress and Fe deficiency (Outten *et al.,* 2004; Balasubramanian *et al.,* 2005). Further, the cyanobacterial SufA and IscA are proposed to regulate Fe-S production in response to Fe limitation. It is proposed that IscA and SufA function to sense Fe-S cluster production and indirectly induce expression of the *suf* operon (Balasubramanian *et al.,* 2005). In addition, the cyanobacterium *Synechocystis* sp. PCC 6803 suf scaffold was repressed under Fe replete conditions by the transcriptional repressor, SufR (Shen *et al.,* 2007, Vuorijoki *et al.,* 2017), suggesting that the suf system is central to sensing Fe deficiency through cofactor availability. In higher plants, the SUF system is also sensitive to low Fe, specifically in the down-regulation of SUFB. While SUFB has been proposed as possible Fe sensor in *Arabidopsis* (Yang *et al.,* 2010), its direct role in regulation and Fe binding has not been studied. However, a SUFB knockdown mutant did accumulate Mg-protoporphyrin IX, suggesting that the loss of SUFB directly affects chlorophyll biosynthesis through the availability of Fe-S clusters for enzymes in the chlorophyll biosynthesis pathway (Hu *et al.,* 2017b). Thus, loss of SUFB may affect retrograde signaling through enzymes of the tetrapyrrole pathway.

New molecular details underlying systemic Fe signaling mechanisms have been recently uncovered in plants. It has long been demonstrated through grafting and split root experiments a Fe deficiency signal is initiated from the shoots to up-regulate root Fe uptake (Grusak and Pezeshgi, 1996; Vert *et al.,* 2003). Recently, phloem Fe homeostasis has been linked to up-regulation of Fe uptake. Oligopeptide Transporter 3 (OPT3) is rapidly induced in response to Fe deficiency and loads Fe into the shoot phloem from the xylem (Zhai *et al.,* 2014; Figure 1-3c). Knockout mutant of OPT3 had low phloem Fe and a constitutive up-regulation of Fe uptake. Alternatively, two phloem Fe exporters, Yellow Stripe Like 1 and 3 (YSL1/YSL3) were down-regulated in Fe deficiency, and mutants resulted in a constitutive Fe deficiency phenotype (Kumar *et al.,* 2017). Phloem signaling peptides, Ironman (IMA)/FEP are highly expressed early in the Fe deficiency response, and over expression of IMA3/FEP1 resulted in increased expression of bHLH039 and up-regulation of root Fe uptake (Grillet *et al.,* 2018; Hirayama *et al.,* 2018). Interestingly, IMA/FEP peptides contain a highly conserved aspartate domain that may bind Fe.

1.7 CONCLUSIONS AND OPEN QUESTIONS IN THE FIELD

As the chloroplast is a major sink for Fe in a plant, it is vital to understand how the chloroplast uses Fe and how it responds to deficiency to maintain photosynthesis. Insights from Fe metabolism of other photosynthetic organisms may translate to the study of chloroplast Fe deficiency regulation. Photosynthetic organisms share the Fe deficiency responses of decreased photosynthetic output and Fe-S cluster assembly regulation. Could regulation of these pathways be somewhat conserved? Could the FdC2 protein found across green lineages be tied to chloroplast Fe regulation in Chlamydomonas and land plants as it is in cyanobacteria? Cyanobacterial suf Fe-S assembly machinery, SufA and IscA, may communicate to sense or modulate Fe-S needs during Fe deficiency. Could components of the chloroplast SUF Fe-S cluster assembly system be required for chloroplast Fe deficiency regulation?

Research in plant Fe deficiency over the past decades has determined how Fe proteins respond to Fe deficiency in the chloroplast and has identified key regulatory factors in root Fe uptake and Fe sequestration. Now, questions that remain are centered around how the leaf Fe deficiency response is regulated and how the plant coordinates its leaf and root Fe deficiency responses. By understanding the regulatory pathways that produce the Fe economy response, eventually we can work backwards to determine the chloroplast Fe sensor, and perhaps the master Fe sensor, that is initiating a signal to alter expression of photosynthetic genes. Could chloroplast responses like down-regulation of SUFB and FD2 be regulated by the same families of transcription factors as the roots? Clearly, phloem mediated Fe signaling is required to coordinate shoot Fe needs with root uptake. How the leaf cell communicates Fe needs that lead to up-regulation of phloem Fe signaling, and whether or not chloroplast Fe status is integrated into this communication, are exciting topics for further study.

1.8 SCOPE OF THIS DISSERTATION

Until now, most studies characterizing leaf Fe deficiency have focused on transcriptome changes in response to Fe deficiency in seedlings grown on nutrient agar supplemented with sucrose. While these transcriptomic studies have provided evidence that regulation of ROS scavenging, photosynthesis, and Fe-S cluster assembly are strong targets of Fe deficiency regulation, how protein changes correlate with transcript changes has been lacking. In addition, photosynthetic deficiency has long been associated with Fe deficiency. However, when specific photosynthetic transcripts and proteins are down-regulated after Fe limitation is sensed, was unclear.

Therefore, as a first approach, we aimed to characterize the leaf response to Fe deficiency, across one week of Fe deficiency and one week of Fe resupply. We focused both on protein and transcript level changes in four week old hydroponically grown *Arabidopsis thaliana*. We also measured plant physiological changes in response to Fe deficiency including

photosynthetic efficiency and respiration rate. The data from this project is described in Chapter 2 and was collected in collaboration with a masters student, Laura Hantzis, in which Laura largely focused on protein level changes and I focused on transcript level changes. Together we found evidence for an Fe economy response that prioritizes mitochondrial function and targets a set of chloroplast proteins (SUFB, FD2, and Cyt-b_6f) for down-regulation.

In Chapter 3 we aimed to determine if the regulation of photosynthetic proteins in response to Fe limitation that we had identified in Chapter 2 was directly tied to Fe status due to less available Fe for cofactors, or if they were down-regulated via signals initiated due to loss of photosynthetic efficiency. We tested this by characterizing the molecular response to Fe deficiency of a photosynthetic deficient mutant, *paa1*. The Fe deficiency response in *paa1* plants did not differ from that in WT plants, suggesting that the down-regulation of photosynthetic proteins is specifically regulated by Fe status.

The down-regulation of the Fe-S assembly scaffold proteins, SUFB, presumably leads to a lower accumulation of chloroplast Fe-S clusters. Therefore, in Chapter 4, we asked if lowered chloroplast Fe-S assembly provides a signal to initiate Fe deficiency responses in the leaf. We compared transcriptomic changes of an inducible *sufb*-RNAi knockdown plants with that of WT Fe deficient plants 2h and 26h after WT was put on a low Fe treatment. We determined that SUFB is not involved in Fe regulation, but that the SUFA protein may be important in chloroplast Fe-S homeostasis. We also identified co-regulated transcripts with *SUFB* in the early Fe economy response and were able to identify candidate transcription factors for regulation of chloroplast Fe economy.

The root Fe deficiency response is regulated mainly by bHLH transcription factors which are also up-regulated in the shoots during deficiency. However, while there is evidence for transcriptional regulation of *SUFB* and *FD2*, the promoters of these transcripts do not have known *cis* elements for bHLH factors, suggesting an alternative means of regulation. We have begun to design reporter constructs using β-Glucuronidase to determine if expression of *SUFB*

and *FD2* is driven by regulation via promoter *cis* elements. The preliminary data for this project, along with variable data correlating *SUFB* down-regulation to induction of root reductase activity, and data for investigating if leaf Fe deficiency protein changes are conserved in crop species is contained in Chapter 5.

Chapter 6 summarizes and synthesizes the results of the Chapters 2-5.

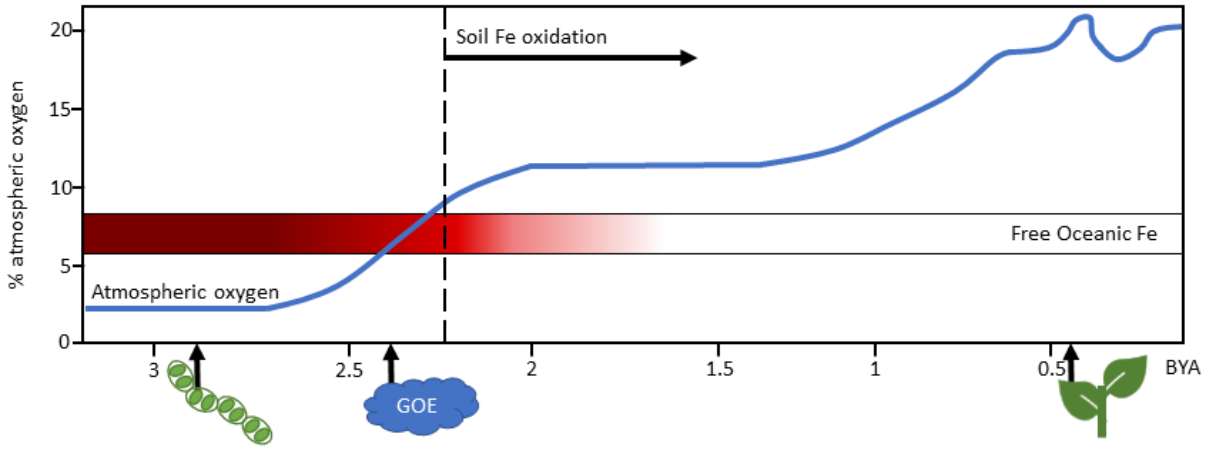

Figure 1-1: Conceptual model of relationship between atmospheric oxygen and Fe availability during earth's history Percent atmospheric oxygen is presented on the y-axis with time on the x axis. The early earth's atmosphere contained about 0.01% oxygen until oxygenic photosynthesis began with the presence of cyanobacterium about 2.7 billion years ago (BYA). The increase in oxygen led to lowered availability of Fe. Banding iron formations in strata are thought to represent times of intermittent Fe oxide formation from free oceanic Fe as atmospheric oxygen began to increase. BIFs are not found prior to 3 BYA, suggesting the low oxygen content allows for free Fe. BIF frequency peaks around 2.5 BYA and are again not found following 1.8 BYA suggesting that Fe oxidation became constant. The start of soil Fe oxidation is dated to around 2.3 BYA. Timeline depicts billions of years ago. Blue line represents general trend of increasing oxygen to current levels. Red gradient represents estimated amount of free Fe(II) based on frequency of banding Fe patterns in strata with darker red representing more free Fe(II). Dotted line represents onset of soil Fe oxidation in the geological record. First occurrence of cyanobacteria, the Great Oxygen Event (GOE) and land plants are noted. Trends are based on data reviewed in Canfield (2005) and Lyons et al. (2014).

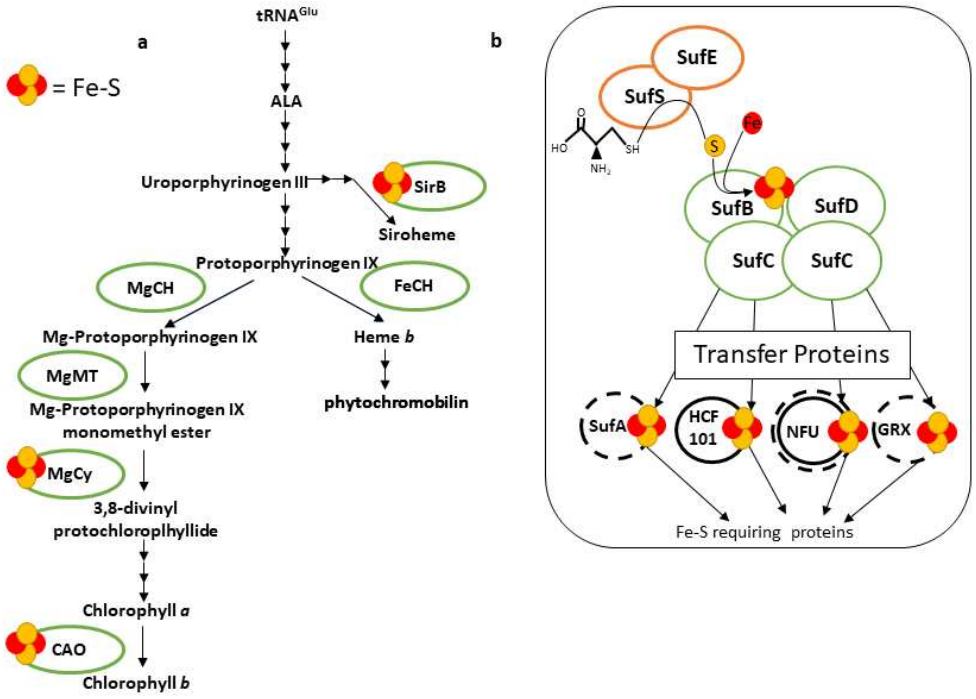

Figure 1-2: Biosynthesis of Fe cofactors in the chloroplast. A. Tetrapyrrole biosynthesis produces heme, siroheme, and chlorophyll. Enzymes requiring Fe-S clusters are denoted. Tetrapyrrole biosynthesis begins with Glutamyl tRNA being converted into ALA which is converted into protoporphyrinogen IX. The pathway then splits to either produce heme by insertion of Fe or chlorophyll by insertion of Mg and production of the chlorophyll antennae. Siroheme cofactor production branches before protoporphyrinogen IX is produced. Each arrow signifies one enzymatic step. B. SUF Fe-S assembly. Fe-S assembly begins with cysteine desluferase via NIFS, stabilized by SUFE. The Fe-S cluster is produced on SUFB and then transferred to carrier molecules for delivery to target proteins. Enzymes necessary for cysteine desulfurase are orange, enzymes of the major scaffold are green, and transfer proteins are black. Dashed lines for the carrier proteins biochemical evidence of their role. Solid lines indicate genetic evidence of their role.

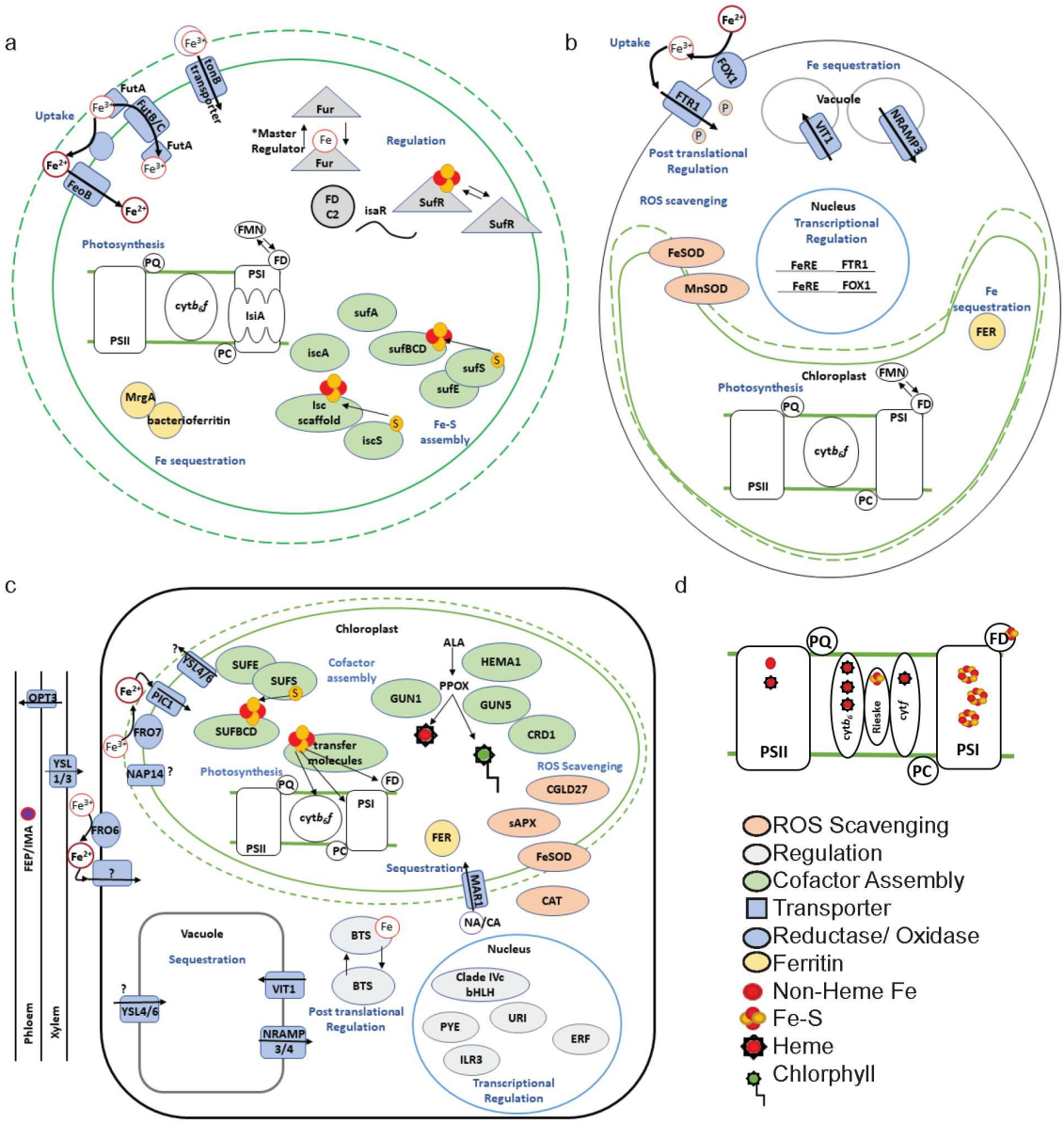

Figure 1-3 Fe responsive proteins and regulatory mechanisms in Cyanobacteria, Chlamydomonas, and land plants (a) Fe responsive proteins in Cyanobacteria, relatives to the ancestors of chloroplasts. Fe is taken up as either Fe^{3+} via siderophore chelation or the FutABC transport system. Fe can also be taken up as Fe^{2+}after reduction, through FeoB. Fe is required for the photosynthetic electron transport chain. During Fe deficiency, IsiA can protect Photosystem I and Ferredoxin (FD) can be replaced by the non-Fe requiring Flavodoxin (FMN). Two operons exist for Fe-S cluster assembly: *isc* and *suf.* Fe is sequestered by bacterioferritin and Fe release is regulated by MrgA. Fur is the master regulator and up-regulates the Fe uptake machinery when not bound to Fe. sufR, isaR, and FDC2 also regulate responses to Fe deficiency**. (b)** Fe responsive proteins in Chlamydomonas. Chlamydomonas takes up Fe^{3+} by FTR1 after Fe^{2+} is oxidized by FOX1. During Fe deficiency, FD can be replaced by FMN. Fe is sequestered in the vacuole by import via VIT1 and can be exported via NRAMP3. Chloroplast Fe is sequestered by Ferritin (FER). The ROS scavenging molecules, FeSOD and MnSOD are

regulated in response to Fe deficiency. The Fe uptake machinery is regulated by Fe Responsive Elements in the promoters of the genes for FOX1 and FTR1 and by phosphorylation via the MAPK pathway. **(c)** Fe responsive proteins in the leaf mesophyll cell with a focus on chloroplast proteins. From the xylem, Fe can be loaded into the phloem by OPT3 or to the mesophyll cell. During Fe deficiency, the FEP/IMA signaling peptides are transported in the phloem. For import into the mesophyll cell, Fe is exported from the xylem by YSL1/3 presumably in a Fe^{3+}-nicocianamine (NA) complex. Fe^{3+} is reduced at the leaf plasma membrane by FRO6 and Fe^{2+} is taken up into the cell. Fe is reduced at the chloroplast inner membrane by FRO7 and taken up by PIC1. NAP14 is also proposed to be a chloroplast Fe uptake protein. YSL4/6 is proposed to be a chloroplast Fe exporter. MAR1 may transport nicocianamine (NA) or citrate (CA) into the chloroplast to sequester free Fe. FER is also required to sequester Fe. Fe-S clusters are formed by the SUF pathway in the chloroplast and transfer molecules insert these Fe-S clusters into photosynthetic proteins. Heme and chlorophyll are produced in the tetrapyrrole pathway. Many enzymes for chlorophyll and heme production are Fe responsive, including GUN5, GUN1, HEMA1, and CRD1. Within the chloroplast, during Fe deficiency, ROS scavenging molecules, sAPX and FeSOD is down-regulated in Fe deficiency while CGLD27 is up-regulated. Outside of the chloroplast, FeSOD and catalase (CAT) is maintained during Fe deficiency. Fe is sequestered in the vacuole, where it is imported by VIT1 and exported by NRAMP3/4. YSL4/6 may also be a vacuolar Fe exporter. Fe deficiency responses are regulated by bHLH transcription factors, and possibly ERF transcription factors. The ubiquitin ligase, Brutus/Brutus-Like (BTS/BTSL) negatively regulates responses to Fe when not bound to Fe. **(d)** Fe requirement of photosynthetic transport chain proteins.

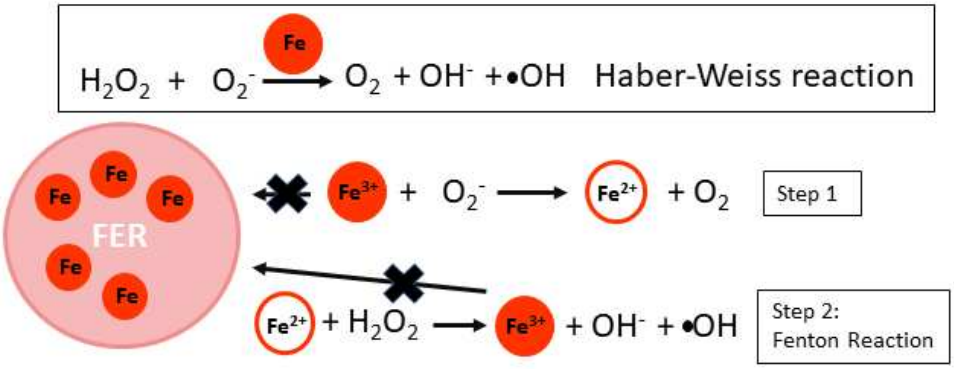

Figure 1-4: Role of Ferritin in preventing Haber-Weiss and Fenton reactions. FER is expressed under normal conditions to prevent accumulation of free Fe^{3+} to avoid build up of ROS. If FER cannot capture free Fe^{3+}, Haber-Weiss reactions which are catalyzed by free Fe can lead to the build up of hydroxyl radicals. Haber-Weiss reactions occur in two steps. First the production of Fe^{2+} and oxygen from Fe^{3+} and superoxide. Second the Fe^{2+} produced in the first step can react with H_2O_2 to produce Fe^{3+} and harmful hydroxyl radicals in a Fenton reaction.

Table 1-1 *Arabidopsis* Fe homeostasis transcripts The name and gene ID of each transcript with a known function in Fe homeostasis is listed. Genes are grouped by the general function of their gene product. Plants that have shown proteins with a homologous function in Fe homeostasis, are listed.

Function	*Arabiodopsis Gene ID*		*Functional homologues*
Reduction	FRO7	AT5G49740	
	FRO3	AT1G23020	
	FRO6	AT5G49730	
Transport	PIC1	AT2G15290	
	NAP14	AT5G14100	
	MAR1	AT5G26820	
	YSL4	AT5G41000	
	YSL6	AT3G27020	
	OPT3	AT4G16370	*Oryza sativa, Brassica juncea*
	YSL1	AT4G24120	*Zea mays*
	YSL3	AT5G53550	*Z. mays*
	VIT1	AT2G01770	*S.cerevisiae, O. Sativa*
	NRAMP3	AT2G23150	*Thlaspi caerulescens*
	NRAMP4	AT5G67330	*Thlaspi caerulescens*
Regulation	BTS	AT3G18290	*S.pombe, O. sativa*
	bHLH115	AT1G51070	
	PYE	AT3G47640	
	bHLH104	AT4G14410	
	ILR3	AT5G54680	
	bHLH38	AT3G56970	
	bHLH101	AT5G04150	
	bHLH39	AT3G56980	
	bHLH100	AT2G41240	
ROS homeostasis	NEET	AT5G51720	eukaryotes
	GRXS17	AT4G04950	*S.cerevisiae, S.pombe, O. sativa*
Sequestration	FER1	AT5G01600	*O. sativa*
	FER2	AT3G11050	*O. sativa*
	FER3	AT3G56090	*O. sativa*
	NAS4	AT1G56430	*O. sativa*
Signaling (predicted)	IMA1/FEP3	AT1G47400	
	IMA2/FEP2	AT1G47395	
	IMA3/FEP1	AT2G30766	
Root specific Fe homeostasis			
Transport	FRD3	AT3G08040	

Uptake	IRT1	AT4G19690	*Poplus tremula, Glycine max, Cucumis sativus, Medicago truncatula*
	FRO2	AT1G01580	*G. Max, C. sativus*
	AHA2	AT4G30190	*G. Max, C. sativus*
Regulation	URI	AT3G19860	
	FIT	AT2G28160	*Lycopersicon esculentum*
	EIN1	AT1G66340	
	EIN3	AT3G20770	

LITERATURE CITED

Abdel-Ghany SE, Ye H, Garifullina GF, Zhang LH, Pilon- Smits EAH, Pilon M (2005) Iron-sulfur cluster biogenesis in chloroplasts. Involvement of the scaffold protein CpIscA. Plant Physiology 138: 161-172

Adams DG, Duggan PS (1999) Tansley Review No. 107. Heterocyst and akinete differentiation in cyanobacteria. New Phytologist 144: 3-33

Ahn CS, Lee JH, Pai HS (2005) Silencing of NbNAP1 encoding a plastidic SufB-like protein affects chloroplast development in Nicotiana benthamiana. Molecules and Cells 20: 112-118

Andaluz S, Lopez-Millan A-F, De las Rivas J, Abadia J, Abadia A (2006) Proteomic profiles of thylakoid membranes and changes in response to iron deficiency. Photosynthesis Research 89: 141-155

Balasubramanian R, Shen G, Bryant DA, Golbeck JH (2006) Regulatory Roles for IscA and SufA in Iron Homeostasis and Redox Stress Responses in the Cyanobacterium Synechococcus sp. Strain PCC 7002. The Journal of Bacteriology 188: 3182

Balk J, Pilon M (2011) Ancient and essential: the assembly of iron–sulfur clusters in plants. Trends in Plant Science 16: 218-226

Balk J, Schaedler TA (2014) Iron Cofactor Assembly in Plants. Annual Review of Plant Biology 65: 125-153

Balparda M, Armas AM, Estavillo GM, Roschzttardtz H, Pagani MA, Gomez-Casati DF. (2020) The PAP/SL1 retrograde signaling pathway is involved in iron homeostasis. Plant Molecular Biology. 1-15.

Bandyopadhyay S, Gama F, Molina-Navarro MM, Gualberto JM, Claxton R, Naik SG, Huynh BH, Herrero E, Jacquot JP, Johnson MK, Rouhier N (2008) Chloroplast monothiol

glutaredoxins as scaffold proteins for the assembly and delivery of 2Fe-2S clusters. Embo Journal 27: 1122-1133

Barkan A (2011) Expression of Plastid Genes: Organelle-Specific Elaborations on a Prokaryotic Scaffold. Plant Physiology 155: 1520-1532

Briat JF, Duc C, Ravet K, Gaymard F. (2010) Ferritins and iron storage in plants. Biochim Biophys Acta. 1800 (8): 806-14.

Ben-Shem A, Frolow F, Nelson N (2003) Crystal structure of plant photosystem I. Nature 426: 630

Bernard DG, Cheng YF, Zhao YD, Balk J (2009) An Allelic Mutant Series of ATM3 Reveals Its Key Role in the Biogenesis of Cytosolic Iron-Sulfur Proteins in Arabidopsis. Plant Physiology 151: 590-602

Blaiseau PL, Lesuisse E, Camadro JM (2001) Aft2p, a novel iron-regulated transcription activator that modulates, with Aft1p, intracellular iron use and resistance to oxidative stress in yeast. The Journal of biological chemistry 276: 34221-34226

Borlotti A, Vigani G, Zocchi G (2012) Iron deficiency affects nitrogen metabolism in cucumber (Cucumis sativus L.) plants. BMC Plant Biology 12: 189

Brumbarova T, Bauer P, Ivanov R (2015) Molecular mechanisms governing Arabidopsis iron uptake. Trends in Plant Science 20: 124-133

Buckhout TJ, Yang TJW, Schmidt W (2009) Early iron-deficiency-induced transcriptional changes in Arabidopsis roots as revealed by microarray analyses. BMC Genomics 10: 147-147

Bughio N, Takahashi M, Yoshimura E, Nishizawa NK, Mori S (1997) Characteristics of light-regulated iron transport system in barley chloroplasts. Soil Science and Plant Nutrition 43: 959-963

Busch A, Rimbauld B, Naumann B, Rensch S, Hippler M (2008) Ferritin is required for rapid remodeling of the photosynthetic apparatus and minimizes photo-oxidative stress in response to iron availability in Chlamydomonas reinhardtii. Plant Journal 55: 201-211

Canfield, D.E., The early history of atmospheric oxygen: Homage to Robert M. Garrels. *Annual Review of Earth and Planetary Sciences* **2005,** 33, 1-36.

Chappell PD, Webb EA (2010) A molecular assessment of the iron stress response in the two phylogenetic clades of Trichodesmium. Environmental Microbiology 12: 13-27

Chauvet AAP, Agarwal R, Haddad AA, Van Mourik F, Cramer WA (2016) Photo-induced oxidation of the uniquely liganded heme f in the cytochrome b 6 f complex of oxygenic photosynthesis. Physical Chemistry Chemical Physics 18: 12983-12991

Chen J-C, Hsieh SI, Kropat J, Merchant SS (2008) A Ferroxidase Encoded by FOX1 Contributes to Iron Assimilation under Conditions of Poor Iron Nutrition in Chlamydomonas. Eukaryotic Cell 7: 541

Connorton JM, Balk J, Rodriguez-Celma J (2017) Iron homeostasis in plants - a brief overview. Metallomics 9: 813-823

Conte S, Stevenson D, Furner I, Lloyd A (2009) Multiple Antibiotic Resistance in Arabidopsis Is Conferred by Mutations in a Chloroplast-Localized Transport Protein. Plant Physiology 151: 559-573

Conte SS, Chu HH, Rodriquez DC, Punshon T, Vasques KA, Salt DE, Walker EL (2013) Arabidopsis thaliana Yellow Stripe1-Like4 and Yellow Stripe1-Like6 localize to internal cellular membranes and are involved in metal ion homeostasis. Frontiers in Plant Science 4

Cottage A, Mott EK, Kempster JA, Gray JC (2010) The Arabidopsis plastid-signalling mutant gun1 (genomes uncoupled1) shows altered sensitivity to sucrose and abscisic acid and alterations in early seedling development. Journal of Experimental Botany 61: 3773-3786

Couturier J, Wu HC, Dhalleine T, Pegeot H, Sudre D, Gualberto JM, Jacquot JP, Gaymard F, Vignols F, Rouhier N (2014) Monothiol GlutaredoxinBolA Interactions: Redox Control of Arabidopsis thaliana BolA2 and SufE1. Molecular Plant 7: 187-205

Crichton RR (2016) Iron metabolism: from molecular mechanisms to clinical consequences, Ed Fourth edition. Chichester, West Sussex: John Wiley & Sons, Ltd.

Czarnecki O, Hedtke B, Melzer M, Rothbart M, Richter A, Schröter Y, Pfannschmidt T, Grimm B (2011) An Arabidopsis GluTR Binding Protein Mediates Spatial Separation of 5-Aminolevulinic Acid Synthesis in Chloroplasts(W). Plant Cell 23: 4476-4491

Deng X, Eriksson M (2007) Two Iron-Responsive Promoter Elements Control Expression of FOX1 in Chlamydomonas reinhardtii. Eukaryotic Cell 6: 2163

Divol F, Couch D, Conejero G, Roschzttardtz H, Mari S, Curie C (2013) The Arabidopsis YELLOW STRIPE LIKE4 and 6 Transporters Control Iron Release from the Chloroplast. Plant Cell 25: 1040-1055

Dong G, Witcher S, Outten FW, Pilon M (2017) The Suf System in Archea, Bacteria, and Eukaryotic Organelles. In: Metalloprotein Active Site Assembly. Michael K Johnson, Robert A Scott (eds) West Sussex, UK

Duc C, Cellier F, Lobréaux S, Briat J-F, Gaymard F (2009) Regulation of iron homeostasis in Arabidopsis thaliana by the clock regulator time for coffee. The Journal of biological chemistry 284: 36271

Duy D, Stube R, Wanner G, Philippar K (2011) The Chloroplast Permease PIC1 Regulates Plant Growth and Development by Directing Homeostasis and Transport of Iron. Plant Physiology 155: 1709-1722

Duy D, Wanner G, Meda AR, von Wiren N, Soll J, Philippar K (2007) PIC1, an ancient permease in Arabidopsis chloroplasts, mediates iron transport. Plant Cell 19: 986-1006

Eckhardt U, Buckhout TJ (1998) Iron assimilation in Chlamydomonas reinhardtii involves ferric reduction and is similar to Strategy I in higher plants. Journal of Experimental Botany 49: 1219-1226

Estavillo G, Crisp P, Pornsiriwong W, Wirtz M, Collinge D, Carrie C, Giraud E, Whelan J, David P, Javot H, Brearley C, Hell R, Marin E, Pogson B (2011) Evidence for a SAL1-PAP Chloroplast Retrograde Pathway That Functions in Drought and High Light Signaling in Arabidopsis. Plant Cell 23: 3992-4012

Fei S, Yu J, Li Y, Deng X (2017) CrMAPK3 regulates the expression of iron-deficiency-responsive genes in Chlamydomonas reinhardtii. BMC Biochemistry 18: 1-10

Fei X, Eriksson M, Li Y, Deng X (2010) A Novel Negative Fe-Deficiency-Responsive Element and a TGGCA-Type-Like FeRE Control the Expression of FTR1 in Chlamydomonas reinhardtii. Journal of Biomedicine and Biotechnology 2010

Fei X, Eriksson M, Yang J, Deng X (2009) An Fe Deficiency Responsive Element with a Core Sequence of TGGCA Regulates the Expression of FEA1 in Chlamydomonas reinharditii. Journal of Biochemistry 146: 157-166

Feng H, An F, Zhang S, Ji Z, Ling H-Q, Zuo J (2006) Light-regulated, tissue-specific, and cell differentiation-specific expression of the Arabidopsis Fe(III)-chelate reductase gene AtFRO6. Plant physiology 140: 1345-1354

Fischer W, Hemp J, Johnson J (2016) Evolution of Oxygenic Photosynthesis. Annual Review of Earth and Planetary Sciences 44: 647

Frazzon J, Fick JR, Dean DR (2002) Biosynthesis of iron-sulphur clusters is a complex and highly conserved process. Biochemical Society Transactions 30: 680-685

Frey PA, Reed GH (2012) The ubiquity of iron. ACS chemical biology 7: 1477

Fukuyama K, Hase T, Matsumoto S, Tsukihara T, Katsube Y, Tanaka N, Kakudo M, Wada K, Matsubara H (1980) Structure Of S-Platensis 2Fe-2S Ferredoxin And Evolution Of Chloroplast-Type Ferredoxins. Nature 286: 522-524

Gabilly ST, Dreyfuss BW, Karamoko M, Corvest V, Kropat J, Page MD, Merchant SS, Hamel PP (2010) CCS5, a Thioredoxin-like Protein Involved in the Assembly of Plastid c-Type Cytochromes. Journal of Biological Chemistry 285: 29738-29749

Gao F, Robe K, Gaymard F, Izquierdo E, Dubos C (2019) The Transcriptional Control of Iron Homeostasis in Plants: A Tale of bHLH Transcription Factors? Frontiers in Plant Science 10

Georg J, Kostova G, Vuorijoki L, Schön V, Kadowaki T, Huokko T, Baumgartner D, Müller M, Klähn S, Allahverdiyeva Y, Hihara Y, Futschik ME, Aro E-M, Hess WR (2017) Acclimation of Oxygenic Photosynthesis to Iron Starvation Is Controlled by the sRNA IsaR1. Current Biology 27: 1425-1436.e1427

Glaesener AG, Merchant SS, Blaby-Haas CE (2013) Iron economy in Chlamydomonas reinhardtii. Frontiers In Plant Science 4

Gonzalez A, Fillat MF, Bes MT, Peleato ML, Sevilla E (2018) The challenge of iron stress in cyanobacteria. In: Cyanobacteria. Ed. Tiwari A

Gonzalez-Vallejo EB, Morales F, Cistue L, Abadia A, Abadia J (2000) Iron Deficiency Decreases the Fe(III)-Chelate Reducing Activity of Leaf Protoplasts. Plant Physiology 122: 337-344

Grillet L, Lan P, Li W, Mokkapati G, Schmidt W (2018) IRON MAN is a ubiquitous family of peptides that control iron transport in plants. Nature plants 4: 953

Grusak MA, Pezeshgi S (1996) Shoot-to-root signal transmission regulates root Fe(III) reductase activity in the dgl mutant of pea. Plant Physiology 110: 329-334

Halliwell B, Gutteridge J (1984) Oxygen toxicity, oxygen radicals, transition metals and disease. Biochemical Journal 219: 1-14

Hantzis LJ, Kroh GE, Jahn CE, Cantrell M, Peers G, Pilon M, Ravet K (2018) A Program for Iron Economy during Deficiency Targets Specific Fe Proteins. Plant Physiology 176: 596-610

Hirayama T, Lei GJ, Yamaji N, Nakagawa N, Ma JF (2018) The Putative Peptide Gene FEP1 Regulates Iron Deficiency Response in Arabidopsis. Plant and Cell Physiology 59: 1739-1752

Holtgrefe S, Bader KP, Horton P, Scheibe R, von Schaewen A, Backhausen JE (2003) Decreased content of leaf ferredoxin changes electron distribution and limits photosynthesis in transgenic potato plants. Plant Physiology 133: 1768-1778

Hopkinson B, Morel F (2009) The role of siderophores in iron acquisition by photosynthetic marine microorganisms. BioMetals 22: 659-669

Hu X, Page MT, Sumida A, Tanaka A, Terry MJ, Tanaka R (2017b) The iron-sulfur cluster biosynthesis protein SUFB is required for chlorophyll synthesis, but not phytochrome signaling . Plant Journal 89: 1184-1194

Hu XY, Kato Y, Sumida A, Tanaka A, Tanaka R (2017a) The SUFBC2D complex is required for the biogenesis of all major classes of plastid Fe-S proteins. Plant Journal 90: 235-248

Hurt E, Hauska G (1981) A Cytochrome f/b6 Complex of Five Polypeptides with Plastoquinol-Plastocyanin-Oxidoreductase Activity from Spinach Chloroplasts. European Journal of Biochemistry 117: 591-599

Lermontova I, Kruse E, Mock HP, Grimm B (1997) Cloning and characterization of a plastidal and a mitochondrial isoform of tobacco protoporphyrinogen IX oxidase. Proceedings of the National Academy of Sciences of the United States of America 94: 8895

Ivanov A, Krol M, Sveshnikov D, Selstam E (2006) Iron Deficiency in Cyanobacteria Causes Monomerization of Photosystem I Trimers and Reduces the Capacity for State Transitions and the Effective Absorption Cross Section of Photosystem I in Vivo1. Plant Physiology 141: 1436-1445

Jensen PE, Bassi R, Boekema EJ, Dekker JP, Jansson S, Leister D, Robinson C, Scheller HV (2007) Structure, function and regulation of plant photosystem I. BBA - Bioenergetics 1767: 335-352

Jeong J, Cohu C, Kerkeb L, Pilon M, Connolly EL, Guerinot ML (2008) Chloroplast Fe(III) chelate reductase activity is essential for seedling viability under iron limiting conditions. Proceedings of the National Academy of Sciences of the United States of America 105: 10619-10624

Jeong J, Merkovich A, Clynel M, Connolly EL (2017) Directing iron transport in dicots: regulation of iron acquisition and translocation. Current Opinion in Plant Biology 39: 106-113

Johnson DC, Dean DR, Smith AD, Johnson MK (2005) Structure, function, and formation of biological iron-sulfur clusters. Annual Review of Biochemistry 74: 247-281

Kastoori Ramamurthy R, Xiang Q, Hsieh E-J, Liu K, Zhang C, Waters BM (2018) New aspects of ironcopper crosstalk uncovered by transcriptomic characterization of Col-0 and the copper uptake mutant spl7 in Arabidopsis thaliana. Metallomics 10: 1824-1840

Keren N, Aurora R, Pakrasi HB (2004) Critical Roles of Bacterioferritins in Iron Storage and Proliferation of Cyanobacteria. Plant Physiology 135: 1666-1673

Khan MA, Castro-Guerrero NA, McInturf SA, Nguyen NT, Dame AN, Wang JJ, Bindbeutel RK, Joshi T, Jurisson SS, Nusinow DA, Mendoza-Cozatl DG (2018) Changes in iron availability in Arabidopsis are rapidly sensed in the leaf vasculature and impaired sensing leads to opposite transcriptional programs in leaves and roots. Plant Cell and Environment 41: 2263-2276

Kim SA, Guerinot ML (2007) Mining iron: Iron uptake and transport in plants. Febs Letters 581: 2273-2280

Kim SA, Lacroix IS, Gerber SA, Guerinot ML (2019) The iron deficiency response in requires the phosphorylated transcription factor URI. Proceedings of the National Academy of Sciences of the United States of America 116: 24933

Kobayashi T (2019) Understanding the Complexity of Iron Sensing and Signaling Cascades in Plants. Plant & cell physiology

Kobayashi T, Nagasaka S, Senoura T, Itai RN, Nakanishi H, Nishizawa NK (2013) Iron-binding haemerythrin RING ubiquitin ligases regulate plant iron responses and accumulation. Nature Communications 4

Kobayashi T, Nishizawa NK (2012) Iron Uptake, Translocation, and Regulation in Higher Plants. Annual Review of Plant Biology, Vol 63 63: 131-152

Kranzler C, Lis H, Finkel OM, Schmetterer G, Shaked Y, Keren N (2013) Coordinated transporter activity shapes high-affinity iron acquisition in cyanobacteria. The ISME Journal 8: 409

Kranzler C, Lis H, Shaked Y, Keren N (2011) The role of reduction in iron uptake processes in a unicellular, planktonic cyanobacterium. Environmental Microbiology 13: 2990-2999

Kumanovics A, Chen OS, Li LT, Bagley D, Adkins EM, Lin HL, Dingra NN, Outten CE, Keller G, Winge D, Ward DM, Kaplan J (2008) Identification of FRA1 and FRA2 as genes involved in regulating the yeast iron regulon in response to decreased mitochondrial iron-sulfur cluster synthesis. Journal of Biological Chemistry 283: 10276-10286

Kumar AM, Söll D (2000) Antisense HEMA1 RNA Expression Inhibits Heme and Chlorophyll Biosynthesis in Arabidopsis. Plant Physiology 122: 49-55

Kumar RK, Chu HH, Abundis C, Vasques K, Rodriguez DC, Chia JC, Huang R, Vatamaniuk OK, Walker EL (2017) Iron-Nicotianamine Transporters Are Required for Proper Long Distance Iron Signaling. Plant Physiology 175: 1254-1268

Kushnir S, Babiychuk E, Storozhenko S, Davey MW, Papenbrock J, De Rycke R, Engler G, Stephan UW, Lange H, Kispal G, Lill R, Van Montagu M (2001) A Mutation of the Mitochondrial ABC Transporter Sta1 Leads to Dwarfism and Chlorosis in the Arabidopsis Mutant starik. The Plant Cell 13: 89-100

Laganowsky A, Gomez SM, Whitelegge JP, Nishio JN (2009) Hydroponics on a chip: Analysis of the Fe deficient Arabidopsis thylakoid membrane proteome. Journal of Proteomics 72: 397-415

Lammers PJ, Sanders-Loehr J (1982) Active transport of ferric schizokinen in Anabaena sp. Journal of bacteriology 151: 288

Larbi A, Abadía A, Abadía J, Morales F (2006) Down co-regulation of light absorption, photochemistry, and carboxylation in Fe-deficient plants growing in different environments. Photosynthesis Research 89: 113-126

Larkin RM (2016) Tetrapyrrole Signaling in Plants. Frontiers in plant science 7: 1586

Thi Tuyet Le C, Brumbarova T, Bauer P (2019) The interplay of ROS and iron signaling. In: Redox Homeostasis in Plants. Signalling and Communication in Plants. Panda A, Yamamoto Y (eds) Springer, Cham pp 43-66

Lenton TM, Dahl TW, Daines SJ, Mills BJW, Ozaki K, Saltzman MR, Porada P (2016) Earliest land plants created modern levels of atmospheric oxygen. Proceedings of the National Academy of Sciences of the United States of America 113: 9704-9709

Leon S, Touraine B, Ribot C, Briat JF, Lobreaux S (2003) Iron-sulphur cluster assembly in plants: distinct NFU proteins in mitochondria and plastids from Arabidopsis thaliana. Biochemical Journal 371: 823-830

Lezhneva L, Amann K, Meurer J (2004) The universally conserved HCF101 protein is involved in assembly of [4Fe-4S]-cluster-containing complexes in Arabidopsis thaliana chloroplasts. Plant Journal 37: 174-185

Li HM, Theg SM, Bauerle CM, Keegstra K (1990) METAL-ION-CENTER ASSEMBLY OF FERREDOXIN AND PLASTOCYANIN IN ISOLATED-CHLOROPLASTS. Proceedings of the National Academy of Sciences of the United States of America 87: 6748-6752

Li M, Zhang J, Jin H, Feng D, Wang J, Wang H-B, Liu B (2019) The Iron Deficiency Response Regulators IAA-LEUCINE RESISTANT3 and bHLH104 Possess Different Targets and Have Distinct Effects on Photosynthesis in Arabidopsis. Journal of Plant Biology 62: 109-119

Liang X, Qin L, Liu P, Wang M, Ye H. (2014) Genes for iron-sulfur cluster assembly are targets of abiotic stress in rice, *Oryza sativa*. Plant, Cell and Environment. 37 (3): 780-794.

Lill R, Muhlenhoff U (2008) Maturation of iron-sulfur proteins in eukaryotes: Mechanisms, connected processes, and diseases. Annual Review of Biochemistry 77: 669-700

Lingam S, Mohrbacher J, Brumbarova T, Potuschak T, Fink-Straube C, Blondet E, Genschik P, Bauer P (2011) Interaction between the bHLH Transcription Factor FIT and ETHYLENE INSENSITIVE3/ETHYLENE INSENSITIVE3-LIKE1 Reveals Molecular Linkage between the Regulation of Iron Acquisition and Ethylene Signaling in Arabidopsis. The Plant Cell 23: 1815-1829

Lodeyro AF, Ceccoli RD, Pierella Karlusich JJ, Carrillo N (2012) The importance of flavodoxin for environmental stress tolerance in photosynthetic microorganisms and transgenic plants. Mechanism, evolution and biotechnological potential. *In*, Vol 586, pp 2917-2924

Long J, Sommer F, Allen M, Lu S-F, Merchant S (2008) FER1 and FER2 Encoding Two Ferritin Complexes in Chlamydomonas reinhardtii Chloroplasts Are Regulated by Iron. Genetics 179: 137-147

Long TA, Tsukagoshi H, Busch W, Lahner B, Salt DE, Benfey PN (2010) The bHLH Transcription Factor POPEYE Regulates Response to Iron Deficiency in Arabidopsis Roots. Plant Cell 22: 2219-2236

Lonnerdal B. (2009) Soybean ferritin: implications for iron status of vegetarians. American Journal of Clinical Nutrition. 89 (5): 1680S-1685S.

Lopez-Millan AF, Duy D, Philippar K (2016) Chloroplast Iron Transport Proteins - Function and Impact on Plant Physiology. Frontiers in Plant Science 7

Lopez-Millan AF, Grusak MA, Abadia A, Abadia J (2013) Iron deficiency in plants: an insight from proteomic approaches. Frontiers in Plant Science 4

Lubberding HJ, de Graf FHJM, Bienfait HF. (1988) Ferric reducing activity in roots of Fe-deficient Phaseoulus vulgaris: source of reducing equivalents. Biochem Physiol Pflanzen. 183: 271-276

Lyons TW, Reinhard CT, Planavsky NJ (2014) The rise of oxygen in Earth's early ocean and atmosphere. Nature 506: 307-315

Ma F, Zhang X, Zhu X, Li T, Zhan J, Chen H, He C, Wang Q (2017) Dynamic Changes of IsiA-Containing Complexes during Long-Term Iron Deficiency in Synechocystis sp. PCC 6803. Molecular Plant 10: 143-154

Mentewab A, Matheson K, Adebiyi M, Robinson S, Elston B (2014) RNA-seq analysis of the effect of kanamycin and the ABC transporter AtWBC19 on Arabidopsis thaliana seedlings reveals changes in metal content. PLoS ONE 9: e109310

Merchant S, Sawaya MR (2005) The Light Reactions: A Guide to Recent Acquisitions for the Picture Gallery. *In*, Vol 17, pp 648-663

Mihara H, Esaki N (2002) Bacterial cysteine desulfurases: their function and mechanisms. Applied Microbiology and Biotechnology 60: 12-23

Moller SG, Kunkel T, Chua NH (2001) A plastidic ABC protein involved in intercompartmental communication of light signaling. Genes & Development 15: 90-103

Moran Lauter A, Peiffer G, Yin T, Whitham S, Cook D, Shoemaker R, Graham M (2014) Identification of candidate genes involved in early iron deficiency chlorosis signaling in soybean (Glycine max) roots and leaves. BMC Genomics 15

Moseley JL, Allinger T, Herzog S, Hoerth P, Wehinger E, Merchant S, Hippler M. (2002) Adaptation to the Fe-deficiency requires remodeling of the photosynthetic apparatus. EMBO J. 21 (24): 6709-6720.

Moulin M, Smith AG (2005) Regulation of tetrapyrrole biosynthesis in higher plants. Biochemical Society Transactions 33: 737-742

Mukherjee I, Campbell NH, Ash JS, Connolly EL (2006) Expression profiling of the Arabidopsis ferric chelate reductase (FRO) gene family reveals differential regulation by iron and copper. Planta 223: 1178-1190

Müller B, Kovács K, Pham H-D, Kavak Y, Pechoušek J, Machala L, Zbořil R, Szenthe K, Abadía J, Fodor F, Klencsár Z, Solti Á (2019) Chloroplasts preferentially take up ferric-citrate over iron-nicotianamine complexes in Brassica napus. Planta 249: 751

Murthy N, Ollagnier-de-Choudens S, Sanakis Y, Abdel-Ghany SE, Rousset C, Ye H, Fontecave M, Pilon-Smits EAH, Pilon M (2007) Characterization of Arabidopsis thaliana SufE2 and SufE3 - Functions in chloroplast iron-sulfur cluster assembly and NAD synthesis. Journal of Biological Chemistry 282: 18254-18264

Nagane T, Tanaka A, Tanaka R (2010) Involvement of AtNAP1 in the regulation of chlorophyll degradation in Arabidopsis thaliana. Planta 231: 939-949

Naumann B, Stauber EJ, Busch A, Sommer F, Hippler M (2005) N-terminal processing of Lhca3 Is a key step in remodeling of the photosystem I-light-harvesting complex under iron deficiency in Chlamydomonas reinhardtii. The Journal of biological chemistry 280: 20431

Nechushtai R, Conlan A, Harir Y, Song L, Yogev O, Eisenberg-Domovich Y, Livnah O, Michaeli D, Rosen R, Ma V, Luo Y, Zuris J, Paddock M, Cabantchik Z, Jennings P, Mittler R (2012) Characterization of Arabidopsis NEET Reveals an Ancient Role for NEET Proteins in Iron Metabolism(W). Plant Cell 24: 2139-2154

Nicolaisen K, Moslavac S, Samborski A, Valdebenito M, Hantke K, Maldener I, Muro-Pastor AM, Flores E, Schleiff E (2008) Alr0397 is an outer membrane transporter for the siderophore schizokinen in Anabaena sp. strain PCC 7120. Journal of bacteriology 190: 7500

Outten FW, Djaman O, Storz G (2004) A suf operon requirement for Fe-S cluster assembly during iron starvation in Escherichia coli. Molecular Microbiology 52: 861-872

Outten FW, Wood MJ, Munoz FM, Storz G (2003) The SufE protein and the SufBCD complex enhance SufS cysteine desulfurase activity as part of a sulfur transfer pathway for fe-s cluster assembly in Escherichia coli. Journal of Biological Chemistry 278: 45713-45719

Page M, Allen M, Kropat J, Urzica E, Karpowicz S, Hsieh S, Loo J, Merchant S (2012) Fe Sparing and Fe Recycling Contribute to Increased Superoxide Dismutase Capacity in Iron-Starved Chlamydomonas reinhardtii(W). Plant Cell 24: 2649-2665

Page MLD, Hamel PP, Gabilly ST, Zegzouti H, Perea JV, Alonso JM, Ecker JR, Theg SM, Christensen SK, Merchant S (2004) A homolog of prokaryotic thiol disulfide transporter CcdA is required for the assembly of the cytochrome b(6)f complex in Arabidopsis chloroplasts. Journal of Biological Chemistry 279: 32474-32482

Pan IC, Tsai H-H, Cheng Y-T, Wen T-N, Buckhout TJ, Schmidt W (2015) Post-Transcriptional Coordination of the Arabidopsis Iron Deficiency Response is Partially Dependent on the E3 Ligases RING DOMAIN LIGASE1 (RGLG1) and RING DOMAIN LIGASE2 (RGLG2). Molecular & cellular proteomics : MCP 14: 2733

Pierella Karlusich JJ, Lodeyro AF, Carrillo N (2014) The long goodbye: the rise and fall of flavodoxin during plant evolution. Journal Of Experimental Botany 65: 5161-5178

Pilon M, Dekruijff B, Weisbeek PJ (1992) New Insights Into The Import Mechanism Of The Ferredoxin Precursor Into Chloroplasts. Journal of Biological Chemistry 267: 2548-2556

Pilon-Smits EAH, Garifullina GF, Abdel-Ghany S, Kato S-I (2002) Characterization of a NifS-like chloroplastic protein from A*rabidopsis.* Implications
for its role in sulfur and selenium metabolism. Plant Physiology 130: 1309-1318

Poor CB, Wegner SV, Li H, Dlouhy AC, Schuermann JP Sanishvili R, Hinshaw JR, Riggs-Gelasco PJ, Outten CE, He C (2014) Molecular mechanism and structure of the Saccharomyces cerevisiae iron regulator Aft2. Proceedings of the National Academy of Sciences 111: 4043

Proudhon D, Wei J, Briat J, Theil E (1996) Ferritin gene organization: Differences between plants and animals suggest possible kingdom-specific selective constraints. Journal of Molecular Evolution 42: 325-336

Ramírez L, Bartoli CG, Lamattina L (2013) Glutathione and ascorbic acid protect Arabidopsis plants against detrimental effects of iron deficiency. Journal of experimental botany 64: 3169

Raux-Deery E, Leech HK, Nakrieko KA, McLean KJ, Munro AW, Heathcote P, Rigby SEJ, Smith AG, Warren MJ (2005) Identification and characterization of the terminal enzyme of siroheme biosynthesis from Arabidopsis thaliana - A plastid-located sirohydrochlorin ferrochelatase containing a 2Fe-2S center. Journal of Biological Chemistry 280: 4713-4721

Raven JA, Allen JF (2003) Genomics and chloroplast evolution: what did cyanobacteria do for plants? Genome Biology 4: 209-209

Ravet K, Touraine B, Boucherez J, Briat JF, Gaymard F, Cellier F (2009) Ferritins control interaction between iron homeostasis and oxidative stress in Arabidopsis. Plant Journal 57: 400-412

Robinson NJ, Procter CM, Connolly EL, Guerinot ML (1999) A ferric-chelate reductase for iron uptake from soils. Nature 397: 694-697

Rodríguez-Celma J, Connorton JM, Kruse I, Green RT, Franceschetti M, Chen Y-T, Cui Y, Ling H-Q, Yeh K-C, Balk J (2019) Arabidopsis BRUTUS-LIKE E3 ligases negatively regulate iron uptake by targeting transcription factor FIT for recycling. Proceedings of the National Academy of Sciences of the United States of America 116

Rodriguez-Celma J, Pan IC, Li W, Lan P, Buckhout TJ, Schmidt W (2013) The transcriptional response of A*rabidopsis* leaves to Fe deficiency. Frontiers in Plant Science 4: 276

Rutherford JC, Jaron S, Ray E, Brown, PO, Winge DR (2001) A second iron-regulatory system in yeast independent of Aft1p. Proceedings of the National Academy of Sciences of the United States of America 98: 14322

Salome PA, Oliva M, Weigel D, Kramer U (2013) Circadian clock adjustment to plant iron status depends on chloroplast and phytochrome function. Embo Journal 32: 511-523

Schaedler TA, Thornton JD, Kruse I, Schwarzlander M, Meyer AJ, van Veen HW, Balk J (2014) A Conserved Mitochondrial ATP-binding Cassette Transporter Exports Glutathione Polysulfide for Cytosolic Metal Cofactor Assembly. Journal of Biological Chemistry 289: 23264-23274

Schorsch M, Kramer M, Goss T, Eisenhut M, Robinson N, Osman D, Wilde A, Sadaf S, Brückler H, Walder L, Scheibe R, Hase T, Hanke GT (2018) A unique ferredoxin acts as a player in the low-iron response of photosynthetic organisms. Proceedings of the National Academy of Sciences of the United States of America 115: E12111

Schwenkert S, Netz DJA, Frazzon J, Pierik AJ, Bill E, Gross J, Lill R, Meurer J (2010) Chloroplast HCF101 is a scaffold protein for 4Fe-4S cluster assembly. Biochemical Journal 425: 207-214

Sharma P, Jha AB, Dubey RS, Pessarakli M (2012) Reactive Oxygen Species, Oxidative Damage, and Antioxidative Defense Mechanism in Plants under Stressful Conditions. Journal of Botany 2012

Shcolnick S, Summerfield T, Reytman L, Sherman L, Keren N (2009) The Mechanism of Iron Homeostasis in the Unicellular Cyanobacterium Synechocystis sp. PCC 6803 and Its Relationship to Oxidative Stress. Plant Physiology 150: 2045-2056

Shen G, Balasubramanian R, Wang T, Wu Y, Hoffart LM, Krebs C, Bryant DA, Golbeck JH (2007) SufR coordinates two 4Fe-4S (2+,1+) clusters and functions as a transcriptional repressor of the sufBCDS operon and an autoregulator of sufR in cyanobacteria. Journal of Biological Chemistry 282: 31909-31919

Shevela D, Eaton-Rye JJ, Shen JR, Govindjee (2012) Photosystem II and the unique role of bicarbonate: A historical perspective. Biochimica Et Biophysica Acta-Bioenergetics 1817: 1134-1151

Shikanai T, Muller-Moule P, Munekage Y, Niyogi KK, Pilon M (2003) PAA1, a P-type ATPase of Arabidopsis, functions in copper transport in chloroplasts. Plant Cell 15: 1333-1346

Shimoni-Shor E, Hassidim M, Yuval-Naeh N, Keren N (2010) Disruption of Nap14, a plastid-localized non-intrinsic ABC protein in Arabidopsis thaliana results in the over-accumulation of transition metals and in aberrant chloroplast structures. Plant, Cell & Environment 33: 1029-1038

Shingles R, North M, McCarty RE (2002) Ferrous ion transport across chloroplast inner envelope membranes. Plant Physiology 128: 1022-1030

Singh A, McIntyre L, Sherman L (2003) Microarray analysis of the genome-wide response to iron deficiency and iron reconstitution in the cyanobacterium Synechocystis sp. PCC 68031. Plant Physiology 132: 1825-1839

Sivitz AB, Hermand V, Curie C, Vert G (2012) Arabidopsis bHLH100 and bHLH101 Control Iron Homeostasis via a FIT-Independent Pathway. Plos One 7

Solti Á, Müller B, Czech V, Sárvári É, Fodor F (2014) Functional characterization of the chloroplast ferric chelate oxidoreductase enzyme. New Phytologist 202: 920-928

Stein RJ, Waters BM (2012) Use of natural variation reveals core genes in the transcriptome of iron-deficient roots. Journal of Experimental Botany 63: 1039-1055

Sun J, Golbeck JH (2015) The Presence of the IsiA-PSI Supercomplex Leads to Enhanced Photosystem I Electron Throughput in Iron-Starved Cells of Synechococcus sp. PCC 7002. The journal of physical chemistry. B 119: 13549

Susek RE, Ausubel FM, Chory J (1993) Signal-Transduction Mutants Of Arabidopsis Uncouple Nuclear Cab And Rbcs Gene-Expression From Chloroplast Development. Cell 74: 787-799

Takahashi Y, Mitsui A, Fujita Y, Matsubara H (1991a) Roles of ATP and NADPH in formation of the fe-s cluster of spinach ferredoxin. Plant physiology 95: 104

Takahashi Y, Mitsui A, Hase T, Matsubara H (1986) Formation of The Iron Sulfur Cluster of Ferredoxin In Isolated-Chloroplasts. Proceedings of the National Academy of Sciences of the United States of America 83: 2434-2437

Takahashi Y, Mitsui A, Matsubara H (1991b) Formation of The Fe-S Cluster of Ferredoxin In Lysed Spinach-Chloroplasts. Plant Physiology 95: 97-103

Takahashi Y, Tokumoto U (2002) A third bacterial system for the assembly of iron-sulfur clusters with homologs in archaea and plastids. Journal of Biological Chemistry 277: 28380-28383

Tanaka A, Tanaka R (2006) Chlorophyll metabolism. Current Opinion in Plant Biology 9: 248-255

Tanaka R, Tanaka A, (2007) Tetrapyrrole biosynthesis in higher plants. Annu. Rev. Plant Biol. 58: 321–346.

Tanaka R, Kobayashi K, Masuda T (2011) Tetrapyrrole metabolism in *Arabidopsis thaliana* The *Arabidopsis* Book 9: e0145

Tejada-Jimenez M, Llamas A, Galvan A, Fernandez E (2019) Role of Nitrate Reductase in NO Production in Photosynthetic Eukaryotes. Plants 8: 56

Teng YS, Su YS, Chen LJ, Lee YJ, Hwang I, Li HM (2006) Tic21 is an essential translocon component for protein translocation across the chloroplast inner envelope membrane. Plant Cell 18: 2247-2257

Terauchi AM, Peers G, Kobayashi M, Niyogi KK, Merchant SS (2010) Trophic status of *Chlamydomonas reinhardtii* influences the impact of iron deficiency on photosynthesis. Photosynthesis Research 105: 39-49

Terzulli A, Kosman DJ (2010) Analysis of the High-Affinity Iron Uptake System at the Chlamydomonas reinhardtii Plasma Membrane. Eukaryotic Cell 9: 815-826

Thimm O, Essigmann B, Altmann T, Buckhout TJ (2001) Response of Arabidopsis to Iron Deficiency Stress as Revealed by Microarray Analysis. Plant Physiology 127: 1030-1043

Thomine S, Vert G (2013) Iron transport in plants: better be safe than sorry. Current Opinion in Plant Biology 16: 322-327

Timperio AM, D'Amici GM, Barta C, Loreto F, Zolla L (2007) Proteomics, pigment composition, and organization of thylakoid membranes in iron-deficient spinach leaves. Journal of Experimental Botany 58: 3695-3710

Tissot N, Robe K, Gao F, Grant-Grant S, Boucherez J, Bellegarde F, Maghiaoui A, Marcelin R, Izquierdo E, Benhamed M, Martin A, Vignols F, Roschzttardtz H, Gaymard F, Briat J-F, Dubos C (2019) Transcriptional integration of the responses to iron availability in Arabidopsis by the bHLH factor ILR3. The New phytologist

Tognetti VB, Zurbriggen MD, Morandi EN, Fillat MF, Valle EM, Hajirezaei MR, Carrillo N (2007) Enhanced plant tolerance to iron starvation by functional substitution of chloroplast ferredoxin with a bacterial flavodoxin. Proceedings of the National Academy of Sciences 104: 11495

Touraine B, Boutin JP, Marion-Poll A, Briat JF, Peltier G, Lobréaux S (2004) Nfu2: a scaffold protein required for [4Fe-4S] and ferredoxin iron-sulphur cluster assembly in Arabidopsis chloroplasts. Plant Journal 40: 101-111

Touraine B, Vignols F, Przybyla-Toscano J, Ischebeck T, Dhalleine T, Wu H.C, Magno C, Berger N, Dubos C, Feussner I, Caffarri S, Havaux M, Rouhier N, Gaymard F. (2019) Iron-Sulfur protein NFU2 is required for branched chain amino acid synthesis in Arabidopsis roots. Journal of Experimental Botany. 70 (6): 1875-1889.

Tripathi D, Singh S, Gaur S, Singh S, Yadav V, Liu S, Singh V, Sharma S, Srivastava P, Prasad S, Dubey N, Chauhan D, Sahi S (2018) Acquisition and Homeostasis of Iron in

Higher Plants and Their Probable Role in Abiotic Stress Tolerance. Frontiers in Environmental Science 5

Urzica EI, Adler LN, Page MD, Linster CL, Arbing MA, Casero D, Pellegrini M, Merchant SS, Clarke SG (2012b) Impact of oxidative stress on ascorbate biosynthesis in Chlamydomonas via regulation of the VTC2 gene encoding a GDP-L-galactose phosphorylase. The Journal of biological chemistry 287: 14234

Urzica EI, Casero D, Yamasaki H, Hsieh SI, Adler LN, Karpowicz SJ, Blaby-Haas CE, Clarke SG, Loo JA, Pellegrini M, Merchant SS (2012a) Systems and Trans-System Level Analysis Identifies Conserved Iron Deficiency Responses in the Plant Lineage. The Plant Cell 24: 3921-3948

Van Hoewyk D, Abdel-Ghany SE, Cohu CM, Herbert SK, Kugrens P, Pilon M, Pilon-Smits EAH (2007) Chloroplast iron-sulfur cluster protein maturation requires the essential cysteine desulfurase CpNifS. Proceedings of the National Academy of Sciences 104: 5686

Vert G, Grotz N, Dedaldechamp F, Gaymard F, Guerinot ML, Briat J-F, Curie C (2002) IRT1, an A*rabidopsis* transporter essential for iron uptake from the soil and for plant growth. The Plant Cell 14: 1223-1233

Vert GA, Briat JF, Curie C (2003) Dual regulation of the Arabidopsis high-affinity root iron uptake system by local and long-distance signals. Plant Physiology 132: 796-804

Vigani G, Solti Á, Thomine S, Philippar K (2019) Essential and Detrimental – an Update on Intracellular Iron Trafficking and Homeostasis (Book review). *In*,

Vuorijoki L, Tiwari A, Kallio P, Aro EM (2017) Inactivation of iron-sulfur cluster biogenesis regulator SufR in Synechocystis sp PCC 6803 induces unique iron-dependent protein-level responses. Biochimica Et Biophysica Acta-General Subjects 1861: 1085-1098

Wacey D, Saunders M, Brasier MD, Kilburn MR (2011) Earliest microbially mediated pyrite oxidation in similar to 3.4 billion-year-old sediments. Earth and Planetary Science Letters 301: 393-402

Wang T, Shen G, Balasubramanian R, McIntosh L, Bryant DA, Golbeck JH (2004) The sufR Gene (sll0088 in Synechocystis sp. Strain PCC 6803) Functions as a Repressor of the sufBCDS Operon in Iron-Sulfur Cluster Biogenesis in Cyanobacteria. The Journal of Bacteriology 186: 956

Waters BM, McInturf SA Stein RJ (2012) Rosette iron deficiency transcript and microRNA profiling reveals links between copper and iron homeostasis in Arabidopsis thaliana. Journal of Experimental Botany 63: 5903-5918

Waters MT, Langdale JA (2009) The making of a chloroplast. EMBO Journal 28: 2861-2873

Xu XM, Adams S, Chuam NH, Moller SG (2005) AtNAP1 represents an atypical SufB protein in Arabidopsis plastids. Journal of Biological Chemistry 280

Xu XM, Moller SG (2006) AtSufE is an essential activator of plastidic and mitochondrial desulfurases in Arabidopsis. Embo Journal 25: 900-909

Xu XM, Møller SG, Cashmore AR (2004) AtNAP7 Is a Plastidic SufC-Like ATP-Binding Cassette/ATPase Essential for Arabidopsis Embryogenesis. Proceedings of the National Academy of Sciences of the United States of America 101: 9143-9148

Yabe T, Morimoto K, Kikuchi S, Nishio K, Terashima I, Nakai M (2004) The Arabidopsis chloroplastic NifU-like protein CnfU, which can act as an iron-sulfur cluster scaffold protein, is required for biogenesis of ferredoxin and photosystem I. Plant Cell 16: 993-1007

Yabe T, Nakai M (2006) Arabidopsis AtIscA-I is affected by deficiency of Fe–S cluster biosynthetic scaffold AtCnfU-V. Biochemical & Biophysical Research Communications 340: 1047-1052

Yadavalli V, Neelam S, Rao ASVC, Reddy AR, Subramanyam R (2012) Differential degradation of photosystem I subunits under iron deficiency in rice. Journal of Plant Physiology 169: 753-759

Yamasaki H, Hayashi M, Fukazawa M, Kobayashi Y, Shikanai T. (2009) *SQUAMOSA* promoter binding protein-like7 is a central regulator for copper homeostasis in *Arabidopsis.* Plant Cell. 21: 347-361.

Yamaguchi-Iwai Y, Stearman R, Dancis A, Klausner RD (1996) Iron-regulated DNA binding by the Aft1 protien controls the iron regulon in yeast. The EMBO Journal 15: 3377-3384

Yang T, Lin W-D, Schmidt W (2010) Transcriptional Profiling of the Arabidopsis Iron Deficiency Response Reveals Conserved Transition Metal Homeostasis Networks. Plant Physiology 152: 2130-2141

Ye H, Abdel-Ghany SE, Anderson TD, Pilon-Smits EAH, Pilon M (2006) CpSufE Activates the Cysteine Desulfurase CpNifS for Chloroplastic Fe-S Cluster Formation. Journal of Biological Chemistry 281: 8958-8969

Ye H, Garifullina GF, Abdel-Ghany SE, Zhang LH, Pilon-Smits EAH, Pilon M (2005) The chloroplast NifS-like protein of Arabidopsis thaliana is required for iron-sulfur cluster formation in ferredoxin. Planta 220: 602-608

Yu H, Yang J, Shi Y, Donelson J, Thompson SM, Sprague S, Roshan T, Wang D-L, Liu J, Park S, Nakata PA, Connolly EL, Hirschi KD, Grusak MA, Cheng N (2017) Arabidopsis Glutaredoxin S17 Contributes to Vegetative Growth, Mineral Accumulation, and Redox Balance during Iron Deficiency. Frontiers in Plant Science 8

Zandalinas SI, Song L, Sengupta S, McInturf SA, Grant DG, Marjault H-B, Castro-Guerrero NA, Burks D, Azad RK, Mendoza-Cozatl DG, Nechushtai R, Mittler R (2019) Expression of a dominant-negative AtNEET-H89C protein disrupts iron-sulfur metabolism and iron homeostasis in Arabidopsis. The Plant journal : for cell and molecular biology

Zhai ZY, Gayomba SR, Jung HI, Vimalakumari NK, Pineros M, Craft E, Rutzke MA, Danku J, Lahner B, Punshon T, Guerinot ML, Salt DE, Kochian LV, Vatamaniuk OK (2014) OPT3 Is a Phloem-Specific Iron Transporter That Is Essential for Systemic Iron Signaling and Redistribution of Iron and Cadmium in Arabidopsis. Plant Cell 26: 2249-2264

Zhang Z-W, Yuan S, Feng H, Xu F, Cheng J, Shang J, Zhang D-W, Lin H-H (2011) Transient accumulation of Mg-protoporphyrin IX regulates expression of PhANGs – New evidence for the signaling role of tetrapyrroles in mature Arabidopsis plants. Journal of Plant Physiology 168: 714-721

Zheng L, Huang F, Narsai R, Wu J, Giraud E, He F, Cheng L, Wang F, Wu P, Whelan J, Shou H (2009) Physiological and Transcriptome Analysis of Iron and Phosphorus Interaction in Rice Seedlings. Plant Physiology 151: 262-274

Zheng LM, Cash VL, Flint DH, Dean DR (1998) Assembly of iron-sulfur clusters - Identification of an iscSUA-hscBA-fdx gene cluster from Azotobacter vinelandii. Journal of Biological Chemistry 273: 13264-13272

Zheng LM, White RH, Cash VL, Jack RF, Dean DR (1993) Cysteine Desulfurase Activity Indicates A Role For Nifs In Metallocluster Biosynthesis. Proceedings of the National Academy of Sciences of the United States of America 90: 2754-2758

CHAPTER 2: A PROGRAM FOR IRON ECONOMY DURING DEFICIENCY IN ARABIDOPSIS ROSETTES TARGETS SPECIFIC FE PROTEINS[2]

2.1 SUMMARY

Iron (Fe) is an essential element for plants, utilized in nearly every cellular process. Because the adjustment of uptake under Fe limitation cannot satisfy all demands, plants need to acclimate their physiology and biochemistry, especially in their chloroplasts, which have a high demand for Fe. To investigate if a program exists for the utilization of Fe under deficiency, we analyzed how hydroponically grown *Arabidopsis thaliana* adjusts its physiology and Fe protein composition in vegetative photosynthetic tissue, during Fe deficiency. Fe deficiency first affected photosynthetic electron transport with concomitant reductions in carbon assimilation and biomass production when effects on respiration were not yet significant. Photosynthetic electron transport function and protein levels of Fe-dependent enzymes were fully recovered upon iron resupply, indicating that the Fe depletion stress did not cause irreversible secondary damage. At the protein level, ferredoxin, the cytochrome-b_6f complex, and Fe-containing enzymes of the plastid sulfur assimilation pathway were major targets of Fe deficiency, whereas other Fe dependent functions were relatively less affected. In coordination, SUFA and SUFB, two proteins of the plastid iron-sulfur cofactor assembly pathway were also diminished early by Fe depletion. Iron depletion reduced mRNA levels for the majority of the affected proteins indicating that loss of enzyme was not just due to lack of Fe cofactors. SUFB and Ferredoxin were early targets of transcript down-regulation. The data reveal a hierarchy for Fe utilization in photosynthetic tissue and indicate that a program is in place to acclimate to impending Fe deficiency.

---

[1] Published in *Plant Physiology,* Authors: Laura J. Hantzis*, Gretchen E. Kroh*, Courtney E. Jahn, Michael Cantrell, Graham Peers, Marinus Pilon and Karl Ravet (Hantzis et al., 2018).
* These authors contributed equally

2.2 INTRODCUTION

Iron (Fe) is a pivotal micronutrient for plants because of its role as a cofactor in proteins involved in electron transport, redox reactions, and catalysis (Balk and Schaedler, 2014). Low bio-availability of Fe in arable soils can decrease agricultural yields and affect the nutritional value of edible plant parts (Reviewed in Briat *et al.*, 2015). Fe can be utilized in three different types of cofactors: heme, iron-sulfur (Fe-S) clusters, or non-heme iron (Balk and Schaedler, 2014). In plants, the plastid has its own Fe-S cluster biosynthesis machinery (Balk and Pilon, 2011) and it is also the site for the synthesis of heme precursors (Moulin and Smith, 2005). In *Arabidopsis* the majority of the Fe in the vegetative shoot (68%) was found to be in the chloroplasts (Shikanai *et al.,* 2003), which indicates that these organelles are a major sink for Fe utilization in green leaves. Therefore, plastids should play a central role in maintaining Fe homeostasis in green tissues, especially when Fe supply becomes limiting.

Research on Fe homeostasis in plants has mainly focused on Fe uptake mechanisms in the roots and Fe distribution within the plants resulting in the identification of several molecular factors involved in whole-plant Fe homeostasis (for recent reviews see: Kobayashi and Nishizawa, 2012; Brumbarova *et al.*, 2015, Krohling *et al.*, 2016). In addition to Fe uptake and redistribution, plants can also acclimate their metabolism when Fe supply cannot meet all needs (Lopez-Millan *et al.,* 2013). A still understudied aspect of the biology of Fe is its utilization within plant cells. We hypothesize that plants implement a mechanism for Fe economy that allows a preferential allocation of Fe to the most important functions, when the cellular demand for Fe in photosynthetic tissue exceeds its potential supply by the roots. Are certain enzymes maintained while others are lost, and is there a regulatory Fe economy system in place to mediate such an acclimation? These crucial questions need to be addressed in order to get a comprehensive view of how plants respond to Fe deficiency.

Nutrient “economy” strategies tend to prioritize, recycle, and remobilize limiting nutrients

(Blaby-Haas and Merchant, 2013). Studies on non-photosynthetic unicellular organisms such as bacteria and yeast have suggested that programs exist to acclimate metabolism to Fe deficiency (Oglesby-Sherrousse *et al.*, 2013; Philpott *et al.*, 2012). Compared to heterotrophs, photosynthetic organisms have to cope with a substantially higher demand for Fe because of the added iron requirement of the chloroplast (reviewed in Blaby-Haas and Merchant, 2013). The response to Fe deficiency in *Chlamydomonas rheinhardtii*, a unicellular alga and a facultative photo-autotroph, depends on whether the cells grow photosynthetically or heterotrophically (Terauchi *et al.*, 2010; Glaesener *et al.*, 2013). Fe economy in *Chlamydomonas* gives a central role to the chloroplast and relies on reduced *de novo* Fe-protein synthesis, turnover of Fe proteins, together with up-regulation of specific enzymes such as Fe superoxide dismutase (Moseley *et al.*, 2002; Page *et al.*, 2012). However, unlike Chlamydomonas, plants absolutely require photosynthesis for growth. In the context of Cu nutrition, another pivotal trace element for photosynthesis, a molecular remodeling has been proposed both in higher plants and in Chlamydomonas but the targets of regulation are different in the two kinds of organisms (Blaby-Haas and Merchant, 2013).

In this study, a hydroponic system was used to control available Fe in order to analyze physiological and molecular level changes upon Fe depletion with an emphasis on chloroplastic Fe-dependent proteins in *Arabidopsis* vegetative shoots. The results suggest that a defined hierarchy is implemented for Fe utilization in chloroplasts when Fe is scarce in the environment.

2.3 METHODS

Plant Material, Hydroponic Growth Conditions and Plant Sampling. *Arabidopsis thaliana* columbia-0 (Col-0) seeds were surface sterilized by three consecutive 5 minutes rinses with 70%, 95% and 70% ethanol, air dried and stratified for three days at 4°C. Seeds were germinated on vertical half-strength Murashigue and Skoog (MS) medium (Sigma-Aldrich, St Louis, MO) supplemented with 1 % (w/v) sucrose (Sigma-Aldrich), 1 % (w/v) phytoagar

(Research Products International, Mt. Prospect, IL) and 10 µM Fe(III)-EDTA (Caisson Labs, Smithfield, UT) in a growth chamber under controlled conditions (in a 8h/16h light/dark cycle, 200 µmol photons.m^{-2}.s^{-1}, HR 70%, 23°C/20°C day/night). The hydroponics setup was in the same growth chamber. One week-old seedlings were transferred to hydroponics, in 5-liter containers, holding 1/5th strength modified Hoagland's solution (Ravet *et al.*, 2011) containing 10 µM Fe(III)-EDTA. Preliminary experiments showed that 10 µM Fe(III)-EDTA is the lowest amount of Fe allowing Arabidopsis growth without visible signs of Fe deficiency symptoms such as growth retardation or chlorosis. The nutrient solution was replaced once a week. Seedlings were grown for 3 weeks in hydroponics before treatment. Then untreated plants (control) were maintained on 10 µM Fe(III)-EDTA for 2 additional weeks, while the treated plants were subjected to one week of Fe depletion (Fe limited to 10 nM Fe(III)-EDTA), followed by one week of Fe resupply (restored to 10 µM Fe(III)-EDTA). Pilot experiments had shown that all the Fe-deficiency symptoms were reversible with one week of Fe-resupply albeit that the plants that had been subjected to depletion lagged in size. To obtain enough biological material we grew 32 plants per hydroponics container. For each experiment, five containers were started, two for deficiency treatment, two for control; with an extra container to replace plants whose roots had sustained damage during transfer from agar media. Data are reported for plants from 8 different hydroponics experiments which passed quality control by visual inspection and chlorophyll fluorescence imaging that was utilized as a non-invasive method to assess plant health and Fe-deficiency.

For shoot material, 3 whole rosettes were pooled as a unique sample. For one root material sample, the entire root system from 3 plants was pooled. Material for molecular analyses was immediately frozen in liquid nitrogen, and stored frozen until further analysis. Samples from both treated and untreated plants were collected at day 0 (before treatment), after 2, 4 and 7 days (Fe-depetion period), and at day 9, 11 and 14 (Fe-resupply period). All sampling was at 2h after the start of the light period.

Elemental Analysis. Rosettes were dried for a week at 55°C. Fifty mg of homogenized dried tissue was digested in 1 mL of nitric acid and heated for 2 h at 60°C and for 6 h at 130°C. Resulting digests were diluted up to 10 mL with di-deionized water and analyzed using inductively coupled plasma-atomic emission spectrometry (ICP-AES) as described (Ravet *et al.*, 2011).

Chlorophyll, Leaf Area Determination and Gas Exchange Measurements. Total chlorophyll was extracted from frozen tissue and chlorophyll a and b concentrations were determined using absorbance at 662 nm and 645 nm as previously described (Porra *et al.*, 1989). Leaf area was measured with a conveyor belt system attached to the LI-3050C in RealTime Capture mode (Li-Cor, Inc., Lincoln, NE). Measurements were made using electronic rectangular approximation with $1mm^2$ resolution. Gas exchange measurements were obtained using a LI-6400 portable photosynthesis system (Li-Cor, Inc., Lincoln, NE, USA) with a custom-built cuvette that enclosed the whole rosette of *Arabidopsis* (Christman *et al.*, 2008). For daytime measurements, cuvette light intensity was at 350 μmol photons x m^{-2} x s^{-1}. CO_2 was maintained at 400 ppm. Temperature and RH in the gas exchange cuvette were set to ambient growth chamber conditions.

Chlorophyll Fluorescence and Redox State of P700 Analyses. Chlorophyll fluorescence images were captured at room temperature using a FluorCam (PSI, Brno, Chech republic) as described (Ravet *et al.*, 2011). Chlorophyll fluorescence numeric measurements were obtained using a FMS2 Fluorometer (Hansatech Instruments, Norfolk, UK). Plants were dark adapted for 30 min prior to analysis. PSII maximum capacity (F_V/F_M), efficiency of the PSII (ϕPSII) and Non-Photochemical Quenching (NPQ) were calculated according to Maxwell and Johnson (2000). Photo-oxidation/reduction of P700 was monitored in dark-adapted leaves at 22 °C as the light-induced absorbance change at 820nm (ΔA_{820}) using a Dual-PAM-100 P700 fluorometer (Walz, Effeltrich, Germany; Klughammer and Schreiber, 2008). The quantum yield of photochemical energy conversion Y(I), the quantum yield of non-photochemical energy conversion due to

donor side limitation Y(ND) and the quantum yield of non-photochemical energy conversion due to acceptor side limitation Y(NA), where Y(I) +Y(ND) + Y(NA) = 1, were calculated according to Klughammer and Schreiber (2008). Data shown are results from analyses conducted at a light intensity of 354 µmol photons m^{-2} s^{-1}.

Immunoblotting and Protein Quantitation. Soluble proteins for SDS-polyacrylamide gel analysis were extracted as described (Abdel-Ghany *et al.*, 2005). Protein concentration was determined according to Bradford (1976) using bovine serum albumin as a standard. For western blotting, 20 µg of total protein was separated by 10 to 15% SDS-PAGE and then transferred onto a nitrocellulose membrane. Each experiment was done at least in biological triplicate with identical results, and representative gels are shown. Quantification of the signals was performed as described (Ravet *el al.,* 2011) using calibration curves based on dilution series (1.5, 1, 0.75, 0.5, 0.25, 0) of control (untreated-day 7) samples. Signal intensity was determined using ImageJ software, and regression curves (R^2>0.9) were determined using SigmaPlot software (version 7.4; Systat Software). Information related to the antibodies used for immunodetection of the various proteins is listed in supplemental Table 2-1. In untreated plants, kept on sufficient Fe, all tested proteins were equally expressed over the time course of the experiments except for adenosine 5'-phosphosulfate reductase (APR), which increased slightly in abundance in older rosettes in the control plants (not shown).

mRNA Expression Analysis. Total RNA was extracted using the Trizol reagent (Life Technologies, Carlsbad, CA, USA) according to the manufacturer's recommendations. The RNA concentration of samples was determined using a Nanodrop Fluorospectrometer and quality was assessed by agarose electrophoresis of aliquots (Sambrook and Russell, 2001) before shipping RNA to the NanoStrings core facility. Gene expression was analyzed at the University of Arizona Genetics Core in Tucson, AZ by NanoString Technology (Geiss *et al.*, 2008). RNA quality was further assessed by analyzing a 1:10 dilution of each total RNA sample in a Fragment Analyzer, which determines the quality by the ratio and resolution of the large and

small rRNA peaks (https://www.aati-us.com/instruments/fragment-analyzer/). In a multiplexed gene expression analysis, 100ng of total RNA was hybridized to reporter probes and capture probes specific to each gene target (Supplemental Table 2-1). Following purification and binding of the hybridized probes to the optical cartridge, the cartridge was scanned on the nCounter Digital Analyzer. *SAND*, *EF1a, UBIQUITIN11* and *ACTIN2* were used as potential reference genes. The *SAND* and *EF1a* mRNA levels varied with treatment at day 4 of treatment whereas the transcripts for *UBIQUITIN11* and *ACTIN2* were stable under Fe deficiency and therefore the latter two were used for normalization. Raw counts for each individual gene were imported into the nSolver Analysis Software 3.0 and were normalized against background and the two reference genes.

Statistical Analysis. JMP software (version 9.0.2; SAS Institute) was used for statistical analysis. Figures and data represent average and SD values based on sampling from at least three independent biological replicates. The number of total samples (n) is given when appropriate. Student's *t* test was used to calculate significant differences (p-value<0.05). Statistical analysis of gene expression was performed in R (version 3.3.3), using the lsmeans and plyr packages. A one-way ANOVA was used to compare treated and control plants for each day, using pair wise comparisons. p-values <0.05 were considered significant comparisons and are indicated in figures.

2.4 RESULTS

Experimental design and characterization of Fe deficiency symptoms in Arabidopsis rosettes

We established hydroponic growth conditions to analyze progressive changes in the vegetative shoot in response to one week of low Fe availability followed by resupply (see Figure 2-1A). As expected, lowering Fe from 10 µM Fe-EDTA in the nutrient solution to 10 nM Fe-EDTA resulted in a strong decrease in Fe content in plant rosettes measured after 7 days (Figure 2-1B). A significant decrease in shoot Fe content was measured as soon as 2 days after

Fe limitation and became more pronounced after 4 and 7 days (Figure 2-1C). For the Fe resupply treatment, Fe in the medium was restored to 10 µM Fe-EDTA, seven days after the initiation of the deficiency treatment (Figure 2-1A). This resupply led to a rise of Fe levels in the rosette which reached control levels after only 4 days of Fe resupply (Figure 2-1C). Among the other elements analyzed, only the levels of sulfur (S) and manganese (Mn) showed significant alterations (Figure 2-1B). The reduction in the Mn content in shoot tissues correlated with the evolution of Fe levels, albeit that the decrease of Mn was not yet significant after 2 days of Fe depletion (Figure 2-1C). An increase in S content in shoots was observed after 7 days of Fe-deficiency and the S levels remained high after plants had recovered from the Fe-depletion, while Fe and Mn were back to control levels at that time (Figure 2-1C). Expression analysis for the Fe status markers ferritin (Petit *et al.*, 2001; Ravet *et al.*, 2009) and IRT1 (Vert *et al.*, 2002; Seguela *et al.*, 2008) indicated that the Fe deficiency response was induced upon depletion and that plants returned to normal Fe status with resupply within a week (supplementary Figure 2-1). As expected, the loss of Fe content during depletion was accompanied by the appearance of chlorosis due to a drop in chlorophyll content, mainly in the young developing leaves of treated plants (Figure 2-2A, B). Importantly, upon Fe resupply plants were able to fully recover their chlorophyll content (Figure 2-2A, B). Furthermore leaf morphology was normal indicating that the visible symptoms of deficiency were fully reversible with resupply (Figure 2-2A). Typical of Fe depletion, treated plants had decreased total rosette biomass (Figure 2-2C) and lagged in primary root growth (S. Figure 2-2). Although Fe deficient plants quickly recovered after resupply, the Fe deficiency treatment caused a delay in growth and development (Figures 2-2A, 2C).

Fe deficiency has strong impact on light-dependent carbon assimilation

Carbon assimilation and release were measured to get estimates for net photosynthetic capacity in the light and dark respiration. The net CO_2 assimilation rate per leaf area in the light was reduced by about 50% in Fe-deficient leaves after 7 days of treatment, while CO_2 release was only slightly, but not significantly, affected in the dark (Figure 2-3). These observations suggest that maintenance of mitochondrial respiration activity may be prioritized over photosynthesis when Fe becomes limiting. Seven days after Fe-resupply, the net CO_2 assimilation rates were no longer different between treated and control plants (not shown).

Fe-deficiency affects photosynthetic electron transport primarily in the younger leaves.

The strong effect of Fe depletion on carbon assimilation led us to investigate the light reactions of photosynthesis. In order to analyze the spatial distribution of photosynthesis-related symptoms caused by Fe depletion within the rosettes, we used a Fluorcam imaging system. (Figure 2-4A). The parameter ϕPSII (PSII efficiency) gives an indication for how much of the light energy absorbed by chlorophyll molecules is used to drive electron transport. The parameter NPQ estimates non-photochemical quenching in PSII antennae, which depends on acidification of the lumen and thus electron transport activity (Maxwell and Johnson, 2000). Compared to the controls, the Fe deficient plants had lower values for ϕPSII and NPQ throughout their rosettes with the strongest effects in the younger leaves (Figure 2-4A, left side). Importantly a week after Fe was resupplied to the plants, both these chlorophyll fluorescence parameters were again identical in control and treated plants, which indicates that the plants had fully recovered their photosynthetic electron transport (Figure 2-4A, right side).

Whereas the imaging system provides a spatial analysis of chlorophyll fluorescence, this setup could only reach an actinic light intensity of about 120 µmol photons m^{-2} s^{-1}, which is less than half the light intensity used to grow the plants and below the level where saturation of the

light reactions typically occurs (Maxwell and Johnson, 2000). Therefore, a FMS fluorometer was used for a more quantitative analysis of chlorophyll fluorescence (Figures 2-4B, C and D). Because the FMS clamp does not allow measurements on the smallest leaves, we conducted the measurements on intermediate leaves considering that these reflect a behavior representative of the entire rosette (Figure 2-4A). F_V/F_M was only slightly decreased by Fe deficiency (Figure 2-4B). This indicates that the majority of PSII centers are still functional after one week and that photoinhibition was minor. This observation was confirmed by Fluorcam measurements (not shown). Importantly, the F_V/F_M recovered with Fe resupply indicating that long-term damage to PSII was avoided (Figure 2-4B). The ΦPSII was measured over a range of light intensities, which showed a consistent trend where the Fe-depleted plants had reduced activity compared to the control plants. For simplicity, only the data obtained at an actinic light intensity close to what was used to grow plants are presented for ϕPSII (Figure 2-4C). ϕPSII is strongly affected by Fe deficiency but is also recovered rapidly upon Fe resupply (Figure 2-4C). Overall, the time course analysis of the ϕPSII over the depletion and resupply period (Figure 2-4C) mirrors the evolution of shoot Fe levels (Figure 2-1C). Because NPQ is induced by high light we chose to analyze the evolution of NPQ over the time course of depletion and resupply at a relatively high light intensity. (Figure 2-4D). The NPQ values strongly diminished after Fe levels dropped, indicative of a lack of electron transport and proton pumping. NPQ recovered with Fe resupply (Figure 2-4D).

To gain insight into how PSI was affected, changes in the redox state of the PSI were analyzed. The Y(I) parameter indicates the quantum yield of photochemical energy conversion in PSI (Klughammer and Schreiber, 2008) (Figure 2-4E). Y(I) was significantly diminished by Fe depletion (Figure 2-4E). In untreated plants, the PSI quantum yield was already limited by electron donors upstream of PSI and this limitation was exacerbated further by Fe depletion (Supplementary Figure 2-3).

In conclusion, the analyses of the light reactions suggest that PSII is only mildly affected by Fe deficiency (small changes in F_V/F_M) but that strong defects are seen in electron transport downstream of PSII. On the other hand, PSI function is strongly compromised by Fe-deficiency and this may be in large part because of upstream limitations. The observations thus suggest that Fe deficiency causes a backup in electron transport at the Fe containing cytochrome-*b_6f* complex which functions downstream of PSII and donates electrons to PSI via the copper protein plastocyanin.

Fe-deficiency triggers specific changes in the abundance of Fe-dependent chloroplast proteins and their transcripts

To study changes in the abundance of selected Fe- and photosynthesis-related chloroplast proteins over the time course of Fe depletion and Fe resupply we used quantitative immunoblotting (Figure 2-5). Fe deficiency caused a decrease in the abundance of several Fe binding proteins and affected all complexes of the electron transport chain (Figure 2-5A). However only mild effects were observed for the subunits of PSII. The three core subunits PSBA (D1 protein), PSBB and PSBC which harbor non-heme iron (Barber 2016) were reduced to 65-75% of control levels at 7 days of Fe depletion whereas no major change was noted before this time. No change was seen for the heme-binding protein PSBE (Figure 2-5A). PSI contains 12 iron atoms in three 4Fe-4S clusters bound by the PSaA, B and C subunits (Merchant and Sawaya, 2005). Surprisingly, the PSaA subunit of PSI, which carries the FeSx cluster, appeared to be slightly increased in abundance after Fe depletion (Figure 2-5A). PSAB and PSAC carry two 4Fe-4S clusters between them. These iron-binding PSI core proteins were only mildly affected by Fe depletion in our conditions (Figure 2-5A). However a stronger effect on protein levels was observed for PSAD, which mediates interactions between the PSI core and ferredoxin but does not bind Fe itself (Setif et al, 2002), and which was reduced to half of the control levels at day 7 of depletion. In comparison to the two photosystems, the effect of Fe

depletion was stronger and observed earlier for subunits of the cytochrome-*b_6/f* complex. The strong decrease in cytochrome-*f* and the [2Fe-2S]-Rieske proteins became evident at 2 days of depletion. NDHK, which is an Fe-S protein of the NDH complex that mediates cyclic electron flow was also affected. By far the strongest effect of Fe depletion was seen for ferredoxin (FDX). The major FDX2 isoform (Hanke et al, 2004) accumulated to only 8% of control levels and showed already very clear changes at day 2. All proteins that changed abundance in response to Fe returned to control levels with 7 days of Fe resupply. The two iron-independent electron carriers, plastocyanin and FNR, were not affected by iron treatment, indicating that Fe deficiency does not affect all ETR components.

The di-iron enzyme chlorophyll cyclase (CRD1/CHl27) which is required for chlorophyll synthesis (Tottey *et al.*, 2003; Bang *et al.*, 2008), was affected by Fe depletion with about 60% of the protein left after 7 days of deletion (Figure 2-5A), which matches chlorophyll levels (Figure 2-2B). Similar down-regulation was observed for 7-Hydroxymethyl Chlorophyll a Reductase (HCAR) a FeS cluster enzyme required for chlorophyll a formation (not shown). However, most of the chlorophyll binding LHC proteins that we could detect were unaffected by Fe depletion with the exception of LHCA2 and LHCA3 which showed significant lower abundance at day 7 (Figure 2-5A).

In summary, the analysis of proteins involved in the light reactions indicate that Fe deficiency triggers a large drop in ferredoxin abundance followed by a progressive loss of cytochrome-*b_6/f* complex components. These changes can help explain the loss of photosynthetic electron transport. In comparison PSI and PSII and associated LHCs are less affected.

No changes were observed for the abundance of RuBisCO (C fixation) and the chloroplastic glutamate 2 oxoglutarate aminotransferase, a 3Fe-4S enzyme (GOGAT, N assimilation). By contrast, the abundance of two key proteins for S assimilation, adenosine 5'-phosphosulfate reductase (APR) a Fe-S protein and sulfite reductase (SIR) a heme and Fe-S

cluster protein, was strongly decreased. Fe depletion had minor effects on the major chloroplast Fe- superoxide dismutase FSD1 and Cu/Zn-superoxide dismutases CSD1 (cytosol) and CSD2 (chloroplast). Two plastid lipopoxygenases that are non-heme iron proteins were also unaffected (Figure 2-5C).

Two major Fe cofactor types are Fe-S clusters and heme. Fe-S clusters for plastidial proteins are synthesized from Fe and sulfide within the chloroplast by the SUF system (Balk and Pilon, 2011). Strikingly, two of the FeS assembly system components SUFA and SUFB, were strongly reduced in abundance (-50%) (Figure 2-5D). Sulfide of FeS clusters originates from desulfurization of cysteine. This is achieved in plant plastids by the cysteine desulfurase NFS2, which is activated by SUFE1 (Pilon-Smits *et al.*, 2002; Ye *et al.*, 2006). Both NFS2 and SUFE1 remained unaffected by Fe depletion. Similarly the putative FeS scaffold HCF101 was also not affected. Heme synthesis requires ferrochelatase (FC) to incorporate Fe into the porphyrin structure (Cornah *et al.*, 2003). Strikingly, FC protein levels were maintained during the Fe depletion (Figure 2-5D).

COX2, which is a core subunit of mitochondrial cytochrome-*c* oxidase, a heme- and Cu-containing complex, was not affected in abundance by Fe depletion. Similarly, the mitochondrial di-iron protein alternative oxidase (AOX) was also not affected (Figure 2-5E). However, strongly affected by Fe depletion were the cytosolic proteins Aconitase1 (ACO1, 4Fe-4S cofactor), xanthine dehydrogenase (XDH1, 2Fe-2S cofactor) as well as heme-containing cAPX (Figure 2-5E). However, the cytosolic nitrate reductase (NR), which also carries heme, did not change in abundance. We tested NBP35, a component of the cytosolic Fe-S biosynthesis machinery (Bych *et al.*, 2008) but we did not observe an effect of the Fe treatment on its abundance (Figure 2-5E). Catalase, a major peroxisomal Fe protein was maintained during Fe deficiency (Figure 2-5E).

We used NanoString Technology for transcript analysis (Figure 2-6) because it can measure transcripts of both nuclear and plastid encoded genes, it is suitable for measurements

with multiple time points with low variability between biological replicates and good dynamic range (Malkov *et al.*, 2009; Veldman-Jones *et al.*, 2015). In our set of genes for interrogation we included the mRNA for all proteins that had shown a change in response to Fe deficiency (Figure 2-5). Multiple isoforms were tested when appropriate. We complemented our list with genes encoding major Fe binding protein subunits and known Fe homeostasis factors for which antibodies are lacking. A complete list of target genes is presented in Supplementary Table 2-1.

The transcript abundance of each gene after 2, 4 or 7 days of Fe deficiency was plotted using a $\log_2$ scale against its control value (Figure 2-6 panels A, B, C). Unaffected transcripts remained on the diagonal, transcripts with lower expression after deficiency fall bellow the diagonal whereas up-regulated transcripts are above. Abundance under control conditions increases to the right in the plots. As expected, after two days of iron deficiency, *FER1* expression was decreased while *PYE*, *BHLH38* and *BHLH100*, markers for plant Fe deficiency (Long *et al.*, 2010; Sivitz *et al.*, 2012), were up-regulated. Generally a good correlation was observed between protein and mRNA abundance. For proteins that did not change in abundance such as chloroplast encoded *PSAA* and *PSAB*, the corresponding transcript levels were also stable. In some cases (*AOX1*, *CSD1*) we noted a slight increase in transcript abundance late in the deficiency treatment. Conversely, a decrease in protein level was generally accompanied by a lower transcript level also. There were, however, noticeable exceptions. Whereas SUFA, APR2 (the major APR isoform) and ACO1 proteins showed much lower accumulation at the protein levels under Fe-depletion, the transcripts for these genes did not diminish over the course of 7 days. It is also noteworthy that transcripts encoding proteins proposed to be involved in Fe transport over the plastid envelope (*PIC1, FRO6, FRO7, YSL4, YSL6*) showed small, statistically not significant, changes after Fe depletion.

Strikingly, among the Fe-related components tested at the transcript level only *SUFB* and *FDX2* were decreased significantly in Fe starved plants compared to control at 2 days after Fe depletion (Figure 2-6A; S. Figure 2-4). For *sAPX* a trend towards reduced transcript

accumulation was already seen at day 2 but it was yet not significantly different from the control (S. Figure 2-4). Transcripts for *SUFB, FDX2* and *sAPX* remained low over the one-week Fe depletion. After 4 and 7 days, many additional genes showed reductions in transcript levels in treated vs. control plants, including both chloroplastic and cytosolic transcripts encoding abundant subunits of the photosynthetic machinery (Figure 2-6C). *PSAA* and *PSAB* transcripts however were unchanged (Figure 2-6C), consistent with protein levels. *SIR* expression was reduced by Fe depletion, but in contrast the transcript for nitrite reductase (*NIR*), which carries the same Fe-S siroheme cofactor was not affected (Figure 2-6). Some of the transcripts such as *CSD1*, *AOX1* and *ACO1* appeared to become up-regulated towards the end of the deficiency treatment.

2.5 DISCUSSION

Responses to low Fe target specific chloroplast functions progressively

The main effects on Fe-related chloroplast proteins are summarized in supplementary figure 2-5. It can be envisioned that Fe deficiency causes a loss of Fe proteins due to lack of cofactor availability, but in addition the Fe proteome can be affected by the regulation of gene expression. The data presented in figures 2-5 and 2-6 indicate that during Fe deficiency specific abundant Fe proteins of the chloroplast such as ferredoxin and the cytochrome-b_6f complex are targeted for down-regulation at the transcript level which has consequences for photosynthesis and other chloroplast metabolism. There are therefore priorities in the regulation of protein and transcript levels in response to low Fe. The implication is that novel, thus far unrecognized regulatory circuits to regulate Fe economy must exist and that Fe protein abundance is not just controlled passively by cofactor availability. This regulation of Fe utilization in green tissue has not been studied in detail in plants before. We propose that Fe economy is an important mechanism to cope with impending Fe deficiency and functions in concert to the up-regulation of root Fe uptake and the adjustment of metabolism (Lopez-Millan *et al*., 2013)

The symptoms observed in Arabidopsis within the first seven days of Fe-depletion treatment were almost all fully reversible with resupply of iron (Figures 2-1, 2-2, 2-4, 2-5). It is thus likely that secondary and irreversible damage was avoided in the depletion protocol, especially in the first days. Therefore, the changes at the molecular level after the onset of Fe-depletion (Figure 2-5 and Figure 2-6), especially the earlier events, are likely to reflect programmed responses which could help the plant to acclimate to a temporary lack of iron.

The Fe depletion treatment affected photosynthesis, especially in the younger leaves, much more than respiration albeit that photosynthesis was not completely blocked, even after 7 days (Figure 2-4). Chloroplast Fe proteins and their transcripts were among the most affected while generally milder effects were seen for the mitochondrial Fe proteins (Figure 2-5 and Figure 2-6). Several cytosolic proteins were also affected (Figure 2-5E) but transcripts for these were mostly stable relative to transcripts for chloroplast proteins, which dominated the pool of differentially regulated genes (Figure 2-6). These observations may be taken as an indication that photosynthesis is more dispensable under Fe deficiency compared to respiration, which also has a strong demand for Fe (Balk and Schaedler, 2014). However, the effect of Fe depletion on the abundance of Fe proteins of the chloroplast was not uniform. For instance, plastid enzymes involved in S assimilation (APR and SIR) were strongly affected whereas expression of the N assimilation enzymes plastid GOGAT (plastid), nitrite reductase (NIR, plastid), and nitrate reductase (NR cytosol) seemed to be less affected (Figure 2-5 and Figure 2-6).

For practical reasons, protein and mRNA levels were analyzed in the entire rosette. It is possible that protein and mRNA was more affected in the youngest leaves, which showed the strongest physiological response. However, the timing of effects also varied for different genes and the temporal analysis of gene expression was especially useful in discerning early and later responses (S. Figure 2-4). Lowering Fe in the media resulted in a measurable reduction in shoot Fe levels after 2 days when other elements and physiological parameters were not significantly

changed yet. Nevertheless, already at day 2 on the molecular level, a clear and notable reduction in the accumulation of the SUFB and leaf ferredoxin (FDX) proteins was observed which was also accompanied by a reduction in transcript levels. These observations suggest that down-regulation of FDX, a 2Fe-2S protein, and SUFB a factor required for all plastid FeS synthesis is a priority under Fe deficiency in the vegetative shoot.

Chlorophyll levels and photosynthetic electron transport parameters became significantly affected at 4 days of depletion, when symptoms had become more severe, and remained low until after Fe resupply. Most light harvesting complex proteins were mildly affected by Fe depletion which agrees with previously reported effects of Fe depletion on thylakoid proteomes (Laganowsky *et al.*, 2009). Exceptions were LHCA2 and LHCA3, which also showed transcriptional regulation. The latter may reflect a remodeling of the PSI antennae to adjust low Fe (Laganowsky *et al.*, 2009; Rodríguez-Celma *et al.*, 2014) as has also been suggested for Chlamydomonas cells depleted of Fe (Moseley *et al.*, 2002). Of the Fe proteins in the major complexes of the photosynthetic electron transport chain the subunits of the cytochrome-b_6f complex were most affected, more than the Fe binding subunits of PSI, while minor damage and no transcriptional down-regulation was observed in PSII as a result of Fe depletion.

Iron sparing in chloroplasts targets abundant Fe proteins.

By far the largest loss in protein abundance was observed for ferredoxin, especially for FDX2 (see S. Figure 2-5). Does the down-regulation of *FDX2* make sense in the context of Fe economy? In regard to this question it is of interest to see if photosynthesis-related symptoms of Fe-deficiency resemble published phenotypes of ferredoxin mutants (Hanke *et al*., 2008; Voss *et al*., 2011; Liu *et al*., 2013). There are several FDX isoforms in Arabidopsis (Hanke et al., 2004). Due to the possible partial redundancy of ferredoxin isoforms, mutants in *FDX2* show mild phenotypes (Hanke *et al*., 2008; Voss *et al*., 2011). This may also explain why in iron deficiency we see FDX2 protein decrease early (day 2) but we do not see effects on

photosynthesis until later (day 4) when also the cytochrome-*b*$_6$*f* complex and to a lesser extend PSI and the NDHK subunit of the NDH complex become affected. Even at 7 days of deficiency when FDX protein levels had dropped by ~90%, was photosynthetic electron transport still at about 50% of capacity compared to control Fe replete conditions. FDX2 comprises roughly 90% of the ferredoxin protein in green tissue (Hanke *et al.*, 2004) and the transcript analysis indicates that *FDX2* is the most abundant nuclear encoded mRNA for an Fe protein (Figure 2-6). FDX is a 2Fe-2S protein and its down-regulation thus will have a relatively large effect on Fe quota. Because FDX proteins seem to accumulate in excess in replete conditions, down-regulation of *FDX2* seems to be an efficient way to economize Fe utilization.

How do the symptoms of Fe deficiency compare to electron transport phenotypes of FDX mutants? Genetic loss of FDX2 is reported to result in mild phenotypes and affected mainly photoreduction of NADP, while cyclic electron flow via the less abundant FDX1 isoform or alternative Fe-S proteins may help maintain NPQ in FDX2 mutants (Voss *et al*., 2011; Liu *et al*., 2013). Chlorophyll fluorescence measurements indicated that both ϕPSII, which is indicative of linear electron flow, and NPQ, which depends on both linear and cyclic electron flow (Maxwell and Johnson, 2000), are affected by Fe deficiency. The observed lower NPQ in Fe deficiency is expected in view of the observed loss in abundance of not only ferredoxin, but also cytochrome-*b*$_6$*f* complex subunits and a subunit of the NDH complex, which are all required for both linear and cyclic electron flow and therefore induction of NPQ.

The 2nd most abundant nucleus-encoded transcript for an Fe protein is PETC (Figure 2-6) which encodes for the Rieske 2Fe-2S-binding subunit of the cytochrome-*b*$_6$*f* complex. Rieske protein was also strongly down-regulated, which involved transcript abundance changes, albeit that this occurred later than for FDX. It is interesting that the two heme containing and chloroplast-encoded subunits of the cytochrome-*b*$_6$*f* complex, Cyt*f* and Cyt*b*$_6$ also undergo transcriptional down-regulation. The dimeric cytochrome-*b*$_6$*f* complex is reported to contain 12 Fe atoms, the same number as is present in PSI (Merchant and Sawaya, 2005). Apparently,

under impending Fe deficiency, down-regulation of the cytochrome-b_6f complex is preferred over removal of PSI for which the core subunits are chloroplast encoded and for which the transcripts have an abundance comparable to the cytochrome-b_6f complex subunits. However, the nucleus encoded PSAD subunit, which does not itself bind Fe, was strongly down-regulated in coordination with FDX, for which it contributes to the docking site on PSI.

It is of interest to place our findings in the context of studies that have reported on the general effects of Fe deficiency on chlorophyll synthesis and photosynthesis which have been well documented in the literature (Spiller and Terry, 1980; Andaluz *et al.*, 2006; Nishio and Terry, 1983; Nishio *et al.*, 1985; Sharma, 2007; Timperio *et al.*, 2007;Laganowski *et al.*, 2009; Msilini *et al.*, 2011; Ciaffi *et al.*, 2013; Paolacci *et al.*, 2014; Rodríguez-Celma *et al.*, 2014). Some studies on Fe depletion in plants had reported that PSI was the major target of Fe deficiency (Nishio *et al.*, 1985; Timperio *et al.*, 2007) whereas we saw a major effect on the cytochrome-b_6f complex and less on PSI. The severity of the applied Fe deficiency, differences in light conditions, and the use of different species, may all help determine if PSI or the cytochrome-b_6f complex is more affected. Our data are consistent, however, with a study on the effects of mild Fe deficiency in hydroponics on the thylakoid proteome of Arabidopsis (Lagonowsky *et al.*, 2009). In Chlamydomonas*,* Fe deficiency activates a genetic program in which remodeling of pigment binding proteins associated with PSI occurs (Moseley *et al.*, 2002). Furthermore, in Chlamydomonas maintenance of respiration is favored over photosynthesis in the chloroplast (Terauchi *et al.*, 2010). Within the Chlamydomonas chloroplast abundant Fe proteins such as ferredoxin and cytochrome-*f* were strongly diminished by Fe deficiency (Page *et al.*, 2012), similar to what we found in Arabidopsis. However, in Chlamydomonas FeSOD was maintained and even up-regulated under deficiency (Page *et al.*, 2012) but this is not the case in Arabidopsis (Figure 2-6) where the major control over FSD1 expression depends on Cu levels and is mediated via the SPL7 transcription factor (Yamasaki *et al.*, 2009).

In order to start to uncover potential mechanisms of Fe economy, we have focused our studies on major Fe proteins of the chloroplast. Untargeted proteomics approaches, as first pioneered with wild-type tomatoes and cloronerva mutans, which lack the metal-chelating nicotianamine molecule (Herbik *et al*., 1996), have the potential to uncover other mechanisms of acclimation to low Fe such as the adjustment of metabolism. A number of studies in various species have investigated the proteome changes after iron deficiency, the majority focusing on the root proteomic response (for a review see Lopez- Millan *et al*., 2013). What can be found in proteomic studies will depend heavily on the experimental protocol and the methods used to fractionate samples and detect proteins even if the same plant species is used. For example, it is not surprising that studies in Arabidopsis aimed to detect changes upon low Fe treatment in either the thylakoid proteome (Laganowsky *et al.,* 2009) or the root phosphoproteome (Lan *et al.,* 2012) upon low Fe treatment show no overlap. Proteomic studies can however help reveal specific responses that might help plants to acclimate to low Fe by adjustments of metabolism (Lopez- Millan *et al*., 2013). In general, proteomic studies have shown changes in protein abundance of oxidative stress response related proteins such as increases in CuZnSOD, MnSOD, peroxidase, and a decrease in catalase (Lopez- Millan *et al*., 2013). However, proteomic studies on tomato leaves showed a decrease in CuZnSOD and an increase in cytosolic ascorbate peroxidase with Fe depletion (Herbik *et al*., 1996). The present study shows little effect of iron deficiency on CuZnSODs or cytosolic ascorbate peroxidase, which might be because the Fe limitation was mild and reversible.

Effects of Fe deficiency on plastid Fe-S assembly and S metabolism.

Two members of the chloroplast Fe-S assembly system, SUFA and SUFB were strongly affected by Fe depletion. SUFB is a key component of the plastid SUF-BCD complex which functions as a scaffold required for the assembly of all plastid Fe-S clusters (Hu *et al.*, 2017b). Down-regulation of SUFB in Fe deficiency had been reported but only at the transcript level, both in Arabidopsis grown on agar media (Xu *et al.*, 2005; Sivitz *et al.*, 2012; Rodriquez Celma

et al., 2014) and in rice (Liang *et al.*, 2014). The now observed very early down-regulation of SUFB protein and transcript (Figure 2-5, Figure 2-6, S. Figure 2-4) when other Fe deficiency symptoms are still mild suggests that SUFB may play a special role in the acclimation to low iron. SUFB is also unique in its regulation in mycobacteria where SUFB protein activity is regulated via an intein, a self-cleaving peptide sequence inserted into the polypeptide (Huet *et al.*, 2006; Topilina *et al.*, 2015). Furthermore, in apicomplexan parasites, *SufB* is the only *suf* component of the apicoplast (plastid) that is encoded within the small apicoplast genome (Lim and McFadden 2010) which may allow for regulation of *SufB* in response to local conditions within the organelle. SufB and SufC are the evolutionary most ancient core of the Fe-S system (Boyd *et al.*, 2014) and it is likely that the first association of iron and sulfur requires SufB (Balk and Pilon, 2011). In the absence of sufficient Fe the risk of forming incomplete clusters may have to be avoided in order to prevent oxidative damage via Fenton chemistry.

The protein abundance of the putative SUFA/CpIscA Fe-S carrier was lower after Fe-deficiency whereas the transcript was not affected. It is possible that for this protein a lack of cofactor causes instability of the resulting apoprotein. A similar mechanism may apply to the FeS enzyme APR. For SUFA/CpIscA it had been observed that the protein is also reduced in abundance in mutants for *nfu2*, a potential scaffold or transfer protein in the plastid Fe-S assembly pathway (Yabe and Nakai, 2006). The chloroplast cysteine desulfurase NFS2 may also be required for other S-dependent cofactor synthesis pathways, which are likely important to maintain (Pilon-Smits and Pilon, 2005) which may be why NFS2 was maintained with Fe deficiency together with its SUFE1 and SUFE3 partners. It is possible that plastid heme synthesis remains required for other cellular compartments (Tanaka *et al.*, 2011; Balk and Schaedler, 2014) which could be why ferrochelatase protein was not affected by Fe depletion.

Two key chloroplastic enzymes of the S reduction pathway, APR and SIR, were strongly affected by Fe depletion. The rapid loss of APR may help prevent the accumulation of toxic sulfite in the absence of sufficient SIR activity. Together a lack of APR and SIR should result in

lower levels of reduced sulfur compounds including glutathione. Lack of reduced sulfur compounds should cause up-regulation of plant sulfate uptake which explains the higher S content after Fe deficiency (Koprivova and Kopriva, 2014); indeed Fe deficiency was shown to increase S uptake capacity in tomato and wheat (Ciaffi *et al.*, 2013; Zuchi *et al.*, 2015)

In plant shoots, micronutrient economy, the idea that certain proteins under deficiency are preferred targets for down-regulation to benefit cofactor delivery to other essential functions is documented for Cu (Burkhead *et al.*, 2009) and Zn (Li *et al.*, 2013). The down-regulation at the transcript level of abundant Fe proteins, coordinated with the SUFB key factor of the Fe-S assembly system, should help to safely economize and perhaps prioritize Fe during Fe deficiency.

Iron economy involves specific response programs.

The transcriptional responses are specific. For instance, the transcript for SIR is down-regulated by low Fe, but the transcript for NIR, which carries the same Fe-S siroheme cofactor, is not. Therefore, at least some of the observed effects seem to be caused by Fe-deficiency proper and not just by downstream defects due to lack of cofactor assembly. We can also compare consequences of Fe deficiency at the molecular level with effects caused by genetically induced loss of Fe-S assembly factors NFS2 (Van Hoewyk *et al.*, 2007) and SUF-BCD (Hu *et al.*, 2017a; Hu *et al.*, 2017b). Loss via RNAi of NFS2 activity (Van Hoewyk *et al.*, 2007) or SUF-BCD activity (Hu *et al.*, 2017b) caused after one-week physiological effects that are very similar to the Fe deficiency described here (Fig 1, 3, 4). RNAi lines induced for loss of NFS2 or SUFBCD complex components had shown a general loss of all Fe-S proteins including strong effects on PSI subunits PSAA, and PSAB and on GOGAT (Van Hoewyk *et al.*, 2007; Hu *et al.*, 2017b). However, we did not see this general loss of plastid Fe-S cluster proteins for Fe deficiency. Conversely, whereas we noted down-regulation of the heme containing subunits of the cytochrome-b_6f subunits together with PETC (Rieske protein) in Fe deficiency, the

genetically induced loss of SUFB, SUFC, or SUFD strongly affected Rieske protein but had marginal effects on CYTb_6 and CYT*f* protein accumulation (Hu *et al.*, 2017b).

Some of the late effects on transcript levels (Figure 2-6C) could be indirect however. Plastocyanin expression depends on active photosynthesis (Vorst *et al.*, 1993), which may be why we observed slightly lower transcript levels for the major PC2 isoform at day 7 of Fe depletion (Figure 2-6). After seven days of Fe depletion the major FeSOD, FSD1, was down-regulated at the transcript level and the cytosolic Cu/ZnSOD, CSD1, was up-regulated at the transcript level albeit that protein levels were not notably changed. FSD1 and CSD1 transcripts respond to Cu (Abdel-Ghany *et al.*, 2005, Yamasaki *et al.*, 2009), which might become more available when Fe is limited. Even if total shoot Cu levels did not change significantly, the lack of biomass formation could have shifted intracellular available Cu pools affecting FSD1 and CSD1 expression (Pilon, 2017).

An important implication of the specific regulation of chloroplast Fe proteins is that there has to be a mechanism of sensing the Fe status and to relay this signal. As expected, ferritin transcripts (*FER1, 3, 4*) were also down-regulated at 2 days after the start of low Fe treatment, similar to *SUFB* and *FDX2* (Figure 2-6). At the same time the transcripts for selected known low Fe markers *BHLH38*, *BHLH100* and *PYE* were up. FIT and PYE are major regulators of root Fe uptake (reviewed in Brumbarova *et al.*, 2015). PYE associates with similar BHLH transcription factors (Selote *et al.*, 2015). Four other BHLH transcription factors, BHLH38, BHLH39 BHLH100 and BHLH101 are Fe responsive (Wang *et al.*, 2007). BHLH100 and BHLH101 act separately from PYE and from BHLH38, BHLH39 and FIT which interact to mediate regulation of root Fe uptake (Yuan *et al.*, 2008) but all are implied in the regulation of Fe uptake or distribution between tissues (Long *et al.*, 2010, Sivitz *et al.*, 2012, Selote *et al.*, 2015). The bHLH family of transcription factor thus plays an important role in Fe homeostasis. Lack of whole plant Fe uptake or lack of Fe allocation to the shoot as observed with mutants for PYE, FIT and BHLH100 and BHLH101 caused stronger Fe deficiency for shoots. Indeed in an experiment on

agar media with a BHLH100/101 double-mutant the down-regulation of low Fe responsive genes including FDX2 was stronger, not weaker, indicating exacerbated Fe depletion (Sivitz *et al.*, 2012). Therefore these bHLH transcription factors do not directly mediate the observed local down-regulation of photosynthetic Fe proteins and ferritin but other bHLH proteins might still be involved. Early changes in FDX2 and SUFB transcript and protein levels due to iron deficiency suggest transcript abundance regulation. We have analyzed the promoter regions of *SUFB* and *FDX2* for promoter motifs via the online tool, AthaMap (Steffens *et al.*, 2004). The *SUFB* promoter does not show any bHLH binding motifs, while the *FDX2* promoter shows only a very low probability of bHLH binding, with only one putative bHLH binding site. At this point the mechanism for sensing Fe-status in the plant shoot and the relay mechanism is unclear, as it is in Chlamydomonas (Blaby-Haas and Merchant, 2013). Knowing how the chloroplast Fe proteome responds locally gives a starting point for unraveling this important novel regulatory circuit in the future.

2.6 CONCLUSION

Fe depletion causes specific effects on the chloroplast Fe-proteome, with strong and early down-regulation of SUFB and Ferredoxin, followed by the cytochrome-b_6f complex. These changes affect photosynthesis. Importantly, these observations imply the existence of a hitherto undiscovered program that mediates Fe economy. The observations provide a foundation to investigate further the mechanisms by which Fe is sensed locally in photosynthetically active plant cells.

2.7 AUTHOR CONTRIBUTIONS

M.P. and K.R. conceived the research plans; K.R. did the pilot experiments; L.H. performed most of the physiological experiments and immunoblots with help from M.C. and supervision by K.R. and M.P.; G.K. did transcript analysis and finalized the experiments and

figures with supervision by M.P.; C.J. provided assistance with gas exchange measurements and M.C. and G.P. with PSI measurements; L.H., G.K., K.R. and M.P. analyzed the data; L.H., K.R. and G.K. drafted the first manuscript with contributions of all the authors; M.P. supervised the overall project and finalized the writing.

2.8 CONTRIBUTIONS

We thank Dr Daniel J. Kliebenstein, Dr Janneke Balk, Dr Catherine Curie, Dr Jean-Francois Briat, Dr Stanislas Kopriva, Dr Hisashi Ito, Dr Toshiharu Shikanai, and Dr Atsushi Sakamoto for providing us with antisera. We thank Dr. Ann Hess for advice with transcriptome analysis.

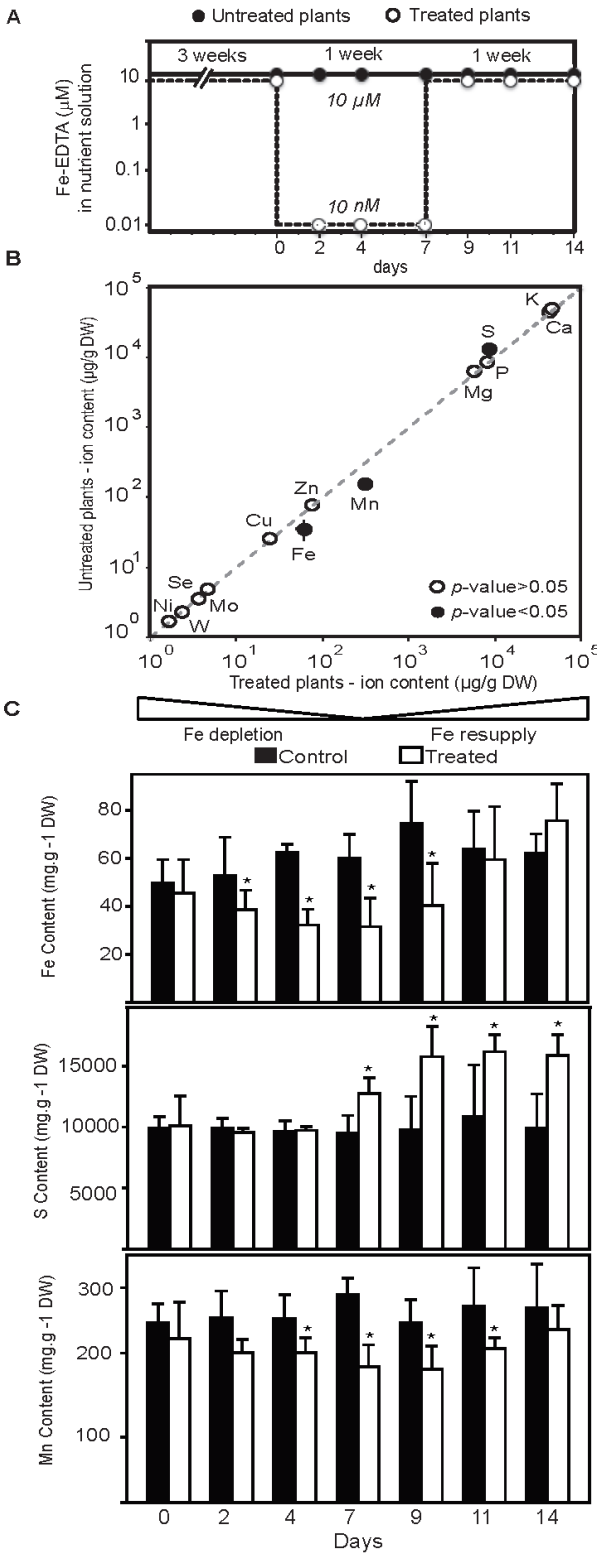

Figure 2-1: Experimental set up and elemental composition of *Arabidopsis* rosettes over the experimental time course. A, *Arabidopsis* plants were grown hydroponically on 10 µM Fe(III)EDTA for 3 weeks and then a subset of plants were transferred to 10 nM Fe(III)EDTA. After 1 week, the deficient plants were resupplied with 10 µM Fe(III)EDTA. Circles represent time points at which data was collected for untreated (black) and treated (white) plants. All analyses were completed before bolting, in order to avoid compounding effects of nutrient re-allocation during flowering and seed set. B, Ionome of untreated vs. treated plants at day 7. The elemental composition was compared in treated and untreated plants at day 7 (n=5-7). Concentration, as µg.g-1 dry weight (DW), of a given element in untreated plants was plotted against its concentration in treated plants. Black circles represent elements that differ significantly (p value <0.05) in treated plants compared to control. C, Changes in elemental content of Fe, S and Mn in *Arabidopsis* rosettes with time. Control (black) and treated (white) plants are compared at each time point in the study with statistical significance denoted by an asterisk (indicating that that treated plants differed from untreated plants on a given time point, p value <0.05; n=5).

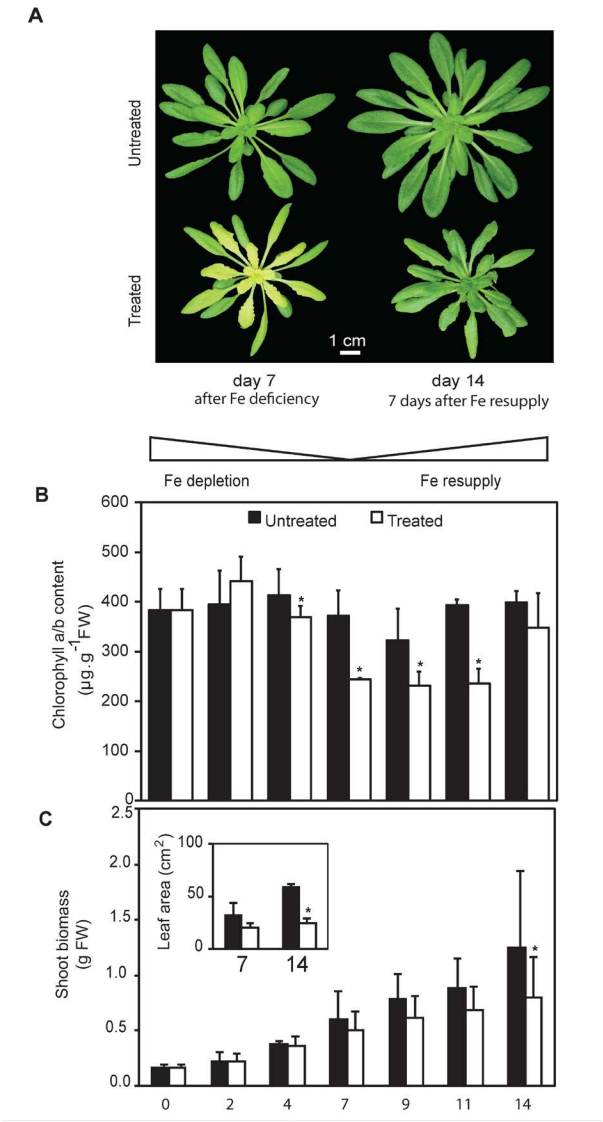

Figure 2-2: Symptoms of Fe deficient *Arabidopsis* and impacts on chlorophyll content and growth. A, Appearance of untreated (top) and treated (bottom) *Arabidopsis* plants. Representative plants were photographed at day 7 (left) and at day 14 (right). B, Total chlorophyll a/b content in Arabidopsis rosette. Values are given as averages ± SD (n = 10). FW, Fresh weight. C, Shoot biomass of *Arabidopsis* during iron deficiency and resupply. Growth of the shoot was monitored by measurement of rosette fresh weight. Values are given as averages ± SD (n = 15). Insert, total leaf area per plant for Fe-deficient plants (day 7) and Fe-resupplied (day 14) plants. Values are given as averages ± SD (n = 15). Black and white bars represent untreated and treated plants, respectively. Stars above bars represent significant differences (*p*-value<0.05) between untreated and treated plants for a given time point.

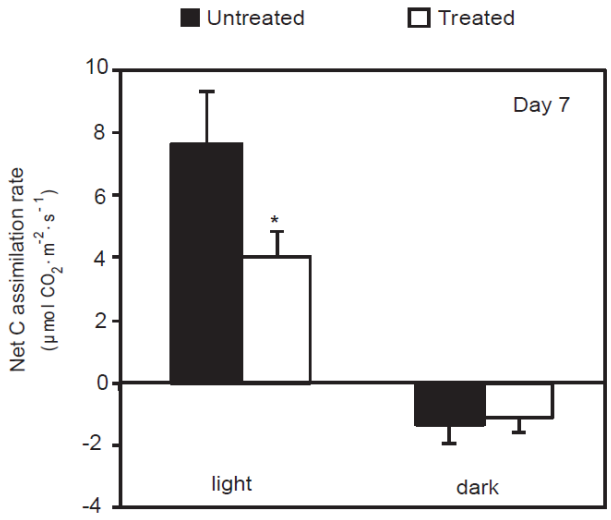

Figure 2-3: Fe-deficiency strongly affects photosynthetic CO_2 assimilation. Net C assimilation was determined in the light (350 μmol photons m^{-2} s^{-1}) and in darkness at the end of the Fe deficiency treatment (top, day 7) and 7 days after Fe was resupplied (bottom, day 14). Values are given as averages ± SD (n = 10). Black and white bars represent treated and control plants, respectively. Stars above bars represent significant differences (*p*-value<0.05) between untreated and treated plants for a given time point.

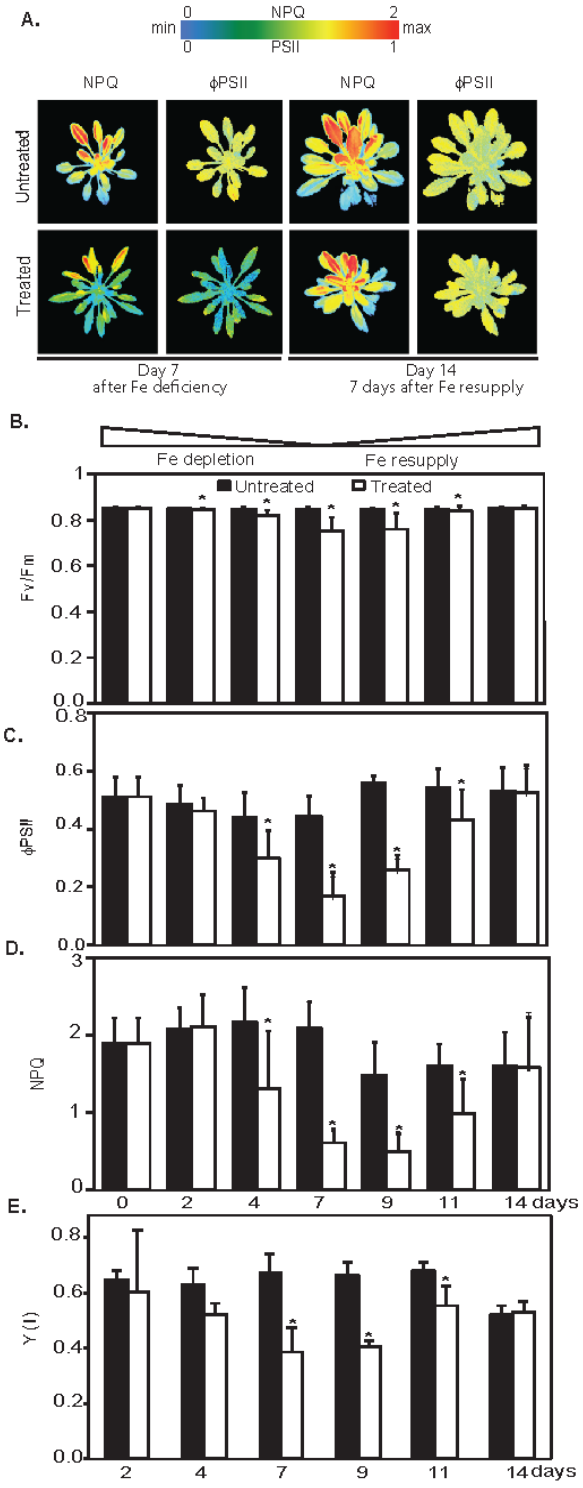

Figure 2-4: Fe-deficiency decreases electron transport though the photosynthetic apparatus, primarily in the younger leaves. A, The non-photochemical quenching (NPQ) and ΦPSII of Arabidopsis untreated (top) and treated plants (bottom). Representative false color chlorophyll fluorescence images are shown for day 7 (Fe deficient) and day 14 (Fe-resupplied) plants. B, C, D, Chlorophyll fluorescence parameters obtained using a FMS Hansatech system. B, F_V/F_m of dark-adapted plants. C, ΦPSII (PSII efficiency) measured at 250 µmol photons $m^{-2}.s^{-1}$. D, Non-Photochemical Quenching (NPQ) measured at 600 µmol photons $m^{-2}.s^{-1}$. E, Quantum yield of photochemical energy conversion Y(I). Photo-oxidation/reduction of P700 was monitored as the light-induced absorbance change at 820nm using a Dual-PAM-100 P700 fluorometer. All PSI parameters were measured over the time course of the treatment with the exception of day 0 because the intermediate leaves of the rosette at this time point were too small to fit in the Dual-PAM-100 leafclip used for the measurements. For panels B, C, D and E the values are given as averages ± SD (n = 6). Black and white bars represent untreated and treated plants, respectively. Stars above bars represent significant differences (*p*-value<0.05) between untreated and treated plants for a given time point.

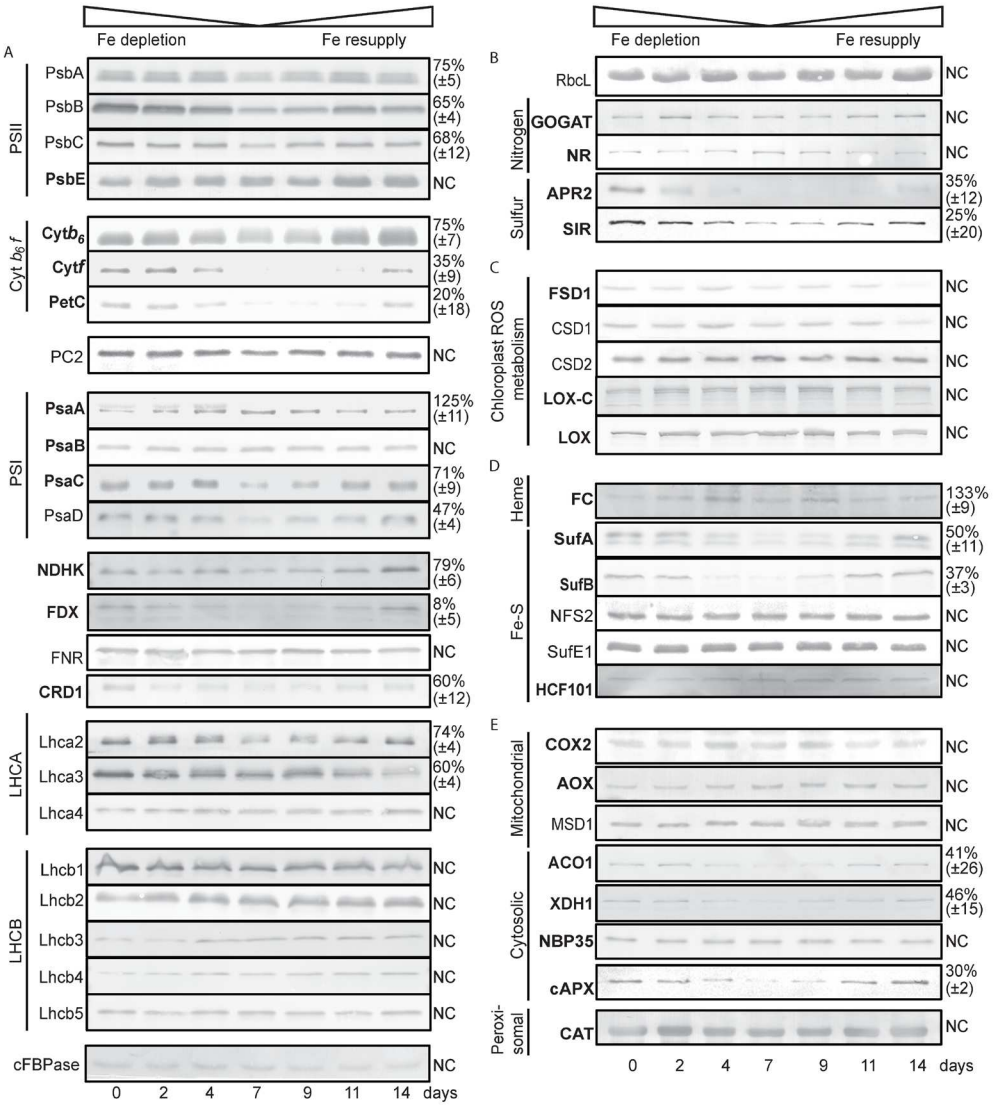

Figure 2-5: Impact of Fe-deficiency on the abundance of Fe-proteins in the *Arabidopsis* rosette. Total protein extracts (20 µg) from treated *Arabidopsis* rosette were fractionated by SDS-PAGE and blotted onto nitrocellulose membranes. The cytosolic fructose-1,6-bisphosphatase (cFBPase) was used as a loading control. Immunoblots are presented for A, proteins related to the photosynthetic light reactions, B, Chloroplast metabolism, C, Plastid ROS related proteins, D, Plastid Fe cofactor assembly, and E, Cytosolic, mitochondrial, and peroxisomal Fe related proteins. Protein name is denoted to the left of the immunoblot. Fe-binding proteins are in bold face. Shown are representative blots of at least 4 independent biological replicates. Immunoblots were quantified on day 7 comparing treated (low Fe) and untreated (control medium) plant samples. Numbers (right) represent the remaining amount of protein (as %) in Fe deficient plants (treated plants, day7) relative to controls (untreated, day 7) for significantly (p-value<0.05) affected proteins. For proteins that did not show a significant change, NC for “no change” is written to the right of the blot.

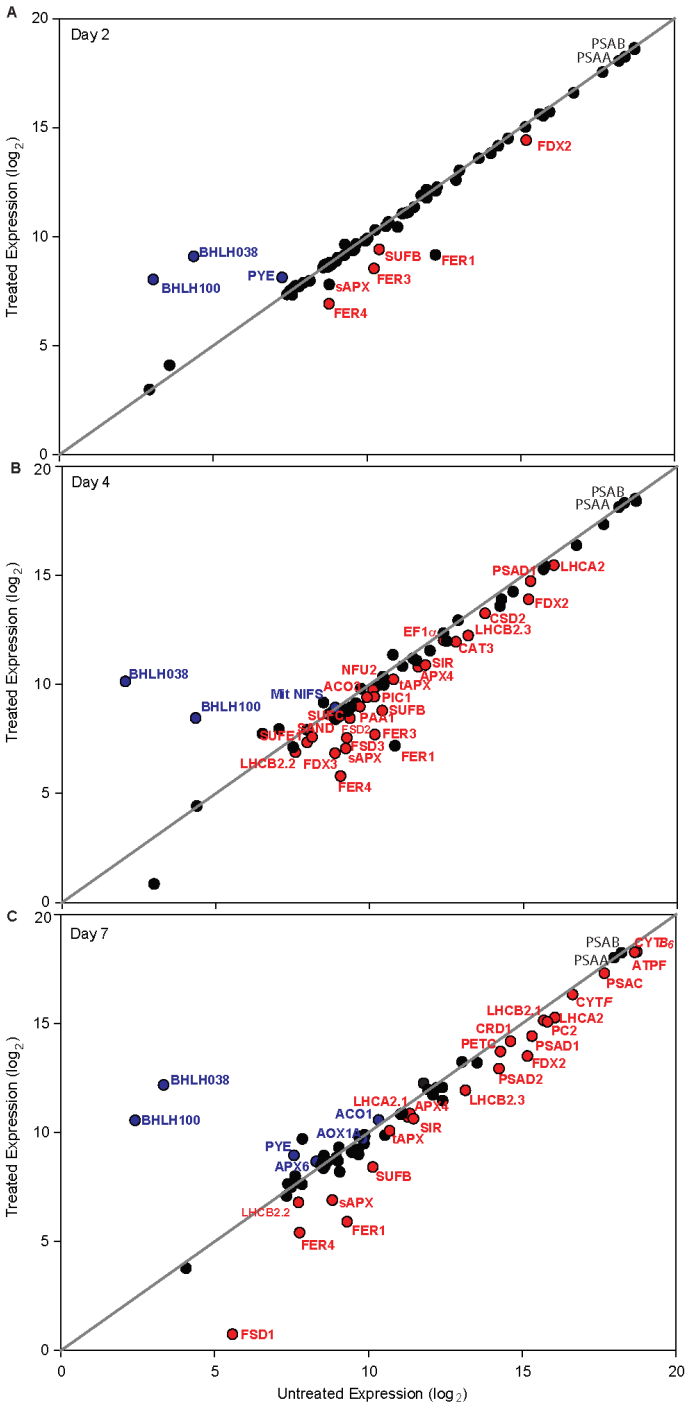

Figure 2-6: Impact of Fe-deficiency on the abundance of Fe related transcripts in the *Arabidopsis* rosette. Total leaf RNA was analyzed for transcript abundance with NanoString Technology. Normalized mRNA expression for treated and control plants is compared using a ^{2}log scale. *UBIQUITIN11* and *ACTIN2* were used for normalization. A, Day 2 after iron deficiency (n =4), B, Day 4 after iron deficiency (n =3), and C, Day 7 after iron deficiency (n=4). Black circles represent unchanged transcripts, red circles represent significantly decreased transcripts, and blue circles represent significantly increased transcripts (p value<0.05).

LITERATURE CITED

Abdel-Ghany SE, Müller-Moulé P, Niyogi KK, Pilon M, Shikanai T (2005a) Two P-Type ATPases Are Required for Copper Delivery in Arabidopsis thaliana Chloroplasts. Plant Cell 17: 1233-1251

Abdel-Ghany SE, Ye H, Garifullina GF, Zhang LH, Pilon- Smits EAH, Pilon M (2005b) Iron-sulfur cluster biogenesis in chloroplasts. Involvement of the scaffold protein CpIscA. Plant Physiology 138: 161-172

Andaluz S, Lopez-Millan A-F, De las Rivas J, Abadia J, Abadia A (2006) Proteomic profiles of thylakoid membranes and changes in response to iron deficiency. Photosynthesis Research 89: 141-155

Ayami N, Saori S, Misa T, Hiromichi M, Atsushi S (2007) The RNAi-Mediated Silencing of Xanthine Dehydrogenase Impairs Growth and Fertility and Accelerates Leaf Senescence in Transgenic Arabidopsis Plants. Plant & Cell Physiology 48: 1484-1484

Balk J, Pilon M (2011) Ancient and essential: the assembly of iron–sulfur clusters in plants. Trends in Plant Science 16: 218-226

Balk J, Schaedler TA (2014) Iron Cofactor Assembly in Plants. Annual Review of Plant Biology 65: 125-153

Bang WY, Jeong IS, Kim DW, Im ChH, Ji C, Hwang SM, Kim SW, Son YS, Jeong J, Shiina T, Bahk JD (2008) Role of Arabidopsis CHL27 Protein for Photosynthesis, Chloroplast Development and Gene Expression Profiling. Plant & Cell Physiology 49: 1350-1350

Barber J (2016) Photosystem II: the water splitting enzyme of photosynthesis and the origin of oxygen in our
atmosphere. Quarterly Reviews of Biophysics e14

Blaby-Haas CE, Merchant SS (2013) Iron sparing and recycling in a compartmentalized cell. Current Opinion in Microbiology 16: 677-685

Bradford MM (1975) A rapid and sensitive method for the quantitation of microgram quantity of protein utilizing the principle of
protein-dye binding. Analytical Biochemistry 72: 248-254

Briat J-F, Dubos C, Gaymard F (2015) Iron nutrition, biomass production, and plant product quality. Trends in Plant Science 20: 33-40

Brumbarova T, Bauer P, Ivanov R (2015) Molecular mechanisms governing Arabidopsis iron uptake. Trends in Plant Science 20: 124-133

Burkhead JL, Reynolds KAG, Abdel-Ghany SE, Cohu CM, Pilon M (2009) Copper homeostasis. New Phytologist 182: 799-816

Bych K, Netz DJA, Vigani G, Bili E, Lilly R, Pierik AJ, Balk J (2008) The Essential Cytosolic Iron-Sulfur Protein Nbp35 Acts without Cfdl Partner in the Green Lineage. Journal of Biological Chemistry 283: 35797-35804

Christman MA, Richards JH, McKay JK, Stahl EA, Juenger TE, Donovan LA (2008) Genetic variation in Arabidopsis thaliana for night-time leaf conductance. Plant, Cell & Environment 31: 1170-1178

Ciaffi M, Paolacci AR, Celletti S, Catarcione G, Kopriva S, Astolfi S (2013) Transcriptional and physiological changes in the S assimilation pathway due to single or combined S and Fe deprivation in durum wheat (Triticum durum L.) seedlings. Journal of Experimental Botany 64: 1663-1675

Cornah JE, Terry MJ, Smith AG (2003) Green or red: what stops the traffic in the tetrapyrrole pathway? Trends in Plant Science 8: 224-230

Geiss GK, Bumgarner RE, Birditt B, Dahl T, Dowidar N, Dunaway DL, Fell HP, Ferree S, George RD, Grogan T, James JJ, Maysuria M, Mitton JD, Oliveri P, Osborn JL, Tao P,

Ratcliffe AL, Webster PJ, Davidson EH, Hood L (2008) Direct multiplexed measurement of gene expression with color-coded probe pairs. Nature Biotechnology 26: 317-325

Glaesener AG, Merchant SS, Blaby-Haas CE (2013) Iron economy in C*hlamydomonas reinhardtii*. Frontiers in Plant Science 337

Hanke GT, Hase T (2008) Variable Photosynthetic Roles of Two Leaf-type Ferredoxins in Arabidopsis, as Revealed by RNA Interference. Photochemistry and Photobiology 84: 1302-1309

Hanke GT, Kimata-Ariga Y, Taniguchi I, Hase T (2004) A Post Genomic Characterization of Arabidopsis Ferredoxins. Plant Physiology 134: 255-264

Herbik A, Giritch A, Horstmann C, Becker R, Balzer HJ, Baumlein H, Stephan UW (1996) Iron and copper nutrition-dependent changes in protein expression in a tomato wild type and the nicotianamine-free mutant chloronerva. Plant Physiology 111: 533-540

Hong Y, Abdel-Ghany SE, Anderson TD, Pilon-Smits EAH, Pilon M (2006) CpSufE Activates the Cysteine Desulfurase CpNifS for Chloroplastic Fe-S Cluster Formation. Journal of Biological Chemistry 281: 8958-8969

Hu X, Page MT, Sumida A, Tanaka A, Terry MJ, Tanaka R (2017) The iron-sulfur cluster biosynthesis protein SUFB is required for chlorophyll synthesis, but not phytochrome signaling . Plant Journal 89: 1184-1194

Hu XY, Kato Y, Sumida A, Tanaka A, Tanaka R (2017) The SUFBC2D complex is required for the biogenesis of all major classes of plastid Fe-S proteins. Plant Journal 90: 235-248

Huet G, Daffé M, Saves I (2005) Identification of the Mycobacterium tuberculosis SUF Machinery as the Exclusive Mycobacterial System of [Fe-S] Cluster Assembly: Evidence for Its Implication in the Pathogen's Survival. Journal of Bacteriology 187: 6137-6146

Klughammer C, Schrieber U (2008) Saturation Pulse method for assessment of energy conversion in PSI. PAM
application notes 1: 11-14

Kobayashi T, Nishizawa NK (2012) Iron Uptake, Translocation, and Regulation in Higher Plants. Annual Review of Plant Biology 63: 131-152

Koprivova A, Kopriva S (2014) Molecular mechanisms of regulation of sulfate assimilation: first steps on a long road. Frontiers in Plant Science 5

Krohling CA, Eutropio FJ, Bertolazi AA, Dobbss LB, Campostrini E, Dias T, Ramos AC (2016) Ecophysiology of iron homeostasis in plants. Soil Science and Plant Nutrition 62: 39-47

Laganowsky A, Gómez SM, Whitelegge JP, Nishio JN (2009) Hydroponics on a chip: Analysis of the Fe deficient Arabidopsis thylakoid membrane proteome. Journal of Proteomics 72: 397-415

Lan P, Li WF, Wen TN, Schmidt W (2012) Quantitative Phosphoproteome Profiling of Iron-Deficient Arabidopsis Roots. Plant Physiology 159: 403-417

Li YL, Zhang Y, Shi DQ, Liu XJ, Qin J, Ge Q, Xu LH, Pan XL, Li W, Zhu YY, Xu J (2013) Spatial-temporal analysis of zinc homeostasis reveals the response mechanisms to acute zinc deficiency in Sorghum bicolor. New Phytologist 200: 1102-1115

Liang XJ, Qin L, Liu PW, Wang MH, Ye H (2014) Genes for iron-sulphur cluster assembly are targets of abiotic stress in rice, Oryza sativa. Plant Cell and Environment 37: 780-794

Liu J, Wang P, Liu B, Feng DR, Zhang J, Su JB, Zhang Y, Wang J, Wang H (2013) A deficiency in chloroplastic ferredoxin 2 facilitates effective photosynthetic capacity during long-term high light acclimation in Arabidopsis thaliana. Plant Journal 76: 861-874

Long TA, Tsukagoshi H, Busch W, Lahner B, Salt DE, Benfey PN (2010) The bHLH Transcription Factor POPEYE Regulates Response to Iron Deficiency in Arabidopsis Roots. Plant Cell 22: 2219-2236

Lopez-Millan AF, Grusak MA, Abadia A, Abadia J (2013) Iron deficiency in plants: an insight from proteomic approaches. Frontiers in Plant Science 4

Malkov VA, Serikawa KA, Balantac N, Watters J, Geiss G, Mashadi-Hossein A, Fare T (2009) Multiplexed measurements of gene signatures in different analytes using the Nanostring nCounter Assay System. BMC Research Notes 2: 1-9

Maxwell K, Johnson GN (2000) Perspectives in Experimental Botany. Chlorophyll fluorescence—a practical guide. Journal of Experimental Botany. Journal of Experimental Botany 51: 659-668

Merchant S, Sawaya MR (2005) The Light Reactions: A Guide to Recent Acquisitions for the Picture Gallery. *In*, Vol 17, pp 648-663

metabolism. Plant Physiology 130: 1309-1318

Moseley JL, Allinger T, Herzog S, Hoerth P, Wehinger E, Merchant S, Hippler M (2002) Adaptation to Fe-deficiency requires remodeling of the photosynthetic apparatus. EMBO Journal 21: 6709-6720

Moulin M, Smith AG (2005) Regulation of tetrapyrrole biosynthesis in higher plants. Biochemical Society Transactions 33: 737-742

Msilini N, Zaghdoudi M, Govindachary S, Lachaal M, Ouerghi Z, Carpentier R (2011) Inhibition of photosynthetic oxygen evolution and electron transfer from the quinone acceptor QA- to QB by iron deficiency. Photosynthesis Research 107
247-256

Nishio JN, Abadia J, Terry N (1985) Chlorophyll-proteins and electron transport during iron-mediated chloroplast development. Plant Physiology 78: 296-299

Nishio JN, Terry N (1983) Iron nutrition-mediated chloroplast development. Plant Physiology 71: 688-691

Oglesby-Sherrouse AG, Murphy ER (2013) Iron-responsive bacterial small RNAs: variations on a theme. Metallomics 5: 276-286

Page MD, Allen MD, Kropat J, Urzica EI, Karpowicz SJ, Hsieh SI, Leo JA, Merchant SS (2012) Fe Sparing and Fe Recycling Contribute to Increased Superoxide Dismutase Capacity in Iron-Starved Chlamydomonas reinhardtii. Plant Cell 24: 2649-2665

Paolacci AR, Celletti S, Catarcione G, Hawkesford MJ, Astolfi S, Ciaffi M (2014) Iron deprivation results in a rapid but not sustained increase of the expression of genes involved in iron metabolism and sulfate uptake in tomato (Solanum lycopersicum L.) seedlings. Journal of Integrative Plant Biology 56: 88-100

Petit J-M, Briat J-F, Lobreaux S (2001) Structure and differential expression of the four members of the A*rabidopsis thaliana* ferritin gene family. Biochemical Journal 359: 575-582

Philpott CC, Leidgens S, Frey AG (2012) Metabolic remodeling in iron-deficient fungi. BBA - Molecular Cell Research 1823: 1509-1520

Pilon M (2017) The copper microRNAs. New Phytologist 213: 1030-1035

Pilon M, Ravet K, Tapken W (2011) The biogenesis and physiological function of chloroplast superoxide dismutases. BBA - Bioenergetics 1807: 989-998

Pilon-Smits EAH, Garifullina GF, Abdel-Ghany S, Kato S-I (2002) Characterization of a NifS-like chloroplastic protein from A*rabidopsis.* Implications for its role in sulfur and selenium metabolism. Plant Physiology 130: 1309-1318

Pilon-Smits EAH, Garifullina GF, Abdel-Ghany S, Kato SI, Mihara H, Hale KL, Burkhead JL, Esaki N, Kurihara T, Pilon M (2003) Characterization of a NifS-like chloroplast protein from Arabidopsis. Implications for its role in sulfur and selenium metabolism (vol 130, pg 1309, 2002). Plant Physiology 131: 379-379

Pilon-Smits EAH, Pilon M (2005) Sulfur metabolism in plastids. *In* RR Wise, JK Hoober, eds, Advances in Photosynthesis and Respiration, The Structure and Function of Plastids, Vol 23. Kluwer Academic Publishers, The Netherlands, pp 387-402

Porra RJ, Thompson WA, Kriedemann PE (1989) Determination of accurate extinction coefficients and simultaneous equations for assaying chlorophylls a and b extracted with four different solvents: verification of the concentration of chlorophyll standards by atomic absorption spectroscopy. Biochimica et Biophysica Acta 975: 384–394

Ravet K, Danford FL, Dihle A, Pittarello M, Pilon M (2011) Spatiotemporal Analysis of Copper Homeostasis in Populus trichocarpa Reveals an Integrated Molecular Remodeling for a Preferential Allocation of Copper to Plastocyanin in the Chloroplasts of Developing Leaves. Plant Physiology 157: 1300-1312

Ravet K, Touraine B, Boucherez J, Briat J-F, Gaymard F, Cellier F (2009) Ferritins control interaction between iron homeostasis and oxidative stress in Arabidopsis. Plant Journal 57: 400-412

Rodriguez-Celma J, Pan IC, Li W, Lan P, Buckhout TJ, Schmidt W (2013) The transcriptional response of A*rabidopsis* leaves to Fe deficiency. Frontiers in Plant Science 4: 276

Sambrook J, Russell DW (2001) Molecular Cloning: A Laboratory Manual, Vol 1. Cold Spring Harbor Laboratory Press, New York, NY

Séguéla M, Briat J-F, Vert G, Curie C (2008) Cytokinins negatively regulate the root iron uptake machinery in Arabidopsis through a growth-dependent pathway. Plant Journal 55: 289-300

Selote D, Samira R, Matthiadis A, Gillikin JW, Long TA (2015) Iron-Binding E3 Ligase Mediates Iron Response in Plants by Targeting Basic Helix-Loop-Helix Transcription Factors. Plant Physiology 167: 273-286

Sétif P, Fischer N, Lagoutte B, Bottin H, Rochaix J-D (2002) The ferredoxin docking site of photosystem I. BBA - Bioenergetics 1555: 204

Sharma S (2007) Adaptation of photosynthesis under iron deficiency in maize. Journal of Plant Physiology 164: 1261-1267

Shikanai T, Muller-Moule P, Yuri M, Niyogi KK, Pilon M (2003) PAA1, a P-Type ATPase of Arabidopsis, Functions in Copper Transport in Chloroplasts. Plant Cell 15: 1333-1346

Sivitz AB, Hermand V, Curie C, Vert G, Bennett M (2012) Arabidopsis bHLH100 and bHLH101 Control Iron Homeostasis via a FIT-Independent Pathway. PLoS ONE 7: 1-12

Spiller S, Terry N (1979) Limiting Factors in Photosynthesis: II. Iron Stress diminishes photochemical capacity by reducing number of photosynthetic units. Plant Physiology 65: 121-125

Steffens NO, Galuschka C, Schindler M, Bulow L, Hehl R (2004) AthaMap: an online resource for in silico transcription factor binding sites in the Arabidopsis thaliana genome. Nucleic Acids Research 32: D368-D372

Tanaka R, Kobayashi K, Masuda T (2011) Tetrapyrrole metabolism in *Arabidopsis thaliana* The *Arabidopsis* Book 9: e0145

Terauchi AM, Peers G, Kobayashi M, Niyogi KK, Merchant SS (2010) Trophic status of *Chlamydomonas reinhardtii* influences the impact of iron deficiency on photosynthesis. Photosynthesis Research 105: 39-49

Timperio AM, D'Amici GM, Barta C, Loreto F, Zolla L (2007) Proteomics, pigment composition, and organization of thylakoid membranes in iron-deficient spinach leaves. Journal of Experimental Botany 58: 3695-3710

Topilina NI, Green CM, Jayachandran P, Kelley DS, Stanger MJ, Piazza CL, Nayak S, Belfort M (2015) SufB intein of Mycobacterium tuberculosis as a sensor for oxidative and nitrosative stresses. Proceedings of the National Academy of Sciences of the United States of America 112: 10348-31035

Tottey S, Block MA, Allen M, Westergren T, Albrieux C, Scheller HV, Merchant S, Jensen PE (2003) Arabidopsis CHL27, located in both envelope and thylakoid membranes, is required for the synthesis of protochlorophyllide. Proceedings of the National Academy of Sciences of the United States of America 100: 16119-16124

Van Hoewyk D, Abdel-Ghany SE, Cohu CM, Herbert SK, Kugrens P, Pilon M, Pilon-Smits EAH (2007) Chloroplast iron-sulfur cluster protein maturation requires the essential cysteine desulfurase CpNifS. Proceedings of the National Academy of Sciences of the United States of America 104: 5686-5691

Veldman-Jones MH, Brant R, Rooney C, Geh C, Emery H, Harbron CG, Wappett M, Sharpe A, Dymond M, Barrett JC, Harrington EA, Marshall G (2015) Evaluating Robustness and Sensitivity of the NanoString Technologies nCounter Platform to Enable Multiplexed Gene Expression Analysis of Clinical Samples. Cancer Research 75: 2587-2593

Vert G, Grotz N, Dedaldechamp F, Gaymard F, Guerinot ML, Briat J-F, Curie C (2002) IRT1, an A*rabidopsis* transporter essential for iron uptake from the soil and for plant growth. The Plant Cell 14: 1223-1233

Vorst O, Kock P, Lever A, Weterings B, Weisbeek P, Smeekens S (1993) The promoter of the *Arabidopsis thaliana* plastocyanin gene contains a far upstream enhancer-like element involved in chloroplast dependent expression. Plant Journal 4: 933-945

Voss I, Goss T, Murozuka E, Altmann B, McLean KJ, Rigby SEJ, Munro AW, Scheibe R, Hase T, Hanke GT (2011) FdC1, a Novel Ferredoxin Protein Capable of Alternative Electron Partitioning, Increases in Conditions of Acceptor Limitation at Photosystem I. Journal of Biological Chemistry 286: 50-59

Wang H-Y, Klatte M, Jakoby M, Baumlein H, Weisshaar B, Bauer P (2007) Iron deficiency-mediated stress regulation of four subgroup Ib BHLH gene in A*rabidopsis thaliana*. Planta 226: 897-908

Xu XM, Adams S, Chuam NH, Moller SG (2005) AtNAP1 represents an atypical SufB protein in Arabidopsis plastids. Journal of Biological Chemistry 280

Yabe T, Nakai M (2006) Arabidopsis AtIscA-I is affected by deficiency of Fe–S cluster biosynthetic scaffold AtCnfU-V. Biochemical & Biophysical Research Communications 340: 1047-1052

Yamasaki H, Abdel-Ghany SE, Cohu CM, Kobayashi Y, Shikanai T, Pilon M (2007) Regulation of copper homeostasis by micro-RNA in A*rabidopsis*. Journal of Biological Chemistry 282: 16369-16378

Yamasaki H, Hayashi M, Fukazawa M, Kobayashi Y, Shikanai T (2009) SQUAMOSA Promoter Binding Protein-Like 7 Is a Central Regulator for Copper Homeostasis in Arabidopsis. Vol 21, pp 347-361

Ye H, Abdel-Ghany SE, Anderson TD, Pilon-Smits EAH, Pilon M (2006) CpSufE activates the cysteine desulfurase CpNifS for chloroplastic Fe-S cluster formation. Journal of Biological Chemistry 281: 8958-8969

Yuan YX, Wu HL, Wang N, Li J, Zhao WN, Du J, Wang DW, Ling HQ (2008) FIT interacts with AtbHLH38 and AtbHLH39 in regulating iron uptake gene expression for iron homeostasis in Arabidopsis. Cell Research 18: 385-397

Zuchi S, Watanabe M, Hubberten HM, Bromke M, Osorio S, Fernie AR, Celletti S, Paolacci AR, Catarcione G, Ciaffi M, Hoefgen R, Astolfi S (2015) The Interplay between Sulfur and Iron Nutrition in Tomato. Plant Physiology 169: 2624-2639

CHAPTER 3: MICRONUTRIENT HOMEOSTASIS AND CHLOROPLAST IRON PROTEIN EXPRESSION IS LARGELY MAINTAINED IN A CHLOROPLAST COPPER TRANSPORTER MUTANT.[3]

3.1 SUMMARY

PAAI is a P-Type ATPase that functions to import copper (Cu) into the chloroplast. *Arabidopsis thaliana paa1* mutants have lowered plastocyanin levels, resulting in a decreased photosynthetic electron transport rate. In nature Fe and Cu homeostasis are often linked and it can be envisioned that *paa1* acclimates its photosynthetic machinery by adjusting expression of its chloroplast Fe-proteome, but outside of Cu homeostasis *paa1* has not been studied. Here, we characterize *paa1* ultrastructure and accumulation of electron transport chain proteins in a *paa1*allelic series. Furthermore, using hydroponic growth conditions, we characterized metal homeostasis in *paa1* with an emphasis on the effects of Fe deficiency. Surprisingly, the *paa1* mutation does not affect chloroplast ultrastructure or the accumulation of other photosynthetic electron transport chain proteins, despite the strong decrease in electron transport rate. The regulation of Fe-related photosynthetic electron transport proteins in response to Fe status was maintained in *paa1,* suggesting that regulation of the chloroplast Fe proteins ignores operational signals from photosynthetic output. The characterization of *paa1* has revealed new insight into the regulation of expression of the photosynthetic electron transport chain proteins and chloroplast metal homeostasis and can help to develop new strategies for the detection of shoot Fe deficiency.

[3] Submitted to Functional Plant Biology, Authors: Gretchen E. Kroh and Marinus Pilon (Under Review)

3.2 INTRODUCTION

The assembly and maintenance of a functional photosynthetic machinery in plants requires coordinated expression of both plastid and nucleus encoded genes (Jarvis and López-Juez 2013). The expression of chloroplast proteins is regulated by both biogenic (developmental) and operational signals (Kleine and Leister 2016; Chan *et al.,* 2016). Factors such as light quality and quantity, drought, herbicides and reactive oxygen species affect photosynthesis, causing operational signaling pathways to tune expression of photosynthesis related nuclear encoded genes (Chan *et al.,* 2016). The assembly of a functional chloroplast also requires metal ion micronutrients such as copper (Cu), iron (Fe) manganese (Mn) and zinc (Zn), which are used in cofactors. In the last two decades we have gained much insight into the delivery and assembly systems for metal cofactors. The delivery system is especially well-characterized for Cu, in *Arabidopsis thaliana,* which in chloroplasts is required in two major Cu enzymes, plastocyanin and copper/zinc superoxide dismutase.

PAA1/HMA6 (P-type ATPase of *Arabidopsis* 1/Heavy Metal ATPase 6) is a P type-ATPase, with an N-terminal Heavy Metal-Binding (HMB) domain and eight predicted trans-membrane domains, that functions as a chloroplast Cu importer (Shikanai *et al.,* 2003; Abdel-Ghany *et al.,* 2005; Blaby-Haas *et al.,* 2014). The *PAA1* locus encodes for two major splice forms, a long transcript encoding for the full transporter, and a short transcript encoding for only the N-terminal, soluble, HMB domain which serves to deliver Cu to PAA1 and was called PCH1 for Plastid copper CHaperone1 (Blaby-Haas *et al.,* 2014). Six loss-of-function alleles have been described for *paa1* and complementation with a wild-type genomic sequence rescued growth and photosynthesis phenotypes (Shikanai *et al.,* 2003). All six *paa1* alleles showed a comparable photosynthetic phenotype, which is partially suppressed by feeding $CuSO_4$, allowing seed set on well-fertilized soil (Shikanai *et al.,* 2003). In *paa1* mutants less Cu is available for plastocyanin (PC) maturation, which leads to a lowered photosynthetic electron transport rate and a growth defect. In addition, maturation of chloroplast Cu/Zn superoxide

dismutase (CSD2) is disturbed in *paa1* plants (Shikanai *et al.,* 2003). It is possible that *paa1* plants acclimate to the loss of PC and CSD2 by means of compensatory mechanisms, but the effects of *paa1* loss-of-function on chloroplast structure and expression of proteins, beyond those that are Cu-related, have not been reported.

While Cu is important, plants require roughly 20x more Fe for photosynthesis. Chloroplasts require at least 24 Fe atoms for one linear photosynthetic electron transport chain (Merchant and Sawaya 2005) and low Fe availability drastically affects plant chloroplast function (Lopez-Millan *et al.,* 2013; Briat *et al.,* 2015). Plants are commonly Fe deficient because of the low bioavailability of soil Fe. When plants are Fe deficient, photosynthesis suffers, resulting in decreased biomass production. Specifically, photosynthetic electron transport is significantly inhibited by Fe deficiency (Larbi *et al.,* 2006; Lopez-Millan *et al.,* 2013, Rodriguez-Celma *et al.,* 2013). A chloroplast Fe deficiency response, which can help to prioritize the use of available Fe under impending deficiency, was uncovered recently in *Arabidopsis* (Hantzis *et al.,* 2018). Major targets of the *Arabidopsis* chloroplast Fe deficiency response which were found to be regulated at the transcript level are subunits of the cytochrome-b_6f complex and leaf ferredoxin as well as the SUFB component of the chloroplast SUF iron-sulfur (Fe-S) assembly system (Hantzis *et al.,* 2018). SUFB is essential for all Fe-S cluster formation in the photosynthetic electron transport chain (Hu *et al.,* 2017). FDX2 is the Fe-regulated major leaf isoform of FDX, a protein that requires a 2Fe-2S cluster (Hanke and Mulo 2013).

It is possible that the disturbance of delivery of one type of metal co-factor to chloroplasts such as Cu could affect photosynthetic gene expression and the homeostasis of other metal cofactors required for chloroplast biogenesis. In this context it is especially compelling to look at Fe homeostasis in *paa1*. Interactions between Cu and Fe homeostasis are well-established in several living systems and especially photosynthetic organisms (Yuan *et al.,* 1995; Hill and Merchant 1995; Lin *et al.,* 1997; Fontaine *et al.,* 2002; Waters *et al.,* 2012; Kastoori Ramamurthy *et al.,* 2018). In plants, it is well documented that starvation of whole

plants for Cu causes an increase in root surface ferric reductase activity and thus slightly increased iron uptake (Mukherjee *et al.,* 2006; Bernal et al., 2012). Conversely, increased Cu accumulation has been reported for Fe deficient plants (Waters and Armbrust 2013; Perea-Garcia *et al.,* 2013). Interestingly, *paa1* plants show a similar photosynthetic defect as wild type (WT) plants subjected to short term Fe deficiency (Hantzis *et al.,* 2018). Roughly 80% of leaf Fe is in the chloroplast. Due to their high expression and Fe content, the observed down-regulation of the cytochrome-b_6f complex and ferredoxin under Fe deficiency could save about half of this Fe for use in other proteins (Hantzis *et al.,* 2018). If operational signals that mediate expression of Fe containing photosynthetic transcripts originate from photosynthetic electron transport, *paa1* should show a chloroplast Fe deficiency response even when grown on sufficient levels of Fe. Conversely if photosynthetic deficiency does not mediate Fe protein expression, *paa1* should respond to Fe deficiency in the same way as wild type plants.

Here we sought to characterize the effects of *paa1* mutation beyond chloroplast Cu protein accumulation by investigating chloroplast ultrastructure, photosynthetic protein expression and metal ion homeostasis with an emphasis on Fe. The results indicate that chloroplast Fe protein expression and biogenesis is maintained in *paa1* despite a large reduction in photosynthesis. These results have impact for our understanding of chloroplast metal ion homeostasis and might be applied to better understand Cu and Fe status in field settings.

3.3 METHODS

Plant material and growth. We utilized 4 of the previously described paa1 alleles and their respective wild-types. *paa1-1 (Landsberg erecta, Ler* background*), paa1-4,* and *paa1-6* (*Columbia gl, Col3* background) are point mutations, which are predicted to fully abolish transporter function; while one allele, *paa1-3 (Columbia, Col0* background*),* carries a 9 base pair (in frame) deletion in the area corresponding to the N-terminal metal binding domain which

also corresponds to PCH1 (Shikanai *et al.,* 2003; Blaby Haas *et al.,* 2014). In *paa1-3* the full transporter protein is detectable, albeit at a reduced level, but PCH1 protein was lost (Tapken *et al.,* 2012; Blaby-Haas *et al.,* 2014). In contrast, for other alleles the transporter is lost but PCH1 may still be detectable as was found for *paa1-1* (Tapken *et al.,* 2012; Blaby-Haas *et al.,* 2014). The primers listed in S. Table 3-3 were used on genomic DNA of plants grown on soil. Following PCR the products were digested with the indicated restriction enzymes followed by agarose electrophoresis to distinguish genotype as indicated in S. Table 3-3. Seeds are deposited in the *Arabidopsis* Biological Resource Center at The Ohio State University, Columbus, OH, USA.

For growth on soil, seeds were stratified for four days at 4˚C in darkness before planting on pre-moistened PRO-MIX HP soil in 4 inch pots. Plants were grown at 23˚C with a light intensity of 200 μmol $m^{-2}s^{-1}$, at 8 h : 16 h, light : dark. All pots were watered with tap water three times per week from the bottom. The fourth and seventh watering solution contained a 1:1000 dilution of Miracle-Gro Liquid All Purpose Plant Food (Scotts Company, Marysville, OH).

For hydroponic growth the procedure outlined by Conn *et al.,* (2013) was adapted. Specifically, seeds were germinated on microcentrifuge tube caps containing 2 mm holes to allow root growth, which were filled with 400 μL of ½ strength Murashige and Skoog medium (Murashige and Skoog 1962, Sigma-Aldrich, St. Louis, MO) supplemented with 0.7% plant agar (PlantMedia, Dublin, OH). Seeds of each line were placed on the agar-filled caps, which were held in hydroponic tubs containing deionized water and stratified for four days at 4°C in darkness. Tubs were then transferred to a growth room set to 23°C and 8 h day length with a light intensity of 200 μmol $m^{-2}s^{-1}$ (Feit Electric LED Full Spectrum Grow Light, Pico Rivera, CA). During the first two weeks of growth, the hydroponics tubs were covered with plastic wrap to induce optimal humidity for germination. After seeds germinated, the deionized water was first replaced with 1/15th strength modified Hoagland's solution and the strength of the solution was increased to 1/10th after two weeks and then to 1/5th four days later. Final salt concentrations in

the 1/5th Hoagland's solution were 0.3 mM NH_4NO_3, 1 mM $Ca(NO_3)_2$, 1.4 mM KNO_3, 0.2 mM KH_2PO_4, 0.4 mM $MgSO_4$, 6.6 mM $MgCl_2$, 12.3 μM H_3BO_3, 2.4 μM $MnSO_4$, 0.2 μM $ZnSO_4$, 0.03 μM MoO_3, 0.5 μM $CuSO_4$, 10 μM Fe(III)EDTA (Hoagland and Arnon 1938). To induce Fe deficiency, plants that were four weeks old (10-14 leaf stage) were transferred to 1/5th Hoagland's supplemented with 10 nM Fe(III)EDTA, whereas control groups were maintained at 10 μM Fe(III)EDTA (Hantzis *et al.,* 2018). Plants were sampled and analyzed seven days after the start of treatment; all sampling and measurements were at 1 h after the start of the light period.

Elemental analysis and biomass measurements. Whole rosette samples were harvested and dried for elemental analysis (2 rosettes per biological rep). Dried rosettes were digested in nitric acid and analyzed for elemental composition via ICP-OES as described (Pilon-Smits *et al.,* 1999; Cohu and Pilon 2007). Elemental concentrations were normalized to the dry weight of the digested sample (n=13-15). Biomass of shoots was measured on dry weight basis. 26 rosettes of treated and control *paa1-4* and 30 rosettes of Col3 were analyzed. Biomass of roots was measured on a fresh weight basis for roots used in Ferric Reductase Assays. Ten root systems of treated and control for both *paa1-4* and Col3 were analyzed.

Chlorophyll fluorescence. Chlorophyll fluorescence imaging using a FluorCam (PSI, Brno, Chech Republic) and quantitative measurement of chlorophyll fluorescence using a FMS2 system (Hansatech Instruments) and calculation of parameters was as described (Maxwell and Johnson 2000).

Protein and mRNA levels. For protein levels four biological replicates, consisting of three rosettes each, for each treatment and each line were analyzed. Proteins were extracted as described in Friso *et al.* (2011) and protein concentration was quantified using the Pierce BCA Protein Assay Kit (Thermo-Fisher, Waltham, MA). Antibodies, immunoblotting and quantification were as described (Hantzis *et al.,* 2018). Antibodies for PsbA, PsbO, RbcL, FDX, PC, cFPbase,

PsaA, PsaB, Rieske, Cyt$b_{6,}$ and Cyt*f* were from Agrisera (Vannas, Sweden). Antibody for SufB was a gift from Dr. Nicolas Rouhier (Université de Lorraine, Nancy, France).

Total RNA was extracted from four biological replicates using the TRIzol extraction method (Life Technologies, Carlsbad, CA). Each replicate consisted of three rosettes for each genotype and treatment. Quality was assessed spectrophotometrically (NanoDrop) and by gel electrophoresis. RNA was treated with DNase I (Invitrogen, Carlsbad, CA) and cDNA was synthesized by SuperScript III Reverse Transcriptase (Invitrogen, Carlsbad, CA) using both random hexamer primers and oligo-dT primers. A separate aliquot from each RNA sample was treated with DNase without reverse transcription to serve as a minus RT control in qPCR. After cDNA synthesis, cDNA was treated with RNase H to remove excess RNA (El Mehdawi *et al.,* 2018). qRT-PCR was assayed as described (El Mehdawi *et al.,* 2018). At least two technical replicates of each biological replicate were included and all technical replicate Ct values of one biological rep were averaged. Relative expression was calculated using the ΔΔCT method (Schmittgen and Livak 2008). Ct values of each gene of interest were first normalized to the reference gene, *UBQ10*, and then normalized to the expression level found in Col3 control rosettes. *UBQ10* expression was analyzed alongside each gene of interest. For each gene of interest and *UBQ10*, a water control was included to ensure no primer dimers or off targets were being amplified in the qPCR reactions. *Tubulin2* was included as a control gene (Wintz *et al.,* 2003; Kobayashi *et al.,* 2013; Ceballos-Laita *et al.,* 2015; Zhu *et al.,* 2016). Additionally, a minus RT control was included to ensure that the qPCR reactions were not contaminated by genomic DNA. Primers for qRT-PCR are listed in the S. Table 3-2. All primers were tested for efficiency and used for gene expression analysis if higher than 95% efficient. Primers for quantitative PCR were designed as described (Udvardi *et al.,* 2008) and are listed (S. Table 3-2).

Root ferric chelate reductase activity. Root ferric reductase activity of whole root systems was measured seven days after Fe deficiency. Roots were first rinsed twice in 1/5th Hoagland's solution lacking Fe for 5 minutes each to remove excess Fe from the epidermal tissue. Ferric chelate reductase activity was measured on a whole root system basis in 1.5 mL of assay solution (1/5 Hoagland's solution, 100 μM Fe (III)EDTA, and 100 μM of the colorimetric Fe (II) chelator, BPDS (batho-phenanthrolinedisulfonic acid, Sigma-Aldrich, St. Louis, MO) for 30 minutes in the dark. Ferric reductase activity is normalized by root fresh weight (n=10). One biological replicate consisted of one whole root system with a fresh weight above 30 mg. The roots were then removed from the assay solution and the absorbance of the solution was read at 535 nm. Reductase activity was calculated on a whole root basis as described in Grusak (1995).

TEM analysis. Leaf samples of four week-old soil grown plants were fixed, sectioned and processed for transmission EM and imaged at Electron Microscopy Services (Colorado Springs, CO) as described (Lundquist *et al.,* 2013).

Statistical analysis. All statistical analysis was done using R version 3.4.4. A t-test was used to determine differences in chlorophyll fluorescence parameters between soil grown *paa1* alleles and WT. For all other assays, a two factor ANOVA was used to determine significance between treated and control Col3 and *paa1-4* plants (p value < 0.05). A Tukey test was conducted in any case where the ANOVA was significant using the lsmeans R package. For each experiment, at least four biological replicates were analyzed.

3.4 RESULTS

Previous characterization of *paa1* was of seedlings grown in long-day conditions (Shikanai *et al.,* 2003). To further characterize the effect of *paa1* on chloroplast structure, we grew plants on soil in short-day growth conditions which delays flowering and favors biomass production for biochemical analysis. We first investigated if the reduction in photosynthetic

electron transport in *paa1* relative to wild-type may also result in changes to chloroplast ultrastructure (Figure 3-1). Using Ler and *paa1-1* as representative lines, we analyzed chloroplast anatomy by Transmission EM (Figure 3-1). The images are characteristic of chloroplasts grown in an intermediate light intensity (Wise 2006) but show no dramatic differences in chloroplast anatomy between Ler wild-type and *paa1-1* under our growth conditions (Figure 3-1a). We quantified the number of thylakoids per granum, the number of total grana stacks per chloroplast, and the number of plastoglobules per chloroplast in the images and did not observe significant differences between *paa1* and wild-type (Figure 3-1b). We conclude that chloroplast architecture is not dramatically impaired by photosynthetic deficiency in *paa1.*

We further analyzed the impact of *paa1* on photosynthetic electron transport using an allelic series of *paa1* plants and their wild-type backgrounds on soil in short-day conditions (Figure 3-2). As expected, the soil grown, *paa1* plants had lowered biomass as evidenced by a clear reduction in leaf area (Figure 3-2a). Previous characterization of *paa1* seedlings grown in long-day light conditions had shown a decrease in electron transport rate and non-photochemical quenching (NPQ) (Shikanai *et al.,* 2003). Chlorophyll fluorescence imaging of soil grown plants on short day conditions also indicated that the parameter flux through PSII (ΦPSII) was lower throughout the rosette, indicative of a reduced electron transport activity. Similarly, the *paa1* mutant alleles were deficient in NPQ induction compared to the wild-types (Figure 3-1a). A quantitative analysis of chlorophyll fluorescence indicated that electron transport is reduced 2-3 fold in the *paa1* alleles with accompanying reductions in NPQ (Figure 3-2b). However, F_V/F_M was unaffected in the *paa1* alleles, suggesting a maintenance of PSII capacity (Figure 3-2b). Therefore, we conclude that only electron transport downstream of PSII function is disrupted in the *paa1* mutant.

It is well established that *paa1* is defective in plastocyanin (PC) and Cu/Zn superoxide dismutase in the chloroplasts but other photosynthesis related proteins have not been reported

(Shikanai *et al.,* 2003). A Commasie Brilliant Blue stained gel for total proteins shows few protein accumulation differences across the *paa1* alleles compared to respective wild type backgrounds (Figure 3a). Since *paa1* alleles show a photosynthesis defect in electron transport, we asked if accumulation of other photosynthetic electron transport chain proteins is affected in the *paa1* alleles (Figure 3b). As expected, *paa1* alleles accumulated less PC (Figure 3-3; Shikani *et al.,* 2003). However, the majority of the other photosynthetic electron transport chain proteins measured, including the cytochrome b_6f complex, subunits of PSII and PSI, the oxygen evolving complex (PsbO), and RuBisCo large subunit, accumulated to a comparable level in the *paa1* alleles and the wild-types. SUFB, which is required for production of Fe-S clusters needed for photosynthetic proteins was also maintained in *paa1* alleles. Interestingly, FDX protein abundance was variable across all *paa1* alleles but generally lower compared to their WT backgrounds (Figure 3-3b). The maintenance of PSII, PSI, Cyt*f,* and SUFB in the *paa1* lines grown on soil suggests that photosynthetic deficiency due to a decrease in PC, surprisingly, does not lead to initiation of operational signals to down-regulate electron transport proteins, with the possible exception of FDX.

The magnitude of the photosynthetic defect in *paa1* (Figure 3-2) is comparable to that reported for short term Fe deficiency in wild-type *Arabidopsis* which resulted in down-regulation of the protein FDX (Hantzis *et al.,* 2018). The observations in figure 3-2 prompted us to further characterize the response of *paa1* to Fe deficiency, which requires a hydroponic system (Figure 3-4). Because previous characterization of Fe deficiency was done using a Columbia ecotype (Hantzis *et al.,* 2018), we selected *paa1-4* in the Col3 background as a representative allele for more detailed analysis in hydroponics since it produces one of the strongest photosynthetic deficiencies of the *paa1* alleles and, unlike *paa1-3*, is a null allele for transporter function (Tapken *et al.,* 2012; Blaby-Haas *et al.,* 2014). After 4 weeks of growth in control (+Fe) media, half of the Col3 and *paa1-4* plants were transferred to deficient conditions (-Fe) whereas the other half were maintained on +Fe media. We compared plants after 7 days of treatment (Figure

3-4). Col3 showed the expected response to Fe depletion (Figure 3-4; Hantzis *et al.,* 2018). In the control hydroponic condition (+Fe), *paa1-4* plants showed decreased rosette size together with decreased root and shoot biomass compared to Col3 (Figure 3-4a; S. Figure 3-1). The biomass of control (+Fe) *paa1-4* was similar to that of Fe deficient (-Fe) Col3 plants (Figure 3-4b). In the hydroponic conditions, relative electron transport rate, estimated by ϕPSII, of the *paa1-4* control (+Fe) plants was decreased to the same level of that as Fe deficient (-Fe) Col3 plants (Figure 3-4c). PC accumulation was decreased in the *paa1-4* grown on +Fe but a recovery is seen in the *paa1-4* grown on -Fe (Figure 3-4d), suggesting that Fe deficiency responses may increase Cu availability in the growth medium.

To assess *paa1-4* response to systemic Fe deficiency we also investigated the influence of the *paa1-4* mutation on root iron reductase activity (FRO2 activity), which is up-regulated during Fe deficiency to increase bioavailability of Fe in the rhizosphere (Robinson *et al.,* 1999). The *paa1-4* plants also showed up-regulation of root Fe reductase activity during Fe deficiency (Figure 3-5a). *Paa1-4* -Fe plants did show a significantly higher reductase activity compared to Col3 -Fe but the fold increase in reductase activity in response to low Fe was comparable between Col3 and *paa1-4:* Col3 presented a 4.9 fold increase and *paa1-4* presented a 4.2 fold increase compared to their +Fe counterparts. *Paa1-4* may respond to a slight Cu deficiency, increasing the activity of other FRO proteins in the root (Mukherjee *et al.,* 2006). Measurement of the elemental composition corroborates the increase in FRO2 activity. Shoot Fe levels were comparable between Col3 and *paa1-4* in control (+Fe) conditions whereas in deficiency (-Fe), Fe was lower in both genotypes (Figure 3-5b). Other elements were comparable between WT and *paa1-4* (see S. Table 3-1). Fe deficiency caused increases in S and Cu shoot concentrations in WT as expected (Paolacci *et al.,* 2014; Waters *et al.,* 2012) and the same was found in *paa1-4* (S. Table 3-1). The shoot Cu levels were not affected by *paa1* mutation, as expected (Tapken *et al.,* 2012).

We next analyzed the accumulation of chloroplast Fe proteins (Figure 3-6a). As expected, SUFB, and the cytochrome-b_6f complex subunits (Cyt*f*, Cytb_6 and Rieske protein) were strongly decreased by Fe deficiency in Col3 (Figure 3-6a). These Fe proteins decreased in *paa1-4* -Fe to a comparable level in Col3 -Fe. FDX, however, showed a variable decrease in abundance across the replicates of either Col3 or *paa1-4* -Fe. Additionally, PSaA was unaffected by the *paa1-4* mutation or by Fe deficiency, suggesting Fe prioritization for photosystem-I is conserved in the mutant. Therefore, we can conclude that at the protein level, SUFB, PSaA, and the cytochrome-b_6f complex subunits are primarily regulated by Fe status and are not affected by lowered photosynthesis per se as seen in *paa1* +Fe.

Because the chloroplast Fe deficiency response results in changes in both protein and transcript levels for Fe dependent proteins (Hantzis *et al.,* 2018), we investigated the accumulation of nucleus-encoded transcripts for three strongly Fe regulated chloroplast proteins by qRT-PCR. In both *paa1-4* and Col3, *SUFB*, *FDX2,* and *Rieske* transcripts were strongly down-regulated in Fe deficiency compared to the control treatment (Figure 3-6b). All these transcripts were maintained in *paa1-4* at the same levels as wild-type. *TUB2* was used to present a stable control gene known to not be responsive to Fe deficiency or photosynthetic deficiency (Wintz *et al.,* 2003; Kobayashi *et al.,* 2013; Ceballos-Laita *et al.,* 2015; Zhu *et al.,* 2016). No differences are seen in regulation of *TUB2* in each of the 4 treatments. We conclude that changes to photosynthetic related Fe transcripts, *SUFB, FDX2,* and *Rieske* are specifically regulated in response to Fe deficiency and maintained in *paa1*.

3.5 DISCUSSION

Does the capacity for photosynthetic activity regulate the expression and maintenance of the photosynthetic machinery? Loss of the PAA1 chloroplast envelope Cu transporter results in a dramatically lowered plastocyanin activity and, as a consequence, a strongly decreased electron transport rate (Shikanai *et al.,* 2003; Abdel-Ghany *et al.,* 2005; Tapken *et al.,* 2012).

Surprisingly, while *paa1* growth is stunted, the chloroplast ultrastructure of *paa1-1* did not show strong differences from WT. The photosynthetic machinery was overall well maintained in *paa1* despite the strong decrease in electron transport and NPQ (Figure 3-2). Further, *paa1* showed minimal changes to the abundance of thylakoid electron transport proteins other than PC (Figure 3-3). These observations indicate that *paa1* mutation, despite the strong loss of PC function, does not induce strong pleiotropic phenotypes (Figure 3-1). The expression of chloroplast Fe-related proteins is strongly down-regulated by limiting Fe availability (Figure 3-6; Hantzis *et al.,* 2018). However, the expression of these proteins was not affected in *paa1* (Figure 3-6), even though the effect on photosynthesis of Fe deficiency in WT is very comparable to the loss of loss of PAA1 in Fe sufficiency. Specifically, in response to Fe status the regulation of protein accumulation of chloroplast Fe related proteins, SUFB, Rieske, Cyt*f,* and PSaA, were maintained in *paa1* at levels comparable to wild-type plants. Similarly, transcript expression and regulation was maintained for *SUFB, FDX2* and *RIESKE* (Figure 3-6). Apparently, a lack of photosynthesis per se does not activate photosynthetic operational signals to down-regulate chloroplast Fe protein expression. These observations highlight the existence of a novel signaling pathway in plants that targets photosynthetic Fe proteins specifically in response to low Fe stress.

A lack of whole plant Cu uptake can cause an increase in the accumulation of Fe, which might help to compensate the lack of the Cu (Waters and Armbrust 2013; Perea-Garcia *et al.,* 2013; Kastoori Ramamurthy *et al.,* 2018). Is there a compensatory response for the lack of plastocyanin in the chloroplast of *paa1* plants, as is seen in microbial photosynthetic systems? Several, cyanobacteria as well as *Chlamydomonas rheinhartii* can replace plastocyanin with an iron containing cytochrome-c_6 when copper deprived (Zhang *et al.,* 1992; Bovy *et al.,* 1992; Hill and Merchant 1995). However, plants cannot replace PC (Weigel et al., 2003). Still, it could be envisioned that *paa1* could compensate for a loss of PC function by up-regulation of other photosynthetic electron transport chain components, but we do not find evidence for this since

major thylakoid Fe proteins are unchanged in *paa1* (Figure 3-3, 3-6). An interesting hallmark of Fe deficiency is the over accumulation of Cu and other divalent cations which may be taken up, inadvertently, by the root iron uptake system comprised of the FRO2 root surface ferric reductase and the membrane transporter (IRT1) (Waters *et al.,* 2012; Thomine and Vert 2013). Increased root reductase activity is a well-established marker of systemic, Fe deficiency (Kobayashi and Nishizawa 2012; Jeong *et al.,* 2017). Hydroponically grown *paa1-4* showed an increase in root ferric reductase activity in response to Fe deficiency, similar to Col3 plants (Figure 3-5). We also observed an increase in whole shoot Cu in both the Col3 and *paa1-4* Fe deficient plants (S. Table 3-1). Previously, the *paa1* mutant was shown to be partially rescued by excess Cu feeding (Shikanai *et al.,* 2003). Fe deficient *paa1-4* did recover PC1 and 2 accumulation during Fe deficiency (Figure 3-4), suggesting that both amount of Cu and leaf Cu availability are important in rescuing the *paa1* specific molecular changes. Therefore, in a surprising twist, Fe deficiency seems to somewhat compensate for a loss of *paa1*.

Of the photosynthetic proteins analyzed, only PC and FDX showed lowered accumulation across the *paa1* alleles grown in soil (Figure 3-3). In hydroponics, the *FDX2* transcript abundance was significantly down-regulated in both Col3 and *paa1-4* in response to Fe deficiency. However, on soil FDX accumulation was variable across the alleles. It is well-established that leaf type *FDX* expression in plants is regulated in response to tissue type, light and chloroplast activity (Elliot *et al.,* 1989; Vorst *et al.,* 1993, Dickey *et al.,* 1994). The regulation of *Arabidopsis FDX2* in response to light and the presence of a functional chloroplast involves cis-acting sequences that reside within the transcribed region (Vorst *et al.,* 1993; Caspar and Quail 1993; Bovy *et al.,* 1995). However, the cis-acting elements and transacting factors that mediate *FDX2* expression have not been mapped. A further consideration with respect to FDX maturation is that the biosynthesis of its Fe-S cluster requires SUFB (Hu *et al.,* 2017), which is not altered in *paa1* alleles. Alternatively, *paa1* is defective also in chloroplast Cu/Zn superoxide

dismutase and superoxide accumulation may inhibit FDX protein maturation (Fisher *et al.,* 2016).

The *paa1* mutant may be useful for the analysis of the expression of photosynthesis-related proteins. When compared to single knockout plastocyanin mutants, the effects on electron transport proteins are stronger in *paa1*. A knockout mutation of PC1 (*pete1)* presented no changes in protein abundance of other electron transport proteins, while a knockdown of PC2 (*pete2)* resulted in only slight decreases in Cyt*f* and PSI component accumulation (Pesaresi *et al.,* 2009; Abdel-Ghany 2009). It was not possible to analyze the effects of electron transport in a *pc1/pc2* double mutant, which is seedling lethal (Weigel *et al.,* 2003). Similarly, a null mutation for Rieske, or *petc*, presents with lowered accumulation of Cytb_6 and PSII which results a dramatic block to linear electron flow and strong pleiotropic growth phenotypes and chlorosis (Maiwald *et al.,* 2003). A similar phenotype is observed in the *Arabidopsis* knockout mutant for CCDA, which is required for cytochrome-b_6f biogenesis (Page *et al.,* 2004). Thus, whereas PC single mutants do not affect photosynthesis enough, double PC mutants or mutants with a strong effect on the cytochrome-b_6f complex are not informative regarding signaling due to pleiotropic defects.

3.6 CONCLUSION

In conclusion, the characterization of *paa1* presented here has shed new light on the regulation of Fe-containing photosynthetic electron transport chain proteins and metal homeostasis. The chloroplast response to iron status is maintained in *paa1* at the transcriptional level, which suggests that down-regulation of chloroplast Fe proteins responds to Fe status directly, and not to operational signals from deficiency of photosynthesis. Therefore, the expression of *SUFB*, and *FDX2* can be used as markers for chloroplast Fe deficiency, just as up-regulation of *FRO2* and *IRT1* have been used as markers of systemic Fe deficiency in the roots (Jeong *et al.,* 2017).

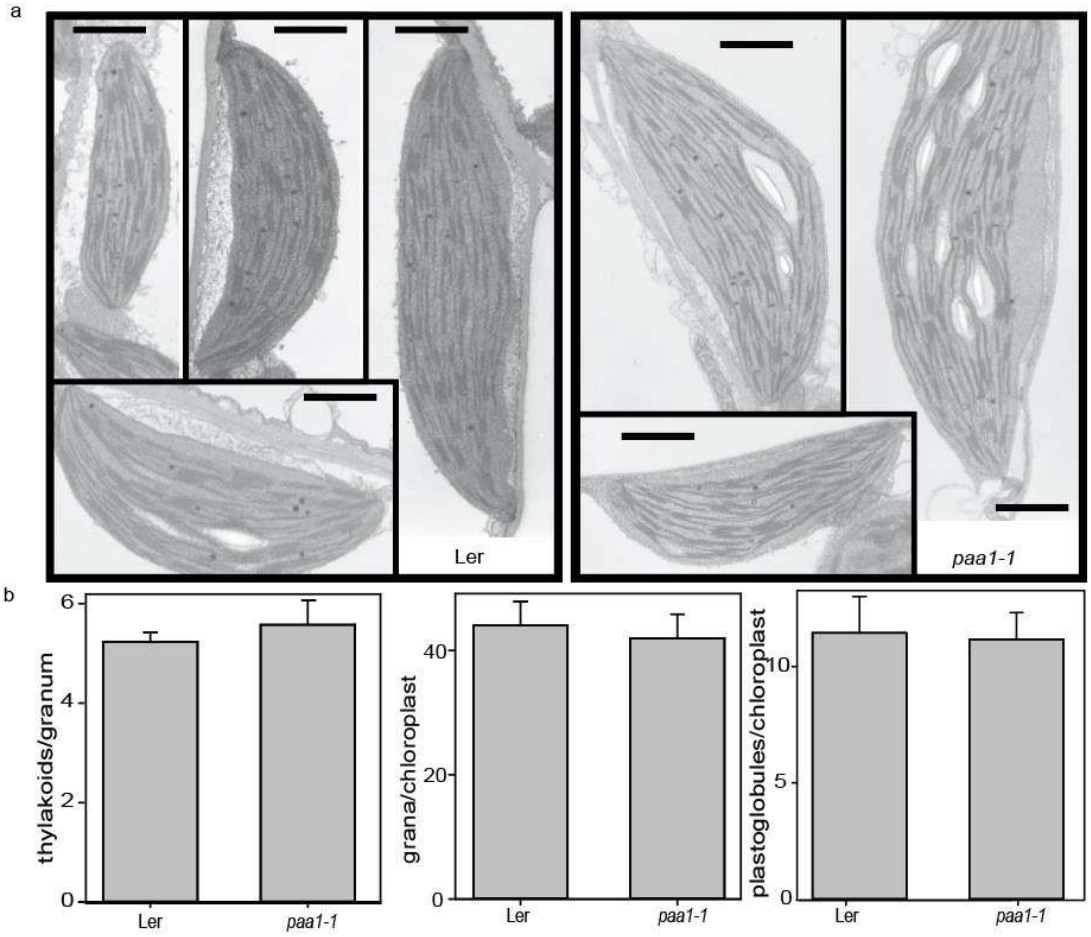

Figure 3-1: Chloroplast anatomy of Ler and *paa1-1*: (a) Representative Transmission Electron microscopy (TEM) images of Ler and *paa1-1* chloroplasts. (b) TEM images were analyzed for number of thylakoid stacks per granum (thylakoids/granum) and the number of grana per chloroplast (grana/chloroplast) as well as the number of plastoglobules per chloroplast. Black bar in images corresponds to 1 μM. Only images that contained a full, well fixed intact chloroplast section were analyzed. The number of thylakoid stacks per granum was estimated by using the measure feature in ImageJ. The measuring scale was set to the cross-section of a known number of grana stacks, and then the remainder of the number of stacks in the grana in the chloroplast section were estimated based on this scale. 13 images of *paa1-1* and 11 images of Ler chloroplasts were quantified. Bars represent averages ± se (n=11-13).

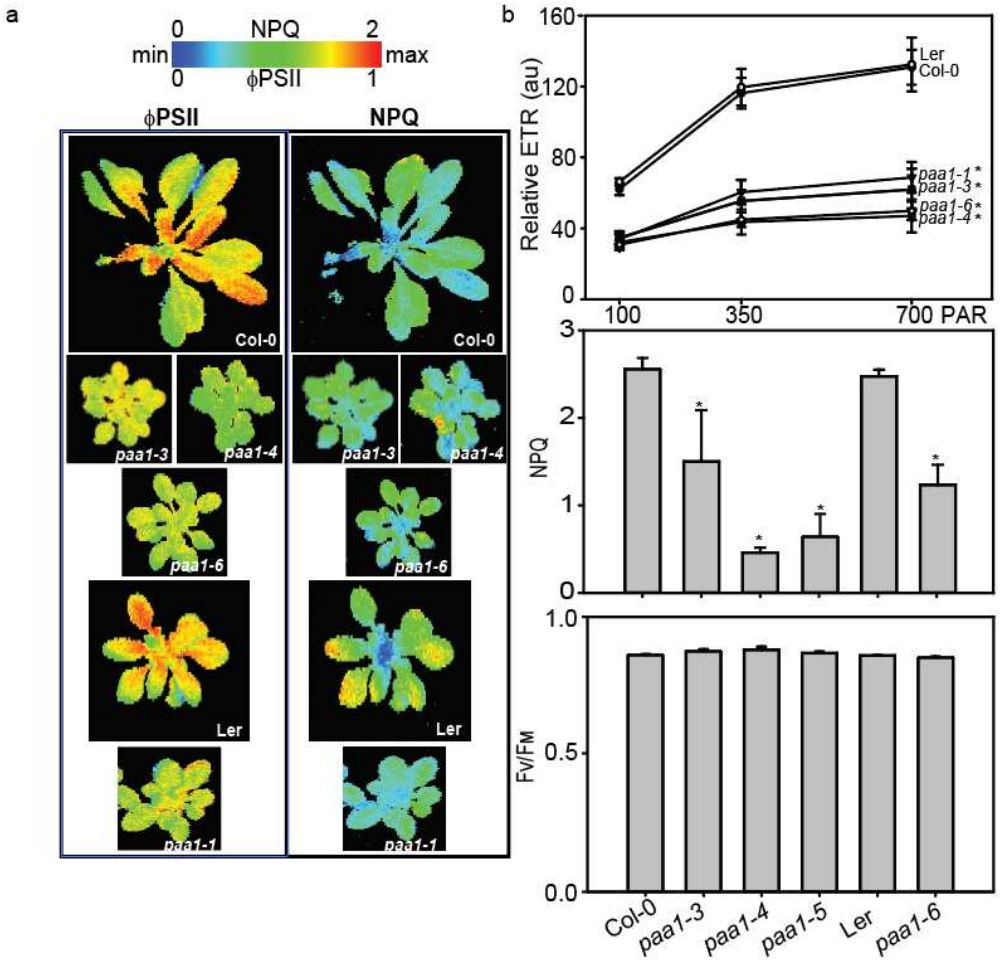

Figure 3-2: *paa1* lines grown in short day conditions on soil are impaired in photosynthetic electron transport downstream of PSII. (a) Representative false color images of the chlorophyll fluorescence parameters flux through PSII (ϕPSII), an estimate of electron transport rate, and non-photochemical quenching (NPQ). The *paa1* lines are grouped with their corresponding wild-type background. (b) Quantitative measurement by chlorophyll fluorescence of relative electron transport rates (ETR) measured at three light intensities (100, 350, and 700 μmol $m^{-2}s^{-1}$), non-photochemical quenching (NPQ) measured at a light intensity of 700 μmol $m^{-2}s^{-1}$, and F_V/F_M. Each point (ETR) and bar (NPQ and F_V/F_M) represents the mean ± se (n=8). Significance of each photosynthetic parameter in the *paa1* line compared to the WT background was determined using a t-test and is denoted by an asterisk.

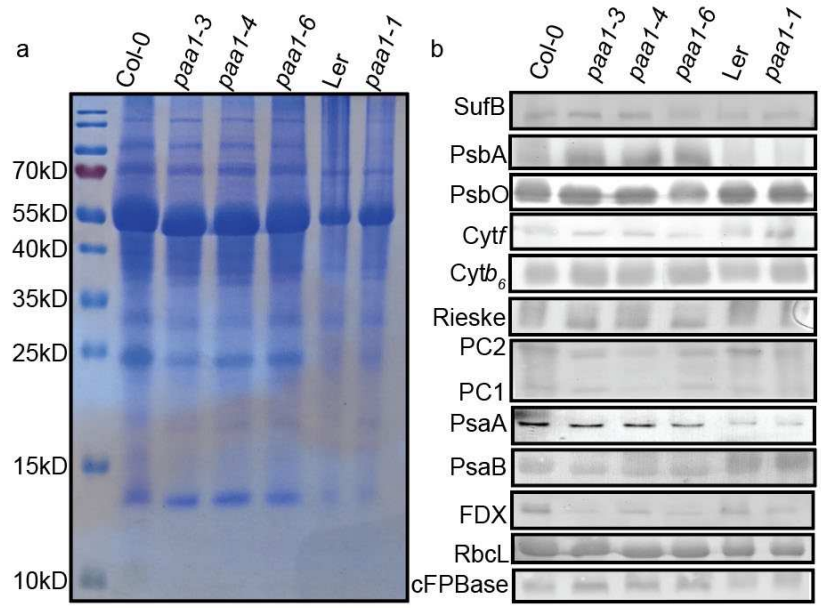

Figure 3-3: Photosynthetic electron transport protein levels are maintained in soil grown *paa1*. (a) Coomassie Brilliant Blue stained gel of total protein in four *paa1* lines compared to the respective WT background. Equal amount of protein was loaded for each mutant and the respective WT background. For mutants in the Columbia background, 60 μg of protein was loaded. For mutants in the Lansberg background, 40 μg of protein was loaded. (b) Immunoblot detection of protein abundance. Antibodies were used for the Fe-S assembly factor SUFB (SUFB), photosystem II subunit A (PsbA), oxygen evolving complex (PsbO), Rieske protein, cytochrome-*f* (Cyt*f*), cytochromeb_6 (Cytb_6), plastocyanin (PC), Photosystem I subunits A and B (PsaA, PsaB), leaf ferredoxin (FDX), RuBisCo large subunit (RbcL), and cytocolic FBPase (cFPBase). cFPBase is included as a loading control. 20 μg of each protein sample was separated on a 15% SDS-PAGE gel and transferred to a 0.2 μm pore Nitrocellulose membrane. Three whole rosettes of each line were collected for one biological replicate and representative images of three biological replicates are presented. All plants were analyzed and sampled 1h after start of the light period when WT plants were six weeks of age (14-16 leaf stage).

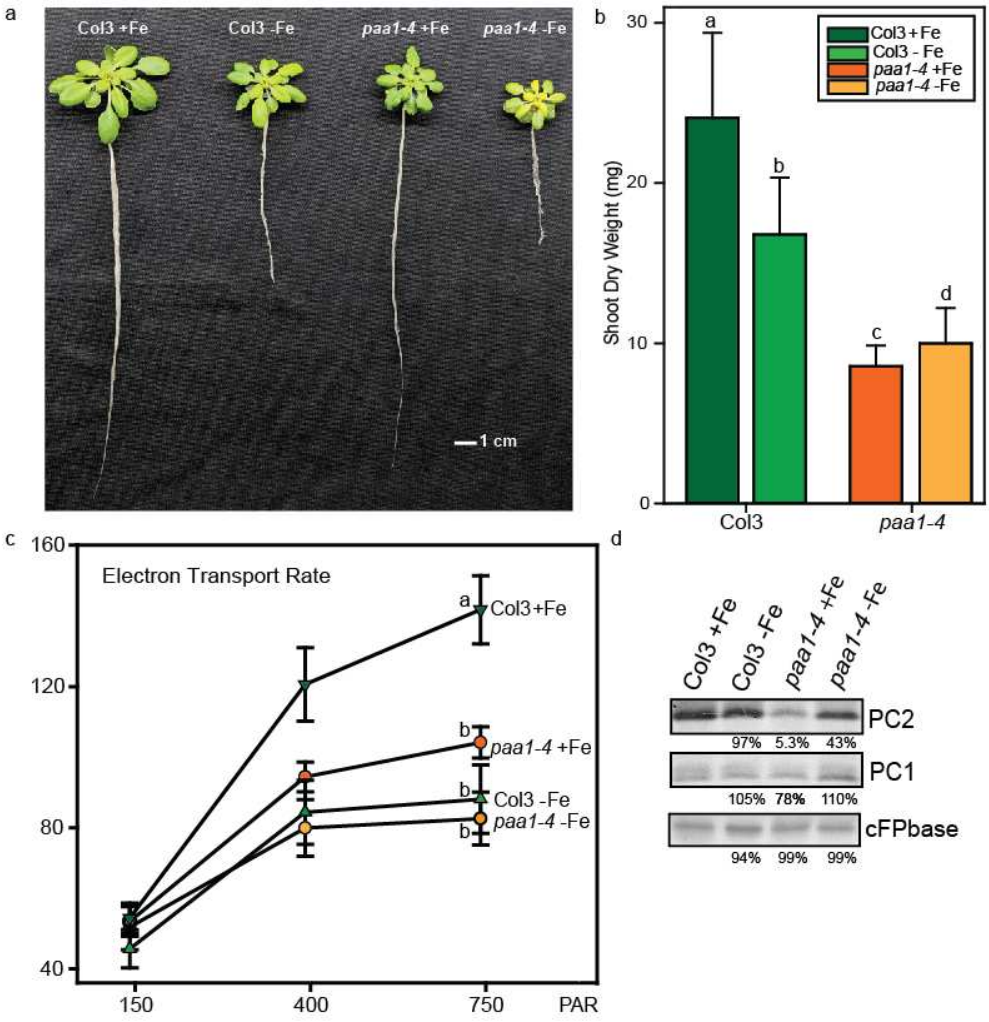

Figure 3-4: Physiological characterization of hydroponically grown *paa1-4:* Four week old hydroponically grown Col3 and *paa1-4* were subject to Fe deficiency (treated) for one week. (a) Representative images of Col3 and *paa1-4* control and Fe deficient plants after one week of Fe deficiency. (b) Accumulation of shoot (n= 22-28) biomass of control and treated Col3 and *paa1-4*. (c) Photosynthetic electron transport by means of chlorophyll fluorescence of control and treated Col3 and *paa1-4.* ETR of hydroponically grown *paa1-4* compared to that of Col3 (n=10). Significance was determined by a 2 factor ANOVA and is denoted by asterisks above bars. Bars represent mean ± se. (d) PC accumulation by western blotting in Col3 and *paa1-4* hydroponically grown plants after 1 week of Fe deficiency. After 7 days of Fe deficiency, rosette samples were flash frozen in liquid N2 and total protein was extracted. 20 μg of each protein sample was separated on a 15% SDS-PAGE gel and transferred to a 0.2 μm pore Nitrocellulose membrane. Band intensity of each treatment group is expressed as a percentage of that of Col3 +Fe. CFPbase is included as a loading control. Representative blot is shown (n=4).

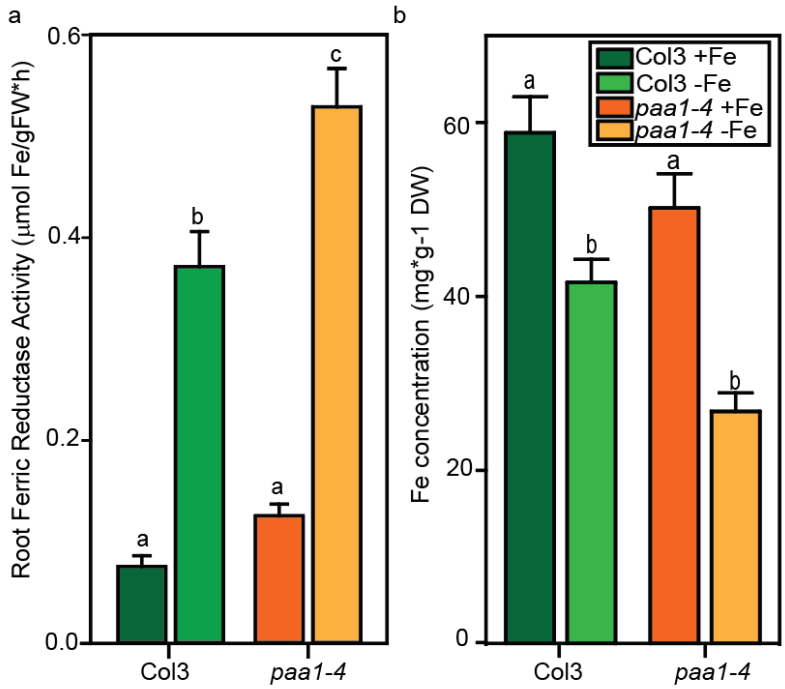

Figure 3-5: Physiological Characterization of Fe deficiency in hydroponically grown *paa1-4*: (a) Root ferric chelate reductase activity of Col3 and *paa1-4* after seven days of Fe deficiency (n=10). (b) Fe concentration of whole rosettes from Col3 and *paa1-4* after seven days of Fe deficiency measured by ICP-OES (n= 11-14). Significance was determined using a two factor ANOVA and is denoted by letters. Bars represent mean ± se.

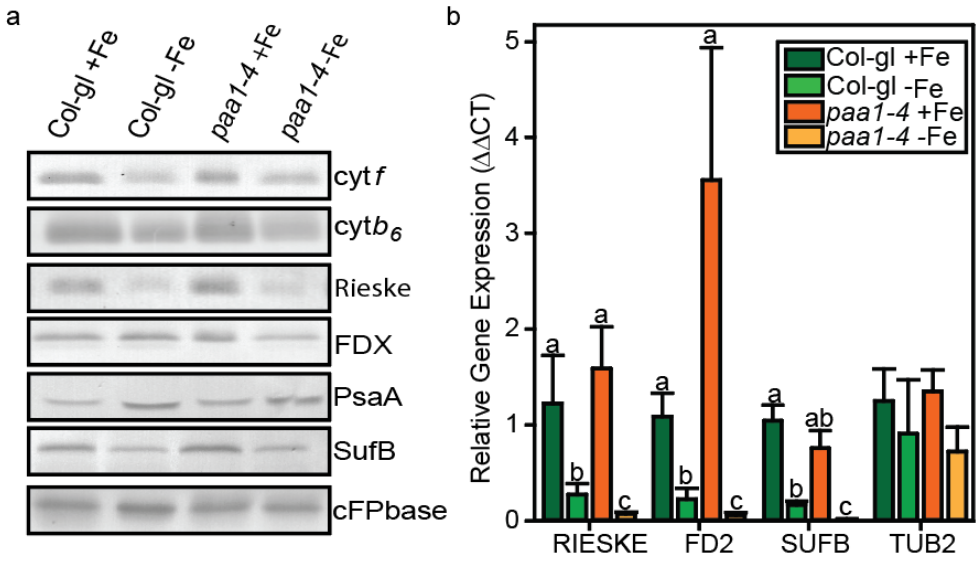

Figure 3-6: Molecular response of chloroplast Fe deficiency markers in *paa1-4*: (a) Selected Protein accumulation in Col3 and *paa1-4*. Analysis of protein abundance was conducted using western blotting. After 7 days of Fe deficiency, rosette samples were flash frozen in liquid N2 and total protein was extracted. 20 μg of each protein sample was separated on a 15% SDS-PAGE gel and transferred to a 0.2 μm pore Nitrocellulose membrane. Representative blots for each protein (n=4). (b) Selected gene expression in Col3 and *paa1-4* by qPCR. Gene expression is normalized to *Ubiquitin 10*. *Tubulin2* is presented as a control gene. Gene expression for each biological rep is calculated based on the mean of at least two technical replicates. Bars represent mean fold change in expression normalized to Col3 control ± se (n=4). Differences in relative expression were analyzed using a 2 factor ANOVA and significance is denoted by an asterisk.

LITERATURE CITED

Abdel-Ghany, SE (2009) Contribution of plastocyanin isoforms to photosynthesis and copper homeostasis in Arabidopsis thaliana grown at different copper regimes. Planta 229: 767-779.

Abdel-Ghany, SE, Müller-Moulé, P, Niyogi, KK, Pilon, M, Shikanai, T (2005) Two P-Type ATPases Are Required for Copper Delivery in Arabidopsis thaliana Chloroplasts. Plant Cell 17: 1233-1251.

Bernal, M, Casero, D, Singh, V, Wilson, GT, Grande, A, Yang, H, Dodani, S, Pellegrini, M, Huijser, P, Connolly, EL, Merchant, SS, Krämer, U (2012) Transcriptome Sequencing Identifies SPL7-Regulated Copper Acquisition Genes FRO4/FRO5 and the Copper Dependence of Iron Homeostasis in Arabidopsis. The Plant Cell 24: 738-761.

Blaby-Haas, CE, Padilla-Benavides, T, Stube, R, Arguello, JM, Merchant, SS (2014) Evolution of a plant-specific copper chaperone family for chloroplast copper homeostasis. Proceedings of the National Academy of Sciences of the United States of America 111: E5480-E5487.

Bovy, A., de, Vrieze, G., Borrias, M. and Weisbeek, P (1992) Transcriptional regulation of the plastocyanin and cytochrome C_{553} genes from the cyanobacterium Anabaena species PCC 7937. Molecular Microbiology 6: 1507-1513.

Bovy, A, Vandenberg, C, Devrieze, G, Thompson, WF, Weisbeek, P, Smeekens, S (1995) Light regulated expression of the Arabidopsis thaliana ferredoxin gene requires sequences upstream and downstream of the transcription initiation site. Plant Molecular Biology 27: 27-39.

Briat, J-F, Dubos, C, Gaymard, F (2015) Iron nutrition, biomass production, and plant product quality. Trends in Plant Science 20: 33-40.

Caspar, T, Quail, PH (1993) Promoter and leader regions involved in the expression of the Arabidopsis ferredoxin A gene. Plant Journal 3: 161-174.

Chan, KX, Phua, SY, Crisp, P, McQuinn, R, Pogson, BJ (2016) Learning the Languages of the Chloroplast: Retrograde Signaling and Beyond. Annual Review of Plant Biology 67: 25-+.

Cohu, CM, Pilon, M (2007) Regulation of superoxide dismutase expression by copper availability. Physiologia Plantarum 129: 747-755.

Conn, SJ, Hocking, B, Dayod, M, Xu, B, Athman, A, Henderson, S, Aukett, L, Conn, V, Shearer, MK, Fuentes, S, Tyerman, SD, Gilliham, M (2013) Protocol: optimising hydroponic growth systems for nutritional and physiological analysis of Arabidopsis thaliana and other plants. Plant Methods 9

Dickey, LF, Nguyen, TT, Allen, GC, Thompson, WF (1994) Light modulation of ferredoxin messenger RNA abundance requires an open reading frame. Plant Cell 6, 1171-1176.

El Mehdawi, AF, Jiang, Y, Guignardi, ZS, Esmat, A, Pilon, M, Pilon-Smits, EAH, Schiavon, M (2018) Influence of sulfate supply on selenium uptake dynamics and expression of sulfate/selenate transporters in selenium hyperaccumulator and nonhyperaccumulator Brassicaceae. New Phytologist 217:194-205.

Elliott, RC, Dickey, LF, White, MJ, Thompson, WF (1989) Cis acting elements for light regulation of pea ferredoxin I gene expression are located within transcribed sequences. Plant Cell 1: 691-698.

Fisher, B, Yarmolinsky, D, Abdel-Ghany, S, Pilon, M, Pilon-Smits, EA, Sagi, M, Van Hoewyk, D (2016) Superoxide generated from the glutathione-mediated reduction of selenite damages the iron-sulfur cluster of chloroplastic ferredoxin. Plant Physiology and Biochemistry 106: 228-235.

Fontaine SL, Quinn J, Merchant S (2002) Comparative Analysis of Copper and Iron Metabolism in Photosynthetic Eukaryotes vs Yeast and Mammals. In: Massaro E.J.

(eds) Handbook of Copper Pharmacology and Toxicology. Humana Press, Totowa, NJ

Friso G, Olinares PDB, van Wijk KJ (2011) The workflow for quantitative proteome analysis of chloroplast development and differentiation, chloroplast mutants, and protein interactions by spectral counting. In Chloroplast Research in Arabidopsis, Jarvis R.P. (ed). pp 265-282, New York, New York

Grusak, MA (1995) Whole root iron(III) reductasae activity throughout the life cycle of iron grown Pisum sativum L (Fabaceae): Relevance to the iron nutrition of developing seeds. Planta 197:111-117.

Hanke, G, Mulo, P (2013) Plant type ferredoxins and ferredoxin-dependent metabolism. Plant Cell and Environment 36: 1071-1084.

Hantzis, LJ, Kroh, GE, Jahn, CE, Cantrell, M, Peers, G, Pilon, M, Ravet, K (2018) A Program for Iron Economy during Deficiency Targets Specific Fe Proteins. Plant Physiology 176: 596-610.

Hill, KL, Merchant, S (1995) Coordinate expression of coproporphyrinogen oxidase and cytochrome c_6 in the green alga Chlamyomonas reinhardtii in response to changes in copper availability. Embo Journal 14: 857-865.

Hoagland DR, and Arnon, D (1938) The water culture method for growing plants without soil. UC College of Agriculture, Ag. Exp. Station, Berkeley, CA. Circular. 347: 1-39

Hu, XY, Kato, Y, Sumida, A, Tanaka, A, Tanaka, R (2017) The SUFBC2D complex is required for the biogenesis of all major classes of plastid Fe-S proteins. Plant Journal 90: 235-248.

Jarvis, P, Lopez-Juez, E (2014) Biogenesis and homeostasis of chloroplasts and other plastids (vol 14, pg 787, 2013). Nature Reviews Molecular Cell Biology 15: 147-147.

Jeong, J, Merkovich, A, Clynel, M, Connolly, EL (2017) Directing iron transport in dicots: regulation of iron acquisition and translocation. Current Opinion in Plant Biology 39: 106-113.

Kastoori Ramamurthy, R, Xiang, Q, Hsieh, E-J, Liu, K, Zhang, C, Waters, BM (2018) New aspects of ironcopper crosstalk uncovered by transcriptomic characterization of Col-0 and the copper uptake mutant spl7 in Arabidopsis thaliana. Metallomics 10: 1824-1840.

Kleine, T, Leister, D (2016) Retrograde signaling: Organelles go networking. Biochimica Et Biophysica Acta-Bioenergetics 1857: 1313-1325.

Kobayashi, T, Nagasaka, S, Senoura, T, Nakanishi, R, Itai, RN, Nakanishi, H, Nishizawa, NK (2013) Iron-binding haemerythrin RING ubiquitin ligases regulate plant iron responses and accumulation. Nature Communications, 4: 2792

Kobayashi, T, Nishizawa, NK (2012) Iron Uptake, Translocation, and Regulation in Higher Plants. Annual Review of Plant Biology 63: 131-152.

Larbi, A, Abadía, A, Abadía, J, Morales, F (2006) Down co-regulation of light absorption, photochemistry, and carboxylation in Fe-deficient plants growing in different environments. Photosynthesis Research 89: 113-126.

Ceballos-Laita, L, Gutierrez-Carbonell, E, Lattanzio, G, Vazquez, S, Conteras-Moreira, B, Abadia, A, Abadia, J, Lopez-Millan, AF (2015) Protein profile of Beta vulgaris leaf apoplastic fluid and changes induced by Fe deficiency and Fe resupply. Frontiers in Plant Science 6

Lin, SJ, Pufahl, RA, Dancis, A, O'Halloran, TV, Culotta, VC (1997) A role for the Saccharomyces cerevisiae ATX1 gene in copper trafficking and iron transport. The Journal of biological chemistry 272: 9215.

Lopez-Millan, AF, Grusak, MA, Abadia, A, Abadia, J (2013) Iron deficiency in plants: an insight from proteomic approaches. Frontiers in Plant Science 4

Lundquist, PK, Poliakov, A, Giacomelli, L, Friso, G, Appel, M, McQuinn, RP, Krasnoff, SB, Rowland, E, Ponnala, L, Sun, Q, van Wijk, KJ (2013) Loss of Plastoglobule Kinases ABC1K1 and ABC1K3 Causes Conditional Degreening, Modified Prenyl-Lipids, and Recruitment of the Jasmonic Acid Pathway. Plant Cell 25: 1818-1839.

Maiwald, D, Dietzmann, A, Jahns, P, Pesaresi, P, Joliot, P, Joliot, A, Levin, JZ, Salamini, F, Leister, D (2003) Knock-out of the genes coding for the Rieske protein and the ATP-synthase delta-subunit of Arabidopsis. Effects on photosynthesis, thylakoid protein composition, and nuclear chloroplast gene expression. Plant Physiology 133: 191-202.

Maxwell, K, Johnson, GN (2000) Chlorophyll fluorescence - a practical guide. Journal of Experimental Botany 51: 659-668.

Merchant, S, Sawaya, MR, 2005. The Light Reactions: A Guide to Recent Acquisitions for the Picture Gallery. 17: 648-663.

Mukherjee, I, Campbell, NH, Ash, JS, Connolly, EL (2006) Expression profiling of the Arabidopsis ferric chelate reductase (FRO) gene family reveals differential regulation by iron and copper. Planta 223: 1178-1190.

Murashige, T, Skoog, F (1962) A revised medium for rapid growth and bio assays with tobacco tissue cultures. Physiologia Plantarum 15: 473-497.

Page, MLD, Hamel, PP, Gabilly, ST, Zegzouti, H, Perea, JV, Alonso, JM, Ecker, JR, Theg, SM, Christensen, SK, Merchant, S (2004) A homolog of prokaryotic thiol disulfide transporter CcdA is required for the assembly of the cytochrome b(6)f complex in Arabidopsis chloroplasts. Journal of Biological Chemistry 279: 32474-32482.

Paolacci, AR, Celletti, S, Catarcione, G, Hawkesford, MJ, Astolfi, S, Ciaffi, M (2014) Iron deprivation results in a rapid but not sustained increase of the expression of genes involved in iron metabolism and sulfate uptake in tomato (Solanum lycopersicum L.) seedlings. Journal of Integrative Plant Biology 56: 88-100.

Perea-García, A, Garcia-Molina, A, Andrés-Colás, N, Vera-Sirera, F, Pérez-Amador, MA, Puig, S, Peñarrubia, L (2013) Arabidopsis copper transport protein COPT2 participates in the cross talk between iron deficiency responses and low-phosphate signaling. Plant physiology 162: 180.

Pesaresi, P, Scharfenberg, M, Weigel, M, Granlund, I, Schroeder, WP, Finazzi, G, Rappaport, F, Masiero, S, Furini, A, Jahns, P, Leister, D (2009) Mutants, Overexpressors, and Interactors of Arabidopsis Plastocyanin Isoforms: Revised Roles of Plastocyanin in Photosynthetic Electron Flow and Thylakoid Redox State. Molecular Plant 2: 236-248.

Pilon-Smits, EAH, Hwang, SB, Lytle, CM, Zhu, YL, Tai, JC, Bravo, RC, Chen, YC, Leustek, T, Terry, N (1999) Overexpression of ATP sulfurylase in Indian mustard leads to increased selenate uptake, reduction, and tolerance. Plant Physiology 119: 123-132.

Qin, G, Gu, H, Zhao, Y, Ma, Z, Shi, G, Yang, Y, Pichersky, E, Chen, H, Liu, M, Chen, Z, Qu, L-J (2005) An Indole-3-Acetic Acid Carboxyl Methyltransferase Regulates Arabidopsis Leaf Development. The Plant Cell 17: 2693-2704

Robinson, NJ, Procter, CM, Connolly, EL, Guerinot, ML (1999) A ferric-chelate reductase for iron uptake from soils. Nature 397: 694-697.

Rodriguez-Celma, J, Pan, I, Li, W, Lan, P, Buckhout, T, Schmidt, W (2013) The transcriptional response of Arabidopsis leaves to Fe deficiency. Frontiers In Plant Science 4,

Schmittgen, TD, Livak, KJ (2008) Analyzing real-time PCR data by the comparative C-T method. Nature Protocols 3: 1101-1108.

Shikanai, T, Muller-Moule, P, Munekage, Y, Niyogi, KK, Pilon, M (2003) PAA1, a P-type ATPase of Arabidopsis, functions in copper transport in chloroplasts. Plant Cell 15: 1333-1346.

Takanori, K, Seiji, N, Takeshi, S, Reiko Nakanishi, I, Hiromi, N, Naoko, KN (2013) Iron-binding haemerythrin RING ubiquitin ligases regulate plant iron responses and accumulation. Nature Communications 4

Tapken, W, Ravet, K, Pilon, M (2012) Plastocyanin Controls the Stabilization of the Thylakoid Cu-transporting P-type ATPase PAA2/HMA8 in Response to Low Copper in Arabidopsis. Journal of Biological Chemistry 287: 18544-18550.

Thomine, S, Vert, G (2013) Iron transport in plants: better be safe than sorry. Current Opinion in Plant Biology 16: 322-327.

Udvardi, MK, Czechowski, T, Scheible, WR (2008) Eleven golden rules of quantitative RT-PCR. Plant Cell 20: 1736-1737.

Vorst, O, Vandam, F, Weisbeek, P, Smeekens, S (1993) Light regulated expression of the Arabidopsis thaliana ferredoxin A gene involves both transcriptional and post transcriptional processes. Plant Journal 3: 793-803.

Waters, BM, Armbrust, LC (2013) Optimal copper supply is required for normal plant iron deficiency responses. Plant Signaling & Behavior 8

Waters, BM, McInturf, SA, Stein, RJ (2012) Rosette iron deficiency transcript and microRNA profiling reveals links between copper and iron homeostasis in Arabidopsis thaliana. Journal of Experimental Botany 63: 5903-5918.

Wise RR.(2006) The diversity of plastid form and function. In The Structure and Function of Plastids. Wise RR and Hoober JK (eds). Springer, The Netherlands pp 3-26

Weigel, M, Varotto, C, Pesaresi, P, Finazzi, G, Rappaport, F, Salamini, F, Leister, D (2003) Plastocyanin is indispensable for photosynthetic electron flow in Arabidopsis thaliana. Journal of Biological Chemistry 278: 31286-31289.

Wintz, H, Fox, T, Wu, Y-Y, Feng, V, Chen, W, Chang, H-S, Zhu, T, Vulpe, C (2003) Expression profiles of Arabidopsis thaliana in mineral deficiencies reveal novel transporters involved in metal homeostasis. The Journal of biological chemistry 278: 47644-47653.

Yuan, DS, Stearman, R, Dancis, A, Dunn, T, Beeler, T, Klausner, RD (1995) The Menkes/Wilson disease gene homologue in yeast provides copper to a ceruloplasmin-

like oxidase required for iron uptake. Proceedings of the National Academy of Sciences of the United States of America 92: 2632.

Zhang, L, McSpadden, B, Pakrasi, H, Whitmarsh, J (1992) Copper-mediated regulation of cytochrome c sub(553) and plastocyanin in the cyanobacterium Synechocystis 6803. Journal of Biological Chemistry 267: 19054-19059.

Zhu, XF, Wang, B, Song, WF, Zheng, SJ, Shen, RF (2016) Putrescine Alleviates Iron Deficiency via NO-Dependent Reutilization of Root Cell-Wall Fe in Arabidopsis. Plant Physiology 170: 558.

CHAPTER 4: IRON DEFICIENCY AND LOSS OF THE CHLOROPLAST IRON-SULFUR CLUSTER ASSEMBLY PROTEIN SUFB TRIGGER OPPOSITIE TRANSCRIPTIONAL RESPONSES IN *ARABIDOPSIS* LEAVES

4.1 SUMMARY

Iron (Fe) deficiency in the leaf results in reduced abundance of several abundant iron-sulfur (Fe-S) cluster proteins of the chloroplast which function in photosynthesis. Therefore, photosynthesis becomes impaired during Fe deficiency. The down-regulation of these abundant plastid Fe-S proteins could be a direct response of sensing low Fe, or could be a result of the down-regulation of the machinery for the assembly of Fe-S cofactors. Specifically, the transcription of *SUFB*, a key component of the plastid Iron-Sulfur (Fe-S) assembly pathway which is required for maturation of all Fe-S containing plastid proteins, is down-regulated early after Fe deficiency is sensed, but prior to the down-regulation of mRNAs encoding abundant chloroplast Fe containing proteins. How the leaf transcriptional response to low Fe is regulated is unclear. In order to identify possible early regulated targets and targets that are co-regulated with mRNA encoding for SUFB and abundant Fe proteins we performed a transcriptome analysis. To investigate if the transcript level down-regulation of *SUFB* is a key regulatory step required for further transcriptional reprogramming under low Fe by limiting Fe-S availability, we compared the transcriptional response of WT Fe deficiency (WT-Fe) in vegetative *Arabidopsis* shoots with that of an inducible *sufb*-RNAi knockdown line that produces less Fe-S clusters. Surprisingly, WT-Fe and the *sufb*-RNAi knockdown presented opposite transcriptional responses. In addition, in the WT-Fe treatment, we identified three ERF transcription factors that are differentially expressed within 26 h after low Fe treatment and found that early regulation of the leaf Fe deficiency response preferentially targets chloroplast localized gene products. Additionally, we found *SUFA*, a putative chloroplast Fe-S cluster carrier protein, expression is

up-regulated when the *sufb*-RNAi knockdown is induced. The results suggest that the regulation of chloroplast Fe-S assembly is downstream of initial Fe deficiency sensing and may, instead, be required to coordinate Fe-S availability with the later down-regulation of Fe-S requiring photosynthetic proteins.

4.2 INTRODUCTION

Iron (Fe) deficiency is common in plants because soil Fe is predominantly found in the ferric Fe form which is not readily available to plants. Plants and other photosynthetic organisms have a high requirement for Fe since it is used as a protein cofactor for functions such as Nitrogen (N) (Tejada-Jimenez *et al.,* 2019) and Sulfur (S) assimilation (Takahashi *et al*., 2011), photosynthetic electron transport (Merchant and Sawaya, 2005), mitochondrial metabolism (Jain and Connolly, 2013), reactive oxygen species (ROS) scavenging (Ravet and Pilon, 2013), and chlorophyll biosynthesis (Tanaka and Tanaka, 2019). Fe is especially important for photosynthesis where one photosynthetic electron transport chain requires at least 24 Fe atoms (Merchant and Sawaya, 2005). Perhaps unsurprisingly, because of the large Fe requirement, photosynthesis is decreased during Fe deficiency (Lopez-Milan *et al*., 2013; Glaesener *et al*., 2013). In order to minimize negative impacts, photosynthetic organisms including plants can respond to Fe deficiency with multiple strategies. They can (1) attempt to increase uptake of Fe from the environment (Robinson *et a.,* 1999; Vert *et al.,* 2002), (2) remodel metabolism to become less dependent on Fe (Laganowsky *et al.,* 2009; Urzica *et al*., 2012; Rodriquez-Celma *et al.,* 2013) and (3) prioritize the use of Fe for specific functions over others, a concept known as Fe economy (Glaesener *et al*., 2013).

In the *Arabidopsis* Fe economy response, the leaf prioritizes mitochondrial function over that of the chloroplast (Hantzis *et al*., 2018), which normally contains about 80% of leaf Fe (Shikanai *et al*., 2003). The leaf specifically decreases abundance of highly expressed Fe-requiring chloroplast proteins, such as the Cytochrome-b_6f (Cyt-b_6f) complex and Ferredoxin 2

(FDX2), which may help to increase Fe for prioritized pathways such as respiration in the mitochondria. *Arabidopsis* also limits Fe sequestration during deficiency by down-regulating expression of Vacuolar Iron Transporter 1 (VIT1) which imports Fe into the vacuole (Gollhofer *et al*., 2014) and Ferritins (FER), which are plastid Fe storage molecules (Ravet *et al*., 2009; Tissot *et al*., 2019) while up-regulating NRAMP3/4 which serves to export Fe from the vacuole (Lanquar *et al*., 2005).

The decrease in abundance of photosynthetic proteins may be partially due to the down-regulation of plastid Fe-S assembly machinery. Of the three types of Fe cofactors, heme, non-heme iron, and iron-sulfur (Fe-S) clusters, the latter seems the most affected (Hantzis *et al*., 2018). Indeed, plastid Fe-S cluster assembly by the so called *suf* pathway is among the most affected chloroplast pathways during Fe deficiency (Pan *et al*., 2015; Rodriguez-Celma *et al*., 2013; Hantzis *et al*., 2018). SUF-mediated Fe-S assembly begins with the two-component cysteine desulfurase, made up of a protein called CpNIFS, which is now called SUFS, together with the SUFE1 protein. The SUFS/SUFE1 complex serves to efficiently remove a S atom from cysteine, an essential function (Pilon-Smits *et al*., 2002; Ye *et al*., 2006; Van Hoewyk *et al*., 2007). The S is subsequently incorporated into an Fe-S cluster on the SUFBCD major assembly scaffold (For a review see Balk and Pilon 2011). Finally, transfer proteins in the SUF pathways help with maturation and insertion of Fe-S clusters into required proteins. The strongest evidence for function as plastid Fe-S transfer proteins is provided for the three NFU proteins (Touraine *et al.,* 2004; Yabe *et al.,* 2004) and for HCF101 (Schwenkert *et al*., 2009) as *Arabidopsis* knockout lines of any of these proteins exhibit defects in maturation of specific Fe-S requiring proteins (Touraine *et al.,* 2004; Yabe *et al.,* 2004; Schwenkert *et al*., 2009). Other candidate Fe-S transfer proteins include SUFA (Abdel-Ghany *et al.,* 2005; Yabe and Nakai, 2006) and Monothiol Glutaredoxins (Bandyopadhyay *et al.,* 2008). In severe Fe deficiency, SUFB, SUFE2, NFU2, SUFA, and HCF101 been found to decrease in abundance at the protein stability level in response to Fe deficiency (Pan *et al*., 2015). In mild Fe deficiency, only SUFB

and SUFA decrease at the protein level, while SUFE1, HCF101, and NFU2 remain abundant (Hantzis *et al*., 2018). However, in both mild and severe Fe deficiency, SUFB is the only SUF pathway protein that is transcriptionally regulated and is down-regulated early in response to Fe deficiency (Xu *et al*., 2005; Rodriguez-Celma *et al*., 2013; Liang *et al*., 2014; Pan *et al*., 2015; Hantzis *et al*., 2018).

The SUF pathway is required for maturation of all Fe-S containing photosynthetic electron transport proteins in plants (Hu *et al*., 2017). In dexamethasone (DEX) inducible *sufb*-RNAi knockdown lines, all Fe-S containing photosynthetic proteins decreased in accumulation (Hu *et al*., 2017). Thus, the induced *sufb*-RNAi knockdown results in a similar photosynthetic response as chloroplast Fe deficiency response, at least at the protein stability level (Hu *et al*., 2017). With mild Fe deficiency, the Cyt-b_6f complex and FDX2 are down-regulated early, but Fe requiring subunits of Photosystem-I (PSI) remained abundant (Hantzis *et al*., 2018). In this regard, mild Fe deficiency and lack of SUFB differ in their effects on PSI while in both cases the Cyt-b_6f complex and FDX protein level are severely decreased.

The regulation of the root Fe deficiency response is well characterized and is regulated both transcriptionally and post transcriptionally (Kobayashi 2019). When Fe deficient, plants increase root Fe uptake (Brumbarova *et al*., 2015; Jeong *et al*., 2017; Kobayashi 2019). *Arabidopsis* responds to Fe deficiency by first acidifying the soil by a root epidermis localized proton pump to solubilize Fe (Santi and Schmidt, 2009). Then ferric Fe is reduced to ferrous Fe via the Ferric Reductase Chelatase 2 (FRO2) enzyme on the root epidermis (Robinson *et al*., 1999). Finally, ferrous Fe can be taken up by the Iron-Regulated Transporter 1 (IRT1) (Vert *et al*., 2002). *Arabidopsis* FRO2 and IRT1 are up-regulated during low Fe via a cascade of Basic Helix Loop Helix (bHLH) transcription factors (TF) in which bHLH class IV TFs interact with another bHLH protein, ILR3/bHLH105, to initiate transcription of FER Like Fe Deficiency Induced Transcription Factor (FIT) expression (Colangelo and Guerinot, 2004; Jakoby *et al*., 2004; Yuan *et al*., 2008). FIT is an orthologue of FER, a bHLH TF that regulates Fe deficiency

responses in tomato (Ling *et al*., 2002). FIT interacts with bHLH class Ib TFs, bHLH38/39 to up-regulate the expression of FRO2 and IRT1 (Bauer *et al.*, 2007). FITalso with bHLH100/101 which are proposed to regulate Fe distribution within the plant (Sivitz *et al*., 2012). IRT1 protein is also regulated post transcriptionally via a E3 ubiquitin ligase (Shin *et al*., 2013) and the bHLH regulatory cascade is negatively regulated by another ubiquitin ligase, Brutus (BTS) (Long *et al.,* 2010; Hindt *et al*., 2017; Rodriguez-Celma *et al.,* 2019). Fe sequestration is also regulated via bHLH transcription factors Popeye (PYE) and ILR3/bHLH105 and post transcriptionally via BTS (Tissot *et al.,* 2019). In *Arabidopsis,* two MYB transcription factors, MYB10 and MYB72 are also reported to regulate root Fe deficiency responses by driving expression of NAS4, a Fe deficiency induced nicotianamine synthase gene (Palmer *et al*., 2013). Recently, the Ethylene Response Transcription Factor (ERF) family has also been linked to regulation of root and systemic Fe deficiency (Lingam *et al*., 2011; Kastoori Ramamurthy *et al.,* 2019; Zhang *et al*., 2019). To date, the only specific target of ERF family transcription factors in Fe deficiency is FIT which is stabilized during Fe deficiency by the ERF transcription factors, Ethylene Insensitive 1 (EIN1) and EIN3 (Lingam *et al*., 2011).

Compared to what we know about the root Fe deficiency response, our understanding of how the Fe deficiency response in the leaf is regulated is limited. The regulation of SUFB may be important in coordinating down-regulation of photosynthetic proteins with Fe-S cluster availability as photosynthetic proteins require Fe-S clusters. Therefore, the transcriptional regulation of photosynthetic proteins during Fe deficiency may be a result of a decrease in Fe-S cluster availability during Fe deficiency. While class IV bHLH TFs, IRL3/bHLH105, PYE, and class 1b bHLH TFs, bHLH101, bHLH100 are expressed in the shoots (Long *et al*., 2010; Sivitz *et al*., 2012; Rodriguez-Celma *et al*., 2013), *SUFB* does not have bHLH *cis* elements enriched in its promoter (Hantzis *et al*., 2018). Thus, so far undiscovered mechanisms of regulation must be required to initiate changes to chloroplast proteins during Fe deficiency.

Fe-S clusters are important in Fe homeostasis in a broad range of organisms. The *suf* pathway found in plants is conserved from bacterial lineages. The *E. coli suf* operon is specifically induced in response to oxidative stress and Fe starvation. *E. coli* mutants lacking the *suf* operon had a decreased growth rate during Fe deficiency compared to wild type *E. coli*, suggesting that the *suf* operon may be essential for Fe-S assembly during Fe starvation (Outten *et al*., 2004). Fe-S availability is also important in the yeast regulation of Fe homeostasis (Ojeda *et al*., 2006). The yeast transcription factors, Aft1 and Aft2 regulate Fe deficiency gene expression changes. The ability of Aft1 to induce transcription is dependent on two monothiol glutaredoxins, Grx3 and Grx4 (Kumanovics *et al*., 2008). When Grx3 and 4 are bridged by an Fe-S cluster, they bind Aft1 and inhibit transcriptional up-regulation of iron acquisition related genes (Poor *et al*., 2014). During Fe starvation, the Fe-S cluster is removed and Aft1 can bind promoter regions of DNA to initiate the Fe deficiency response.

In plants, the SUF pathway is integral to maintaining photosynthetic proteins, and it is a major target of regulation during leaf Fe deficiency. Specifically, *SUFB* is down-regulated early after Fe deficiency is sensed, but prior to the decrease of mRNAs encoding abundant chloroplast Fe containing proteins. Therefore, it is possible that a decrease in SUFB leading to a decrease in chloroplast Fe-S availability could act as a trigger for the transcriptional regulation of the chloroplast Fe deficiency response. Alternatively, the down-regulation of SUFB could be a required response to coordinate down-regulation of Fe-S containing photosynthetic proteins with Fe-S availability. We investigated if the down-regulation of *SUFB* transcription affects regulatory steps required for further transcriptional reprograming in Fe deficiency. We compared the transcriptional response of SUFB down-regulation in leaves by inducible RNAi knockdown of *Arabidopsis SUFB* with the transcriptomic responses of *Arabidopsis* wild-type (WT) early after Fe limitation. Interestingly, the transcriptome response of plants to loss of SUFB and to Fe deficiency was opposite in that no Fe responsive transcripts are differentially expressed in the

sufb-RNAi knockdown. In addition, we found that the *SUFA* transcript, which is not Fe responsive, is significantly up-regulated in the *sufb*-RNAi knockdown.

4.3 METHODS

Plant lines. The Dexamethasone (DEX) inducible RNAi knockdown mutants *sufb1-12, sufb2-2, sufc2-10-2, and sufd2-13* were a gift from Dr. Ryouichi Tanaka (Hokkaido University, Sapporo, Japan) and are described in Hu *et al*. (2017). Knockout lines for *sufa1-2* were obtained from the Arabidopsis Biological Resource Center (Ohio State University). RNAi lines of *grsx3,4,5,7,8* were a gift from Dr. Matthew Escobar (California State University, San Marcos).

Plant growth and sampling. The *sufb, sufc, and sufd*-RNAi lines were grown alongside Col-0 hydroponically, similar to the procedure outlined in Conn *et al*., (2013). Opaque microcentrifuge caps containing a 2 mm hole were filled with 400 μL of ½ MS medium containing 0.7% agar and seeds were placed on the MS agar for germination. Seeded agar filled caps were placed in hydroponic tubs containing deionized water, covered with plastic wrap to increase humidity, and stratified at 4°C for 4 days in the dark. Tubs were then transferred to a growth room (23°C, 8 h: 16 h light dark cycle) and grown at a light intensity of 200 μmol $m^{-2}s^{-1}$ (Fluence RAZR4 LED). When plants germinated, they were transferred to 1/15th strength Hoagland's solution. After two weeks of growth they were transferred to 1/10th strength Hoagland's and then to 1/5th strength four days later. Final salt concentrations in the 1/5th Hoagland's solution were 0.3 mM NH_4NO_3, 1 mM $Ca(NO_3)_2$, 1.4 mM KNO_3, 0.2 mM KH_2PO_4, 0.4 mM $MgSO_4$, 6.6 mM $MgCl_2$, 12.3 μM H_3BO_3, 2.4 μM $MnSO_4$, 0.2 μM $ZnSO_4$, 0.03 μM MoO_3, 0.5 μM $CuSO_4$, 10 μM Fe(III)EDTA (Hoagland and Arnon, 1938). The *sufb, sufc,* and *sufd*-RNAi lines were maintained on sufficient Fe conditions throughout the experiment. To induce Fe deficiency in Col-0, plants that were four weeks old (10 -14 leaf stage) were transferred to 1/5th

Hoagland's supplemented with 10 nM Fe(III)EDTA, whereas control groups were maintained at 10 μM Fe(III)EDTA (Hantzis *et al*., 2018).

For RNA-sequencing, *sufb2-2* was chosen as a representative line. 26 days after stratification, *sufb2-2* and Col-0 hydroponic grown plants were foliar sprayed with 15 μM DEX (Sigma Aldrich, St. Louis MO) in 0.02% tween (v/v) (Bio-Rad, Hercules, CA) to ensure induction of the RNAi transcript for RNA-sequencing. All plants were sprayed with the DEX solution in a chemical fume hood. Two days later at 4 weeks of age, half of the Col-0 plants were transferred to low Fe (Figure 4-1a). Samples of *sufb2-2*, WT+Fe, and WT-Fe for RNA sequencing were taken at 2 h (Timepoint (TP A)) and 26 h (TP B) after Col-0 was transferred to low Fe. TP A was 2 days after DEX treatment, and TP B was 3 days after DEX treatment. All sampling was done 2 h after the onset of the light period. Three whole rosettes were pooled into one biological replicate and 3 biological replicates were sequenced. Samples were also taken for protein analysis at TP B and 7 days after low Fe treatment and 9 days after DEX treatment (TP C). For all other experiments with *sufb, sufc, and sufd* lines, plants were foliar sprayed with 10 μM DEX in 0.02% tween (v/v) which was determined to be sufficient for RNAi induction (Hu *et al*., 2017).

For analysis of *sufa* and *grxs* responses to Fe deficiency, seeds were sowed on nutrient agar containing Fe as outlined in Rodriguez-Celma *et al*. (2013). Seven days after growth on full nutrient agar with 40 μM Fe(III)EDTA, half of each line was transferred to low Fe plates containing no Fe and Ferrozine to sequester excess Fe while the other half was maintained at 40 μM Fe(III)EDTA. 7 days after transfer to low Fe plates, shoots were collected for protein and transcript analysis, and nutrient composition.

RNA-sequencing. Rosette samples for RNA-sequencing were flash frozen in liquid nitrogen. Tissue was homogenized using a Qiagen Tissue Lyser and RNA was isolated using a Qiagen RNeasy Plant Mini Kit. RNA quality was assessed by an Aligent Tapestation 4200 using a high sensitivity RNA screen tape. RNA quantity was measured with a Qubit 2.0 Fluorometer

using a broad range assay kit and between 25 and 60 ng/μL RNA of each sample was sent to Novogene Corp. (Davis, CA) for library preparation, RNA-sequencing, and bioinformatic analysis. Library preparation was done using poly-A selection for nuclear encoded mRNA. RNA was sequenced at a depth of 150 paired end reads for a sequencing coverage of at least 55 x 10^6 reads per sample.

Bioinformatic analysis. Reads from Illumina sequencing were trimmed for quality and to remove adapter sequences by Novogene. Reads were aligned and mapped to the TAIR10 genome using HISAT2 2.1.0 beta (Kim *et al*., 2015) and FPKM values were calculated using HTseq v0.6.1 (Anders *et al*., 2015). Differential expression was determined using DEseq version 1.10.1 and p-value was adjusted using Bonferroni adjustment. The differential expression threshold was set at a fold change of 1.5x and a p-value of less than 0.05. Differential expression at each timepoint within and across WT-Fe and *sufb2-2* +Fe treatments were compared using Interactivenn (Heberle *et al*., 2015).

Promoter analysis to determine putative transcription factor binding was done by analyzing promoter sequences of differentially expressed genes at TP B in AthaMap (http://www.athamap.de/search_gene.php; Bulow *et al*., 2010). Promoter region was set to 1000 bp upstream of the start site of transcription. To determine if specific *cis* elements were over enriched in the differentially expressed genes (DEGs) from our RNA-seq compared to the rest of the genome, we used the TAIR Motif Search (https://www.arabidopsis.org/tools/bulk/motiffinder/index.jsp). Promoter region was set to 1000 bp upstream of the start of transcription and *cis* elements were only reported if they occurred more than 3 times in a promoter. Enrichment of *cis* elements was determined if the probability of motif occurrence in DEG promoters was significantly higher than the probability of motif occurrence across the *Arabidopsis* genome ($p<0.05$). *Cis* elements analyzed were as follows: the E-Box for bHLH (CANNTG; Toledo-Ortiz *et al*., 2003), the GCC-Box for ERF (GCCGCC; Hao *et al*., 1998), and the motif GATATT for RVE MYB (Franco-Zorrilla *et al*., 2014).

To determine conservation of the transcription factors, ERF53, RA2.12, and CRF2, sequences were taken from NCBI for *Phaseolus vulgaris, Glycine max, Populus, Vitis vinifera, Arabidopsis thaliana, Brassica napus, Oryza sativa, Zea mays, Physcomitrella patens, and the* cyananobacterium *Synechococcales bacterium UBA10510.* Sequences from *Populus* were taken from species with sequences most similar to *Arabidopsis thaliana:* the ERF53 sequence was from *Populus euphratica;* the CRF2 sequence was from *Populus tomentosa;* RA2.12 sequence was from *Populus trichocarpa.* Sequences were aligned in MEGA X (Kumar *et al*., 2018) by Muscle and phylogenic analysis was analyzed by the maximum likelihood method (Jones *et al.,* 1992). The consensus tree is a representative of 500 replicates and numbers on the branches represent the percentage of replicates in which the taxa cluster together in the bootstrap test (Felsenstein, 1985). For presentation purposes, alignments were constructed by M-coffee (Notredame *et al*., 2000) and the AP2 domain was determined using ScanProsite (De Castro *et al*., 2006).

Gene expression analysis via qPCR. For gene expression (mRNA level) analysis of hydroponically grown plants using qPCR, three rosettes were pooled for one biological replicate, and 3 biological replicates were analyzed. For gene expression analysis of seedlings grown on plates, 10 shoots were pooled for one biological replicate and 3-4 biological replicates were analyzed. Tissue was homogenized using a Qiagen tissue lyser and RNA was isolated using the TRIzol extraction method. 2 μg of RNA was treated with 12 U DNAse I (Invitrogen, Carlsbad, CA) and cDNA was synthesized using superscript III cDNA synthesis kit (Invitrogen, Carlsbad, CA). For qPCR, each biological replicate was run in two technical replicates. A second RNA sample from each biological replicate was treated with DNAse I only, to serve as a -RT control. Gene expression (relative transcript abundance) was normalized to expression of *Ubiquitin 10* (*UBQ10*) and then to the level of gene expression of WT +Fe using the ΔΔCT method

(Schmittgen and Livak, 2008). All primers were tested for 95% efficiency or better and were designed according to Udvardi *et al*. (2008) and are listed in Dissertation Chapter 3.

Protein analysis. Three rosettes per sample for hydroponically grown plants and 10 shoots per sample of plate grown seedlings were pooled for protein analysis. At least 3 biological reps were analyzed. Total protein was extracted using the method outlined by Friso *et al*. (2011) and concentration was quantified by the Pierce Rapid Gold BCA protein quantification kit (Pierce, Rockford, Il). For western blotting, samples were denatured by heating at 95^{o}C and treatment with 100 mM DTT. 20 μg protein per sample was separated by SDS-PAGE (15% gel). After separation, proteins were transferred to a 0.2 μM pore nitrocellulose membrane. Primary antibodies for FDX, Cyt*f,* Cytb_6*,* Rieske, PSaA, and cFPbase were obtained from Agrisera (Vannas, Sweden). Primary antibody for SUFB was a gift from Dr. Nicolas Rouhier (Université de Lorraine, Nancy, France). Detection of secondary antibodies was by alkaline phosphatase (Sigma Aldrich, St. Louis, MO). For protein quantification, a dilution series of a WT+Fe sample was included. Blot images were scanned into a computer to generate a TIFF file and then intensity of bands was measured using Image Studio Lite by LiCor (Lincoln, NE) and a standard curve was generated to compare intensity of other samples from the same gel.

Elemental Analysis. Shoot elemental analysis was analyzed at TP C for hydroponic experiments. Two rosettes were pooled for one biological replicate and tissue was dried at 60^{o}C for two weeks and then digested in HNO_3 (Pilon-Smits *et al*., 1999). Digested samples were resuspended in 1% HNO_3 and analyzed on an ICP-OES. Concentration of elements in each sample was normalized by dry weight. At least 7 biological reps of each treatment were analyzed.

Ferric Chelate Reductase Activity. Root Fe reductase activity was measured at TP C according to Grusak (1995). One whole root system was measured per replicate. Roots were excised from the plant and were rinsed twice with 1/5th strength Hoagland's solution without Fe

to rinse off Fe from the hydroponic solution. Roots were then transferred to the assay solution which contained 1/5th Hoagland's, 100 μM Fe(III)EDTA and 100 μM bathophenanthrolinedisulfonic acid (BPDS). After 30 minutes in the assay solution, roots were removed, patted dried and weighed. The absorbance of the assay solution was measured at 535 nm and used to calculate the reductase activity. Reductase activity was calculated on a root fresh weight basis. At least 5 root systems per treatment were analyzed.

Chlorophyll Fluorescence. Chlorophyll fluorescence was measured to assess photosynthetic capacity of plants at TP C. False color images were taken using a FluorCam Quenching Analysis setting (Photo Systems Instruments, Brno, Czech Republic). A whole *Arabidopsis* plant was used for measurements and measurements were taken under a light intensity of 100 μmol m^{-2} s^{-1}. Plants were dark adapted for 30 min and parameters, ϕPSII and NPQ were calculated according to Maxwell and Johnson (2000).

Statistical Analysis. A 2 factor ANOVA was run in R version 3.4.4 to determine differences between treated and control plants (p value <0.05). A Tukey test was used to determine which treatment groups were significant in the ANOVA using the lsmeans R package. Data visualization was done using Sigma Plot version 7.4 and BioVinci version 1.15.

4.4 RESULTS

Induction of sufb-RNAi knockdown produces similar SUFB transcript and protein levels as that of WT Fe deficiency.

To induce the *sufb*-RNAi knockdown in *sufb2-2,* WT plants and the inducible *sufb2-2*-RNAi line were sprayed with DEX 26 days after germination. Two days later (at 4 weeks of age), a subset of WT plants was transferred to low Fe (10nM Fe(III)EDTA). *Sufb2-2*-RNAi plants were maintained on sufficient levels of Fe for the duration of the experiment. Samples for RNA-sequencing were taken 2 h (TP A) and 26 h (TP B) after WT was transferred to low Fe (Figure

4-1a). The *sufb*-RNAi line had been induced 2 days earlier to TP A and 3 days earlier to TP B. Protein samples to measure SUFB accumulation were taken at TP B and 7 days after WT low Fe treatment, or 9 days after DEX treatment (TP C) (Figure 4-1a).

There were minimal developmental differences between the WT plants and induced *sufb2-2*-RNAi plants (from here on referred to as *sufb2-2*) at the beginning of the Fe deficiency treatment of the WT plants (Figure 4-1b). By TP B, chlorosis was present in the young leaves of the induced *sufb2-2* line (Figure 4-1b). *SUFB* transcript level was verified to be decreased in *sufb2-2* at TP A and TP B as expected, and the *SUFB* transcript level of WT-Fe matched that of the transgenic line at TP B (Figure 4-1c). Because we were interested in comparing the early transcriptional response of WT-Fe with *sufb2-2*, loss of SUFB protein at TP B in the *sufb2-2* line was verified via western blotting before samples were sent for RNA sequencing. SUFB protein accumulation was lowered in the transgenic line compared to both WT+Fe and WT-Fe at TP B (Figure 4-1d, e). While *SUFB* mRNA is regulated early after Fe deficiency, decreases in SUFB protein accumulation are minimal in the first days after transfer to low Fe (Hantzis *et al*., 2018). Therefore, SUFB protein accumulation was also measured at TP C to ensure that the WT Fe deficiency response resulted in SUFB protein accumulation similar to that of *sufb2-2.* SUFB protein level of WT-Fe matched that of *sufb2-2* after 7 days of deficiency (Figure 4-1d, e).

Loss of SUFB in shoots does not influence physiological changes in response to low Fe

We first aimed to characterize general Fe homeostasis parameters in induced *sufb*-RNAi plants. To determine physiological changes in response to Fe deficiency we measured shoot Fe accumulation and root Fe reductase activity at TP C. We analyzed the response of *sufb2-2* alongside a second inducible *sufb*-RNAi knockdown, *sufb1-12,* to account for any differences in knockdown alleles. Rosette Fe concentration was measured by elemental composition. No differences in rosette Fe accumulation were seen between induced *sufb*-RNAi lines and WT+Fe, whereas Fe was significantly decreased in the rosettes of WT-Fe compared to WT+Fe

(Figure 4-2a). The systemic Fe deficiency response of the WT plants was also measured by root a ferric reductase chelate assay (FRO activity). FRO activity was significantly up-regulated in WT -Fe plants compared to WT+Fe and induced *sufb* lines (Figure 4-2b). Therefore, shoot SUFB activity is not limiting for root FRO activity or shoot Fe accumulation (Figure 4-2a, b).

Fe deficiency is known to result in decreased photosynthesis, specifically by decreased electron transport downstream of PSII, with accompanying reduction in the induction of Non-Photochemical Quenching (NPQ) (Hantzis *et al*., 2018). Therefore, we analyzed ϕPSII and NPQ via chlorophyll fluorescence as measures of efficiency of electron flow in the light at TP C. Both WT-Fe and the *sufb2-2* knockdown present symptoms of decreased photosynthesis in the youngest leaves. Therefore, we measured chlorophyll fluorescence using a FlourCam because it has the advantage of measuring fluorescence across the entire rosette, allowing visualization of parameters that represent photosynthetic efficiency in both young and old leaves. Both *sufb2-2* and WT-Fe had a decrease in ϕPSII compared to WT+Fe in the youngest leaves (Figure 4-2c). However, while NPQ was lowered in WT-Fe compared to WT+Fe in the youngest leaves, NPQ was increased in the youngest leaves of *sufb2-2* compared to WT+Fe (Figure 4-2c).

Overview of RNA-sequencing quality

For RNA-sequencing, three biological replicates, comprised of three whole rosettes, for each treatment were sequenced at TP A and TP B. The number of raw reads per sequenced sample ranged from 61 million reads to 100 million reads. Raw reads were filtered for low quality reads with more than 10% ambiguous base calling. Clean reads on average made up 97% of the raw reads/sample. The Q20 rate, which represents that the error in base calling was 1/100 bases was above 98% for every sample, suggesting that incorrect base calling rate was low (S. Table 4-1). Within each treatment group WT+Fe, WT-Fe, *sufb2-2* at each time point, correlation between biological replicates was high, with a Pearson correlation coefficient of

above .98 for each group (data not shown). Overall, sequences of biological replicates within each treatment had minimal variation in gene expression.

Few transcripts are differentially expressed in sufb2-2 and WT-Fe

Overall, transcriptional changes in response to WT-Fe and *sufb2-2* +Fe were minimal (Figure 4-3) with only 86 and 147 differentially expressed gene IDs present at TP A and TP B in WT-Fe and only 79 and 235 differentially expressed gene IDs present at TP A and TP B in *sufb2-2* +Fe. To determine similarities and differences in differential gene expression between WT-Fe and *sufb2-2* we produced a heat map to visualize patterns of expression. At both TP A and TP B, WT+Fe, WT-Fe, and *sufb2-2* had independent patterns of differential expression. More interestingly, when comparing the differentially expressed genes from each treatment, WT-Fe and *sufb2-2* +Fe had opposite patterns of expression (Figure 4-4). For example, bHLH transcription factors that were up-regulated in WT-Fe at TP B were not differentially expressed in *sufb2-2.*

The WT-Fe transcriptional response is specific to low Fe and presents transcripts that are co-regulated with SUFB

Although few transcripts were differentially expressed, the WT-Fe response is specific to Fe deficiency, as many Fe responsive transcripts, commonly used as markers for Fe deficiency (Kim *et al*., 2019), were differentially expressed at TP B (Figure 4-5b). Specifically, known bHLH transcription factors that regulate Fe deficiency (*PYE, bHLH100*, and *bHLH101*) were up-regulated compared to WT+Fe with at least 4 fold induction, while mRNA encoding for Fe sequestration proteins, such as the vacuolar Fe importer, *VIT1,* and Fe storage molecules, *Ferritins 1, 3*, and *4* (*FER1, FER3, FER4*), were down-regulated compared to WT+Fe by the same degree (Figure 4-5b).

The down-regulation of *SUFB* in TP B in WT-Fe compared to WT+Fe allowed us to identify transcripts that displayed co-regulation with *SUFB* during Fe deficiency and to determine which functional categories the gene products of DEGs represented. To determine functional categories, transcripts were grouped by the functions of their gene products. Few gene product functional categories were enriched in the DEGs at TP B. The largest functional categories of differentially expressed gene products were transcription factors (TFs), signaling components, ion homeostasis proteins, and redox homeostasis components (Figure 4-5b). Comparatively, at TP A, before *SUFB* is down-regulated, DEGs encoding kinases and transmembrane proteins were largest functional categories being regulated (Figure 4-5a). Interestingly, only one other transcript whose gene product is required for Fe cofactor assembly was differentially expressed at TP B; *CYSG*, required for siroheme biosynthesis. Within the WT-Fe transcriptional response, we identified two sets of novel gene expression changes co-regulated with *SUFB*: a set of cytosolic glutaredoxins (GRXS) and a set of ERF family transcription factors (RA2.12, ERF53, and CRF2) are differentially expressed in WT-Fe compared to WT+Fe.

A set of cytosolic GRXS that are known to be co-regulated by N status (Patterson *et al*., 2016; Walters and Escobar, 2016) were down-regulated 3.2-4.6 fold in response to deficiency compared to WT+Fe (Figure 4-5b). N assimilation is also regulated in response to Fe deficiency (Mai and Bauer, 2016). Therefore, because these co-regulated GRXS transcripts are known to be responsive to N status, we aimed to determine if this set of co-regulated GRXS could be responsible for Fe sensing in leaves. To test this, we measured protein and transcript accumulation for chloroplast proteins known to be down-regulated 7 days after low Fe treatment (Hantzis *et al*., 2018) in an RNAi knockdown line of *grxs3/4/5/7/8* grown on nutrient agar (Figure 4-6). When compared to the WT Fe deficiency response, the Fe deficiency response of *grxs3/4/5/7/8* did not differ, as SUFB, FDX2, and the Rieske component of the Cyt-b_6f complex were all down-regulated at the transcript and protein level in *grxs3/4/5/7/8* on low Fe and PSaA

was maintained. Therefore, loss of *GRXS3/4/5/7/8* did not disrupt leaf Fe homeostasis and, therefore, these proteins do not seem to be required in wild-type abundance in order to mediate initial regulation of the leaf Fe deficiency response.

Ethylene Response Factor Transcription factors have recently been identified as regulating root Fe deficiency responses along with bHLH transcription factors deficiency (Lingam *et al*., 2011; Kastoori Ramamurthy *et al.,* 2019; Zhang *et al*., 2019). Three Ethylene Response Transcription Factors were differentially expressed at TP A and TP B (Figure 4-5a, b, Figure 4-7). ERF53 which has previously been characterized as an early regulatory factor in salt stress (Hsieh *et al*., 2013) was up-regulated 2 fold by TP A compared to WT+Fe (Figure 4-5a, visualized by Integrative Genome Viewer (IGV) Figure 4-7). *ERF53* was not differentially expressed at TP B (Figure 4-5a,b). Two other ERF transcription factors, *RA2.12* and *CRF2* were down-regulated by about 1.5 fold at TP B compared to WT+Fe (Figure 4-5b, Figure 4-7). To determine if these ERF transcription factors may be conserved, we analyzed the protein sequence similarity across the green lineage with a focus on dicot species. These three ERF transcription factors were especially conserved in higher plants and CRF2 and RA2.12 sequences from the different species were considerably more similar to the corresponding protein sequences in *A. thaliana* compared to the sequence for ERF53 (S Figure 4-1, S. Table 4-2). Higher plants had an average protein sequence similarity (as estimated by coverage) with *A. thaliana* of 84% for CRF2, and 82% for RA2.12, compared to only 65% for ERF53 (S Table 4-2). ERF transcription factors contain an AP2 DNA binding domain. Within the sequence alignments, it is the AP2 domain that was most conserved across the protein sequences of each ERF transcription factor (S Figure 4-2).

Sufb2-2 and WT-Fe present opposite transcriptional responses

To determine similarities and differences between the transcriptional response of WT-Fe and *sufb2*-2, we first determined transcriptome changes specific to the loss of SUFB by

identifying shared gene expression changes across TP A and B of *sufb2-2.* Only 47 common differentially expressed transcripts were shared across the timepoints, with 44 of these being up-regulated compared to WT+Fe (S Figure 4-3). Among these up-regulated transcripts was *SUFA*, a candidate Fe-S cluster transfer molecule. *SUFA* expression was induced by 4 fold at TP B. No other SUF pathway transcripts were differentially expressed. *SUFA* transcript levels were stable in Fe deficiency (Figure 4-5), although SUFA protein accumulation does decrease (Pan *et al*., 2015; Hantzis *et al*., 2018). At TP B only, *VIT1*, a vacuolar Fe importer, which is known to be down-regulated during Fe deficiency (Gollhofer *et al*., 2014), was up-regulated in *sufb2-2* compared to WT+Fe (S Figure 4-3). However, *VIT1* up-regulation in *sufb2-2* compared to WT+Fe was not consistent across TP A and TP B.

We then compared transcriptome changes specific to *sufb2-2* with transcriptome changes in both WT-Fe TP A and WT-Fe TP B. When differential expression was compared between WT-Fe and *sufb2-2* +Fe, no DEGs were shared at TP A, and only the down-regulation of *SUFB* (due to RNAi) compared to WT+Fe was shared at TP B (Figure 4-8). This suggests that the decrease in chloroplast Fe-S cluster production resulting from down-regulation of *SUFB* that occurs early in Fe deficiency is not responsible for triggering Fe deficiency signaling in the leaf.

SUFA transcription is induced in knockdowns of components of SUFBCD major scaffold.

RNA-sequencing of *sufb2-2* revealed that *SUFA* transcript was over expressed compared to WT whenever *SUFB* transcript was decreased, as visualized by read coverage generated from Integrated Genome Viewer (IGV; Figure 4-8a). We sought to investigate if this was conserved across other SUFB knockdown lines and knockdown lines for other components of the SUFBCD complex (Hu *et al*., 2017). We also determined if the protein level of SUFA correlates to these transcript level changes. Interestingly, when we measured protein accumulation of SUFA via western blotting, SUFA protein was absent from induced *sufb, sufc,*

and *sufd*-RNAi knockdown lines, and SUFB was decreased at the protein level in all *sufb, sufc* and *sufd* lines compared to WT as previously reported (Figure 4-8b; Hu *et al*., 2017). We used qPCR to determine transcript level changes of *SUFA* in the induced *sufb, sufc* and *sufd* lines and saw similar results to our RNA-seq data, in which *SUFA* transcript was significantly up-regulated in all lines lacking components of the major Fe-S scaffold compared to WT+Fe (Figure 4-8c). To determine if this up-regulation of *SUFA* is specific to loss of *SUFB*, we analyzed the transcript abundance of SUFB in the induced *sufb, sufc* and *sufd* knockdown lines. As previously reported, *SUFB* was only decreased in the *sufb*-RNAi knockdowns (Figure 4-8b, c, Hu *et al*., 2017), suggesting that *SUFA* transcript accumulates in response to a deficiency in the major scaffold of the SUF pathway.

Mutational loss of SUFA leads to increased protein accumulation of several Fe requiring photosynthetic proteins.

We further investigated the role of SUFA in chloroplast Fe homeostasis, specifically in response to Fe deficiency. We deprived *sufa*-KO plants of Fe on nutrient agar and compared the protein and transcript response to WT Fe deficiency. *sufa* maintained Fe regulation of the known chloroplast Fe markers, however, *sufa* accumulated more Rieske, Cytb_6, and FDX2 proteins compared to WT at the protein level when grown on sufficient levels of Fe (Figure 4-10). No significant differences were seen at the transcript level between *sufa* and WT transcript changes. However, there was a trend for *sufa* to accumulate more transcript levels of *FDX2* and *RIESKE* (Figure 4-10).

Early Fe deficiency in WT mainly targets chloroplast localized gene products

Because chloroplast metabolism is a target of the leaf Fe deficiency response, we also analyzed gene product localization at TP B for up and down-regulated genes in WT-Fe compared to WT+Fe, using the GO localization annotations from TAIR. At TP B, the largest

portion of both up-regulated and down-regulated transcripts are targeted to the chloroplast, suggesting that chloroplast metabolism is an initial target of leaf Fe deficiency (Figure 4-11a). Specifically, 38% of differentially regulated gene products were localized to the chloroplast compared to 26.8% localized to the cytoplasm. Additionally, since SUFB is a chloroplast localized protein, we wanted to determine if loss of SUFB alters regulation of chloroplast localized gene products. We analyzed predicted cellular targets of gene products of DEGs that were up-regulated in both timepoints of *sufb2-2* compared to WT+Fe. Only 11% of gene products encoded by DEGs up-regulated in *suf2-2* compared to WT+Fe were predicted to localize to the chloroplast compared to about 32% that were predicted to localize to the cytosol (Figure 4-11b). Only two genes in addition to *SUFB* were down-regulated in response to loss of SUFB in both timepoints.

ERF, MYB, and bHLH transcription factors are predicted to regulate co-regulated genes with SUFB in WT-Fe

To determine whether co-regulated transcripts that are differentially expressed alongside *SUFB* in WT-Fe share promoter elements, we analyzed promoter sequences of differentially expressed genes at TP B. We analyzed the promoters of DEGs that were up and down-regulated in WT-Fe compared to WT+Fe at TP B using AthaMap (Figure 4-12a). We first determined the percentage of up-regulated gene promoters that have at least one putative binding site for each transcription factor family. Of the up-regulated and down-regulated genes at TP B, 100% had at least one putative promoter binding site for ERF and MYB transcription factors (Figure 4-12a). Comparatively, only 57% of down-regulated genes and 76% of up-regulated genes had at least one putative promoter bHLH binding site (Figure 4-12a). While other transcription factor families had *cis* elements present in all up and down-regulated gene promoters, only transcription factors from ERF, MYB, and bHLH families were differentially expressed in the RNA seq. We also investigated the promoters of the four up-regulated bHLH

Fe related transcription factors, *PYE*, *bHLH100*, *bHLH101*, *bHLH28*, along with *BRUTUS*, the E3 ubiquitin ligase that is known to regulate Fe deficiency responses. We found that in all 5 of these transcripts, promoters contained putative ERF *cis* elements. We then determined the number of putative transcription factors within each transcription factor family that are predicted to bind promoter *cis* elements of DEGs. The ERF family had the highest number of transcription factors that were predicted to bind to promoters of DEGs at TP B. 37 ERF transcription factors were predicted to bind to promoters of down-regulated genes and 35 were predicted to bind to up-regulated genes (Figure 4-12a).

We analyzed promoters of DEGs up-regulated across all timepoints in *sufb2-2* compared to WT+ Fe to determine whether co-regulated transcripts that are differentially expressed specifically in response to loss of *SUFB* share promoter elements (Figure 4-12a). Transcription factor families that had at least one putative binding site across all up-regulated gene promoters included ERF (AP2/EREBP), MYB, GARP, C2H2, HD, AT-HOOK, NAC and Trihelix (Figure 4-12a). We found that 33 ERF and 27 MYB transcription factors were predicted to bind to promoter elements of up-regulated genes, a much higher prediction than any other transcription factor family (Figure 4-12a).

To determine if bHLH, MYB, and ERF *cis* elements are more commonly found in the promoters of the DEGs in response to Fe deficiency, suggesting a higher probability of regulation by these transcription factor families, we analyzed *cis* element enrichment. Specific bHLH, MYB, and ERF transcription factor families have all been linked to Fe deficiency regulation in roots (Kobayashi, 2019). To determine if specific *cis* elements were enriched in promoters of DEGs, we compared the probability of *cis* element occurrence for bHLH, ERF, and MYB *cis* elements in the promoters of TP B DEGs with the probability of *cis* element occurrence across the *Arabidopsis* genome. To determine if genes encoding chloroplast localized proteins may be regulated by a specific class of transcription factor, we also analyzed enrichment in promoters of DEGs whose gene products are predicted to localize to the chloroplast. In

promoters of DEGs up-regulated in WT-Fe compared to WT+Fe, there was a preference for bHLH and MYB *cis*-elements as almost all DEGs had enriched MYB *cis* elements (Figure 4-12b). ERF *cis* elements were not enriched in up-regulated DEG promoters. These same patterns remained when only promoters of up-regulated chloroplast localized gene products were analyzed. Promoters of all down-regulated DEGs in WT-Fe compared to WT+Fe, were enriched for bHLH and MYB *cis* elements. However, promoters of down-regulated chloroplast localized gene products were only enriched for bHLH and ERF *cis* These data suggest that bHLH, ERF, and MYB family transcription factors may all regulate transcripts in leaf Fe deficiency.

ERF and MYB transcription factors were also predicted to bind to promoters of up-regulated DEGs in *sufb2-2* compared to WT+Fe. Therefore, to determine if bHLH, ERF, and MYB regulation may be specific to regulation of up-regulated transcripts in *sufb2-2* compared to WT+Fe we analyzed enrichment of bHLH, ERF, and MYB *cis* elements in the promoters of these genes. Because SUFB protein is localized to the chloroplast, we performed this analysis for all up-regulated DEGs as well as those whose gene products are predicted to localized to the chloroplast. In promoters of transcripts up-regulated across the two *sufb2-2* timepoints compared to WT+Fe, *cis* elements of bHLH were enriched in all up-regulated DEGs (Figure 4-12b). bHLH *cis* elements were also enriched in chloroplast localized DEG promoters along with ERF *cis* elements, although not to the same extent. No MYB *cis* elements were enriched in promoters of up-regulated DEGs in *sufb2-2* compared to WT+Fe.

4.5 DISCUSSION

The transcriptional response in leaves to low Fe and to loss of SUFB does not share common differentially expressed genes.

Because down-regulation of *SUFB* by inducible RNAi and Fe deficiency treatment resulted in a comparable expression level of SUFB protein and similar leaf symptoms at each of

the sampling points (Figure 4-1), it was of interest to compare the transcriptional response for both treatments. We could therefore distinguish transcript abundance changes that are due to loss of SUFB function and, thus, loss of Fe-S assembly in chloroplasts from changes due to low Fe availability, which was an important aim of this study. Overall, the transcriptional response of the leaf to Fe deficiency was found to be independent from the transcriptional response to loss of chloroplast Fe-S cluster assembly resulting from loss of SUFB (Figure 4-4, Figure 4-8). Therefore, our data indicate that a loss of chloroplast Fe-S assembly and thus photosynthetic activity is not the trigger that signals transcriptional changes of nuclear genes in the response to low Fe in the vegetative shoot.

Arabidopsis SUFB has previously been proposed as an Fe sensor for plastid Fe homeostasis as its activity is stimulated by addition of Fe (Xu *et al*., 2005). However, the *sufb2-2* line shared few transcriptomic changes with WT-Fe (Figure 4-4, 4-8), suggesting that chloroplast Fe-S cluster availability is not regulating Fe deficiency responses. Instead, the initial down-regulation of *SUFB* to lower Fe-S cluster assembly may be necessary for adjusting Fe protein biogenesis and perhaps photosynthetic output to Fe status, as loss of SUFB results in loss of photosynthetic electron transport proteins (Hu *et al*., 2017). While the inducible *sufb*-RNAi knockdown was previously found to accumulate lower levels of Fe-S photosynthetic proteins, the corresponding transcripts for these proteins were not differentially expressed in our RNA-sequencing analysis. This further suggests that the down-regulation of SUFB during Fe deficiency may influence protein maturation by coordinating a decrease in Fe-S cluster availability with the down-regulation of Fe-S requiring photosynthetic electron transport proteins.

Previously published studies that have characterized genes and proteins required for the Fe deficiency response report mis-regulation of Fe-homeostasis in mutants, for example, the disruption of root FRO activity and IRT1 mediated Fe uptake. For example, loss-of-function mutants in the Iron Man/Fe Uptake Inducing Peptide (IMA/FEP) phloem mobile peptides in *Arabidopsis* presented Fe deficiency chlorosis when at normal Fe levels (Grillet *et al*., 2019).

Further, IMA/FEP loss-of-function lines did not induce root FRO activity on sufficient or deficient levels of Fe compared to WT (Grillet *et al*., 2019). Over-expression lines of IMA1, and inducible over-expression FEP1 lines had up-regulation of Fe responsive bHLH transcription factors, *bHLH38*, *bHLH39*, *bHLH100*, and *bHLH101*, as well as Fe storage proteins, *FER1*, *FER3* and vacuolar Fe importers (Grillet *et al*., 2019; Hirayama *et al*., 2019). *Arabidopsis* mutants of Oligo-Peptide Transporter 3 (OPT3) which functions in systemic Fe deficiency signaling, over accumulates Fe in the shoots (Zhai *et al*., 2014).

Targeted down-regulation of chloroplast localized gene products is specific to the WT-Fe response

In WT-Fe compared to WT+Fe, 38% of both up-regulated and down-regulated gene products co-regulated with SUFB at TP B (26 h after low Fe) are localized to the chloroplast (Figure 4-11), suggesting that alterations to chloroplast metabolism is an initial plant response to sensing changes in Fe status. *Sufb2-2* had only 11% of up-regulated DEG products being chloroplast localized (Figure 4-11). The low percentage of chloroplast localized changes in *sufb2-2* suggests that targeting of chloroplast metabolism is a specific response to Fe status and not to lack of available chloroplast Fe-S clusters.

SUFB down-regulation is an important early Fe deficiency response regardless of plant growth conditions

While transcriptome analysis is a useful tool to study early changes in gene expression in response to Fe deficiency, most published transcriptome studies in Fe deficiency have focused on seedling stage plants, grown on nutrient agar supplemented with sucrose (Sivitz *et al*., 2012; Rodriguez-Celma *et al*., 2013; Zhai *et al.,* 2014; Kim *et al*., 2019). Because of our specific interest in photosynthetic regulation in vegetative shoots in response to Fe deficiency, we analyzed transcriptomes in rosettes of photosynthetically active hydroponically grown

Arabidopsis. Interestingly, regulation of *SUFB* is observed regardless of the developmental stage of the plants. *SUFB* was down-regulated after 3 days of Fe deficiency at the seedling stage, along with chlorophyll biosynthesis (Rodriguez-Celma *et al*., 2013). In the current study, *SUFB* was down-regulated only 26h after Fe deficiency (Figure 4-1), but preceded regulation of chlorophyll biosynthesis-related genes (Figure 4-5). *SUFB* was also reported to be down-regulated in the roots in response to Fe deficiency (Yang *et al*., 2010). Thus, the down-regulation of *SUFB* in leaves and roots seems to be vital for the Fe deficiency response, and perhaps for initial down-regulation of plastid metabolism but, at least in leaves, SUFB is not a regulatory Fe protein.

Chloroplast Fe-S availability may alter intracellular Fe homeostasis.

The down-regulation of SUF Fe-S cluster assembly during Fe deficiency may be important for altering cellular Fe distribution for prioritization of Fe. The vacuolar Fe importer, *VIT1,* was up-regulated in *sufb2-2* at TP B compared to WT+Fe (S Figure 4-3). *VIT1* is known to be down-regulated during Fe deficiency to decrease Fe sequestration in the vacuole (Figure 4-5; Gollhofer *et al*., 2014). Because *sufb2-2* does not accumulate high levels of rosette Fe, most likely, the loss of SUFB results in lowered plastid Fe use which may, in turn, result in increased cytosolic Fe levels which could trigger the up-regulation of *VIT1* transcript in *sufb2-2.*

Other plastid Fe-S cluster machinery has been found to alter Fe homeostasis at the transcriptional level (Zandalinas *et al*., 2019). *Arabidopsis* NEET is reported to be localized to both the mitochondria and chloroplast and has been proposed to function to transfer Fe-S clusters. A line which expressed a dominant negative form of NEET, and in which native NEET function was inhibited, resulted in down-regulation of many SUF pathway transcripts including *SUFB*, as well as Fe related transcription factors, *PYE, bHLH39*, and *ILR3* compared to WT (Zandalinas *et al*., 2019). Moreover, vacuolar Fe export was up-regulated in the NEET dominant negative line compared to WT. *NEET* is also down-regulated during Fe deficiency (Nechushtai

et al., 2012; Figure 4-5). The *sufb2-2* line did not exhibit differential expression of *NEET* or any other Fe responsive bHLH transcription factors.

A novel proposed role for SUFA as a monitor Fe-S homeostasis in the chloroplast

One of the most up-regulated transcripts in *sufb2-2* was *SUFA* whose gene product is chloroplast localized (Figure 4-8). SUFA is a putative carrier protein that is known to either bind Fe or Fe-S clusters (Abdel-Ghany *et al.*, 2005). Within the chloroplast, SUFA may be vital in modulating the supply of Fe-S clusters. In WT on low Fe, SUFA protein accumulation is repressed, but transcript level is unchanged (Pan *et al*., 2015; Hantzis *et al*., 2018). However, its biochemical role *in vivo* has not been determined. Unlike the components of the SUFBCD major scaffold, SUFA knockouts do not have clear a clear phenotype (Abdel-Ghany *et al.*, 2005; Yabe and Nakai, 2006). sufA is not vital for SUF Fe-S cluster assembly in *E. coli* either; the mutational loss of sufA in *E. coli* subject to iron deficiency was not lethal, whereas the mutational loss of other suf components in Fe deficient *E.coli* were lethal (Outten *et al*., 2004). In the cyanobacterium *Synechococcus* PCC 7002, sufA has been proposed to sense capacity of the cell to produce Fe-S clusters during photosynthetic oxidative stress (Balasubramanian *et al*., 2006).

Surprisingly, in the current study, *SUFA* transcript level increased by greater than 3 fold in knockdowns of the major scaffold proteins while SUFA protein accumulation was largely absent (Figure 4-8). While the overaccumulation of *SUFA* mRNA is not seen in Fe deficiency (Figure 4-5, Hantzis *et al*., 2018), the *SUFA* transcript levels are maintained while protein levels decrease (Pan *et al*., 2015; Hantzis *et al*., 2018). Our data suggests that this regulation of *SUFA* during Fe deficiency may be responding to down-regulation of *SUFB* and not directly from Fe deficiency. Additionally, the *sufa* knockout mutant had the same response to Fe deficiency as WT but accumulated more FDX, Rieske, and Cyt*f* protein (Figure 4-8). This novel finding that *SUFA* expression is induced by loss of components of the SUFBCD scaffold may suggest a

mechanism for SUFA under Fe deficiency. SUFA may be acting to sequester either Fe or Fe-S clusters to regulate Fe-S protein insertion with availability of Fe-S requiring proteins in the chloroplast (Figure 4-10). Under normal conditions when the major SUF scaffold is fully functional, SUFA may hold excess Fe or Fe-S clusters while the Fe-S requiring proteins are being translated and folded (Figure 4-13). When there is a deficiency in the major scaffold, for instance in WT-Fe, SUFA protein is degraded, but transcript remains high. When Fe is resupplied to a plant, SUFA protein can be rapidly translated while SUFB and chloroplast Fe-S containing proteins are recovered. In this case, the quick recovery of SUFA protein may serve to hold Fe until the major scaffold is recovered, or to hold new Fe-S clusters as photosynthetic proteins are recovered. Lack of SUFA in the knockdown may result in the plant producing more proteins that are a sink for chloroplast Fe-S clusters.

ERF transcription factors may regulate Fe deficiency transcriptional changes to chloroplast localized gene products

A second important aim of the present study was identify *cis* elements known as binding sites for bHLH, ERF, and MYB transcription factors by assessing expression at 26h after Fe limitation. A set of bHLH transcription factors have been well characterized in their regulation of the root Fe deficiency response (Gao *et al*., 2019). While Fe responsive bHLH transcription factors are expressed in the shoots as well (Long *et al*., 2010; Rodriguez-Celma *et al*., 2013; Sivitz *et al*., 2012), *SUFB* does not have promoter *cis* elements for bHLH transcription factors (Hantzis *et al*., 2018), suggesting a yet undiscovered regulatory pathway. Enrichment analysis found enrichment of bHLH transcription factor *cis* elements in transcripts of both up and down-regulated chloroplast localized gene products, while ERF *cis* elements were only over enriched in transcripts of down-regulated chloroplast localized gene products (Figure 4-12). Enrichment of ERF *cis* elements has also been reported in early (6 h) differentially expressed transcripts in the leaf Fe deficiency response of *Glycine max* (Soybean; Moran Lauter *et al*., 2014).

Conversely, *sufb2-2* up-regulated transcripts compared to WT+Fe had over-enriched bHLH and ERF *cis* elements in promoters of genes encoding chloroplast localized gene products (Figure 4-12b), perhaps further supporting Fe related ERF regulation of chloroplast down-regulated gene products.

We identified three ERF family transcription factors that were differentially expressed in WT-Fe compared to WT+Fe (Figure 4-5). ERF transcription factors are reported to respond to abiotic stress (Mizoi *et al*., 2012; Xie *et al*., 2019) and have recently been linked to Fe deficiency (Lingam *et al*., 2011; Kastoori Ramamurthy *et al*., 2018; Zhang *et al*., 2019). For example, two ERF transcription factors, Ethylene Insensitive 1 and 3 (EIN1, EIN3) were determined to stabilize FIT in the root iron deficiency response by directly screening for FIT interacting proteins (Lingam *et al*., 2011). Two other ERF transcription factors (MbERF4 and MbERF72) were recently found to suppress root Fe uptake by repressing the root proton pump in apple species. A higher expression of MbERF4 and 72 correlated with a Fe sensitive apple variety, while a low expression correlated with an Fe tolerant apple variety (Zhang *et al*., 2019). Moreover, the PAP/SAL1 retrograde signaling pathway which allows communication between chloroplast and nucleus and mitochondria and nucleus has recently been linked with ERF factors and ethylene signaling in Fe deficiency (Balparda *et al*., 2020). Mutants in the PAP/SAL1 pathway respond with increased Fe accumulation in roots and shoots, and an increased FRO2 and IRT1 gene expression. The increase in Fe uptake in the PAP/SAL1 mutant lines may be through PAP/SAL1 regulation of ERF1, as ERF1 was also determined to be over expressed in the mutants compared to WT (Balparda *et al*., 2020). Other Fe responsive ERF family transcription factors have also been identified via gene expression changes such as in the current study (Kastoori Ramamurthy *et al*., 2018). Down-regulation of ERF transcription factors was also seen in the transcriptional analysis of *Arabidopsis* WT-Fe plants and *spl7* mutant plants, which are defective in up-regulation of Cu uptake under Cu deficiency and results in an Fe overload (Kastoori Ramamurthy *et al*., 2018).

Some ERF family proteins are found to be down-regulated in response to low Fe in gene expression studies, suggesting Fe regulated ERF transcription factors may be regulated to stop driving the expression of specific targets (Liu *et al*., 2017a; Liu *et al*., 2017b; Balparda *et al*., 2020). Similarly, ERF transcription factors, *CRF2* and *RA2.12,* expression at TP B was down-regulated compared to WT+Fe (Figure 4-7). The down-regulation of these ERF factors may result in repression of chloroplast localized transcripts. RA2.12 has a been found to directly regulate the reactive oxygen species burst in early stages of stress responses by binding to the promoter of RbohD (Respiratory burst oxidase Homolog D), and constitutive expression of *RA2.12* resulted in enhanced stress responses (Yao *et al*., 2017). The down-regulation of *RA2.12* upon -Fe may correlate with the down-regulation ROS scavenging in the early stages of Fe deficiency. CRF2 is important in cytokinin responses. Cytokinin has been reported to negatively regulate the root Fe deficiency response (Seguela *et al*., 2008).

Conversely to regulation of *RA2.12* and *CRF2*, *ERF53* was up-regulated (>2 fold) at TP A (2 h after low Fe) but was not differentially expressed 24 hours later. ERF53 was reported to be important in early responses to salt and drought stress but was found to be rapidly degraded by the RGLG1/RGLG2 E3 ubiquitin ligases (Hsieh *et al*., 2013). RGLG1/RGLG2 have also previously been proposed to regulate root and shoot Fe responses post-transcriptionally (Pan *et al*., 2015). It is possible that *ERF53* is induced early in the leaf Fe deficiency response to initiate abiotic stress responses but then is degraded by RGLG1/RGLG2 as bHLH transcription factors are up-regulated to initiate later Fe specific responses.

4.6 CONCLUSION

Here, we present evidence that chloroplast Fe-S cluster assembly is regulated downstream of Fe deficiency sensing and thus may be necessary to coordinate down-regulation of photosynthetic proteins with Fe cofactor availability. Deficiency in Fe-S cluster assembly did not induce major changes to the leaf Fe response, despite sharing similarities in photosynthetic

electron transport chain protein accumulation. Overall, the transcriptional response of *sufb2-2* was opposite that of WT-Fe both in respect to gene regulation and cellular location of regulated gene products. However, *sufb2-2* showed up-regulation of *SUFA* transcript but no SUFA protein over-accumulation, suggesting a novel role of SUFA in maintenance of Fe-S homeostasis. Additionally, *sufb2-2* presented up-regulation of the vacuolar Fe transporter, *VIT1*. Overall, transcriptional changes in *sufb2-2* suggest that a lack of plastid Fe use may lead to an increase in cytosolic Fe assembly into Fe-S clusters and alterations in intracellular Fe homeostasis.

4.7 CONTRIBUTIONS: We would like to thank Dr. Tai Montgomery for his guidance in experimental design and analysis of the RNA-sequencing data. We would also like to thank Dr. Anireddy Reddy for his help in analysis of the RNA-sequencing data and Jessica Warren for her help in training G.K. on methods to assess RNA quality.

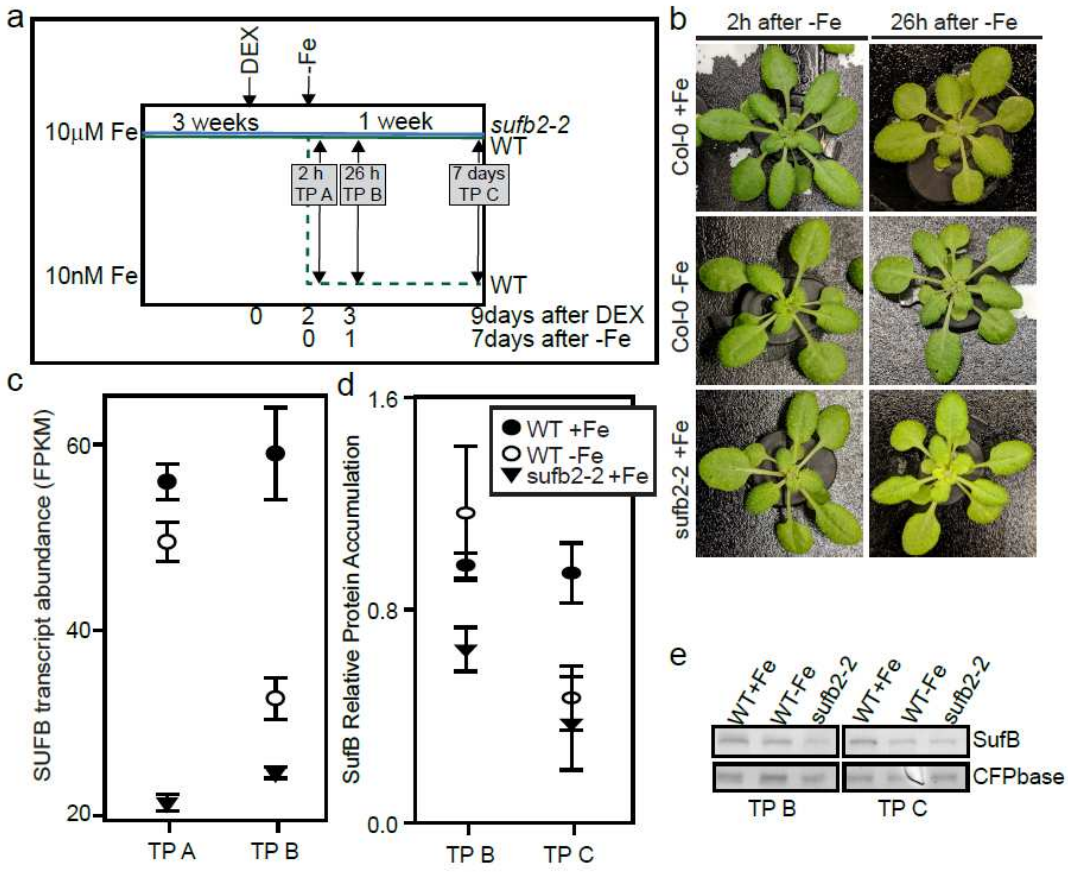

Figure 4-1: Experimental Design and molecular characterization of plants for RNA-seq samples. (a) Experimental set up and sampling times. Plants were grown on +Fe (10 μM Fe(III)EDTA) for 3 weeks and WT plants were transferred to low Fe (10 nM Fe(III)EDTA) at 4 weeks of age. Plants were foliar sprayed with Dex 2 days prior to the start of WT-Fe treatment. Samples for RNA seq and protein were taken at 2 h (TP A) and 26 h (TP B) after the start of low Fe treatment. Physiological measurements were taken 7 days after the start of low Fe treatment (TP C) along with a second set of protein samples. (b) Representative images of WT+Fe, WT-Fe, and *sufb2-2* +Fe used for RNA-sequencing at TP A and TP B (c) *SUFB* accumulation at transcript level at TP A and TP B. Each dot represents FPKM of *SUFB* and standard error. (d) Relative protein accumulation of SUFB at TP B and TP C (n=3). Each dot represents mean relative protein accumulation and standard error. (e) Representative blots for SUFB at TP B and TP C used for protein quantification. cFPBase is presented as a loading control. Proteins were separated by SDS-PAGE (15% gel) and transferred to a 0.2 μM pore nitrocellulose membrane (n=3-4).

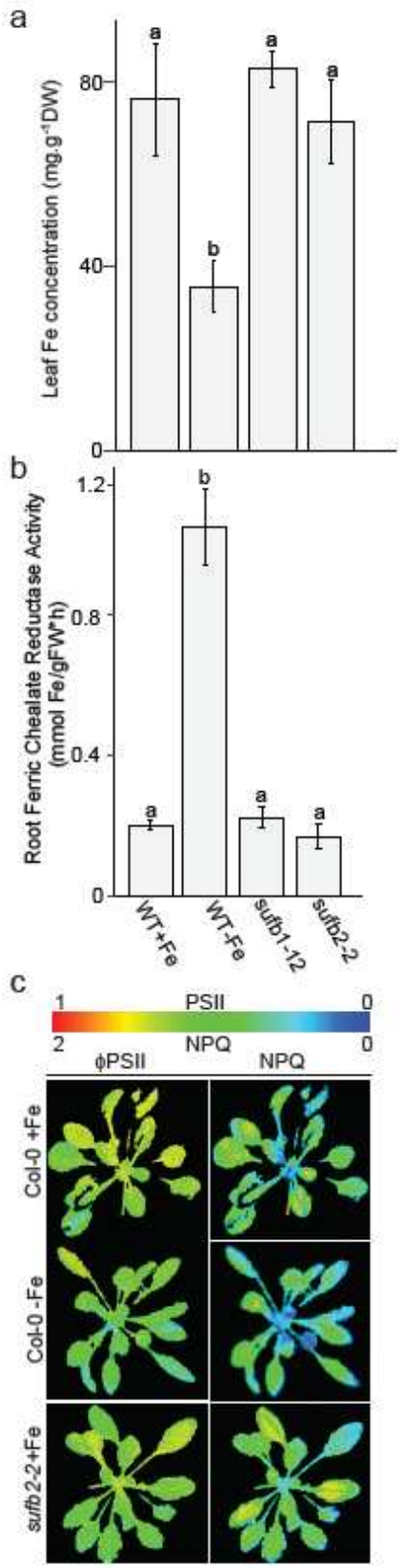

Figure 4-2: Characterization of Fe homeostasis at TP C. (a) Rosette Fe accumulation analyzed by ICP-OES in WT+Fe, WT-Fe, and two *sufb* lines. Fe content was normalized to rosette dry weight (n=8). (b) Root ferric chelate reductase activity for WT+Fe, WT-Fe, and two *sufb* lines (n=5-10). Reductase activity was normalized by root fresh weight. Each bar represents mean and standard error. Significance was determined by an ANOVA and is denoted by a letter above bar. (c) False color images of chlorophyll fluorescence parameters, ϕPSII, indicative electron transport downstream of PSII, and NPQ, for WT+Fe, WT-Fe and *sufb2-2*. Red coloration correlates to higher NPQ and ϕPSII, blue correlates to lower NPQ and ϕPSII

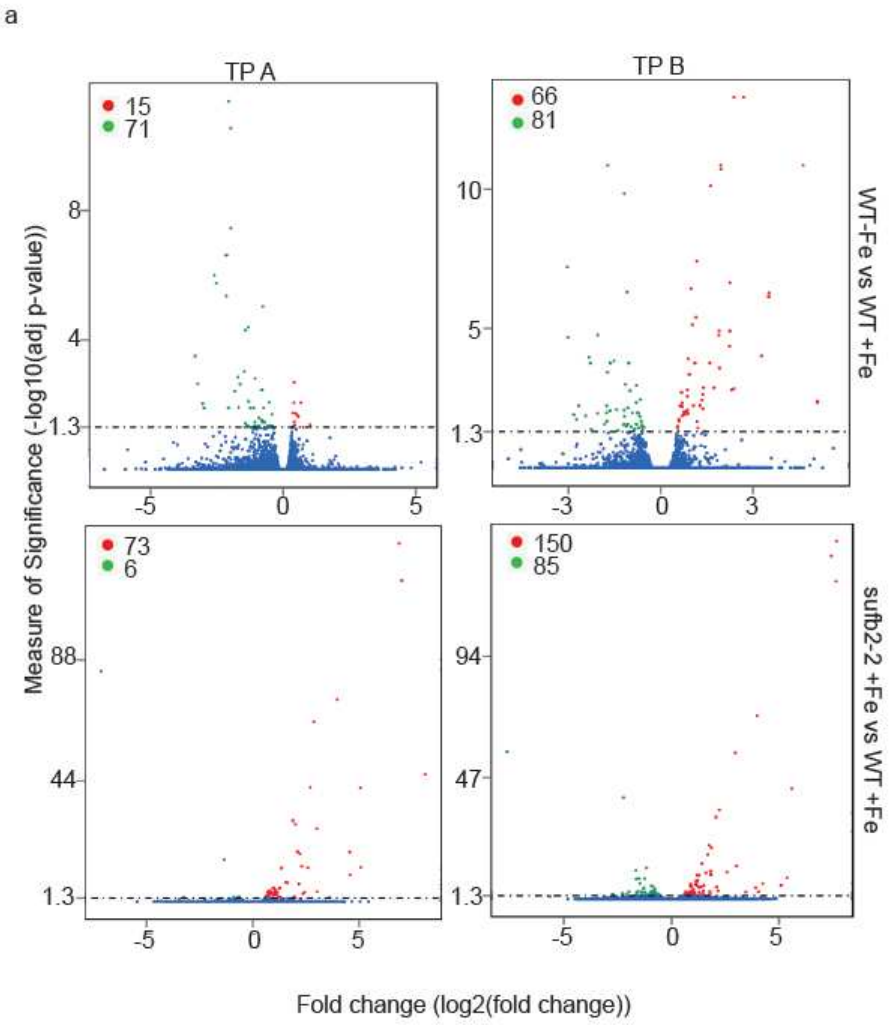

Figure 4-3: Transcript abundance in WT-Fe and *sufb2-2* at TP A and TP B. Volcano plots of differentially expressed genes WT-Fe and *sufb2-2.* Significance ($-\log_{10}$ of the adjusted p-value) is plotted against $\log_2$Fold Change. Red dots represent up-regulated genes, green dots represent down-regulated genes, and blue dots represent unchanged genes. Down-regulated genes are those that are decreased in expression in WT-Fe or *sufb2-2* compared to WT+Fe; Up-regulated genes are these that have increased expression in WT-Fe or *sufb2-2* compared to WT+Fe.

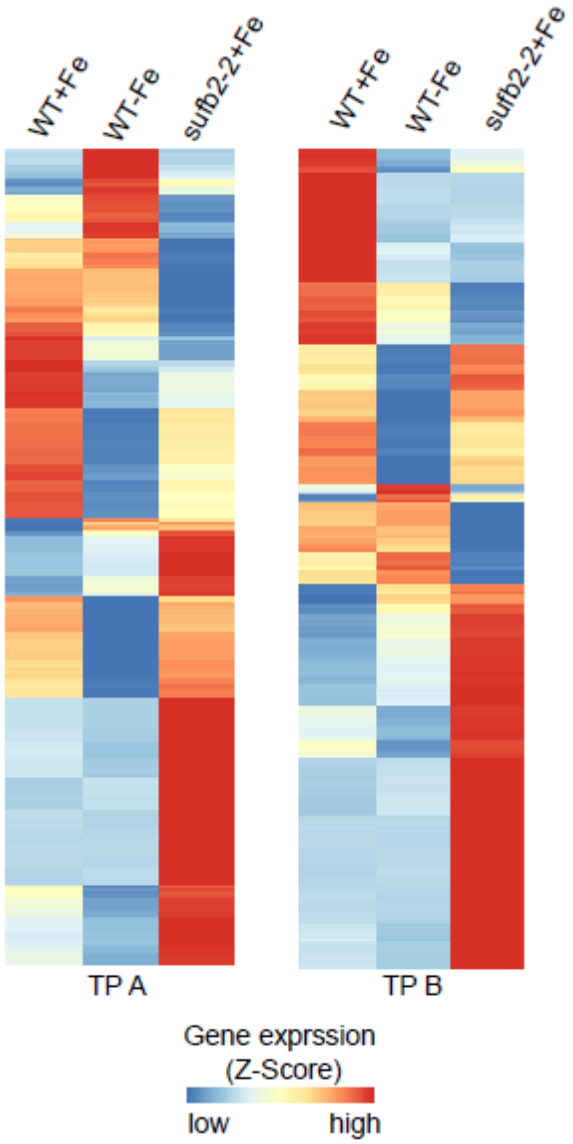

Figure 4-4: Pattern of expression of differentially expressed genes in WT+Fe, WT-Fe, and *sufb2-2*. Heat maps were constructed using normalized FPKM values for significant differentially expressed genes (p>0.05) across TPA and TPB. Normalization was done by calculating a Z score for each transcript. Z score was calculated for each individual gene by subtracting mean FPKM and then dividing by the standard error. High Z-scores are red, while low Z scores are blue. Heatmap was generated using the R-package pheatmap.

Figure 4-5
a

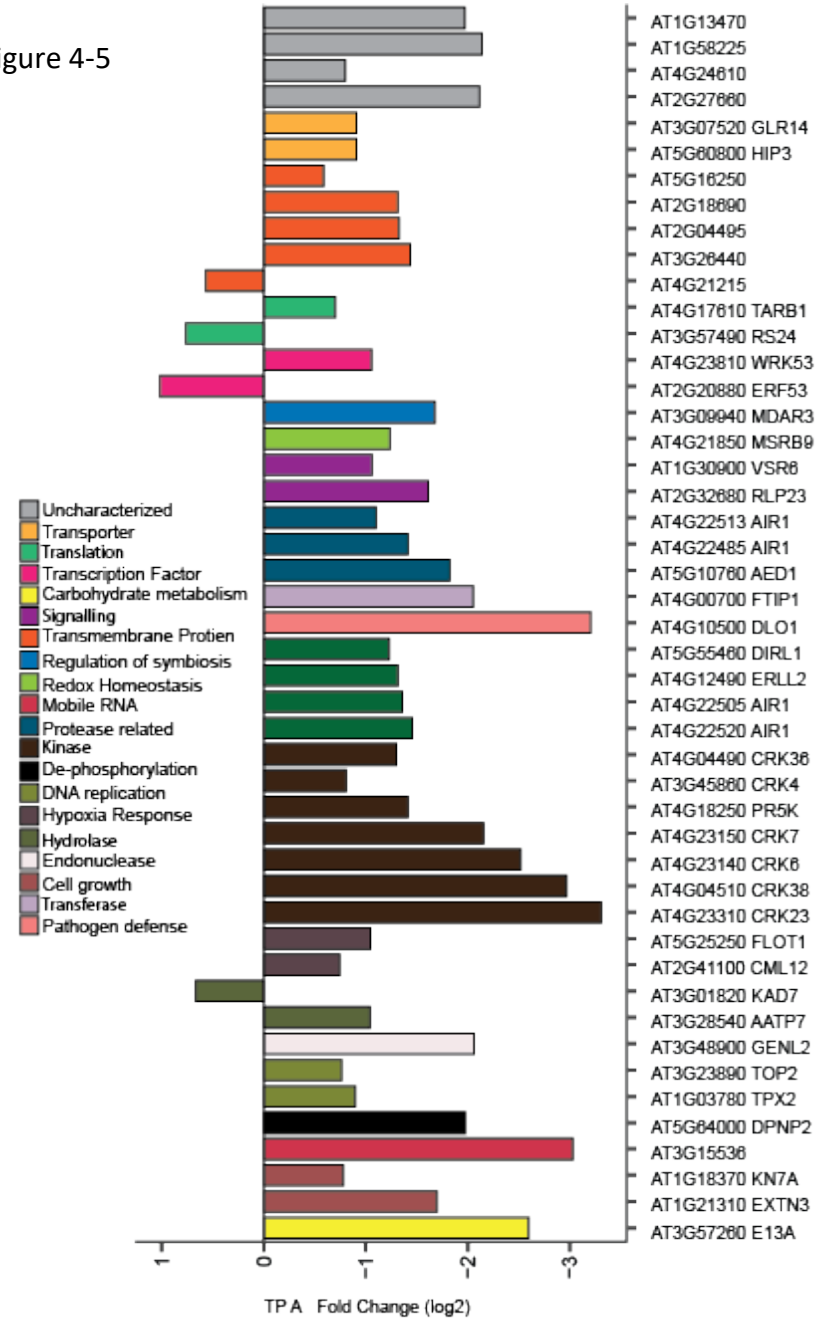

Figure 4-5A (figure legend on pg. 166)

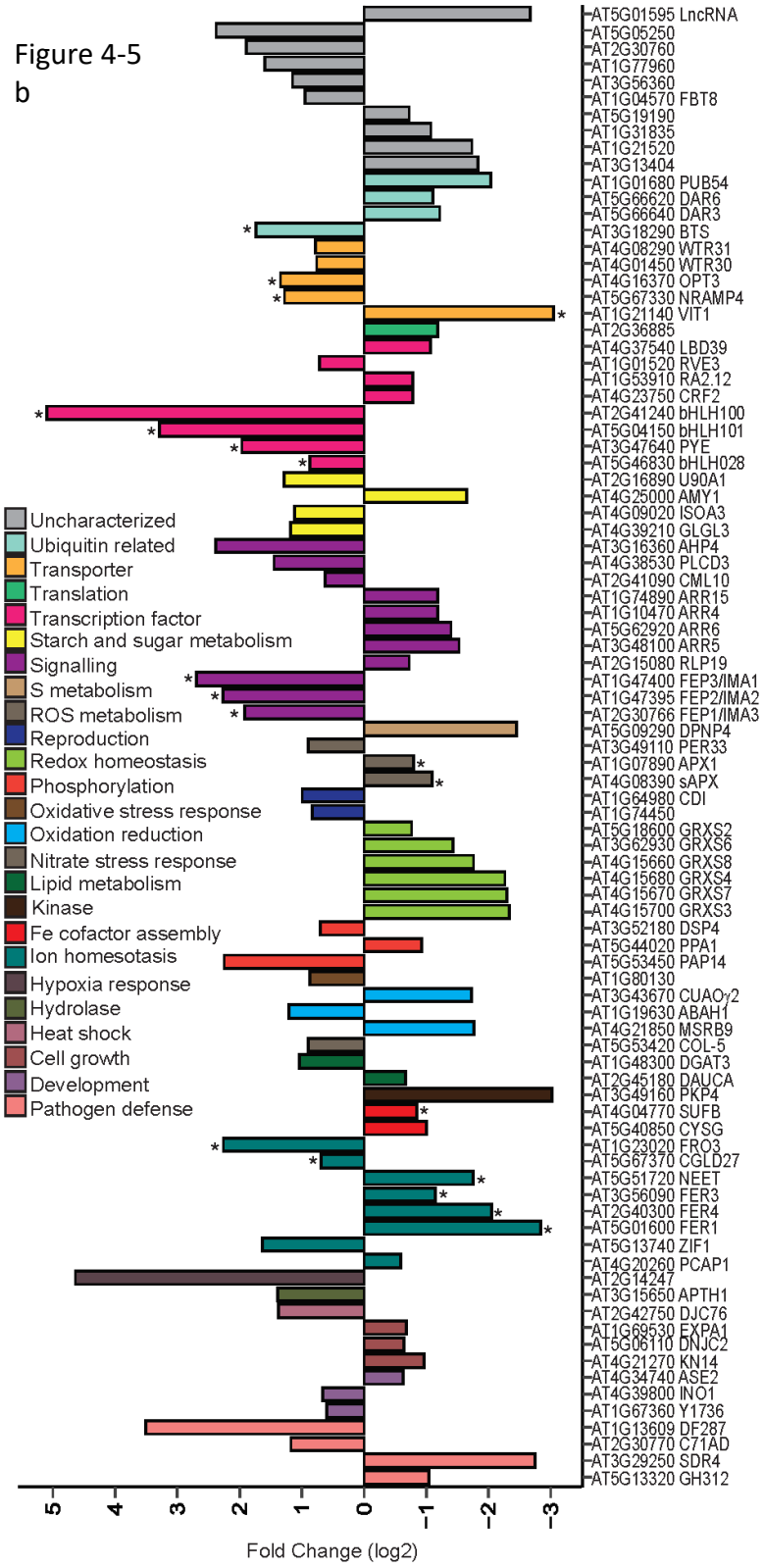

Figure 4-5: a. Fold change of significant DEGs in WT-Fe compared to WT+Fe at TP A and b. TP B Log_2 Fold Change is plotted for all DEGs in WT-Fe. ATG numbers are shown on the right side of the graph. For genes that are annotated, the name of the gene is also included. Colors correspond to general function of the gene product. Asterisks denote known Fe responsive transcripts.

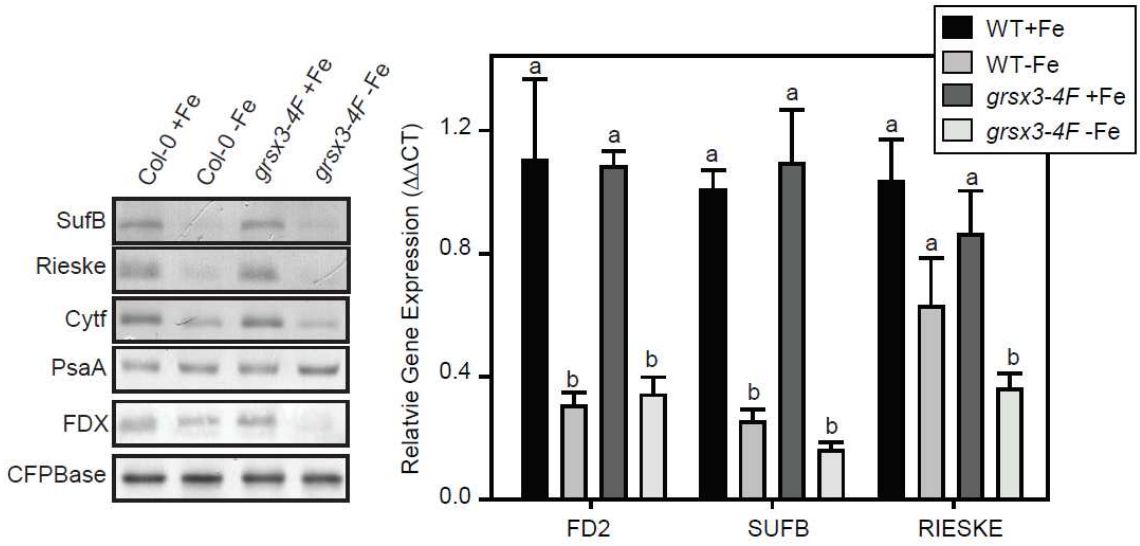

Figure 4-6: Protein and transcript accumulation of photosynthetic Fe proteins in *grxs3/4/5/7/8* knockdown line after 7 days of Fe deficiency. A. Protein and transcript accumulation of leaf proteins that are targeted during Fe deficiency (FDX, Cyt*f*, Rieske, SUFB and PSaA) in WT and *grxs3/4/5/7/8*. Proteins were separated by SDS-PAGE (15% gel) and transferred to a 0.2 μM pore nitrocellulose membrane (n=4). cFPBase is included as a loading control. B. Gene expression is measured by qPCR. Transcript abundance is normalized to *UBQ10* and then to gene expression of WT (n=3).

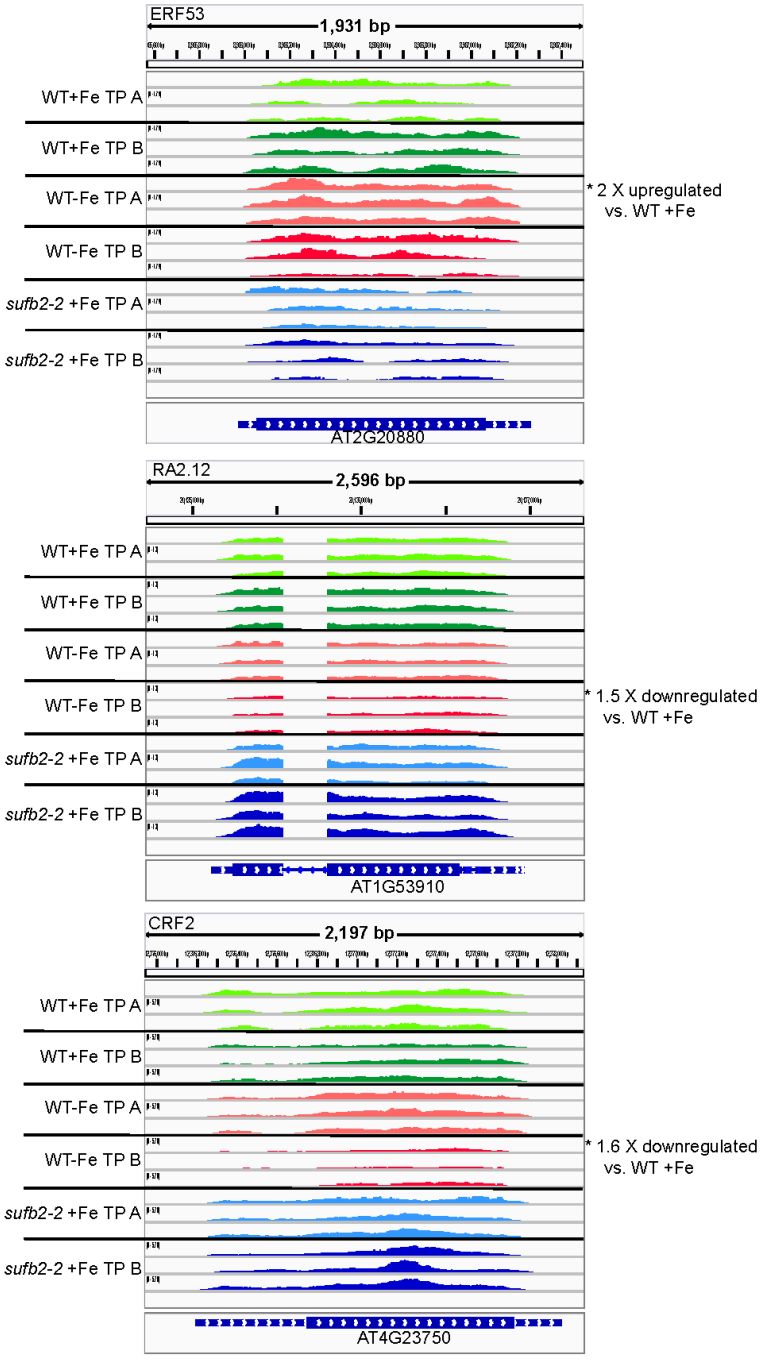

Figure 4-7: Differential expression of 3 ERF family transcripts during Fe deficiency Read coverage of three biological replicates for ERF53, RA2.12, and CRF2 in WT+Fe, WT-Fe, and *sufb2-2* +Fe by Integrative Genome Viewer (IGV). Height of peaks within each lane represents number of reads per area of the genome. Length of the genome area in view is denoted by number of base pairs above the read coverage. Location in genome is denoted by the ATG number at bottom of read coverage. Significant differential expression and fold change of the average FPKM compared to WT+Fe is denoted to the right of the read coverage.

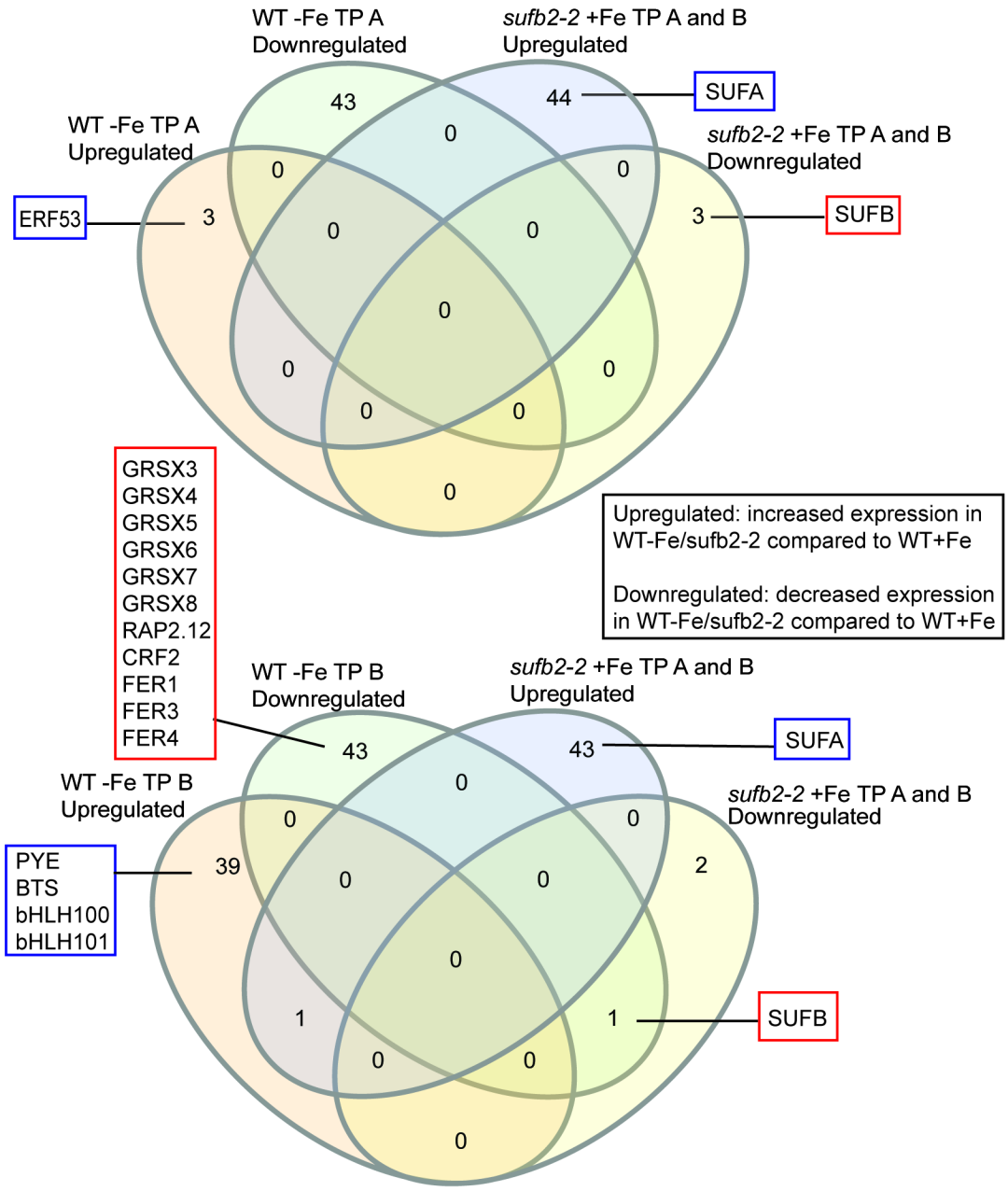

Figure 4-8: **Differentially expressed genes in WT-Fe TPA and TPB compared to differentially expressed genes in *sufb2-2*.** Numbers in each of the Venn diagram segment shows the number of differentially up or down-regulated transcripts shared between the different WT-Fe timepoints and gene expression changes specific to loss of SUFB. Only significantly differentially expressed genes with a fold change of at least 1.5 x higher or lower than WT+Fe are represented. Down-regulated genes are those that are decreased in expression in WT-Fe or *sufb2-2* compared to WT+Fe; Up-regulated genes are these that have increased expression in WT-Fe or *sufb2-2* compared to WT+Fe. Names of transcripts to side of Venn diagrams are examples of genes regulated in each segment of the Venn diagram.

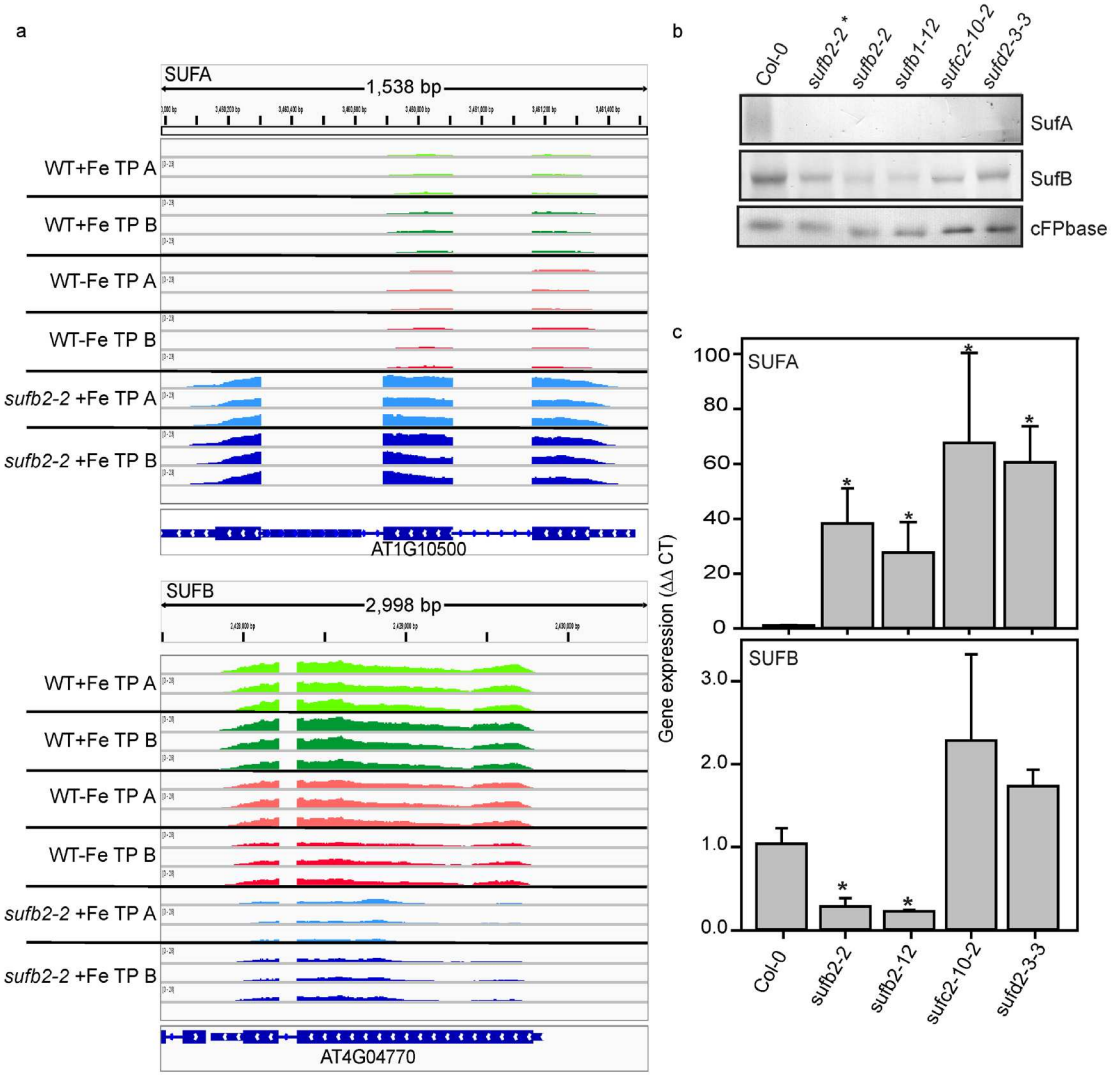

Figure 4-9: SUFA protein and transcript accumulation in *sufb/c/d* knockdown lines. (a) read coverage of *SUFB* and *SUFA* transcripts of 3 biological reps of WT+Fe, WT-Fe and *sufb2-2* from IGV. Height of peaks within each lane represents number of reads per area of the genome. Length of the genome area in view is denoted by number of base pairs above the read coverage. Location in genome is denoted by the ATG number at bottom of read coverage. (b) protein accumulation of SUFA in *sufb/c/d* knockdowns compared to WT. Samples were taken 5 days after DEX induction. Asterisk denotes *sufb2-2* sample was taken from RNA-seq sampling. Representative blots of 3 reps are shown. Proteins were separated on a SDS-PAGE (15% gel) and transferred to a 0.2 μM pore nitrocellulose membrane. (c) transcript abundance of SUFA in *sufb/c/d* knockdowns analyzed by qPCR. Rosettes of knockout lines were collected 3 days after DEX treatment. Transcript abundance is normalized to *UBQ10* and then to SUFA abundance of WT (n=3). Significance was determined by an ANOVA and is denoted by an asterisk above the bar.

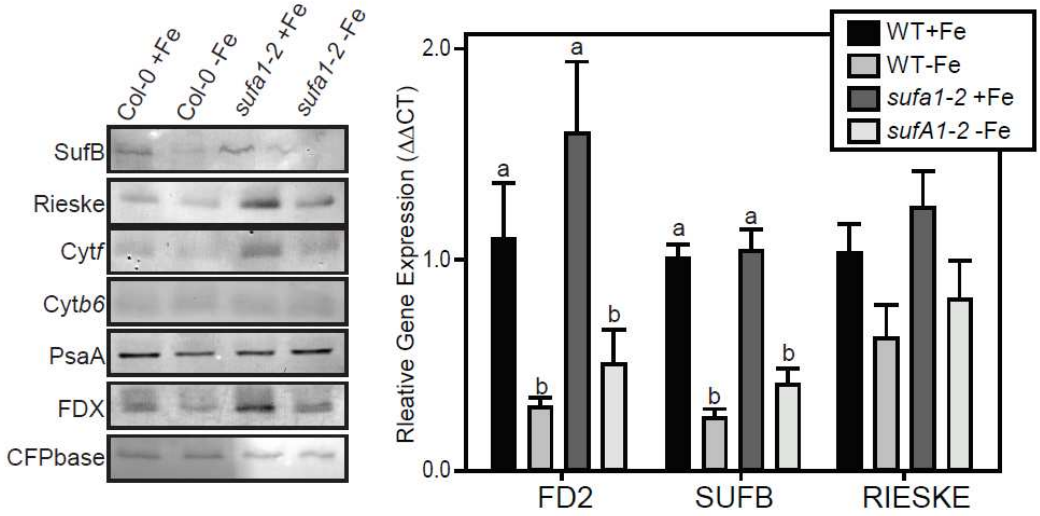

Figure 4-10: Protein and transcript accumulation of photosynthetic proteins in *sufa* under normal and low Fe conditions. Protein accumulation of Fe deficiency markers in WT and *sufa1-2* shows a higher accumulation of FDX, Cyt*f*, and Rieske. Proteins were separated by SDS-PAGE (15% gel) and transferred to a 0.2 μM pore nitrocellulose membrane (n=4). Gene expression of chloroplast Fe markers by qPCR. Transcript abundance is normalized to *UBQ10* and then to gene expression of WT (n=3). Significance was determined by an ANOVA and is denoted by letters above bars.

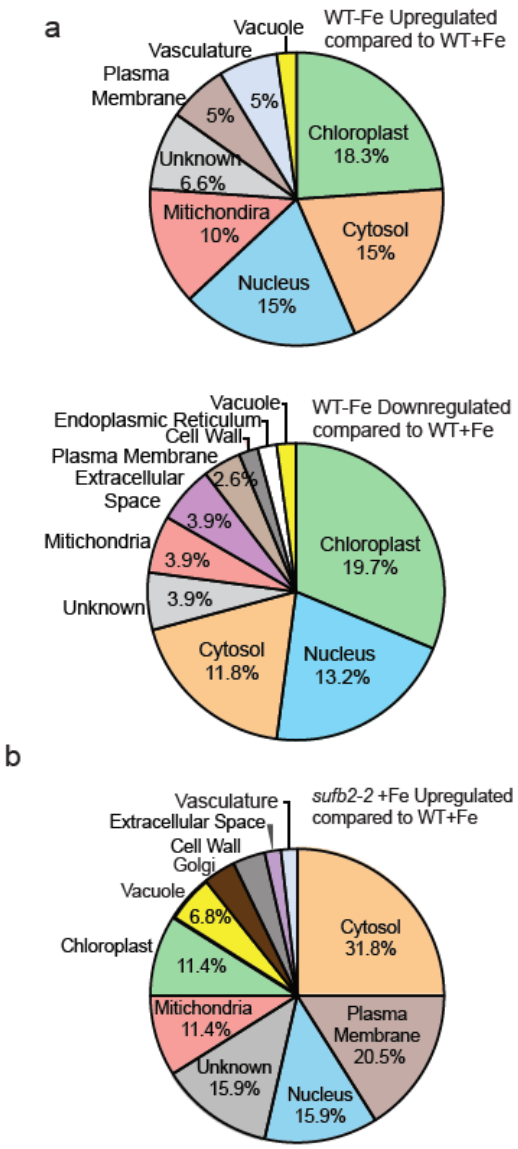

Figure 4-11: Predicted sub-cellular location of gene products of differentially expressed genes. (a) Predicted cellular location of gene products of DEGs at TP B for up and down-reguated DEGs in WT-Fe. (b) Predicted cellular location of gene products of DEGs at TP B for up-regulated DEGs in *sufb2-2* +Fe. Only significantly differentially expressed genes with a fold change of at least 1.5 x higher or lower than WT+Fe are represented. Down-regulated genes are those that are decreased in expression in WT-Fe or *sufb2-2* compared to WT+Fe; Up-regulated genes are these that have increased expression in WT-Fe or *sufb2-2* compared to WT+Fe.

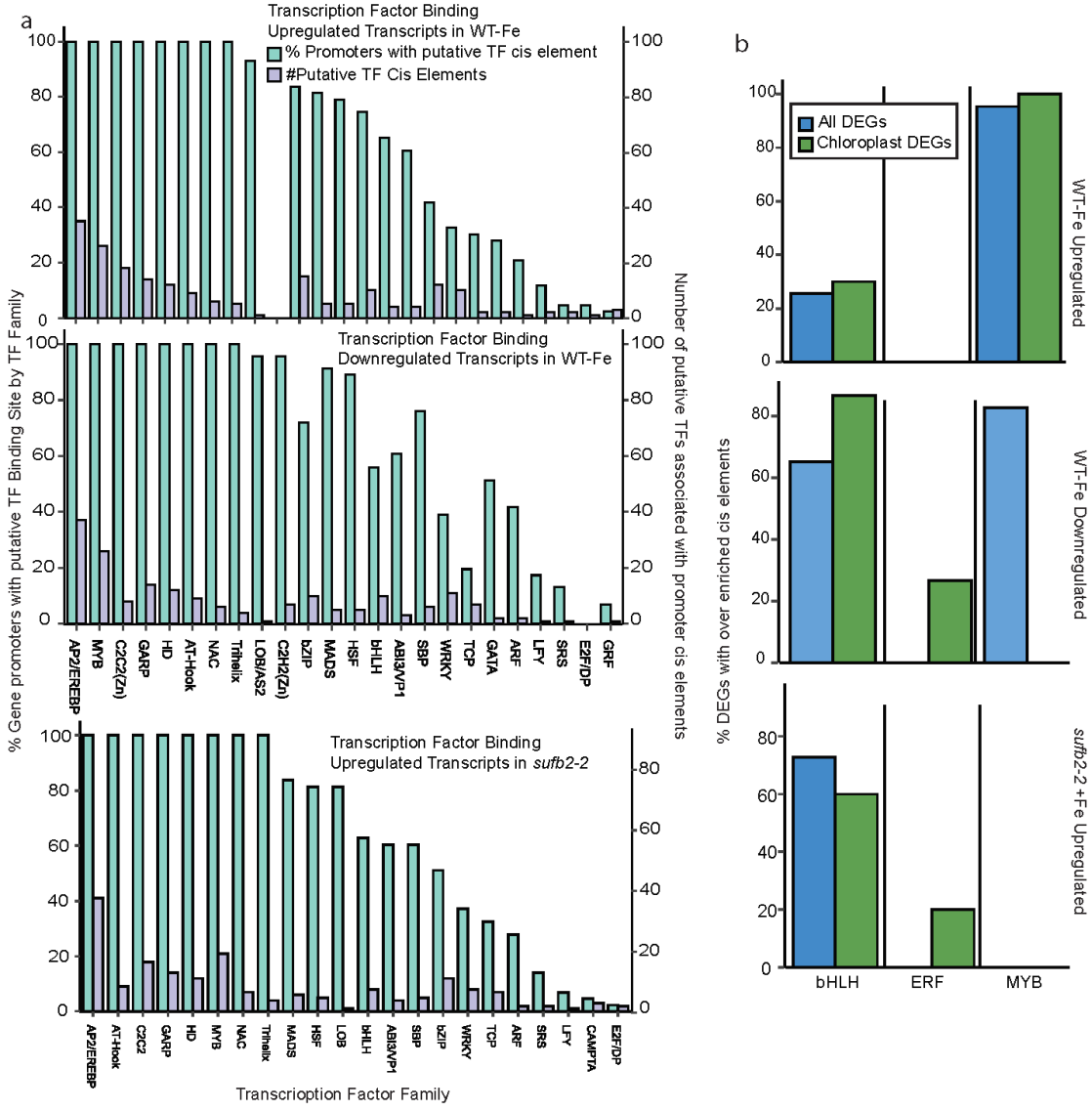

Figure 4-12: Analysis of promoter *cis* elements for transcription factor binding in differentially expressed genes. (a) Transcription factor family binding site enrichment in promoters of up-regulated genes in *sufb2-2*+Fe and up and down-regulated genes in WT-Fe for the indicated treatment comparison in each graph. Green bars represent the percentage of differentially expressed genes that contain at least one putative transcription factor binding site in a specific transcription factor family. Purple bars represent the number of transcription factors within each family that are predicted to bind to promoter sequences of DEGs. (b) Percent of DEGs up and down-regulated that are over enriched for *cis* elements of bHLH, ERF, and MYB Transcription factors in WT-Fe. Percent of DEGs up-regulated that are over enriched for *cis* elements of bHLH and ERF Transcription factors in *sufb2-2* +Fe. No MYB *cis* elements are over enriched in *sufb2-2*+Fe DEG promoters. Enrichment was analyzed for all DEGs and, separately, for DEGs of gene products localized to the chloroplast. Abundance of *cis* elements in DEG promoters were compared to the rate that the same *cis* elements are found across the genome ($p<0.05$). Only significantly differentially expressed genes with a fold change of at least 1.5 x higher or lower than WT+Fe are represented in both a and b.

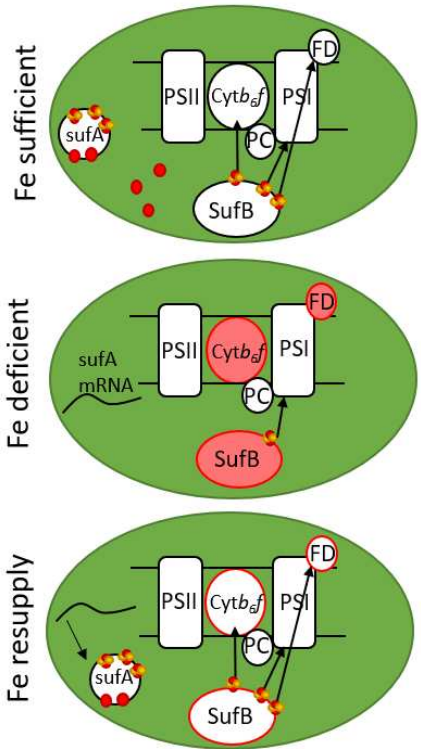

Figure 4-13: Hypothetical model of SUFA as a regulator of Fe-S insertion into apo-proteins. During Fe sufficient conditions, SUFBCD produces Fe-S clusters and they are inserted into apoproteins via Fe-S carrier proteins. SUFA may act to sequester excess Fe to be used in Fe-S assembly or excess Fe-S clusters to be inserted into proteins. During Fe deficiency, SUFB is down-regulated at the protein and transcript level resulting in less Fe-S clusters for proteins. SUFA transcript remains normal, but protein is degraded. Upon Fe resupply, as SUFB and Fe-S requiring proteins are recovering, SUFA can be quickly translated to hold excess Fe/Fe-S for requiring proteins as they recover.

LITERATURE CITED

Abdel-Ghany SE, Ye H, Garifullina GF, Zhang LH, Pilon- Smits EAH, Pilon M (2005) Iron-sulfur cluster biogenesis in chloroplasts. Involvement of the scaffold protein CpIscA. Plant Physiology 138: 161-172

Anders S, Pyl PT, Huber W (2015) HTSeq—a Python framework to work with high-throughput sequencing data. Bioinformatics 31: 166-169

Balasubramanian R, Shen G, Bryant DA, Golbeck JH (2006) Regulatory Roles for IscA and SufA in Iron Homeostasis and Redox Stress Responses in the Cyanobacterium Synechococcus sp. Strain PCC 7002. The Journal of Bacteriology 188: 3182

Balk J, Pilon M (2011) Ancient and essential: the assembly of iron–sulfur clusters in plants. Trends in Plant Science 16: 218-226

Balparda M, Armas AM, Estavillo GM, Roschzttardtz H, Pagani MA, Gomez-Casati DF. (2020) The PAP/SL1 retrograde signaling pathway is involved in iron homeostasis. Plant Molecular Biology. 1-15.

Bandyopadhyay S, Gama F, Molina-Navarro MM, Gualberto JM, Claxton R, Naik SG, Huynh BH, Herrero E, Jacquot JP, Johnson MK, Rouhier N (2008) Chloroplast monothiol glutaredoxins as scaffold proteins for the assembly and delivery of 2Fe-2S clusters. Embo Journal 27: 1122-1133

Bauer P, Ling H-Q, Guerinot ML (2007) FIT, the FER-LIKE IRON DEFICIENCY INDUCED TRANSCRIPTION FACTOR in Arabidopsis. Plant Physiology and Biochemistry 45: 260-261

Brumbarova T, Bauer P, Ivanov R (2015) Molecular mechanisms governing Arabidopsis iron uptake. Trends in Plant Science 20: 124-133

Bülow L, Brill Y, Hehl R (2010) AthaMap-assisted transcription factor target gene identification in Arabidopsis thaliana. Database: The Journal of Biological Databases and Curation 2010

Colangelo EP, Guerinot ML (2004) The essential basic helix-loop-helix protein FIT1 is required for the iron deficiency response. Plant Cell 16: 3400-3412

Conn SJ, Hocking B, Dayod M, Xu B, Athman A, Henderson S, Aukett L, Conn V, Shearer MK, Fuentes S, Tyerman SD, Gilliham M (2013) Protocol: optimising hydroponic growth systems for nutritional and physiological analysis of Arabidopsis thaliana and other plants. Plant Methods 9

de Castro E, Sigrist C, Gattiker A, Bulliard V, Langendijk-Genevaux P, Gasteiger E, Bairoch A, Hulo N (2006) ScanProsite: detection of PROSITE signature matches and ProRule-associated functional and structural residues in proteins. Nucleic Acids Research 34: W362-365

Felsenstein J (1985) Phylogenies and the Comparative Method. The American Naturalist 125: 1-15

Franco-Zorrilla JM, Lopez-Vidriero I, Carrasco JL, Godoy M, Vera P, Solano R (2014) DNA-binding specificities of plant transcription factors and their potential to define target genes. Proceedings of the National Academy of Sciences 111: 2367

Friso G, Olinares PDB, van Wijk KJ (2011) The workflow for quantitative proteome analysis of chloroplast development and differentiation, chloroplast mutants, and protein interactions by spectral counting. In Chloroplast Research in Arabidopsis, Jarvis R.P. (ed). pp 265-282, New York, New York

Gao F, Robe K, Gaymard F, Izquierdo E, Dubos C (2019) The Transcriptional Control of Iron Homeostasis in Plants: A Tale of bHLH Transcription Factors? Frontiers in Plant Science 10

Glaesener AG, Merchant SS, Blaby-Haas CE (2013) Iron economy in Chlamydomonas reinhardtii. Frontiers In Plant Science 4

Gollhofer J, Timofeev R, Lan P, Schmidt W, Buckhout TJ (2014) Vacuolar-Iron-Transporter1-Like proteins mediate iron homeostasis in Arabidopsis. PLoS ONE 9: e110468

Grillet L, Lan P, Li W, Mokkapati G, Schmidt W (2018) IRON MAN is a ubiquitous family of peptides that control iron transport in plants. Nature plants 4: 953

Grusak MA (1995) Whole-Root Iron(III)-Reductase Activity Throughout The Life-Cycle Of Iron-Grown Pisum-Sativum L (Fabaceae) - Relevance To The Iron Nutrition Of Developing Seeds. Planta 197: 111-117

Hantzis LJ, Kroh GE, Jahn CE, Cantrell M, Peers G, Pilon M, Ravet K (2018) A Program for Iron Economy during Deficiency Targets Specific Fe Proteins. Plant Physiology 176: 596-610

Hao D, Ohme-Takagi M, Sarai A (1998) Unique mode of GCC box recognition by the DNA-binding domain of ethylene-responsive element-binding factor (ERF domain) in plant. Journal Of Biological Chemistry 273: 26857-26861

Heberle H, Meirelles GV, Da Silva FR, Telles GP, Minghim R (2015) InteractiVenn: a web-based tool for the analysis of sets through Venn diagrams. BMC bioinformatics 16: 169

Hindt MN, Akmakjian GZ, Pivarski KL, Punshon T, Baxter I, Salt DE, Guerinot ML (2017) BRUTUS and its paralogs, BTS LIKE1 and BTS LIKE2, encode important negative regulators of the iron deficiency response in Arabidopsis thaliana. Metallomics 9: 876-890

Hirayama T, Lei GJ, Yamaji N, Nakagawa N, Ma JF (2018) The Putative Peptide Gene FEP1 Regulates Iron Deficiency Response in Arabidopsis. Plant and Cell Physiology 59: 1739-1752

Hoagland DR, and Arnon, D (1938) The water culture method for growing plants without soil. UC College of Agriculture, Ag. Exp. Station, Berkeley, CA. Circular. **347**: 1-39

Hsieh E-J, Cheng M-C, Lin T-P (2013) Functional characterization of an abiotic stress-inducible transcription factor AtERF53 in Arabidopsis thaliana. Plant Molecular Biology 82: 223-237

Hu XY, Kato Y, Sumida A, Tanaka A, Tanaka R (2017) The SUFBC2D complex is required for the biogenesis of all major classes of plastid Fe-S proteins. Plant Journal 90: 235-248

Jain A, Connolly EL (2013) Mitochondrial Iron Transport and Homeostasis in Plants. Frontiers in Plant Science 4

Jakoby M, Wang HY, Reidt W, Weisshaar B, Bauer P (2004) FRU (BHLH029) is required for induction of iron mobilization genes in Arabidopsis thaliana. Febs Letters 577: 528-534

Jeong J, Merkovich A, Clynel M, Connolly EL (2017) Directing iron transport in dicots: regulation of iron acquisition and translocation. Current Opinion in Plant Biology 39: 106-113

Jones DT, Tayolor WR, Thronton JM (1992) The rapid generation of mutation data matrices from protein sequences. Computational Applied Bioscience. 8(3): 275-82

Kastoori Ramamurthy R, Xiang Q, Hsieh E-J, Liu K, Zhang C, Waters BM (2018) New aspects of ironcopper crosstalk uncovered by transcriptomic characterization of Col-0 and the copper uptake mutant spl7 in Arabidopsis thaliana. Metallomics 10: 1824-1840

Kim D, Langmead B, Salzberg SL (2015) HISAT: a fast spliced aligner with low memory requirements. Nature Methods 12

Kim SA, Lacroix IS, Gerber SA, Guerinot ML (2019) The iron deficiency response in requires the phosphorylated transcription factor URI. Proceedings of the National Academy of Sciences of the United States of America 116: 24933

Kobayashi T (2019) Understanding the Complexity of Iron Sensing and Signaling Cascades in Plants. Plant & Cell Physiology 60: 1440-1446

Kumanovics A, Chen OS, Li LT, Bagley D, Adkins EM, Lin HL, Dingra NN, Outten CE, Keller G, Winge D, Ward DM, Kaplan J (2008) Identification of FRA1 and FRA2 as genes

involved in regulating the yeast iron regulon in response to decreased mitochondrial iron-sulfur cluster synthesis. Journal of Biological Chemistry 283: 10276-10286

Kumar S, Stecher G, Li M, Knyaz C, Tamura K (2018) MEGA X: Molecular Evolutionary Genetics Analysis across Computing Platforms. Molecular biology and evolution 35: 1547

Laganowsky A, Gomez SM, Whitelegge JP, Nishio JN (2009) Hydroponics on a chip: Analysis of the Fe deficient Arabidopsis thylakoid membrane proteome. Journal of Proteomics 72: 397-415

Lanquar V, Ramos MS, Lelievre F, Barbier-Brygoo H, Krieger-Liszkay A, Kramer U, Thomine S (2010) Export of Vacuolar Manganese by AtNRAMP3 and AtNRAMP4 Is Required for Optimal Photosynthesis and Growth under Manganese Deficiency. Plant Physiology 152: 1986-1999

Liang XJ, Qin L, Liu PW, Wang MH, Ye H (2014) Genes for iron-sulphur cluster assembly are targets of abiotic stress in rice, Oryza sativa. Plant Cell and Environment 37: 780-794

Ling HQ, Bauer P, Bereczky Z, Keller B, Ganal M (2002) The tomato fer gene encoding a bHLH protein controls iron-uptake responses in roots. Proceedings of the National Academy of Sciences of the United States of America 99: 13938

Lingam S, Mohrbacher J, Brumbarova T, Potuschak T, Fink-Straube C, Blondet E, Genschik P, Bauer P (2011) Interaction between the bHLH Transcription Factor FIT and ETHYLENE INSENSITIVE3/ETHYLENE INSENSITIVE3-LIKE1 Reveals Molecular Linkage between the Regulation of Iron Acquisition and Ethylene Signaling in Arabidopsis(C)(W). Plant Cell 23: 1815-1829

Liu W, Li Q, Wang Y, Wu T, Yang Y, Zhang X, Han Z, Xu X (2017a) Ethylene response factor AtERF72 negatively regulates Arabidopsis thaliana response to iron deficiency. Biochemical and Biophysical Research Communications 491: 862-868

Liu W, Umuhoza Karemera NJ, Wu T, Yang Y, Zhang X, Xu X, Wang Y, Han Z (2017b) The ethylene response factor AtERF4 negatively regulates the iron deficiency response in Arabidopsis thaliana. PLoS ONE 12: e0186580

Long TA, Tsukagoshi H, Busch W, Lahner B, Salt DE, Benfey PN (2010) The bHLH Transcription Factor POPEYE Regulates Response to Iron Deficiency in Arabidopsis Roots. Plant Cell 22: 2219-2236

Lopez-Millan A, Grusak MA, Abadia A, Abadia J (2013) Iron deficiency in plants: an insight from proteomic approaches. Frontiers In Plant Science 4

Mai H-J, Bauer P (2016) From the proteomic point of view: Integration of adaptive changes to iron deficiency in plants. Current Plant Biology 5: 45-56

Maxwell K, Johnson GN (2000) Perspectives in Experimental Botany. Chlorophyll fluorescence—a practical guide. Journal of Experimental Botany. Journal of Experimental Botany 51: 659-668

Merchant S, Sawaya MR (2005) The Light Reactions: A Guide to Recent Acquisitions for the Picture Gallery. The Plant Cell. 17, pp 648-663

Mizoi J, Shinozaki K, Yamaguchi-Shinozaki K (2012) AP2/ERF family transcription factors in plant abiotic stress responses. BBA - Gene Regulatory Mechanisms 1819: 86-96

Moran Lauter A, Peiffer G, Yin T, Whitham S, Cook D, Shoemaker R, Graham M (2014) Identification of candidate genes involved in early iron deficiency chlorosis signaling in soybean (Glycine max) roots and leaves. BMC Genomics 15

Nechushtai R, Conlan A, Harir Y, Song L, Yogev O, Eisenberg-Domovich Y, Livnah O, Michaeli D, Rosen R, Ma V, Luo Y, Zuris J, Paddock M, Cabantchik Z, Jennings P, Mittler R (2012) Characterization of Arabidopsis NEET Reveals an Ancient Role for NEET Proteins in Iron Metabolism(W). Plant Cell 24: 2139-2154

Notredame C, Higgins DG, Heringa J (2000) T-coffee: a novel method for fast and accurate multiple sequence alignment. Journal of Molecular Biology 302: 205-217

Ojeda L, Keller G, Muhlenhoff U, Rutherford J, Lill R, Winge D (2006) Role of glutaredoxin-3 and glutaredoxin-4 in the iron regulation of the Aft1 transcriptional activator in Saccharomyces cerevisiae. Journal Of Biological Chemistry 281: 17661-17669

Outten FW, Djaman O, Storz G (2004) A suf operon requirement for Fe-S cluster assembly during iron starvation in Escherichia coli. Molecular Microbiology 52: 861-872

Palmer CM, Hindt MN, Schmidt H, Clemens S, Guerinot ML (2013) MYB10 and MYB72 Are Required for Growth under Iron-Limiting Conditions. Plos Genetics 9

Pan IC, Tsai H-H, Cheng Y-T, Wen T-N, Buckhout TJ, Schmidt W (2015) Post-Transcriptional Coordination of the Arabidopsis Iron Deficiency Response is Partially Dependent on the E3 Ligases RING DOMAIN LIGASE1 (RGLG1) and RING DOMAIN LIGASE2 (RGLG2). Molecular & Cellular Proteomics : MCP 14: 2733

Patterson K, Walters LA, Cooper AM, Olvera JG, Rosas MA, Rasmusson AG, Escobar MA (2016) Nitrate-Regulated Glutaredoxins Control Arabidopsis Primary Root Growth. Plant physiology 170: 989

Pilon-Smits EAH, Garifullina GF, Abdel-Ghany S, Kato S-I (2002) Characterization of a NifS-like chloroplastic protein from A*rabidopsis.* Implications for its role in sulfur and selenium metabolism. Plant Physiology 130: 1309-1318

Pilon-Smits EAH, Hwang SB, Lytle CM, Zhu YL, Tai JC, Bravo RC, Chen YC, Leustek T, Terry N (1999) Overexpression of ATP sulfurylase in Indian mustard leads to increased selenate uptake, reduction, and tolerance. Plant Physiology 119: 123-132

Poor CB, Wegner SV, Li H, Dlouhy AC, Schuermann JP, Sanishvili R, Hinshaw JR, Riggs-Gelasco PJ, Outten CE, He C (2014) Molecular mechanism and structure of the Saccharomyces cerevisiae iron regulator Aft2. Proceedings of the National Academy of Sciences 111: 4043

Ravet K, Pilon M (2013) Copper and Iron Homeostasis in Plants: The Challenges of Oxidative Stress. Antioxidants & Redox Signaling 19: 919-932

Ravet K, Touraine B, Boucherez J, Briat JF, Gaymard F, Cellier F (2009) Ferritins control interaction between iron homeostasis and oxidative stress in Arabidopsis. Plant Journal 57: 400-412

Robinson NJ, Procter CM, Connolly EL, Guerinot ML (1999) A ferric-chelate reductase for iron uptake from soils. Nature 397: 694-697

Rodriguez-Celma J, Pan I, Li W, Lan P, Buckhout T, Schmidt W (2013) The transcriptional response of Arabidopsis leaves to Fe deficiency. Frontiers In Plant Science 4

Santi S, Schmidt W (2009) Dissecting iron deficiency-induced proton extrusion in Arabidopsis roots. New Phytologist 183: 1072-1084

Schmittgen TD, Livak KJ (2008) Analyzing real-time PCR data by the comparative C-T method. Nature Protocols 3: 1101-1108

Schwenkert S, Netz DJA, Frazzon J, Pierik AJ, Bill E, Gross J, Lill R, Meurer J (2010) Chloroplast HCF101 is a scaffold protein for 4Fe-4S cluster assembly. Biochemical Journal 425: 207-214

Séguéla M, Briat J-F, Vert G, Curie C (2008) Cytokinins negatively regulate the root iron uptake machinery in Arabidopsis through a growth-dependent pathway. Plant Journal 55: 289-300

Shikanai T, Muller-Moule P, Munekage Y, Niyogi KK, Pilon M (2003) PAA1, a P-type ATPase of Arabidopsis, functions in copper transport in chloroplasts. Plant Cell 15: 1333-1346

Shin L-J, Lo J-C, Chen G-H, Callis J, Fu H, Yeh K-C (2013) IRT1 DEGRADATION FACTOR1, a RING E3 Ubiquitin Ligase, Regulates the Degradation of IRON-REGULATED TRANSPORTER1 in Arabidopsis. The Plant Cell 25: 3039-3051

Sivitz AB, Hermand V, Curie C, Vert G (2012) Arabidopsis bHLH100 and bHLH101 Control Iron Homeostasis via a FIT-Independent Pathway. Plos One 7

Takahashi H, Kopriva S, Giordano M, Saito K, Hell R (2011) Sulfur Assimilation in Photosynthetic Organisms: Molecular Functions and Regulations of Transporters and Assimilatory Enzymes. Annual Review of Plant Biology 62: 157

Tanaka A, Tanaka A (2019) The Biochemistry, Physiology, and Evolution of the Chlorophyll Cycle. In: Advances in Botanical Research Metabolism, Structure and Function of Plant Tetrapyrroles: Introduction Microbial and Eukaryotic Chlorophyll Synthesis and Catabolism, Grimm P. (ed) pp 184-207 London UK

Tejada-Jimenez M, Llamas A, Galvan A, Fernandez E (2019) Role of Nitrate Reductase in NO Production in Photosynthetic Eukaryotes. Plants 8: 56

Tissot N, Robe K, Gao F, Grant-Grant S, Boucherez J, Bellegarde F, Maghiaoui A, Marcelin R, Izquierdo E, Benhamed M, Martin A, Vignols F, Roschzttardtz H, Gaymard F, Briat J-F, Dubos C (2019) Transcriptional integration of the responses to iron availability in Arabidopsis by the bHLH factor ILR3. The New Phytologist 223: 1433-1446

Toledo-Ortiz G, Huq E, Quail P (2003) The Arabidopsis basic/helix-loop-helix transcription factor family(w). Plant Cell 15: 1749-1770

Touraine B, Boutin JP, Marion-Poll A, Briat JF, Peltier G, Lobréaux S (2004) Nfu2: a scaffold protein required for [4Fe-4S] and ferredoxin iron-sulphur cluster assembly in Arabidopsis chloroplasts. Plant Journal 40: 101-111

Udvardi MK, Czechowski T, Scheible WR (2008) Eleven golden rules of quantitative RT-PCR. Plant Cell 20: 1736-1737

Urzica EI, Casero D, Yamasaki H, Hsieh SI, Adler LN, Karpowicz SJ, Blaby-Haas CE, Clarke SG, Loo JA, Pellegrini M, Merchant SS (2012) Systems and Trans-System Level Analysis Identifies Conserved Iron Deficiency Responses in the Plant Lineage. The Plant Cell 24: 3921-3948

Van Hoewyk D, Abdel-Ghany SE, Cohu CM, Herbert SK, Kugrens P, Pilon M, Pilon-Smits EAH (2007) Chloroplast iron-sulfur cluster protein maturation requires the essential

cysteine desulfurase CpNifS. Proceedings of the National Academy of Sciences 104: 5686

Vert G, Grotz N, Dedaldechamp F, Gaymard F, Guerinot ML, Briat JF, Curie C (2002) IRT1, an Arabidopsis transporter essential for iron uptake from the soil and for plant growth. Plant Cell 14: 1223-1233

Walters LA, Escobar MA (2016) The AtGRXS3/4/5/7/8 glutaredoxin gene cluster on Arabidopsis thaliana chromosome 4 is coordinately regulated by nitrate and appears to control primary root growth. Plant Signaling & Behavior 11

Xie Z, Nolan TM, Jiang H, Yin Y (2019) AP2/ERF Transcription Factor Regulatory Networks in Hormone and Abiotic Stress Responses in. Frontiers in plant science 10: 228

Xu XM, Adams S, Chuam NH, Moller SG (2005) AtNAP1 represents an atypical SufB protein in Arabidopsis plastids. Journal of Biological Chemistry 280

Yabe T, Morimoto K, Kikuchi S, Nishio K, Terashima I, Nakai M (2004) The Arabidopsis chloroplastic NifU-like protein CnfU, which can act as an iron-sulfur cluster scaffold protein, is required for biogenesis of ferredoxin and photosystem I. Plant Cell 16: 993-1007

Yabe T, Nakai M (2006) Arabidopsis AtIscA-I is affected by deficiency of Fe–S cluster biosynthetic scaffold AtCnfU-V. Biochemical & Biophysical Research Communications 340: 1047-1052

Yang T, Lin W-D, Schmidt W (2010) Transcriptional Profiling of the Arabidopsis Iron Deficiency Response Reveals Conserved Transition Metal Homeostasis Networks1[C][W]. Plant Physiology 152: 2130-2141

Yao Y, He RJ, Xie QL, Zhao XH, Deng XM, He JB, Song L, He J, Marchant A, Chen XY, Wu AM (2017) ETHYLENE RESPONSE FACTOR 74 (ERF74) plays an essential role in controlling a respiratory burst oxidase homolog D (RbohD)-dependent mechanism in response to different stresses in Arabidopsis. New Phytologist 213: 1667-1681

Ye H, Abdel-Ghany SE, Anderson TD, Pilon-Smits EAH, Pilon M (2006) CpSufE activates the cysteine desulfurase CpNifS for chloroplastic Fe-S cluster formation. The Journal of biological chemistry 281: 8958

Yu H, Yang J, Shi Y, Donelson J, Thompson SM, Sprague S, Roshan T, Wang D-L, Liu J, Park S, Nakata PA, Connolly EL, Hirschi KD, Grusak MA, Cheng N (2017) Arabidopsis Glutaredoxin S17 Contributes to Vegetative Growth, Mineral Accumulation, and Redox Balance during Iron Deficiency. Frontiers in Plant Science 8

Yuan YX, Wu HL, Wang N, Li J, Zhao WN, Du J, Wang DW, Ling HQ (2008) FIT interacts with AtbHLH38 and AtbHLH39 in regulating iron uptake gene expression for iron homeostasis in Arabidopsis. Cell Research 18: 385-397

Zandalinas SI, Song L, Sengupta S, McInturf SA, Grant DG, Marjault H-B, Castro-Guerrero NA, Burks D, Azad RK, Mendoza-Cozatl DG, Nechushtai R, Mittler R (2019) Expression of a dominant-negative AtNEET-H89C protein disrupts iron-sulfur metabolism and iron homeostasis in Arabidopsis. The Plant Journal

Zhai ZY, Gayomba SR, Jung HI, Vimalakumari NK, Pineros M, Craft E, Rutzke MA, Danku J, Lahner B, Punshon T, Guerinot ML, Salt DE, Kochian LV, Vatamaniuk OK (2014) OPT3 Is a Phloem-Specific Iron Transporter That Is Essential for Systemic Iron Signaling and Redistribution of Iron and Cadmium in Arabidopsis. Plant Cell 26: 2249-2264

Zhang G, Liu W, Feng Y, Li D, Li K, Sun Q, Zhai L, Wu T, Zhang X, Xu X, Wang Y, Han Z (2019) Ethylene Response Factors MbERF4 and MbERF72 Suppress Iron Uptake in Woody Apple Plants by Modulating Rhizosphere pH. Plant & cell physiology

CHAPTER 5: ADDITIONAL OBSERVATIONS ON PLASTID FE DEFICIENCY

5.1 SUMMARY

We have identified SUFB, FDX2, and Cyt-b_6f as major targets of down-regulation during the leaf response to Fe deficiency, with SUFB and FDX2 being transcriptionally down-regulated after only 2 days of low Fe treatment (Chapter 2: Hantzis et al., 2018). We wanted to determine if regulation of SUFB and FDX2 in response to Fe status is driven by *cis* elements in their promoters by designing transgenic *Arabidopsis* plants containing constructs in which the upstream regions of SUFB and FDX2 are fused to the reporter β-Glucuronidase (GUS). My second goal aimed to determine if loss of SUFB in the leaf results in up-regulation of the root Fe uptake machinery by measuring root Fe reductase activity in the Dexamethasone (DEX) inducible *sufb*-RNAi knockdown. As a third aim we investigated if the regulation of SUFB, FDX2, and the Cyt-b_6f complex subunits in response to Fe deficiency is conserved in economically important crop plants. Here, the preliminary results of each of these projects is presented and discussed.

5.2 INTRODUCTION

Transcriptional responses to Fe deficiency in the root are largely regulated by a cascade of bHLH transcription factors that culminate in the up-regulation of the ferric reductase enzyme FRO2, and Fe uptake protein IRT1 (Kobayashi *et al.,* 2019). In comparison, much more is still to be discovered about how the leaf contributes to Fe homeostasis and regulates its response to Fe status.

We had found that *SUFB* and *Ferredoxin 2 (FDX2)* transcripts are down-regulated early after low Fe treatment (Hantzis *et al.,* 2018). However, no bHLH *cis* elements are predicted to be present in the *SUFB* promoter, and very few are predicted to be present in the *FDX2* promoter (Hantzis *et al.,* 2018). Therefore, the regulation of *SUFB* and *FDX2* transcripts could

be via a different class of transcription factor (Chapter 4), or by post transcriptional regulation, such as mRNA turnover. We aimed to determine if *SUFB* and *FDX2* are regulated transcriptionally via *cis* elements contained in their promoter regions. To do this, we constructed promoter reporter fusions whereby the upstream regulatory regions (~2000 bp) of Arabidopsis *SUFB* and *FDX2* with and without the 5'UTRs were fused to the β-glucuronidase (GUS) coding sequence from *Escherichia coli*. Constructs were transformed into *Arabidopsis thaliana* for analysis of GUS expression in response to Fe status. If the decreased expression of *SUFB* and *FDX2* is driven by reduced promoter activity in response to Fe deficiency, GUS activity should decrease as Fe availability decreases.

The early down-regulation of *SUFB in* leaves during Fe deficiency results in a similarities with the *sufb*-RNAi inducible knockdown lines specifically in the physiological response and photosynthetic protein accumulation (Hantzis *et al.,* 2018; Hu *et al.,* 2017; for details see Dissertation Chapter 4). Fe deficiency causes up-regulation of root Fe uptake systems (Kobayashi, 2019). Would inducible loss of leaf SUFB also cause this up-regulation of Fe uptake in the root? To test this, we aimed to characterize the systemic Fe deficiency response of the *sufb*-RNAi inducible knockdown by measuring root ferric reductase activity in plants grown on sufficient levels of Fe. Evidence of a systemic Fe deficiency response in the *sufb*-RNAi inducible knockdown during normal Fe conditions would suggest that SUFB, or availability of chloroplast Fe-S clusters, is involved in regulation of the root Fe deficiency response (Robinson *et al.,* 1999). To test the hypothesis that down-regulation of SUFB is required for systemic Fe deficiency signaling, we measured the root ferric reductase activity of a plant containing an inducible *sufb*-RNAi knockdown system. We also measured rosette Fe concentrations which are known to decrease in response to Fe deficiency in WT plants (Hantzis *et al.,* 2018). We expected that the induction of the *sufb*-RNAi transcript would result in up-regulation of root ferric reductase activity because in other mutants that are known to disrupt Fe

homeostasis, such as *opt3*, both root Fe reductase activity and Fe accumulation in the leaves are altered on normal levels of Fe deficiency (Zhai *et al.,* 2014).

Fe deficiency is common in crop plants and leads to a decrease in crop output and nutritional value of crops for human consumption (Briat *et al.,* 2015). A system to detect crop Fe deficiency early could be useful in improving Fe content of crops for human consumption. Therefore, we aimed to determine if the leaf Fe deficiency response that targets SUFB, FDX2, and Cytb_6f as seen in *Arabidopsis* is conserved in economically important plants.

5.3 METHODS

Plant material. Arabidopsis ecotype Col-0 was used for development of GUS expressing lines and as a wild-type control for all experiments. *sufb* and *sufc*-RNAi Dexamethasone (DEX) inducible knockdowns are described in Hu *et al.,* 2017. To determine conservation of the leaf Fe deficiency molecular response in economically important plants, we grew *Glycine max* (Soybean, cultivar Williams 82), *Zea mays* (Maize, accession NSL202126), *Solanum lycopersicum* (Tomato, cultivar Eden Brothers), and *Oryza sativa* (Rice, accession PI 584595). *O. sativa* and *Z. mays* seeds were obtained from the USDA National Plant Germplasm System. *S. lycopersicum* and *G. max* seeds were a gift from Dr. Christina Walter's private seed stores.

Cloning procedures, strains, plasmids and media. Standard cloning procedures were used (Sambrook and Russel, 2001). *E. coli* strain DH5-alpha (Sambrook and Russel, 2001) was used for cloning and DNA amplification, transformation was by the $CaCl_2$/heat shock method. The pBI101.2 vector has been described (Jefferson *et al.,* 1987). Plasmid were purified using the Qiagen Plasmid Mini or Midi Prep Kits according to manufacturer's instructions (Qiagen, Hilden, Germany). Sanger sequencing of isolated DNA was done at GeneWiz (South Plainfield, NJ; www.genewiz.com). *Agrobacterium tumefacians* strain GV3101 (Van Larebeke *et al.,* 1974) was transformed by a freeze thaw method (Holsters *et al.,* 1978). Bacteria were cultured in LB with appropriate antibiotics. Kanamycin sulfate and Gentamycin were used at 50 μg/ml. For long

term maintenance, strains were stored in 16% (w/v) glycerol at -80 ºC. A list of isolated plasmids and strains and their location in the freezer is given in Table 5-3.

Promoter sequence amplification. Upstream regulatory sequences for *SUFB* and *FDX2* were obtained from the TAIR10 release of the *Arabidopsis* Genome. For the promoter sequences (P-constructs) we used the region from upstream of the transcription start site up until the next coding sequence. For the full upstream region, we included the 5'UTR upstream of the translation initiation sites. For *SUFB,* the full upstream region used was 1,955 bp long, including a 65 bp 5' UTR. For *FDX2* the full upstream region used was 2,175 bp long including a 175 bp 5'UTR. Four constructs were produced: SUFB Promoter + UTR (SUFBPU); SUFB Promoter (SUFBP); FDX2 Promoter + UTR (FDX2PU); FDX2 Promoter (FDX2P). For primers, see Table 5-1.

Sequences were amplified from genomic DNA of *Arabidopsis* ecotype Col-0 by PCR using the high fidelity Phusion DNA polymerase (ThermoFisher, Waltham, MA) according to manufacturer's protocol. FDX2 promoter DNA was amplified by 30 cycles of 5 sec at 98ºC, 20 sec at 63ºC for annealing, and 4 min at 72ºC for extension. SUFB promoter DNA was amplified with 5 cycles of 5 sec at 98ºC, 20 sec at 70ºC for annealing, and 4 min at 72ºC for extension followed by 30 cycles of 5 sec at 98ºC, 20 sec at 65ºC for annealing, and 4 min at 72ºC for extension. Because the upstream regulatory region of *SUFB* shared sequence similarity with sequences on chromosome 1, 4 and 5, we first amplified the entire promoter and coding sequence of *SUFB.* We then amplified the *SUFB* regulatory regions from this amplicon. For subsequent cloning of the promoter sequences in the pBI101.2 vector, forward primer sequences contained a *Hind*III restriction site and reverse primer sequences contained a *BamH*I site. Kanamycin resistant colonies were tested for the presence of the construct by colony PCR before sequencing. (for primers, see Table A-1).

For *SUFB* promoter constructs, insertions were observed in the vector sequences compared to the TAIR10 sequence and are denoted in Figure 5-1. Therefore, we analyzed the

conservation of these regions across *Arabidopsis* ecotypes to predict if the changes in the construct sequences would affect promoter regulation. *Arabidopsis* ecotypes aligned to the Col-0 *SUFB* promoter were Lansberg (Ler), Burren (Bur), Cantania (Ct), Wassilewskija (Ws), Wu, Zurich (Zu), Edinburgh (Edi), Wilna (Wil), Tsu, San Feliu (Sf). Sequences were extracted from NCBI and aligned using Muscle in MEGA (Kumar *et al.,* 2018). The sequencing regions in question were not conserved across the *Arabidopsis* ecotypes, suggesting they are not important for promoter regulation. Therefore, we chose two plasmids from each SUFBPU and SUFBP for further transformation. The final vectors are named respectively pSUFBPU (SUFB promoter and 5'UTR fused to GUS), pSUFBP (SUFB promoter fused to GUS), pFDX2PU (FDX2 promoter and 5'UTR fused to GUS) and pFDX2P (FDX2 promoter fused to GUS), schematic construct maps are indicated in Figure 5-2.

Arabidopsis transformation. Agrobacterium-mediated transformation was performed using the floral dip method (Clough and Bent, 1998). Before floral dip, open flowers and siliques were removed. Bacteria were resuspended in a 5% (w/v) sucrose (Sigma Aldrich St. Louis, MO) solution with 0.05% (v/v) Silwet (Lehle Seeds, Round Rock, TX) at a cell density equivalent to an OD_{600} of 0.8. Buds were submerged into the *Agrobacterium* sucrose solution for one minute. After dipping, plants were kept in a dark, high humidity environment for 12 hours to increase probability of *Agrobacterium* transformation. After 12 hours, plants were placed back in the light to set seed.

For selection of transformed lines, T0 seeds were sterilized in 10% bleach and stratified for 4 days at 4°C before planting on ½ MS media (Murashige and Skoog, 1962) (0.4% agar) with 1% sucrose, 0.05 mg/mL kanamycin for selection of transformed lines, and 0.05 mg/mL cefotaxime to kill excess *Agrobacterium*. Plates were incubated in a growth chamber (at 23°C and a 16 h : 8 h light cycle light intensity of 150 μmol $m^{-1}s^{-2}$). Seedlings that grew on the kanamycin plates (from T0 seeds) were transferred to soil for propagation. Seed line nomenclature was as follows: T0 seeds were named for their respective construct (ex: FDPU

T0). Seedlings that were resistant to kanamycin (T1 plants) were named as their construct followed by a letter (ex: FDPU-A). Seeds propagated from the T1 plants that expressed GUS and were PCR verified were named with their construct followed by a letter and number (ex: FDPU-A1). All seeds have been stored at 4°C and location of seeds is denoted in Table 5-3

Verification of transgenic lines. Kanamycin resistant seedlings were further verified to be transformed by PCR and by measuring for GUS activity by histochemical staining. For PCR verification, T2 plants were genotyped to confirm successful transformation. Genotyping primers are listed in Table 5-1 and were designed to span the promoter and GUS sequences. Plant lines that have been confirmed by both qualitative GUS assays and PCR verification were given nomenclature as listed in Table 5-2. For GUS histochemical staining, a young leaf from each T1 plant was incubated in GUS buffer containing 50 mM sodium phosphate, 0.1% v/v Triton-X100, 10 mM EDTA, 0.5 mM K_3FeCN_6, 0.5 mM K_4FeCN_6, and 1 mM 5-bromo-4-chloro-3-indolyl-beta-D-glucuronide cyclohexylammonium salt (X-Gluc; Gold Biotechnology, St. Louis, MO) the GUS substrate, at 37°C for 12 hours. After staining, the GUS buffer was removed and replaced with 95% ethanol for 12 hours, or until all chlorophyll was removed from the leaf. GUS activity was qualitatively measured by the presence of blue coloring in the leaf. T1 seeds were collected only from plants that were positive for GUS activity.

Quantitative analysis of GUS activity. GUS activity was measured using a quantitative enzyme activity 4-methylumbelliferyl β D-glucuronide (MUG; Sigma Aldrich, St. Louis, MO) assay (Gallagher, 1992; Jefferson *et al.,* 1987). Total protein was extracted from rosettes of FDPU line A1 (3 rosettes/ biological replicate) using a GUS extraction buffer containing 1 M $NaHPO_4$ pH 7.0, 14.4 M β-mercaptoethanol, 0.5 M Na_2EDTA pH 8.0, 30% (w/v) Sarcosyl, 10% (v/v) Triton X-100. Protein concentration was determined using the Bradford method (Bradford, 1976) and quantified using a BSA standard curve (1 mg/mL BSA). 300 μg of extracted protein was diluted 0.5x in the GUS assay buffer containing 2 mM 4-methylumbelliferyl b-D-glucuronide

(MUG) and incubated at 37°C for 30 min. For each sample, 50 μL aliquots of the reaction mixture were removed after 0, 10, 20, and 30 min and the reaction was stopped by addition to 1.95 mL of 2 M Na_2CO_3. GUS converts MUG into 4-methylumbelliferone (4-MU) which is fluorescent. The fluorescence was read using a DyNA Quant 200 Fluorometer (Hoefer Inc. San Francisco CA) calibrated by a 4-MU standard solution to 500 units. The 4-MU standard solution was diluted from 1 mM 7-hydroxy-4-methylcoumarin (4-MU; Sigma Aldrich) to 250, 500, 750, 1000, 1250, 1500, and 1750 nM solutions for a standard curve. 4-MU concentration was calculated based on the 4-MU standard curve. GUS activity was determined from the slope of a fitted line after plotting 4-MU concentration vs time and was normalized based on the concentration of protein in the 50 μL aliquot.

Plant growth. To assess FDPU line A1 response to Fe deficiency, plants were grown hydroponically for a pilot study as described in Dissertation Chapter 4. FDPU A1 was grown alongside Col-0 and at 4 weeks of age, half of each line was transferred to low Fe (10 nM Fe(III)EDTA) while the rest of the plants were maintained on normal levels of Fe (10 μM Fe(III)EDTA). Across the weeks of Fe deficiency, rosette samples were taken prior to low Fe treatment, and after 2 and 7 days of low Fe treatment. 3 rosettes were pooled for one biological replicate. A second set of FDPU line A were grown on nutrient agar plates, as described in Dissertation Chapter 4. At the end of one week of Fe deficiency plants were collected for MUG assays and nutrient analysis (10 seedlings per biological replicate).

To characterize root Fe reductase activity of inducible RNAi *sufb* and *sufc* knockdowns, plants were grown hydroponically following the method described in Dissertation Chapter 4. Knockdown lines were grown alongside *Arabidopsis* Col-0. All knockdown lines and a subset of Col-0 were grown on sufficient levels of Fe (10 μM Fe(III)EDTA) for the duration of the experiment. A second subset of Col-0 was transferred to low Fe (10 nM Fe(III)EDTA) for one

week at 4 weeks of age. Induction of the RNAi for experiments described here was done by foliar spraying plants with 10 μM DEX in 0.02% tween at four weeks of age.

For analysis of crop plant responses to Fe deficiency, seeds were germinated in moist paper towels in the dark for one week. After germination, plants were transferred to hydroponics and grown on ½ Hoagland's solution supplemented with 10 μM Fe(III)EDTA. When plants were four weeks old, half of each species was transferred to low Fe (10 nM Fe(III)EDTA) for one week. Plants were sampled 7 days after Fe for chlorophyll fluorescent parameters, and nutrient accumulation by ICP (as described in Dissertation Chapter 4). Samples were also taken for protein analysis.

Elemental Analysis. Shoot elemental analysis was analyzed after 7 days for both hydroponic and plate experiments as described in Dissertation Chapter 4. For hydroponic experiments, 2 rosettes were pooled for one biological replicate. For plate experiments, 10 shoots were pooled for one biological replicate.

Chlorophyll fluorescence. Photosynthetic efficiency was measured by chlorophyll fluorescence by a Fluorescence Monitoring System (Hansatech corp.). A leaf of intermediate age was used for measurement of fluorescence parameters. All photosynthetic parameters were calculated as described in Maxwell and Johnson (2000).

Protein extraction and western blotting detection. Proteins were extracted using the method outlined in Friso *et al.* (2011) and quantified as described in Dissertation Chapter 4. For western blotting, total protein sample was separated by SDS-PAGE (15% gel) and transferred to 0.2 μM pore nitrocellulose. All antibodies used (for Cyt*f,* Cytb_6*,* Rieske, PsaA, PsaC, PsaB, and cFPBase) were obtained from Agrisera. Detection of blots was done by alkaline phosphatase tagged to the secondary antibody. To assess equal loading, a separate SDS-PAGE (15% gel) was used for Coomassie Brilliant Blue (CBB) staining. For each sample, 40 μg of protein was loaded.

Bioinformatics analysis. We analyzed the conservation of the *Arabidopsis* protein sequence in the four crop species included in the study. Conservation analysis was done using NCBI Blast by the compositional matrix adjustment method (Yu and Altschul, 2005) with the query sequence being the respective protein sequence from *Arabidopsis.* All antibodies used for western blotting were raised against *Arabidopsis* proteins. The FDX antibody is specific for all three FD isoforms and therefore, each FD protein sequence comparison for each *Arabidopsis* FD isoform was done.

5.4 RESULTS AND DISCUSSION

GUS reporter transgenic Arabidopsis lines

At the time of completion of this dissertation, line selection for GUS fusions is still ongoing. We currently have 5 lines of FDPU and SUFBP that are verified to express GUS via histochemical staining. Only FDPU lines have been verified also by PCR (Table 5-2). FDP and SUFBPU constructs have been again transformed and seeds from T0 plants will be selected for kanamycin resistance and GUS expression.

For all plants that showed kanamycin resistance on plates, GUS expression was measured qualitatively. Of the four constructs, only two have thus far shown evidence of both kanamycin resistance and GUS expression—FDPU and SUFBP (Table 5-2). FDPU lines that have GUS activity have been verified by PCR to contain the construct. SUFBP lines still need to be verified by PCR. FDPU A1 was the first line to show GUS activity, and has since then been used as a positive control in the GUS assays. All other FDPU GUS expressing lines are shown in Figure 5-3. Plants that were shown to express GUS were propagated to the next generation in order to select for homozygosity.

A pilot study for determination of GUS activity in response to Fe deficiency was performed using FDPU line A. The FDPU A1 line showed the same physiological response to leaf Fe deficiency as Col-0. As expected, both Col-0 and FDPU A1 low Fe plants accumulate

less Fe in the shoots (Figure 5-4a) and have lowered ϕPSII and NPQ compared to their Fe sufficient counter parts (Figure 5-4b). Thus, GUS expression does not affect Fe homeostasis in the FDPU A1 line.

GUS enzyme activity was measured over one week of Fe deficiency treatment in the FDPU A1 line. For FDPU A1 +Fe plants we measured an increase in GUS activity over the time course, while FDPU A1 -Fe plants did not show this increase in GUS activity (Figure 5-5). However, the variation within each timepoint resulted in no significant differences across +Fe and -Fe plants.

The large variation in the GUS activity assay may be attributed to differences in individual plants grown in hydroponics as only 3 plants were pooled per biological replicate. An alternative way to grow plants on low Fe is using agar plates with nutrient agar. This allows for more plants to be pooled. Therefore, we tested this method of growth using FDPU A1 plants. After 7 days of low Fe treatment, FDPU A1 on the low Fe plates accumulated significantly less Fe compared to those on the high Fe plates (Figure 5-6). Further, we have evidence that *FDX2* and *SUFB* are down-regulated in plants grown on low Fe plates as seen in hydroponic plants (See Figures 4-6 and 4-10). Samples were also collected for quantitative MUG assays and are currently stored (see table 5-3).

The optimal parameters of the MUG assay have been determined in the preliminary experiments on FDPU A1, and preliminary data suggests a trend for GUS activity to be higher in the Fe sufficient plants. To complete the study and determine if promoter regulation is driving FDX2 and SUFB expression during Fe deficiency in the leaf, more lines of each construct must be analyzed for GUS activity in response to low Fe. Growing the plants on plates may decrease variability in the assay by pooling more plants per biological replicate.

To complement this study on regulation of *SUFB* and *FDX2* in response to Fe status, current projects in the Pilon Lab are characterizing the Fe deficiency response of *SUFB* and *FDX2* constitutive expressing *Arabidopsis* transgenic lines. If the regulation of *SUFB* and *FDX2*

are important in regulating leaf Fe during deficiency, the constitutive expression of these transcripts should result in plants with less sensitivity to Fe deficiency.

Increased root ferric reductase activity in presence of loss of leaf SUFB.

While testing the hypothesis that SUFB is required for proper regulation of the leaf Fe deficiency response, we found an interesting initial result of increased root ferric reductase activity in induced *sufb*-RNAi lines (Figure 5-7a). The induced *sufb2-2* and *sufb1-12* lines had increased root ferric reductase activity hen grown on sufficient levels of Fe compared to WT+Fe (Figure 5-7a).

To determine if the increase in root ferric reductase activity is correlated with loss of SUFB in leaves, we performed a time course analysis. *Sufb2-2* and *sufb1-12* were grown alongside WT+Fe and WT-Fe according to hydroponic growth methods outlined in Dissertation Chapter 4. At 4 weeks of age, plants were foliar sprayed with 10 μM DEX. A subset of WT was not sprayed. A second subset of WT was transferred to low Fe (10 nM Fe(III)EDTA), while all other plants were maintained on normal levels of Fe (10 μM Fe(III)EDTA). Solutions were changed at day 4 after DEX application to maintain Fe concentrations. Root ferric reductase activity was measured (as described in Dissertation Chapter 4) at 0, 3, 5, 7, 9, 11, and 14 days after DEX application (Figure 5-7b).

Induced lines of *sufb2-2* showed an increase in root ferric reductase activity only at day 9 after DEX application compared to WT+Fe (Figure 5-7b). Induced lines of *sufb1-12* showed an increase in root ferric reductase activity at day 3 and 5 after DEX application compared to WT+Fe. DEX treatment did not alter WT root ferric reductase activity as both WT+Fe sprayed with and without DEX did not show differences in root ferric reductase activity. However, we only observed an increase in root ferric reductase activity in WT-Fe after 3 days of Fe deficiency, suggesting that replenishing the solutions on day 4 may have introduced some Fe

contamination to the WT-Fe plants. However, the increases at certain timepoints of root ferric reductase activity in *sufb2-2* and *sufb1-12* remained of interest.

To simplify the experiment and to understand the relationship between loss of SUFB in the shoots and induction of root ferric reductase activity, we compared non-induced and induced lines of *sufb1-12*, *sufb2-2*, *sufb2-11*, and *sufc2-10-2.* SUFC is another protein in the major scaffold of the SUF Fe-S cluster assembly system and the inducible knockdown shows the same molecular and physiological symptoms as the inducible knockdown of SUFB (Hu *et al.,* 2017). Plants were grown hydroponically on 10 μM Fe(III)EDTA. At four weeks of age, half of each line were foliar sprayed with 10 μM DEX, and root ferric reductase activity was measured at 0, 3, 5, and 7 days after DEX. Non-induced lines were used as controls. In this experiment, no increase in root ferric reductase activity was observed in induced plants compared to non-induced plants (Figure 5-7c).

In addition, we measured shoot Fe concentration of the induced *sufb*-RNAi lines compared to the non-induced SUFB lines, WT+Fe, and WT-Fe. We found no difference in Fe accumulation between any of the induced lines compared to WT+Fe or their non-induced counterparts. In contrast, WT-Fe accumulated about half as much Fe as WT+Fe (Figure 5-7d).

Overall, variation in root ferric reductase activity in response to loss of SUFB was observed on a few occasions but was not consistent across experiments. Further, as shown in detail in Dissertation Chapter 4, the inducible *sufb2-2* line presents opposite transcriptional responses compared to WT-Fe, suggesting that SUFB does not play a pivotal role in leaf Fe deficiency regulation or sensing. However, the variation in root ferric reductase activity may suggest that the loss of SUFB alters the Fe homeostasis within the leaf cell which leads to initiation of a mild Fe deficiency signal. To investigate the role of SUFB in intercellular Fe homeostasis, an understanding of how Fe is partitioned within the cell in the induced *sufb* knockdowns would be useful. If less Fe is imported into the chloroplast in the induced *sufb* lines

and root ferric reductase activity is up-regulated in these conditions, it could suggest that the chloroplast Fe concentration is required for sensing leaf Fe status. Alternatively, the knockout mutant *fro7,* a chloroplast envelope localized ferric reductase enzyme that is required for chloroplast Fe import and is known to have lowered chloroplast Fe (Jeong *et al.,* 2008), could also be used to indirectly asses this question. *Fro7* should be analyzed for its SUFB protein and transcript accumulation to determine if these are lowered compared to WT+Fe, which may suggest that down-regulation of *SUFB* is more tied to chloroplast Fe status than overall leaf Fe status.

Conservation of leaf Fe deficiency protein changes in crop plants

To determine if antibodies raised from *Arabidopsis* proteins would have cross-reactivity with the homologous protein in other plant species, we analyzed sequence conservation of Cyt*f,* Cytb_6*,* Rieske, PsaA, PsaC, FDX1, FDX2, and FDX3. For most of the proteins, a high conservation of amino acid sequence was observed between each species and *Arabidopsis* (Table 5-4). However, the FDX isoforms were less conserved in all the species compared to *Arabidopsis*. Overall, the majority of proteins sequences are conserved across crop species, suggesting that the antibodies raised against *Arabidopsis* proteins should react with the same proteins from the crop species.

Protein accumulation for each of the crop species and for control *Arabidopsis was analyzed for both plants* grown on normal and low Fe levels (Figure 5-8). No major differences are seen in total protein in the Coomassie stained gel within each species. But, all crop species samples are loaded at a lower level compared to *Arabidopsis* protein samples (Figure 5-8a). The only blots that showed *Arabidopsis* positive controls were Cyt*f,* PsaA, and PsaB. However, the only differences in Cyt*f* accumulation between normal and low Fe conditions are in *Arabidopsis* and *O. sativa* (Figure 5-8b). In both *Arabidopsis* and *O. sativa,* PsaA is maintained under Fe deficiency as seen previously (Hantzis *et al.,* 2018). There is some evidence that the

Cytb_6 antibody could detect Cytb_6 protein in *S. lycopersicum* and that the cFPBase antibody could detect cFPBase in *Z. mays* and *G. max* (data not shown), but the presence of bands was weak and should be checked.

The lack of a decrease in Cyt*f* protein accumulation in response to Fe deficiency in several of the crops may be explained by physiological data. There was no real difference in chlorophyll fluorescence parameters, ϕPSII and NPQ, between normal and low Fe conditions within each species (Figure 5-9a). *O. sativa* does show a slightly lower ϕPSII in the low Fe condition. In addition, the low Fe treatments did not show a much lower accumulation of shoot Fe. Only the *G. max* and *S. lycopersicum* low Fe plants had a significantly lower Fe shoot concentration than their controls. However, even the Fe concentration in the low Fe treated *G. max* and *S. lycopersicum* may not have been low enough to induce Fe deficiency responses.

There is some evidence in *O.sativa* that a slight Fe deficiency results in the same decrease in Cyt*f* protein accumulation in response to Fe deficiency as seen in *Arabidopsis*. Overall, differences were not seen in abundance of the leaf proteins known to be regulated in response to Fe deficiency in *Arabidopsis.* One reason for this could be the very mild Fe deficiency in the leaves. The Fe concentration of leaves of low Fe treated plants may still have been sufficient for growth. This project did allow us to determine which antibodies may be useful in detecting proteins in different species but must be repeated to determine optimal Fe concentrations for the plant species in the study.

5.5 COLLABORATORS

Substantial contributions to the selection and verification of GUS transgenic lines were made by two undergraduates: Chase Alsup, a CSU student, and Karen Bacalia, an REU student in the summer of 2019. Karen also collected all data for the preliminary MUG assays

and physiological characterization of the FDPU A1 line. The crop Fe deficiency response project was carried out by an REU student (Tyler Hempstead) in summer 2019.

a.

5′ttcattcgacaattttataacagagactaatccaatactacaatttcactccaaaacctcaacaacac
ctacactcttccccaaagccatacaatagatgcaacaatcacaacagcaacccctacagtcttcaaagct
gactttgccataacatgtcctagctcttccacattctccttcatggtcaagagttcaccctccatcttct
taatcagctcttcctccatctgcttagcgtttttattaaggagctccatattagccatcacgttcattct
gaggtcactaatattctctacaactctcttacacttctcatttaccatcttaatttcgtccaagagagct
tcatcaacccatttgaacaagtgctcttcattttctctctataaaacataatttccaatcatttactcct
tcaatcaatcaaatatatcacaaaatcgaaatgtgtaccttcattgctatcgcacaacggtagaatctcc
ggtatggattctccttttgttttcgatgtgaatgtaatgatctcttctccacaccaacatttcgaggggac
accaggaggacagacacgaaatcctgaactggaagcggatgagtagtagctgttggtgctcattttctta
taaaattgtcgaatgaagaaccctaatcgaccaaatcgattttgcagaagaagaagaatgaaaacgacgt
cgttttctttctcttttgatgagttaaacgaaatgaaaacgacgtcgttttcttaacgggtctgggtat
tagtcgggttaatcgcaatcgcggtacagtaaacgcggatttgtggttaatcccggttaaatgaatggtt
caattggaaatgtatgtttaagcatgaatccgaaagtagatgatgtaattttgggaatatgaaagttgat
ggtggaaatttaagggcccaaaagtccgggggtgaaagctgagaatcgaaatagtttatggctcgaaaat
cagctaacccaagtagaatcgatactgattgtgtctagtgctttaattatctctagtagatcttcaaggt
ttatgccttgtccctagtacattttgctatctcggtctggtgggtgaggtgtgatggtgtttgtacttat
gtctctggtttcagcggcttcttgctttcctctctgtcgatttactattagttttgacttcggtgtaaaa
tctatccgatcttattggtgtttccggcgttcacatttttaggagaagtttaggtcttatttttcccat
agtttttatttttctttgaattttgtctcttgattcaatttcgttggtttaaaatgtttccttatatat
gtttttggttttacttcctttttttcagctaagtttctcaaaatattccgttggtctgttggcttatgta
tttcaacttgtattctactttagtttctaatataattcagatgagaaaaaaaaaagaattaaaactgatt
tcagtgtaccaaactaaactgaaatgaatgaaccaacaaatttttaaaataaaatattattaagtttttga
aataaaagatcaaactaatttttttttttcattaacaaaaacaagaaaccaacccgtaaatcggattataa
aatatctaatatctttgtttgttttgtccaagtataaaaaatatctaatatctaaaagagatttttaaca
aataaagaagagatcaacgttatttttttttttataattagttagtggaaaacgtatgtggtttataattg
agctgaaaagtgaaaatccaacaaaaaaatcgtctcgtggctgacacgagactatcttcaatctacggct
cagaaaattccataaatattaacatttcatctcttcttcatttttttcctaatcgttgtttttttttctaa
cacacgactccaaaaaaaaaaaaaaaaaacaatcttctttttacttctcctaagagccacaccaacaacaa**A**
TGTTACGTCCTGTAGAAACCCCAACCCGTGAAATCAAAAAACTCGACGGCCTGTGGGCAT…3′

(Figure continued onto next page)

b.

5’cgattctacgagaacatcatttgtttattggatatgctttttttaaagaatcaagagaatacgaaaac
aacttgtactcaagaatgtttactataattctctagtggatctttataagagctggagattagtttggat
tttatcttaaagtatccagttatcaaaaaatgagattgttaggacttttttacccgagagtatttagtt
acaaaaaagaaagttagtttaatattagataaactataattgcaactaacggtcagtagaaagctatata
agttatataacgaatctgaatatgacttagttatcttgttggattgtctagatatgttttgccttttac
ggaaagattcgatttggaacaacttctgaattaacctgaaaaacgtaattaaacattgacttgttggttg
tttgtagaatggttggtttatactttccgaatgtggctatgtgaaatcacattttgattatatgtataaa
gttgagatataatttttaaaatttgcaaaaaattattagttttgttaaaataataggagatgcaaactaaa
taaattctcttcttaactaaaaaagcaatagatttgttacattgaatgatggatagatttgtgagttgtg
actttgcttaagctaccccaacagataacggatatatcatatagatgttgagtaagaaagaaaaaaaaac
atttacgattgcattctcgtaatgggctttatgattttaaggcccaatagatgaagtaaggctaatgcac
aactttaagaaacgtaattctagcaagtgtttatcgactgcgttgtaggtttcttgtgttcgtggcacta
tggattaggttttaatatggtttctaatttcgttgatttcagtggcataagtccagttgttgcttgtggc
aaactgtttcatgtacaaaaacacttacatcattactaaattatgtcatgggtttggtttcgttaacaat
aagtcaatctccttgatgagttttatctatatgattatctatttgtctatttgcaacatgtagtagattg
aaatggggctgcaaaatatgctcttgcaattcctagttagatctagcttttgataatacgattatctaat
ttgtcatttcgatatgatagatagattgtttttaaaagagatctcaaccacttttctttaactaaaataa
aaaatttagtcacttttttattaaaaataactaaaaagttttaaacctatcaggacacttccatcaacagt
atttaaaagagatatttattattaaaataatacaaagtggtgaaaagaagagagaagtgagaatcgtctc
tgttttcagaaactctgaaaaatgtttatggccacgtgtttttccagaaatgattgattttattctttt
attaaaatttaatactttatctaaattcaattaaaataagcaatattttattcatgagaaactctttttt
gagaatcaaccgatgtagatggtctcatactctactttgttgattgtgtttaagtttctgaggatttttc
tactttccgacgttatgccaagaggctggtcttcactagaaaactacttccacccaattcaagcaagtat
gacctcttctcccaacaatttattcatgtactgaaaggccattagaagttgactgaagtgtgaaggtgga
gattatgtattcacttgttgatttggtatacattctatgtaaggttcaattatttacgttatataattat
aatggagtaatttacagtaattgggttaaaatggtttgattcggtcaggttgatacggtttggaagttaa
acccggcctagatatgatgttacaaccagtccacatcttttatgattttagtggaacaaacgaagagtta
tttagacgatacaaacaaggtccgaataagtgtgagctgtcccaagtaagaccacgtaatactcacctca
acaagatagtgttcttaaagtgtgtcaaacacaatcacacacacacaaatcataaaacacaaagacgata
atccatcgatccacagaatagacgccacgtggtagataggattctcactaaaaagttctcacctttaat
ctttctccacgccatttccacaagccataatcctcaaaaatctcaactttatctcccaaaacacaaaaca
aaaaaaa**ATGTTACGTCCTGTAGAAACCCCAACCCGTGAAATCAAAAAACTCGACGGCCTGTGGGCAT**…3
’

Figure 5-1 *SUFB* and *FDX2* promoter sequences. a. Promoter sequence from *SUFB*. b. Promoter sequence from *FDX2*. Black lowercase letters represent the promoter sequence. Red letters represent the 5’UTR. The beginning of the GUS coding sequence is denoted in bolded capital letters. The start of translation is underlined. Highlighted amino acids denote an insertion in the vector sequence compared to TAIR10 release of the *Arabidopsis* genome.

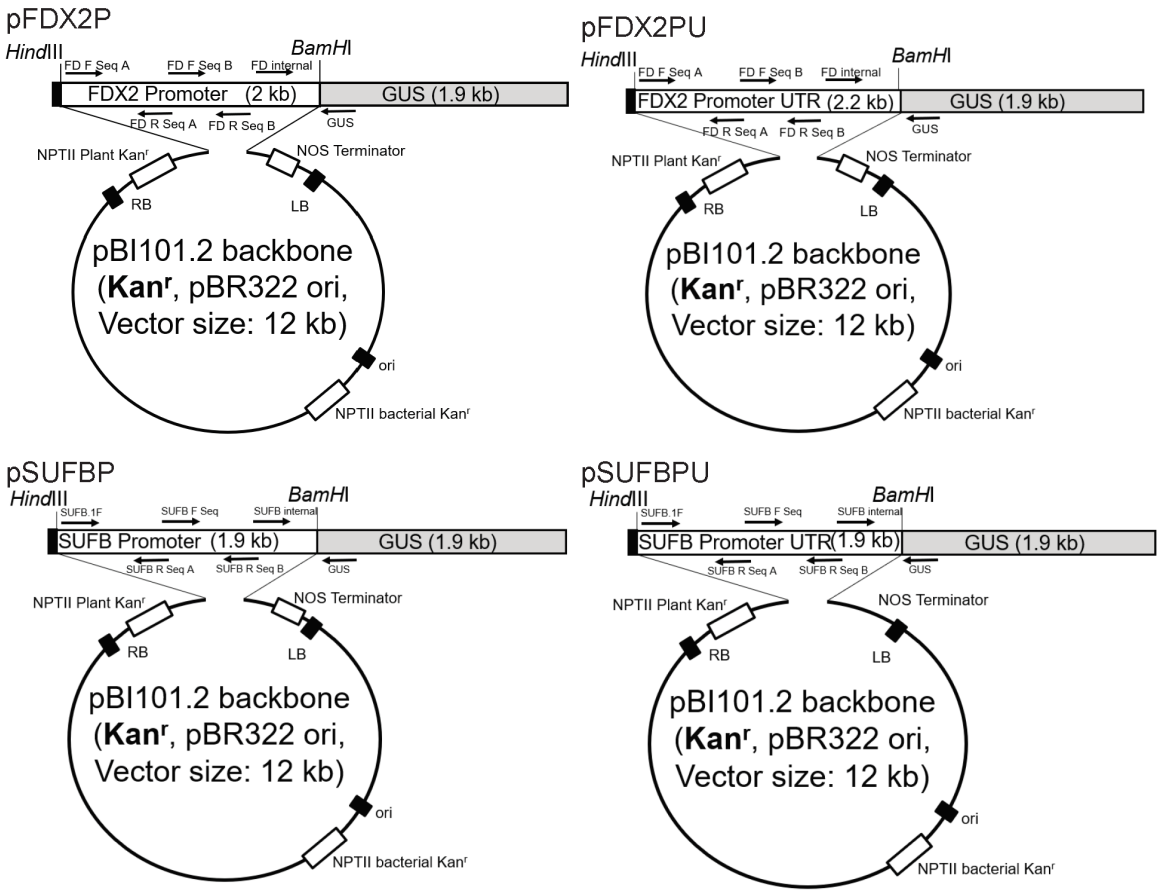

Figure 5-2 Vector constructs for pFDX2P, pFDX2PU, pSUFBP, and pSUFBPU. Backbone vector used for transformation was pBI101.2. Vector name is denoted above vector. For each construct, the size of the promoter or promoter + 5'UTR sequence is denoted. *Hind*III and *BamH*I sites were used for inserting the construct into the vector and their location is labeled. Locations of primers used for sequencing are denoted above and below the construct with their orientation relative to the sequence indicated by the direction of an arrow. The pBI101.2 vector contains a Kan resistance marker within the right and left boarders for Kan selection in plants, as well as a Kan resistance gene on the plasmid for selection in bacteria.

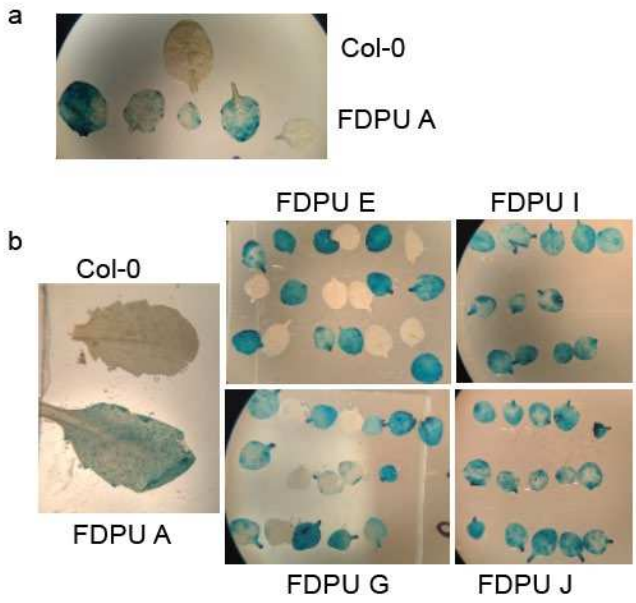

Figure 5-3 Histochemical detection of GUS activity in FDPU confirmed lines: a. FDPU line A was the first transgenic line that was positive for GUS activity after staining. Five leaves from individual FDPU A T1 plants were incubated at 37ºC with the X-Gluc GUS substrate solution. b. GUS activity in subsequent FDPU transgenic T1 lines. FDPU A was used as a positive control. All staining was done for 12 hours at 37ºC and chlorophyll was removed from leaves by extraction with 95% ethanol in the light.

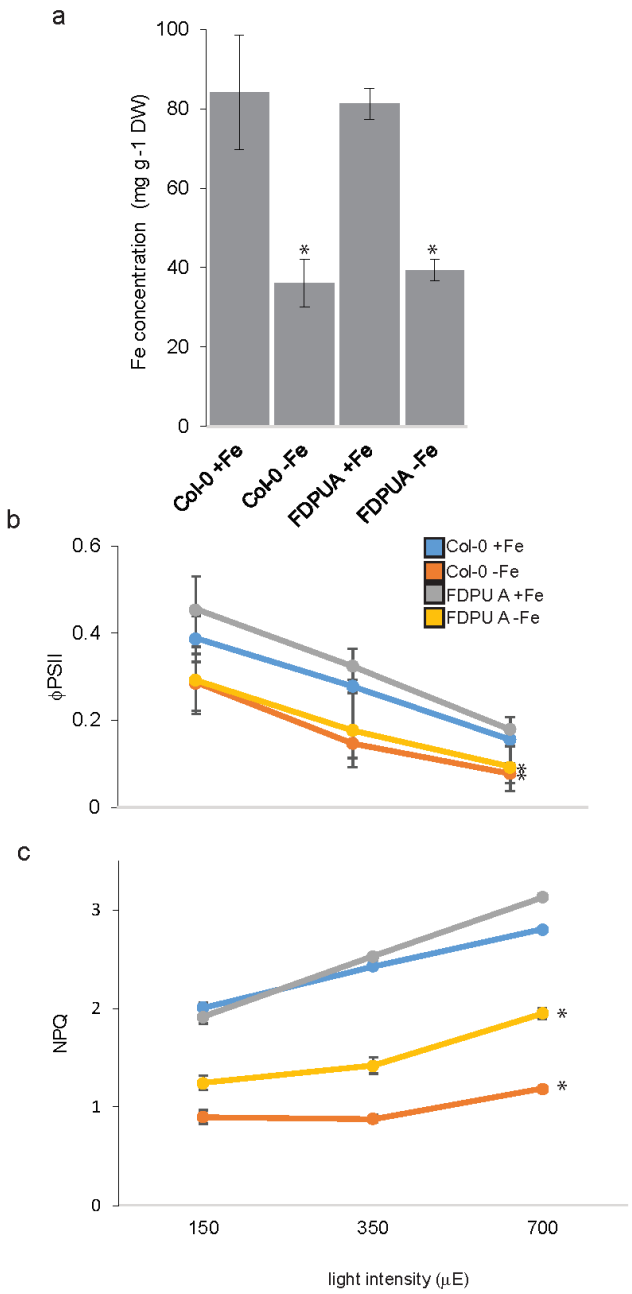

Figure 5-4 Physiological assessment of FDPU after 7 days of low Fe treatment: a. Fe concentration of whole rosettes of Col-0 and FDPU A1 plants grown on normal and low Fe. 2 rosettes were pooled per biological replicate. Fe concentration was normalized to sample dry weight. Bars represent mean +/- standard error (n=3). b. chlorophyll fluorescence parameters, ϕPSII and NPQ, for Col-0 and FDPU A1 plants grown on 10 μM Fe(III)EDTA and 10 nM Fe(III)EDTA. Measurements were taken at 150, 350, and 700 μE. Each point represents mean +/- standard error at each light intensity (n=3). Significance was determined by a t-test between normal and low Fe treatments for each line and is denoted by an asterisk.

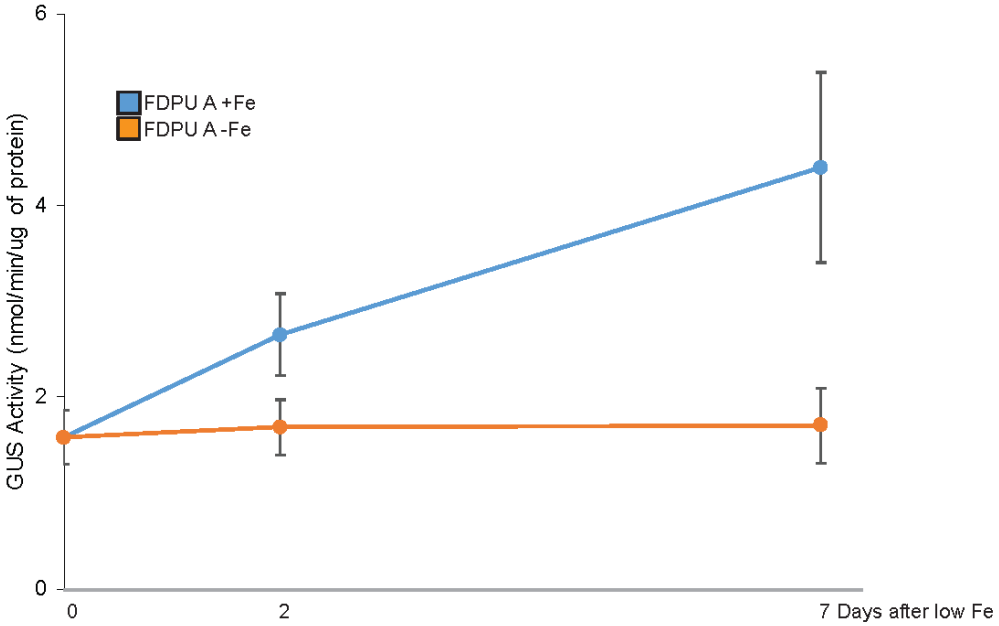

Figure 5-5 GUS activity measured by the MUG assay across 7 days of low Fe treatment: GUS activity was measured using the fluorometric MUG assay at 0, 2, and 7 days after FDPU A1 was transferred to low Fe. Concentration of 4-MU was calculated using a standard curve based on the fluorescence of the samples. Each point represents mean +/- standard error (n=3).

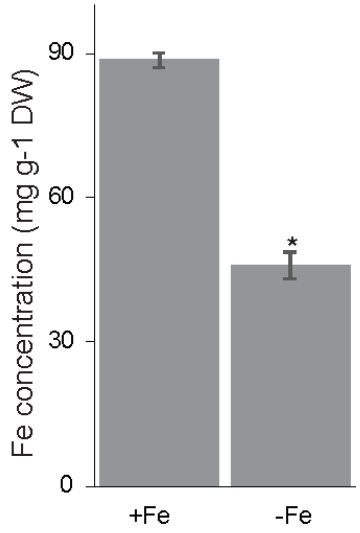

Figure 5-6 Fe concentration in FDPU A1 seedlings grown on plates: FDPU A1 lines were grown on nutrient agar plates with full nutrients and 40 μM Fe(III)EDTA for one week and then either maintained at 40 μM Fe(III)EDTA plates or transferred to 0 Fe plates. Bars represent mean +/- standard error (n=3). Significance was measured by a t-test and denoted by an asterisk.

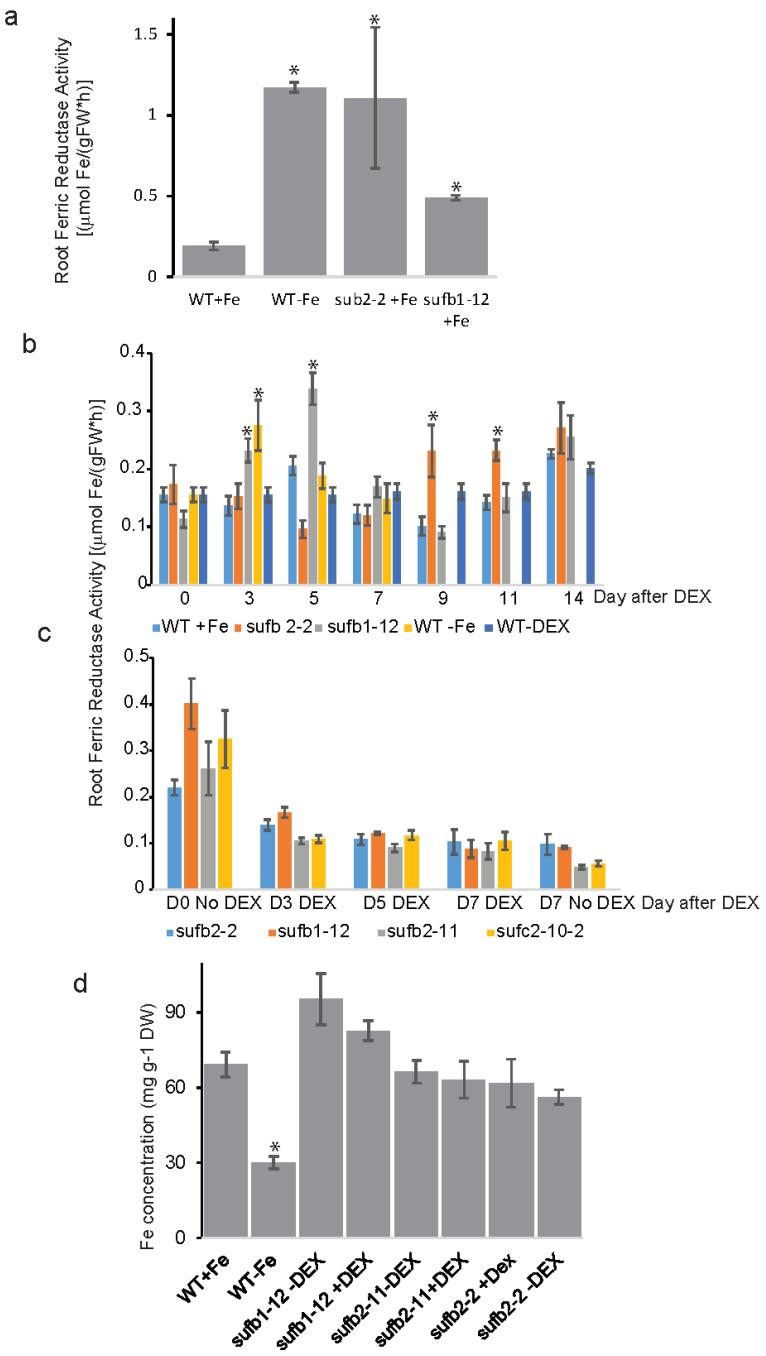

Figure 5-7 Characterization of root Fe reductase activity in *sufb*-RNAi induced lines: a. Initial assays on root Fe reductase activity in *sufb2-2* and *sufb1-12* induced lines after 7 days of DEX foliar application (n=3-7) b. Time course analysis of root ferric reductase activity in induced *sufb* lines compared to WT+Fe and WT-Fe (n=4-5). c. Time course analysis of root ferric reductase activity in induced and non-induced *sufb* and *sufc* lines (n=5). Root reductase activity is normalized by root dry weight. Bars represent mean +/- standard error. d. Soot Fe concentration of induced and non-induced *sufb* lines alongside WT+Fe and WT-Fe. Fe concentration is normalized by sample dry weight. Significance was determined by a t-test to compare treatment groups to WT+Fe and is denoted with an asterisk.

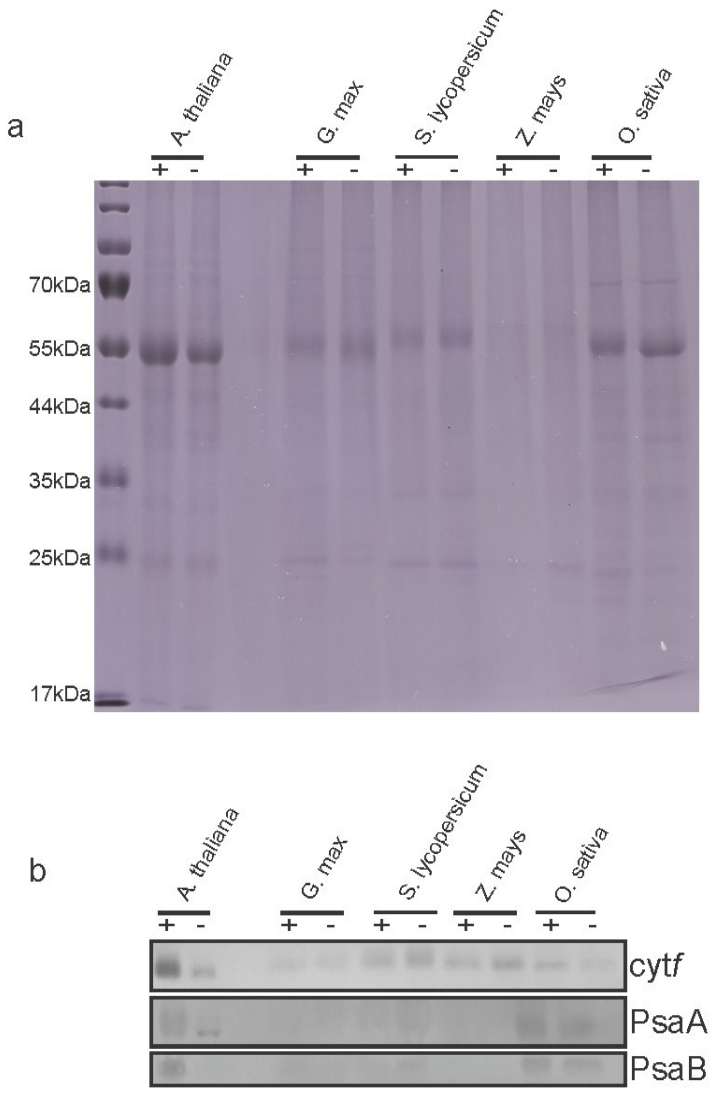

Figure 5-8 Protein accumulation of Cyt*f*, PsaA, and PsaB in crop species on normal media and low Fe treatment. a. SDS-PAGE (15% gel) analysis of total protein. Proteins were visualized by Coomassie Brilliant Blue staining. 40 μg of protein was loaded per sample. b. Western blot analysis of protein accumulation of Cytochrome-*f* (Cyt*f*), and Photosystem I subunits A and B (PsaA and PsaB) in *Glycine max* (Soybean), *Solanum lycopersicum* (Tomato), *Zea mays* (Maize), and *Oryza sativa* (Rice) compared to *Arabidopsis* (*A. thaliana*). Samples from plants grown on 10 μM Fe(III)EDTA are denoted by (+) while samples from Fe deficient plants are denoted by (-). Proteins were separated by SDS-PAGE (15% gel) and transferred to a 0.2 μM pore nitrocellulose.

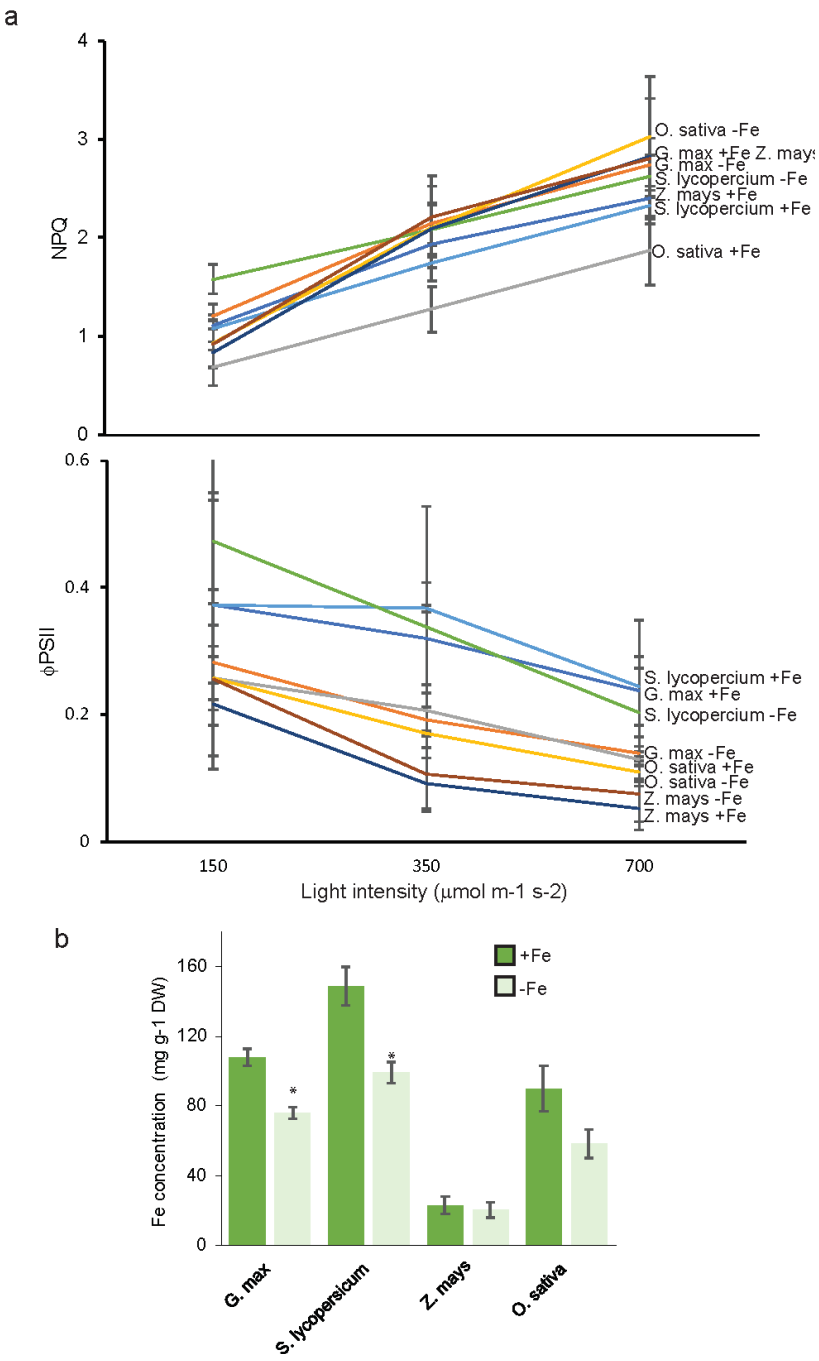

Figure 5-9 Physiological assessment of crop species during low Fe treatment: a. chlorophyll fluorescence parameters, ϕPSII and NPQ, for *Glycine max* (Soybean), *Solanum lycopersicum* (Tomato), *Zea mays* (Maize), and *Oryza sativa* (Rice) grown on low and normal Fe treatments. Chlorophyll fluorescence was measured at 3 light intensities (150, 350, and 700 μE as indicated). Each point represents mean +/- standard error (n=3). b. Shoot Fe concentration for all species grown on normal and low concentrations of Fe. Bars represent mean +/- standard error (n=3). Significance was measured by a t-test between normal and low Fe treatments for each species and is denoted by asterisk.

Table 5-1 Verification of GUS expression and constructs in kanamycin resistant transformed plants. Seeds from Kanamycin resistant FDPU and SFUBP seedlings were tested for GUS activity via histochemical staining. FDPU lines were also verified to contain the FDPU-GUS construct in the genome by PCR.

LINE	GUS STAIN	PCR
FDPU A 1	yes	yes
FDPU A 4	yes	yes
FDPU A 6	yes	yes
FDPU A 7	yes	yes
FDPU A 8	yes	yes
FDPU A 10	yes	yes
FDPU B	yes	yes
FDPU E 1	yes	yes
FDPU E 4	yes	yes
FDPU E 9	yes	yes
FDPU E 10	yes	yes
FDPU E 11	yes	yes
FDPU G 19	yes	yes
FDPU G 22	yes	yes
FDPU I 27	yes	yes
FDPU I 31	yes	yes
FDPU I 26	yes	yes
FDPU I 43	yes	yes
FDPU I 45	yes	yes
FDPU J 47	yes	yes
FDPU J 45	yes	yes
FDPU J 48	yes	yes
FDPU J 51	yes	yes
FDPU J 55	yes	yes
FDPU J 58	yes	yes
SUFBP A	yes	TBD
SUFBP B	yes	TBD
SUFBP C	yes	TBD
SUFBP D	yes	TBD
SUFBP E	yes	TBD

Table 5-2 Primer sequences used for vector construction. Name of primer along with sequence and the step of vector construction for which the primer was used are listed below. Forward primers are labeled as “F” in use column, reverse primers are labeled as “R”. All files are located in GUS fusions folder (GK desktop) and contain exact location of primer in sequence and melting temperature of primer. An asterisk denotes that the primer was also used for colony PCR for respective construct.

Name	Primer sequence	Use
FD2.1F	5’gatcaagcttcgattctacgagaacatcatttg3’	F primer for amplification of FDPU and FDP from gDNA. Underlined is *Hind*III site File: FD sequence.docx
FD2.2R	5’gatcggatccgtgtgtgattgtgtttgacac3’	R primer for amplification of FDP from gDNA. Underlined is *BamH*I site File: FD sequence.docx
FD2.3R	5’ gatcggatccttttttttgttttgtgttttgggagata3’	R primer for amplification of FDPU from gDNA. Underlined is *BamH*I site File: FD sequence.docx
SUFB.1F	5’ TTCATTCGACAATTTTATAACAGAGAC 3’	F primer for amplification of entire promoter + coding sequence of *SUFB* Also used in sequencing File: SUFB sequence.docx
SUFB.1R	5’CGTGATTCACAAATATTAACAAACAC 3’	R primer for amplification of entire promoter + coding sequence of *SUFB* File: SUFB sequence.docx
SUFB.2F	5’gatcaagctttgagttaaacgaaatgaaaacgac3’	F primer for amplification of SUFBPU and

		SUFBP from gDNA. Underlined is *Hind*III site File: SUFB sequence.docx
SUFB.3R	5′ gatcggatccgtgttagaaaaaaaacaacgattagga 3′	R primer for amplification of SUFBP from gDNA. Underlined is *BamH*I site File: SUFB sequence.docx
SUFB.4R	5′ gatcggatcctgttgttggtgtggctcttag 3′	R primer for amplification of SUFBPU from gDNA. Underlined is *BamH*I site File: SUFB sequence.docx
FD_seq_FA	5′ cgattctacgagaacatcatttg 3′	Sequencing reactions for FDPU and FDP File: Primers for colony pcr and sequencing.docx
FD_seq_FB	5′ cgttgatttcagtggcataagtc 3′	Sequencing reactions for FDPU and FDP File: Primers for colony pcr and sequencing.docx
FD_internal	5′ cacttgttgatttggtatacattc 3′ *	Sequencing reactions for FDPU and FDP File: Primers for colony pcr and sequencing.docx
GUS	5′ ccgtcgagttttttgatttcac 3′ *	Sequencing reactions for all constructs File: Primers for colony pcr and sequencing.docx
FD_seq_RA	5′ caaagtcacaactcacaaatctatc 3′	Sequencing reactions for FDPU and FDP

		File: Primers for colony pcr and sequencing.docx
FD_seq_RB	5’gttgatggaagtgtcctgatag 3’	Sequencing reactions for FDPU and FDP File: Primers for colony pcr and sequencing.docx
Sufb_seq_F	5’ tagtcgggttaatcgcaatc 3’	Sequencing reactions for SUFBPU and SUFBP File: Primers for colony pcr and sequencing.docx
Sufb_internal	5’ ctaaactgaaatgaatgaaccaac 3’ *	Sequencing reactions for SUFBPU and SUFBP File: Primers for colony pcr and sequencing.docx
Sufb_seq_RB	5’ cggaaacaccaataagatcgg 3’	Sequencing reactions for SUFBPU and SUFBP File: Primers for colony pcr and sequencing.docx
GUS2	5’ ctgcccaacctttcggtataa 3’	Colony PCR GUS primer File: Primers for pcr.docx
FD2 F	5’ atagacgccacgtggtagatag 3’	Colony PCR FDPU primer. Located in 5’UTR File: Primers for pcr.docx
SufB F	5’ cctaagagccacaccaacaa 3’	Colony PCR SUFBPU primer. Located in 5’UTR File: Primers for pcr.docx

Table 5-3 Location of plasmids, primers, and seeds for GUS promoter fusion transgenic lines. Notes column describes the contents of the box.

Box Name	Location	Notes
“Seeds Nov. 2018 Fd-gus Sufb-gus”	Fridge 1	All transformed lines for FD and SUFB constructs
“FDPU T1 DNA”	Freezer 3	gDNA for genotyping FDPU lines
“FD SUFB Gus DNA KB”	Freezer 3	gDNA for genotyping FD and SUFB lines (Karen B)
“GK primers FD2 and SUFB GUS”	Freezer 3	All primer stocks for transgenic lines (listed in Table 5-2)
“GK plasmid isolation”	Freezer 3	CONFIRMED (re-isolated) stock tubes labeled in green (SUFB) and red (FD)
“SufB FD Gus plasmids for seq”	Freezer 3	Original plasmid isolations and dilutions (SUFBP and FDPU known to be good)
“GK glycerols”	-80 Freezer Fe shelf	E. coli and Agro glycerol stocks
“FDPU A MUG”	-80 Freezer Fe shelf	Agar grown FDPU A1 shoots +/-Fe for MUG assay

Table 5-4 Percent protein sequence similarity to *A. thaliana.* Protein similarity to *Arabidopsis thaliana* for selected proteins from *Glycine max* (Soybean), *Solanum lycopersicum* (Tomato), *Zea mays* (Maize), and *Oryza sativa* (Rice) was determined by NCBI Blast and accounts for substitutions of amino acids with similar biochemical properties. Protein sequences analyzed were for Cytochrome-*f* (Cyt*f*), Cytochrome-b_6 (Cytb_6), Reiske protein, Photosystem subunits A and C (PSaA, PSaC) and Ferredoxin isoforms, 1, 2, 3 (FDX1, FDX2, FDX3)

		G. max	***Z. mays***	***S. lycopersicum***	***O. sativa***
Cyt*f*	ATCG00540	93%	94%	95%	94%
Cytb_6	ATCG00720	98%	99%	99%	99%
Rieske	AT4G03280	83%	78%	84%	79%
PsaA	ATCG00350	98%	98%	99%	98%
PsaC	ATCG01060	100%	96%	100%	96%
FDX1	AT1G10960	78%	72%	76%	71%
FDX2	AT1G60950	78%	73%	76%	68%
FDX3	AT2G27510	84%	89%	54%	70%

LITERATURE CITED

Bradford MM (1976) A rapid and sensitive method for the quantitation of microgram quantities of protein utilizing the principle of protein-dye binding. Analytical biochemistry 72: 248

Briat J-F, Dubos C, Gaymard F (2015) Iron nutrition, biomass production, and plant product quality. Trends in Plant Science 20: 33-40

Clough SJ, Bent AF (1998) Floral dip: a simplified method for Agrobacterium-mediated transformation of Arabidopsis thaliana. Plant Journal 16: 735-743

Friso G, Olinares PDB, van Wijk KJ (2011) The workflow for quantitative proteome analysis of chloroplast development and differentiation, chloroplast mutants, and protein interactions by spectral counting. In Chloroplast Research in Arabidopsis, Jarvis R.P. (ed). pp 265-282, New York, NY

Gallagher SR (1992) Quantification of GUS activity by fluorometry. In: GUS Protocols: using the GUS gene as a reporter of gene expression. Gallagher SR (ed) Academic Press Inc. New York NY pp 47-59

Hantzis LJ, Kroh GE, Jahn CE, Cantrell M, Peers G, Pilon M, Ravet K (2018) A Program for Iron Economy during Deficiency Targets Specific Fe Proteins. Plant Physiology 176: 596-610

Holsters M, de Waele D, Depicker A, Messens E, van Montagu M, Schell J (1978) Transfection and transformation in Agrobacterium tumefaciens. 163: 181-187

Hu XY, Kato Y, Sumida A, Tanaka A, Tanaka R (2017) The SUFBC2D complex is required for the biogenesis of all major classes of plastid Fe-S proteins. Plant Journal 90: 235-248

Jefferson RA, Kavanagh TA, Bevan MW (1987) GUS fusions: β-glucuronidase as a sensitive and versatile gene fusion marker in higher plants. EMBO Journal 6: 3901-3907

Jeong J, Cohu C, Kerkeb L, Pilon M, Connolly EL, Guerinot ML (2008) Chloroplast Fe(III) chelate reductase activity is essential for seedling viability under iron limiting conditions.

Proceedings of the National Academy of Sciences of the United States of America 105: 10619-10624

Kobayashi T (2019) Understanding the Complexity of Iron Sensing and Signaling Cascades in Plants. Plant & cell physiology

Kumar S, Stecher G, Li M, Knyaz C, Tamura K (2018) MEGA X: Molecular Evolutionary Genetics Analysis across Computing Platforms. Molecular biology and evolution 35: 1547

Maxwell K, Johnson GN (2000) Perspectives in Experimental Botany. Chlorophyll fluorescence—a practical guide. Journal of Experimental Botany. Journal of Experimental Botany 51: 659-668

Murashige T, Skoog F (1962) A REVISED MEDIUM FOR RAPID GROWTH AND BIO ASSAYS WITH TOBACCO TISSUE CULTURES. Physiologia Plantarum 15: 473-497

Robinson NJ, Procter CM, Connolly EL, Guerinot ML (1999) A ferric-chelate reductase for iron uptake from soils. Nature 397: 694-697

Sambrook J, Russell DW (2001) Molecular Cloning: A Laboratory Manual, Vol 1. Cold Spring Harbor Laboratory Press, New York, NY

Van Larebeke N, Engler G, Holsters M, Van Den Elsacker S, Zaenen I, Schilperoort RA, Schell J (1974) Large plasmid in Agrobacterium tumefaciens essential for crown gall-inducing ability. Nature 252: 169

Yu Y-K, Altschul SF (2005) The construction of amino acid substitution matrices for the comparison of proteins with non-standard compositions. Bioinformatics 21: 902-911

Zhai ZY, Gayomba SR, Jung HI, Vimalakumari NK, Pineros M, Craft E, Rutzke MA, Danku J, Lahner B, Punshon T, Guerinot ML, Salt DE, Kochian LV, Vatamaniuk OK (2014) OPT3 Is a Phloem-Specific Iron Transporter That Is Essential for Systemic Iron Signaling and Redistribution of Iron and Cadmium in Arabidopsis. Plant Cell 26: 2249-2264

CHAPTER 6: SUMMARIZING DISCUSSION

The aim and major findings of this dissertation

Iron deficiency is common in plants because soil Fe is poorly bioavailable. To minimize the potential stress caused by Fe deficiency, plants can increase uptake of Fe from soil, economize Fe for specific functions, alter metabolism, or remobilize Fe (for details see Chapter 1). Compared to the root Fe deficiency response, which is well-characterized, still much remains to be discovered regarding how the vegetative shoot confronts Fe deficiency. The leaf is a strong sink for Fe and the chloroplast itself contains about 80% of leaf Fe (Shikanai *et al.,* 2003). Furthermore, the photosynthetic electron transport chain requires at least 24 Fe atoms (Merchant and Sawaya, 2005). Therefore, it is vital to understand how the chloroplast responds to Fe limitation and how this response is regulated.

The overall goal of this dissertation was to characterize the leaf response to Fe limitation at the molecular and physiological levels and to determine how molecular changes are regulated in response to low Fe. In a first step towards this goal, we characterized how Fe limitation affects the abundance of Fe requiring proteins and corresponding mRNAs in leaves. We observed that an Fe economy program became activated as a result of Fe limitation in which the plant prioritized Fe for the mitochondria and targeted chloroplast SUFB, FDX2, and Cyt-b_6f complex for down-regulation. Additionally, we found that transcript abundance for *SUFB*, *FDX2*, and *Cyt-b_6f* complex subunits decreased prior to protein abundance, indicating a genetic program that underlies Fe economy.

We next aimed to find out more about what triggers these changes in gene expression. In Chapter 3, we analyzed the molecular Fe deficiency response of a photosynthetic electron transport mutant, *paa1,* to determine if the decrease in abundance of photosynthetic electron transport proteins can be due to operational signals stemming from a loss of photosynthetic

efficiency. The evidence presented in Chapter 3 indicated that this was not the case. Therefore, regulation of expression of abundant chloroplast Fe proteins could be a direct target in the leaf Fe economy response.

We next aimed to identify transcripts that are differentially expressed early after low Fe treatment and determine if loss of chloroplast Fe-S clusters could be initiating a signal for Fe economy (Chapter 4). We compared transcriptome changes of WT-Fe to that of a *sufb*-RNAi inducible knockdown line, which displays phenotypes very similar to plants subjected to low Fe. Because *SUFB* is itself a target of Fe deficiency regulation, loss of SUFB function during acclimation to low Fe could be a trigger for the regulation of abundant Fe proteins, in which case a large overlap would be expected for transcripts regulated by low Fe and loss of SUFB. Surprisingly, the results in Chapter 4 revealed that the transcriptional response of the *sufb*-RNAi knockdown was opposite that of the WT-Fe response despite sharing similarities in decreased abundance of photosynthetic proteins. This observation indicates that the leaf Fe economy response is not downstream of chloroplast Fe-S assembly and photosynthetic capacity.

Overall, the work presented in this dissertation has (1) provided an understanding of the leaf Fe economy response, (2) determined direct photosynthetic electron transport targets of low Fe regulation, and (3) provided evidence that regulation of SUFB is important in coordinating Fe-S cluster assembly with loss of photosynthetic proteins as opposed to producing a trigger to signal Fe deficiency.

Leaf Fe economy primarily targets chloroplast metabolism

In Chapter 2, we found that photosynthetic output was more dispensable in the leaf Fe economy response compared to respiration. The decrease in photosynthetic output was attributed to the down-regulation of abundant photosynthetic electron transport proteins, FDX2 and the Cyt-b_6f complex. Several, previous seedling studies had identified PSI, which binds 12 Fe atoms, as a major target of Fe deficiency reprograming (Anadaluz *et al.,* 2006; Laganowsky

et al., 2009; Rodriquez Celma *et al.,* 2013). Surprisingly, the abundance of PSI proteins was relatively well maintained in our studies in which plants were grown hydroponically and were relatively mature. In previous studies plants were grown with more severe Fe limitations, and at different developmental stages or on agar media (Anadaluz *et al.,* 2006; Laganowsky *et al.,* 2009; Rodriquez Celma *et al.,* 2013). Perhaps the regulation of PSI in response to low Fe is highly dependent on the severity of Fe limitation, developmental stage of the plant, and growth conditions.

Apart from photosynthetic electron transport, the SUF Fe-S assembly pathway in the chloroplasts was also strongly targeted. *SUFB* transcript had previously been found to be regulated in response to Fe deficiency in both the leaves and roots (Xu *et al.,*2005; Yang *et al.,* 2010; Liang *et al.,*2014; Pan *et al.,* 2015). SUFB and SUFA both had strong decreases in protein abundance across the week of Fe deficiency, and *SUFB* mRNA was down-regulated after only 2 days of low Fe treatment (Hantzis *et al.,*2018), suggesting down-regulation of chloroplast Fe-S assembly is a vital early response of leaf Fe economy.

Chapter 4 provides evidence that nuclear encoded transcripts, encoding for chloroplast localized gene products, are primary targets of differential regulation as early as 1 day after low Fe treatment. In Chapter 2, we found that photosynthetic electron transport was not impaired until after 4 days of low Fe treatment. Further, seedling Fe deficiency transcriptome studies have found that the chlorophyll biosynthesis pathway is regulated 3 days after low Fe treatment (Rodriquez-Celma *et al.,* 2013). Thus, while photosynthesis is not measurably impacted until later after the start of low Fe treatment, regulation of chloroplast targeted gene products may be a priority early after leaf Fe limitation is sensed.

Regulation of photosynthetic electron transport proteins is most likely a direct target of leaf Fe economy

Photosynthetic electron transport protein expression could be regulated directly in response to low Fe or result indirectly from loss of available Fe required for cofactors. In Chapter 3, we found that of the photosynthetic proteins regulated in response to leaf Fe limitation, Cyt-b_6f complex was a direct target of Fe economy while FDX2 may be regulated by multiple signals. Ferredoxin has also been strongly linked to Fe status before, in plants, in Chlamydomonas, and in cyanobacteria (Thimm *et al.,* 2001; Terauchi *et al.,* 2010; Lopez-Milan *et al.*, 2013; Rodriguez-Celma *et al.,* 2013; Georg *et al.,* 2017). Plant FDX2 had also been found to be regulated in response to light and chloroplast activity (Elliot *et al.,*1989; Vorst *et al.,*1993, Dickey *et al.,*1994). Our data in Chapter 3 support the regulation of FDX2 in response to photosynthetic output as the mRNA for FDX2 was highly variable in *paa1* grown on sufficient levels of Fe.

The down-regulation of photosynthetic electron transport proteins may make Fe available for other cellular functions when Fe starved. The photosynthetic electron transport proteins are highly expressed (see Chapter 2) and have a strong Fe requirement (Merchant and Sawaya, 2005). Down-regulating these proteins in leaf Fe economy could allow for prioritization of Fe for mitochondrial and cytosolic functions.

Chloroplast Fe-S cluster assembly may be targeted in leaf Fe economy to coordinate Fe-S assembly with photosynthetic electron transport protein maturation

Hu *et al.* (2017) found severe losses of photosynthetic electron transport proteins in the *sufb*-RNAi knockdown lines. Conversely, transcripts for nuclear encoded photosynthetic electron transport proteins were not differentially expressed in the *sufb*-RNAi knockdown in our RNA-seq data even 4 days after DEX induction. Taken together, these studies suggest that the down-regulation of SUFB may act as a method of post-transcriptional regulation to coordinate photosynthetic protein maturation with availability of Fe-S clusters.

SUFB has been strongly linked with Fe deficiency in both shoots and roots in previous transcriptional studies. Xu *et al.* (2005) reported that Fe stimulated the activity of the purified *Arabidopsis* SUFB protein, and Yang *et al.* (2010) proposed SUFB as an Fe sensor because its transcript is regulated by Fe status. Further, the *suf* operon in *E. coli* and in *Synechococcus* sp. PCC 7002, was required for bacterial growth during Fe deficiency (Outten *et al.,* 2004; Balasubramanian *et al.,* 2005). We provided evidence that SUFB is not involved in initiation or regulation of leaf Fe economy as the *sufb*-RNAi line presented an opposite transcriptional response compared to WT-Fe. However, at one RNA-sequencing timepoint, the *sufb*-RNAi knockdown had up-regulation of *VIT1,* a known vacuolar Fe importer that is down-regulated in response to Fe limitation (see Chapter 4). Thus, the loss of SUFB may alter intercellular Fe homeostasis by leading to decreases chloroplast Fe use, resulting less chloroplast Fe import, and, therefore, more cytosolic Fe being sequestered in the vacuole.

Genetic regulation in leaf Fe economy may be driven by bHLH, ERF, and MYB transcription factors

While bHLH transcription factors are vital for the regulation of Fe uptake at the root surface, in comparison, few targets of these bHLH transcription factors have been identified in the shoots (Sivitz *et al.,* 2012; Rodriguez-Celma *et al.,* 2013). In Chapter 4, we found that in comparison to the rest of the genome, ERF and bHLH TFs were over enriched in promoters of down-regulated chloroplast localized transcripts while bHLH and MYB TFs were over enriched in promoters of up-regulated chloroplast localized transcripts. It may be possible that ERF and MYB transcription factors work in concert with bHLH transcription factors in the shoots to regulate chloroplast localized transcripts in the Fe economy response. There is some evidence for this in the roots where Ethylene Insensitive 1 and 3 (EIN1, EIN3), two ERF transcription factors stabilize FIT, a bHLH transcription factor, to up-regulate FRO2 and IRT1 expression

(Lingam *et al.,* 2011). Additionally, MYB10 and MYB72 drive expression of nicotianamine synthase in the roots during Fe deficiency (Palmer *et al.,* 2013).

SUFA may regulate SUF Fe-S homeostasis

SUFA is proposed to be a Fe-S carrier molecule and may bind either Fe or Fe-S clusters but knockout mutants of SUFA are phenotypically like WT (Abdel-Ghany *et al.,* 2005; Yabe and Nakai, 2006). SUFA was found to be strongly down-regulated at the protein level, but not the transcript level, during the leaf Fe economy response (Chapter 2). Additionally, in the inducible *sufb, sufc,* and *sufd*-RNAi knockdown lines, *SUFA* mRNA was over-expressed but SUFA did not accumulate at the protein level. This suggests that the regulation of the SUFA protein observed in leaf Fe economy is in response to the loss of SUFB and not directly responding to Fe status. Thus, SUFA may be regulated by deficiencies within the SUF system. In Chapter 4, the *sufa* knockout seemed to accumulate more FDX2 and Rieske protein, which may suggest that SUFA is responsible for holding excess Fe-S clusters for Fe-S requiring proteins. The maintenance of the *SUFA* transcript during Fe limitation may allow for rapid synthesis of the SUFA protein when Fe is resupplied to store Fe-S clusters as Fe-S assembly and photosynthetic electron transport protein maturation are recovered.

Outlook and future directions

How is the leaf Fe economy response regulated? Future work in the field must focus on how early targets of leaf Fe economy, especially SUFB, are regulated at the transcriptional level. Understanding the regulation of *SUFB* in response to Fe limitation is especially important because down-regulation of SUFB may be required for regulation of photosynthetic protein maturation. Further, the method of regulation of SUFB may also apply to co-regulated transcripts with *SUFB*. An important first step in understanding regulation of *SUFB* is to

determine if regulation is promoter driven. As described in Chapter 5, promoter-GUS reporter constructs are being transformed into *Arabidopsis* to determine if *SUFB* and *FDX2* regulation in response to Fe limitation is promoter driven. In the case of promoter regulation, bHLH, ERF, and MYB transcription factors may all be important in coordinating leaf Fe economy. To determine if the ERF transcription factors that we identified in our RNA-seq (ERF53, CRF2, and RA2.12; Chapter 4) are regulating leaf Fe economy responses, we can analyze the molecular response to Fe limitation in respective knockout mutants.

What is the role of SUFA in the SUF pathway? While we provided evidence that SUFA may be regulating Fe-S homeostasis, to further test this hypothesis, *sufa* knockout lines should be subject to a week of Fe deficiency followed by resupply. While the knockout lines may not present a different leaf Fe economy response compared to WT, they may recover photosynthesis more rapidly as SUFA will be absent to store newly synthesized Fe-S clusters resulting in an increased abundance of Fe-S requiring photosynthetic proteins as a sink for Fe-S clusters.

How might Fe be sensed in the leaves? Fe sensor molecules have remained elusive. Fe is proposed to be initially sensed in the shoots and a signal relayed to the roots for up-regulation of Fe uptake and transport. This dissertation has provided evidence that photosynthetic output and SUF Fe-S assembly are not triggering this shoot derived signal. However, some evidence for chloroplast Fe concentration being of importance in regulating cellular Fe homeostasis was also observed in the dissertation projects. *Sufb2-2* had variation in *VIT1* expression and root reductase activity, suggesting that perhaps Fe homeostasis was altered by the decreased chloroplast Fe use. This hypothesis that a decrease of Fe-S cluster assembly results in altered Fe homeostasis could be further investigated by analyzing expression of Fe homeostasis and economy genes in the inducible NIFS/SUFS knockdown line, that is also defective in Fe-S assembly (Van Hoewyk *et al.,* 2007). Some evidence of regulation by chloroplast Fe concentration was also present in knockout mutants of FRO7, which is responsible for reducing

Fe for import into the chloroplast (Jeong *et al.,* 2008). *Fro7* presented chlorosis, decreased accumulation of Cyt-b_6f, and had lower Fe concentration in its chloroplasts (Jeong *et al.,* 2008). Further analysis of the response of *fro7* to Fe sufficiency to characterize the root Fe reductase activity, and accumulation of SUFB transcript and protein in the shoots, may determine if Fe sensing is reliant on chloroplast Fe status and if chloroplast Fe status is integrated into systemic Fe signaling.

LITERATURE CITED

Abdel-Ghany SE, Ye H, Garifullina GF, Zhang LH, Pilon- Smits EAH, Pilon M (2005) Iron-sulfur cluster biogenesis in chloroplasts. Involvement of the scaffold protein CpIscA. Plant Physiology 138: 161-172

Andaluz S, Lopez-Millan A-F, De las Rivas J, Abadia J, Abadia A (2006) Proteomic profiles of thylakoid membranes and changes in response to iron deficiency. Photosynthesis Research 89: 141-155

Balasubramanian R, Shen G, Bryant DA, Golbeck JH (2006) Regulatory Roles for IscA and SufA in Iron Homeostasis and Redox Stress Responses in the Cyanobacterium Synechococcus sp. Strain PCC 7002. The Journal of Bacteriology 188: 3182

Dickey LF, Nguyen TT, Allen GC, Thompson WF (1994) Light-Modulation Of Ferredoxin Messenger-RNA Abundance Requires An Open Reading Frame. Plant Cell 6: 1171-1176

Elliott, RC, Dickey, LF, White, MJ, Thompson, WF (1989) Cis acting elements for light regulation of pea ferredoxin I gene expression are located within transcribed sequences. Plant Cell 1: 691-698.

Georg J, Kostova G, Vuorijoki L, Schön V, Kadowaki T, Huokko T, Baumgartner D, Müller M, Klähn S, Allahverdiyeva Y, Hihara Y, Futschik ME, Aro E-M, Hess WR (2017) Acclimation of Oxygenic Photosynthesis to Iron Starvation Is Controlled by the sRNA IsaR1. Current Biology 27: 1425-1436.e1427

Hantzis LJ, Kroh GE, Jahn CE, Cantrell M, Peers G, Pilon M, Ravet K (2018) A Program for Iron Economy during Deficiency Targets Specific Fe Proteins. Plant Physiology 176: 596-610

Hu XY, Kato Y, Sumida A, Tanaka A, Tanaka R (2017) The SUFBC2D complex is required for the biogenesis of all major classes of plastid Fe-S proteins. Plant Journal 90: 235-248

Jeong J, Cohu C, Kerkeb L, Pilon M, Connolly EL, Guerinot ML (2008) Chloroplast Fe(III) chelate reductase activity is essential for seedling viability under iron limiting conditions. Proceedings of the National Academy of Sciences of the United States of America 105: 10619-10624

Laganowsky A, Gomez SM, Whitelegge JP, Nishio JN (2009) Hydroponics on a chip: Analysis of the Fe deficient Arabidopsis thylakoid membrane proteome. Journal of Proteomics 72: 397-415

Liang XJ, Qin L, Liu PW, Wang MH, Ye H (2014) Genes for iron-sulphur cluster assembly are targets of abiotic stress in rice, Oryza sativa. Plant Cell and Environment 37: 780-794

Lingam S, Mohrbacher J, Brumbarova T, Potuschak T, Fink-Straube C, Blondet E, Genschik P, Bauer P (2011) Interaction between the bHLH Transcription Factor FIT and ETHYLENE INSENSITIVE3/ETHYLENE INSENSITIVE3-LIKE1 Reveals Molecular Linkage between the Regulation of Iron Acquisition and Ethylene Signaling in Arabidopsis. The Plant Cell 23: 1815-1829

Lopez-Millan AF, Grusak MA, Abadia A, Abadia J (2013) Iron deficiency in plants: an insight from proteomic approaches. Frontiers in Plant Science 4

Merchant S, Sawaya MR (2005) The Light Reactions: A Guide to Recent Acquisitions for the Picture Gallery. *In*, Vol 17, pp 648-663

Outten FW, Djaman O, Storz G (2004) A suf operon requirement for Fe-S cluster assembly during iron starvation in Escherichia coli. Molecular Microbiology 52: 861-872

Palmer CM, Hindt MN, Schmidt H, Clemens S, Guerinot ML (2013) MYB10 and MYB72 Are Required for Growth under Iron-Limiting Conditions. Plos Genetics 9

Pan IC, Tsai H-H, Cheng Y-T, Wen T-N, Buckhout TJ, Schmidt W (2015) Post-Transcriptional Coordination of the Arabidopsis Iron Deficiency Response is Partially Dependent on the E3 Ligases RING DOMAIN LIGASE1 (RGLG1) and RING DOMAIN LIGASE2 (RGLG2). Molecular & cellular proteomics : MCP 14: 2733

Rodriguez-Celma J, Pan IC, Li W, Lan P, Buckhout TJ, Schmidt W (2013) The transcriptional response of A*rabidopsis* leaves to Fe deficiency. Frontiers in Plant Science 4: 276

Shikanai T, Muller-Moule P, Munekage Y, Niyogi KK, Pilon M (2003) PAA1, a P-type ATPase of Arabidopsis, functions in copper transport in chloroplasts. Plant Cell 15: 1333-1346

Sivitz AB, Hermand V, Curie C, Vert G (2012) Arabidopsis bHLH100 and bHLH101 Control Iron Homeostasis via a FIT-Independent Pathway. Plos One 7

Terauchi AM, Peers G, Kobayashi M, Niyogi KK, Merchant SS (2010) Trophic status of *Chlamydomonas reinhardtii* influences the impact of iron deficiency on photosynthesis. Photosynthesis Research 105: 39-49

Thimm O, Essigmann B, Altmann T, Buckhout TJ (2001) Response of Arabidopsis to Iron Deficiency Stress as Revealed by Microarray Analysis. Plant Physiology 127: 1030-1043

Van Hoewyk D, Abdel-Ghany SE, Cohu CM, Herbert SK, Kugrens P, Pilon M, Pilon-Smits EAH (2007) Chloroplast iron-sulfur cluster protein maturation requires the essential cysteine desulfurase CpNifS. Proceedings of the National Academy of Sciences 104: 5686

Vorst O, Vandam F, Weisbeek P, Smeekens S (1993) Light-Regulated Expression Of The Arabidopsis-Thaliana Ferredoxin-A Gene Involves Both Transcriptional And Posttranscriptional Processes. Plant Journal 3: 793-803

Xu XM, Adams S, Chuam NH, Moller SG (2005) AtNAP1 represents an atypical SufB protein in Arabidopsis plastids. Journal of Biological Chemistry 280

Yabe T, Nakai M (2006) Arabidopsis AtIscA-I is affected by deficiency of Fe–S cluster biosynthetic scaffold AtCnfU-V. Biochemical & Biophysical Research Communications 340: 1047-1052

Yang T, Lin W-D, Schmidt W (2010) Transcriptional Profiling of the Arabidopsis Iron Deficiency Response Reveals Conserved Transition Metal Homeostasis Networks. Plant Physiology 152: 2130-2141

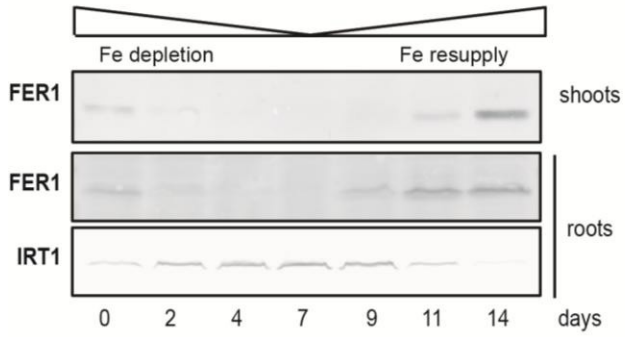

Supplemental Figure 2-1: Response of Fe status markers to Iron deficiency treatment. As markers for Fe deficiency, we analyzed the accumulation of two proteins that are known to be highly regulated by Fe status in plants: the Fe storage protein ferritin (FER) and the root high- affinity Fe transporter IRT1 responsible for primary uptake from the rhizosphere. Fe positively regulates FER synthesis (Petit et al., 2001; Ravet et al., 2009), while it negatively impacts IRT1 expression (Vert et al., 2002; Seguela et al., 2008). Under control growth conditions, some IRT1 protein was detected in roots, indicative of a fairly low Fe supply, which was, however, sufficient for some accumulation of the Ferritin Fe sequestration component in both roots and shoots (day 0). The low Fe treatment (10 nM Fe-EDTA) led to the rapid disappearance of Ferritin in both shoots and roots. Conversely, IRT1 levels increased, reaching a maximum at day 7. Upon Fe resupply to 10 µM Fe-EDTA, Ferritin accumulated concomitantly with the progressive disappearance of IRT1. These data indicate that the Fe deficiency response was induced upon depletion and that plants returned to normal Fe status with resupply within a week. *Methods*: Total protein extracts (20 µg) from treated *Arabidopsis* shoots and roots were fractionated by SDS-PAGE and blotted onto nitrocellulose membranes, then probed with antisera for IRT1 and FER1. Presented blots are representatives of 4 independent biological replicates.

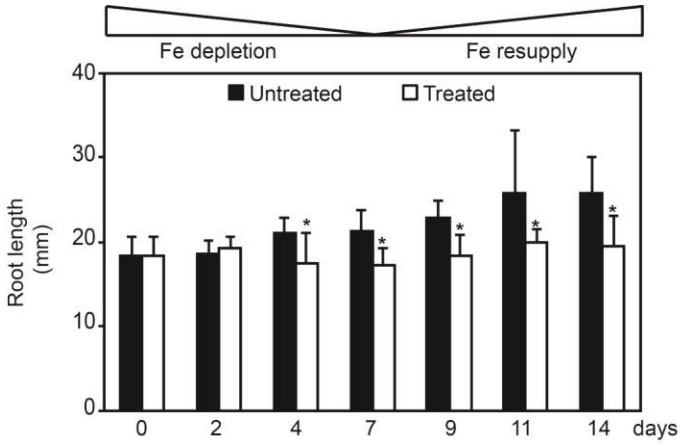

Supplemental Figure 2-2: Growth of *Arabidopsis* thaliana roots during the Fe-deficiency and the Fe-recovery treatment. Growth was monitored by measurement of the primary root length. Values are given as averages ± SD (n = 15). Black and white bars represent untreated and treated plants, respectively. Stars above bars represent significant differences (*p*-value<0.05) between untreated and treated plants.

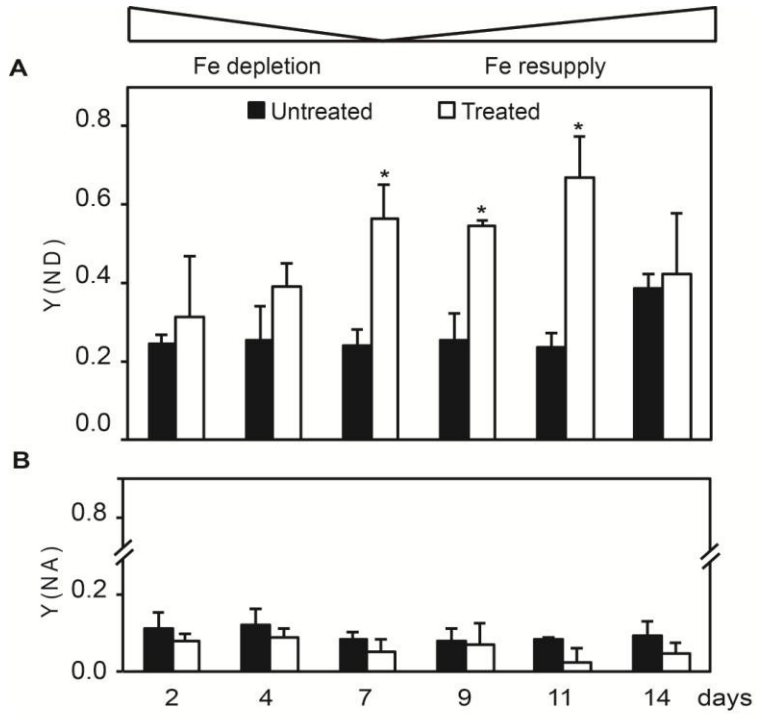

Supplemental Figure 2-3: Loss of PSI quantum yield results mainly from limitations upstream of PSI. Y(ND) indicates the quantum yield of non-photochemical energy conversion due to donor side limitations upstream of PSI (Klughammer and Schreiber, 2008). The Y(NA) parameter which indicates acceptor side limitations downstream of PSI (Klughammer and Schreiber, 2008). A, Quantum yield of non-photochemical energy conversion due to donor side limitation Y(ND). Y(ND) is relatively large in the control plants, suggesting that electron transport to PSI from upstream components was limiting, which is as expected because oxidation of the plastoquinone pool by the cytochrome-b_6f complex is considered a constriction point in electron transport (Maxwell and Johnson, 2000). Fe deficiency caused a further increase in Y(ND) but plants recovered with Fe resupply. B, quantum yield of non-photochemical energy conversion due to acceptor side limitation Y(NA). Y(NA) was relatively low and did not change significantly with Fe treatments. For A, and B, black and white bars represent untreated and treated plants, respectively. Stars above bars represent significant differences (p-value<0.05) between untreated and treated plants. Values are given as averages ± SD (n = 6). *Methods:* The quantum yield of non-photochemical energy conversion due to donor side limitation Y(ND) and the quantum yield of non-photochemical energy conversion due to acceptor side limitation Y(NA) were determined according to Klughammer and Schreiber (2008). Photo-oxidation/reduction of P700 was monitored as the light-induced absorbance change at 820nm using a Dual-PAM-100 P700 fluorometer.

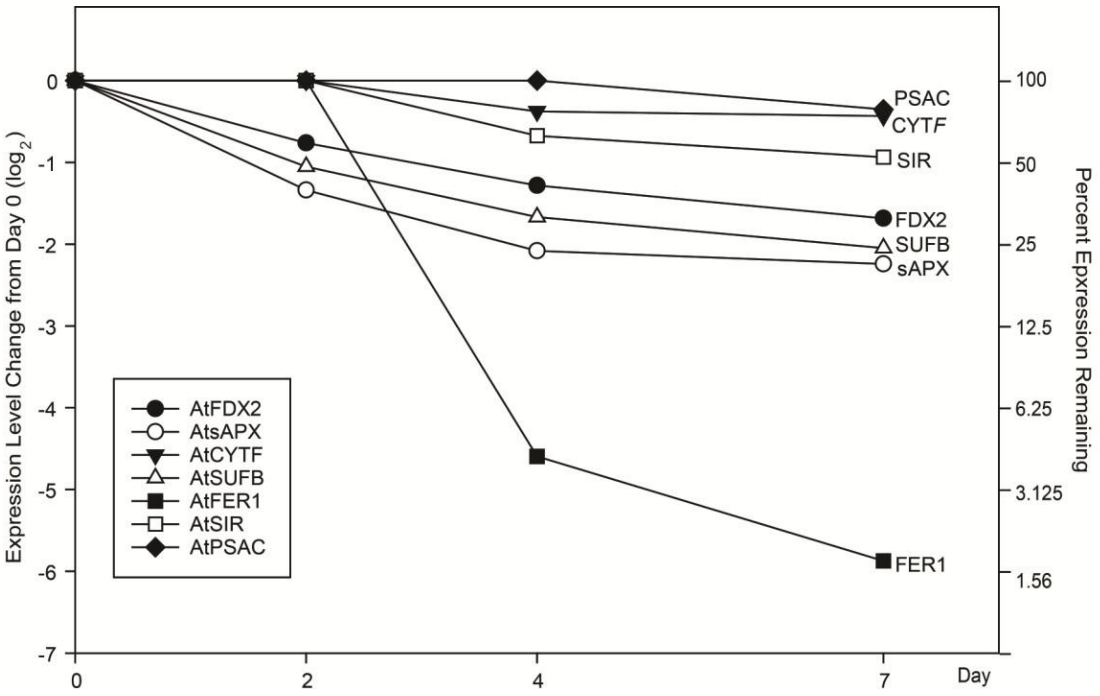

Supplemental Figure 2-4: Transcript changes over the course of iron deficiency. Changes in transcript level from day 0 for selected transcripts were measured using NanoStrings Technology. Expression at day 2, 4, and 7 was compared to expression at day 0. Biological replicates were n=4 for day 0, 2 and 7 and n=3 for day 4. The mRNA encoding the iron signature protein, *FER1* shows the strongest decreased expression over the time course. *SUFB, sAPX*, and *FDX2* show decreases in transcript level starting at day 2 of iron deficiency, while *CYTf* and *SIR* do not show a decrease until day 4. In contrast, expression of *PSAC* transcript is not affected by iron deficiency until day 7.

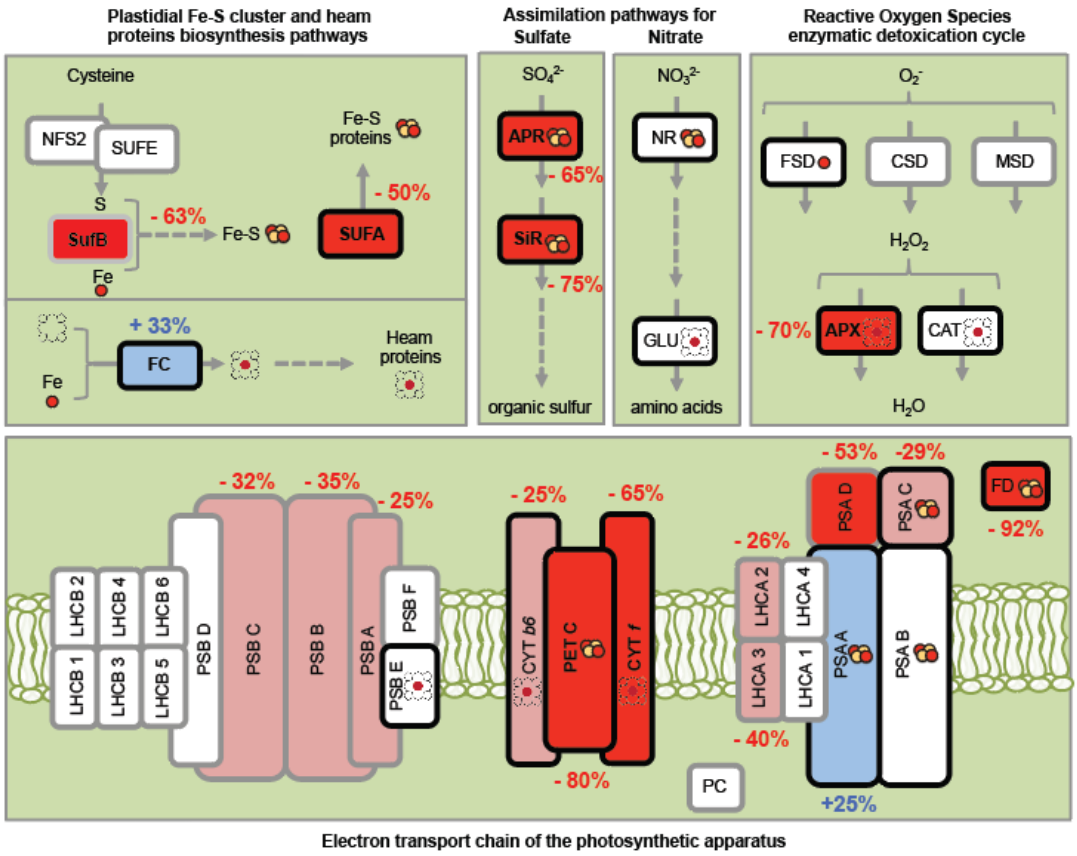

Electron transport chain of the photosynthetic apparatus

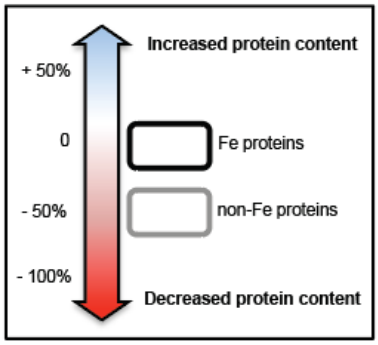

Supplemental Figure 2-5: The effect of Fe deficiency treatment (7 days) on the abundance of chloroplast proteins arranged by metabolic pathway. Proteins with increased expression relative to +Fe control are indicated in blue whereas decreased expression is visualized in red. Numbers indicate the % change in abundance.

Supplemental Table 2-1: Proteins and Transcripts tested over the course of iron deficiency and resupply (see insert). A total of 57 proteins and 72 transcripts were analyzed. For the proteins analyzed, the antibody used for detection is listed. For the transcripts analyzed, the normalized log_2 transcript counts for each day are listed. Antibodies obtained from Agrisera (Vännäs, Sweden) are denoted by an AS accession number. References for antibody sources other than Agrisera are: (a) Abdel- Ghany et al., 2005a, (b) Kliebensein et al., 1998, (c) Abdel-Ghany et al., 2005b, (e)Ye et al., 2006, (f) Pilon-Smits et al., 2002, (g) Bych et al., 2008, (h) Stockel and Oelmuller, 2004, (i) Dellagi et al., 2005, (j) Vert et al, 2002, (k) Kopriva et al., 1999, (l),Yonekura-Sakakibara et al., 2000,(m) Hooks et al., 2014, (n) Munshi et al., 2006. Antibody for detection of SUFB (d) was provided by Nicolas Rouhier (Nancy, France)

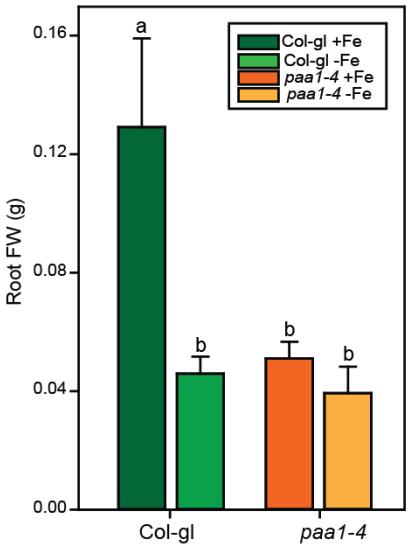

Supplemental Figure 3-1 Root biomass of hydroponically grown *paa1-4:* Fresh weight of root systems of hydroponically grown Col3 and *paa1-4* in response to Fe deficiency. Roots were used to measure Ferric Reductase Activity (n=10)

Supplemental Table 3-1 Elemental analysis of Col3 and *paa1-4*. Elemental concentration ($mg \cdot kg^{-1}DW$) of Col3 and *paa1-4* rosettes after 7 days of Fe deficiency treatment. For each element, values represent mean ± standard error. Statistical significance is denoted by asterisk

	Col3 10 μM Fe	Col3 10 nM Fe	*paa1-4* 10 μM Fe	*paa1-4* 10 nM Fe
Ca	428 x 10^2 ± 15.3 x 10^2	445 x 10^2 ± 12.9 x 10^2	467 x 10^2 ± 18.5 x 10^2	406 x 10^2 ± 16.6 x 10^2
Cu	14 ± 1.7	48 ± 1.6*	32 ± 3.2	57 ± 4.0*
Fe	59 ±4.2	42 ± 2.7*	52 ± 4.0	24 ± 2.3*
K	444 x 10^2 ± 16.5 x 10^2	507 x 10^2 ± 10.8 x 10^2	479 x 10^2 ± 31.3 x 10^2	472 x 10^2 ±16.9 x 10^2
Mg	587 x 10^2 ± 20.5 x 10^2	695 x 10^2 ± 12.9 x 10^2	690 x 10^1 ± 30.5 x 10^2	650 x 10^2 ± 11.6 x 10^2
Mn	78.0 ± 2.70	70.3 ± 3.02	116 ± 12.9	86.7 ± 11.4
Mo	2.9 ± 0.1	3.3 ± 0.2	5.5 ± 1.1	3.4 ± 0.7
P	855 x 10^1 ± 27.9 x 10^1	877 x 10^1 ± 15.7 x 10^1	937 x 10^1 ± 21.6 x 10^1	814 x 10^1 ± 12.7 x 10^1
S	779 x 10^1 ± 25.2 x 10^1	1260 x 10^1 ± 35.3 x 10^1*	847 x 10^1 ± 26.2 x 10^1	1080 x 10^1 ± 43.7 x 10^1*
Zn	55 ± 3.7	49 ± 2.8	67 ± 3.1	53 ± 6.2

Supplemental Table 3-2 Quantitative PCR primers

AT4G04770	**SufB-F:** 5'-CCTTACATCCAGGTAAAGAATCCA-3' **SufB-R:** 5'-CAGAAACCAGAGATCATTGCC-3'
AT1G60950	**FD2-F:** 5'-CAGTCTCCGTTCCCTTCCAT-3' **FD2-R:** 5'-CCAGCTTCCTCAGCAGCATC-3' Liu *et al.* (2013)
AT4G03280	**Rieske-F:** 5'-ATTCCAGCAGACAGAGTTCC-3' **Rieske-R:** 5'-CTACATCGTTTCCAAGGGCA-3'
AT3G18780	**TUB2-F:** 5'-GTTCTCGATGTTGTTCGTAAG-3' **TUB2-R:** 5'-TGTAAGGCTCAACCACAGTAT-3' Li *et al.* (2008)
AT4G05320	**UBQ10-F:** 5'-CGTTAAGACGTTGACTGGGAAAACT-3' **UBQ10-R:** 5'-GCTTTCACGTTATCAATGGTGTCA-3' Lasanthi-Kudahettige *et al.* (2007)

Supplemental Table 3-3 *Paa1* Genotyping: PCR primers and restriction digest procedures for Genotyping

PAA1-1F: 5'-TACTGCAAGGGATATTCTCATTCA-3'
PAA1-1R: 5'-CCTGCGACCTGTAGTTGC-3'
Digest with Hinf1. *WT*: four fragments, with a main band at 281 bp; *paa1-1*: three fragments with a main band at 422 bp
PAA1-3F: 5'-CCGTCTTTCAGGAGTATCTCAAG-3'
PAA1-3R: 5'- GCAACCATTCTTTGAGACAGAAC-3'
Digest with Taq1. *WT*: 168 + 262 bp; *paa1-3*: 420 bp
PAA1-4F: 5'-CAGGAGTTAAACCAGCTGAG-3'
PAA1-4R: 5'-GTGGGGATAATATGCGAAACAT-3'
Digest with Nde1. *WT*: 217 bp; *paa1-3*: 22 + 195 bp
PAA1-6F: 5'-GCCAGATTTAGTTCCTGCATC-3'
PAA1-6R: 5'-GCTTCACGGTCTTCATGG-3'
Digest with Mse1. Six bands are produced in *WT*, seven in *paa1-6.* A 182 bp fragment is present in *WT* but cleaved in *paa1-6*.

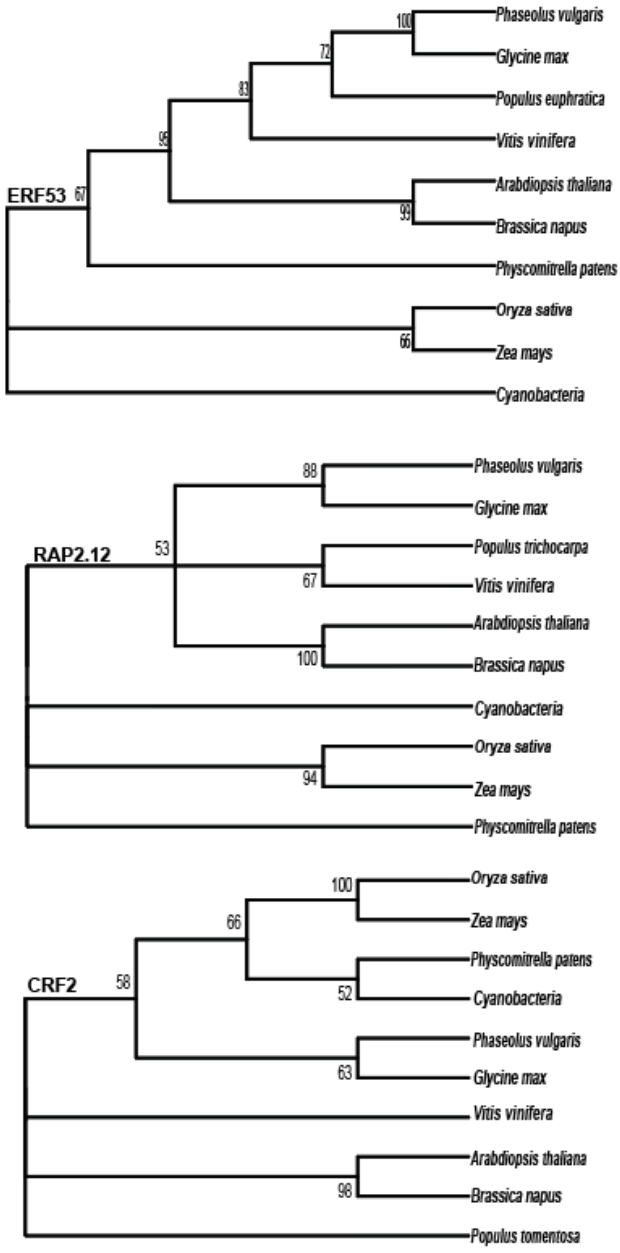

Supplemental Figure 4-1: Phylogenetic analysis of ERF transcription factors differentially expressed in WT-Fe. Phylogenetic trees of ERF53, RA2.12, and CRF2 across selected photosynthetic organisms. Sequences were taken from NCBI, aligned with Muscle. Trees are the least parsimonious of 500 replications. Numbers represent bootstrap values

Supplemental Figure 4-2a (figure legend on pg 244)

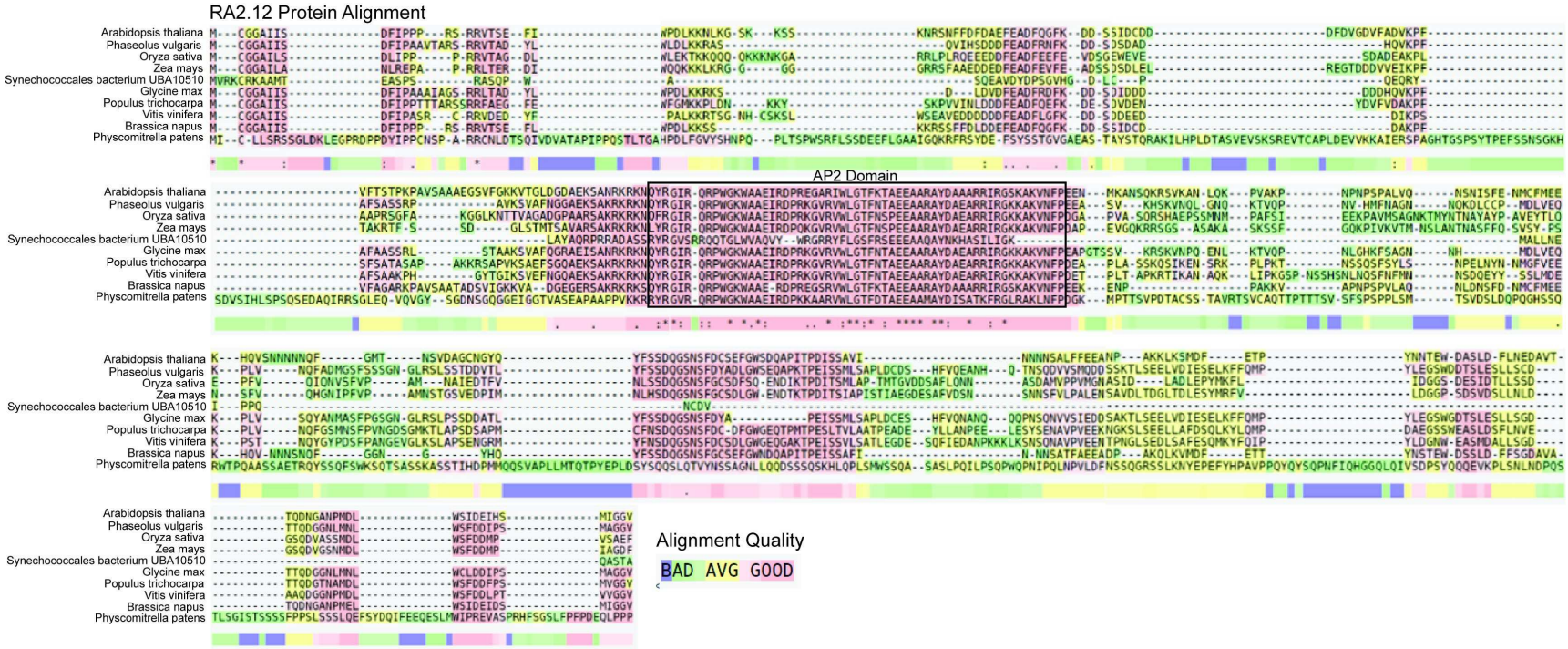

Supplemental Figure 4-2b (figure legend on pg. 244)

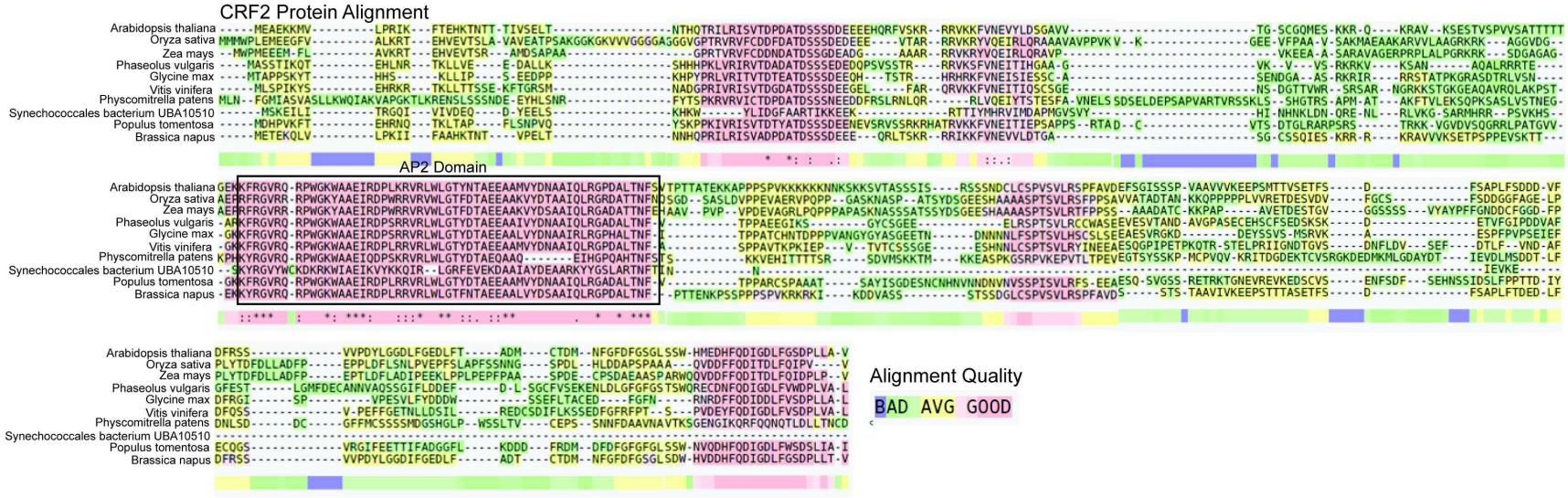

Supplemental Figure 4-2c

Supplemental Figure 4-2. Alignments of ERF53, CRF2, and RA2.12 proteins across the green lineage. a. ERF53 alignment, b. CRF2 alignment, c. RA2.12 alignment. Species name is listed on the left of the sequences. AP2 domain is boxed. Alignment quality is depicted by colors with blue-green being bad quality and pink-red being good quality.

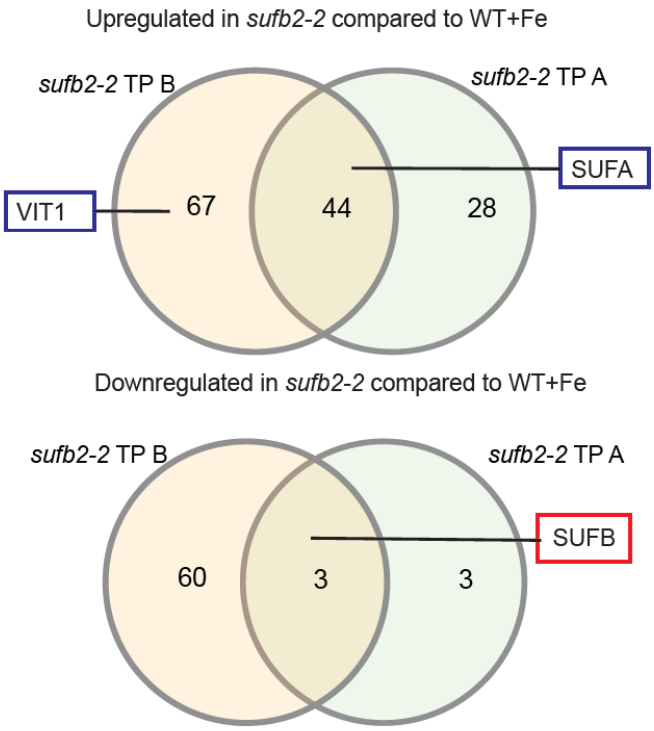

Supplemental Figure 4-3: Transcript changes specific to the loss of SufB. Numbers in each of the Venn diagram segment represent the number of differentially up or down-regulated transcripts shared across TP A and TP B. Only significantly differentially expressed genes with a fold change of at least 1.5 x higher or lower than WT+Fe are represented. Down-regulated genes are those that are decreased in expression in *sufb2-2* compared to WT+Fe; Up-regulated genes are these that have increased expression in *sufb2-2* compared to WT+Fe.

Supplementary Table 4-1: Sequencing Quality of RNA-seq Samples: Number of raw and cleaned (trimmed for quality) reads are presented for each sample. Q20 score represents the probability of one incorrect base call in 100 bases.

Sample name	*Raw Reads*	*Clean Reads*	*Q20 score*
WT+Fe R1 2 h	8.1×10^7	7.9×10^7	98.8
WT+Fe R2 2 h	8.9×10^7	8.6×10^7	98.6
WT+Fe R3 2 h	7.0×10^7	6.8×10^7	98.8
WT+Fe R1 26 h	10.0×10^7	9.8×10^7	98.3
WT+Fe R2 26 h	7.2×10^7	7.0×10^7	98.8
WT+Fe R3 26 h	8.8×10^7	8.5×10^7	98.7
WT-Fe R1 2 h	7.0×10^7	6.8×10^7	98.7
WT-Fe R2 2 h	9.0×10^7	8.7×10^7	98.7
WT-Fe R3 2 h	9.2×10^7	9.0×10^7	98.8
WT-Fe R1 26 h	7.1×10^7	6.9×10^7	98.7
WT-Fe R2 26 h	6.8×10^7	6.6×10^7	98.7
WT-Fe R3 26 h	8.4×10^7	8.2×10^7	98.7
sufb2-2+Fe R1 2 h	7.5×10^7	7.2×10^7	98.7
sufb2-2 +Fe R2 2 h	7.5×10^7	7.4×10^7	98.6
sufb2-2+Fe R3 2 h	8.2×10^7	8.1×10^7	98.7
sufb2-2+Fe R1 26 h	7.1×10^7	7.0×10^7	98.6
sufb2-2 +Fe R2 26 h	7.2×10^7	7.1×10^7	98.5
sufb2-2+Fe R3 26 h	6.1×10^7	6.0×10^7	98.1
average:	7.7×10^7	7.5×10^7	98.6

Supplementary Table 4-2 percent similarity to *Arabidopsis thaliana* ERF transcription factor proteins. Protein sequences for CRF2, RA2.12, and ERF53 for each species was compared to that of *Arabidopsis thaliana* using BLAST. Coverage refers to the percentage of the sequence that was similar to the *A. thaliana* sequence. Identical refers to the percentage of amino acids that were identical in each sequence compared to the *A. thaliana* sequence.

Species	*CRF2*		*RA2.12*		*ERF53*	
	coverage	identical	coverage	identical	coverage	identical
O. sativa	60%	38%	75%	38%	50%	62%
Z. mays	31%	51%	81%	36%	57%	44%
P. vulgaris	100%	40%	88%	45%	50%	55%
G. max	100%	40%	81%	45%	91%	45%
V. vinifera	100%	45%	80%	48%	77%	49%
P. patens	67%	32%	16%	52%	30%	48%
Synechoccales bacterium UBA10510	17%	45%	62%	34%	44%	47%
*Populus sp**	98%	40%	87%	47%	38%	66%
B. napus	100%	71%	84%	72%	98%	62%

* Sequences from *Populus* were as follows: for CRF2: *Populus tomentosa*; for RA2.12: *Populus trichocarpa;* For ERF53: *Populus euphratica*

LITERATURE CITED

Abdel-Ghany SE, Müller-Moulé P, Niyogi KK, Pilon M, Shikanai T (2005a) Two P-Type ATPases Are Required for Copper Delivery in Arabidopsis thaliana Chloroplasts. Plant Cell 17: 1233-1251

Abdel-Ghany SE, Ye H, Garifullina GF, Zhang LH, Pilon- Smits EAH, Pilon M (2005b) Iron-sulfur cluster biogenesis in chloroplasts. Involvement of the scaffold protein CpIscA. Plant Physiology 138: 161-172

Bych K, Netz DJA, Vigani G, Bili E, Lilly R, Pierik AJ, Balk J (2008) The Essential Cytosolic Iron-Sulfur Protein Nbp35 Acts without Cfdl Partner in the Green Lineage. Journal of Biological Chemistry 283: 35797-35804

Dellagi A, Rigault M, Segond D, Roux C, Kraepiel Y, Cellier F, Briat J-F, Gaymard F, Expert D (2005) Siderophore-mediated upregulation of Arabidopsis ferritin expression in response to Erwinia chrysanthemi infection. Plant Journal 43: 262-272

Hooks MA, Allwood JW, Harrison JKD, Kopka J, Erban A, Goodacre R, Balk J (2014) Selective induction and subcellular distribution of ACONITASE 3 reveal the importance of cytosolic citrate metabolism during lipid mobilization in Arabidopsis. Biochemical Journal 463: 309-317

Kliebenstein DJ, Monde RA, Last RL (1998) Superoxide dismutase in Arabidopsis: An eclectic enzyme family with disparate regulation and protein localization. Plant Physiology 118: 637-650

Klughammer C, Schrieber U (2008) Saturation Pulse method for assessment of energy conversion in PSI. PAM application notes 1: 11-14

Kopriva S, Muheim R, Koprivova A, Trachsel N, Catalano C, Suter M, Brunold C (1999) Light regulation of assimilatory sulphate reduction in Arabidopsis thaliana. Plant Journal 20: 37

Lasanthi-Kudahettige, R, Magneschi, L, Loreti, E, Gonzali, S, Licausi, F, Novi, G, Beretta, O, Vitulli, F, Alpi, A, Perata, P, (2007) Transcript profiling of the anoxic rice coleoptile. Plant Physiology 144: 218-231.

Li LC, Qin GJ, Tsuge T, Hou XH, Ding MY, Aoyama T, Oka A, Chen Z, Gu H, Zhao Y, Qu LJ (2008) *SPOROCYTELESS* modulates *YUCCA* expression to regulate the development of lateral organs in *Arabidopsis.* New Phytologist 179 (3): 751-764.

Liu, J, Wang, P, Liu, B, Feng, DR, Zhang, J, Su, JB, Zhang, Y, Wang, J, Wang, H (2013) A deficiency in chloroplastic ferredoxin 2 facilitates effective photosynthetic capacity during long-term high light acclimation in Arabidopsis thaliana. Plant Journal 76: 861-874.

Munshi MK, Kobayashi Y, Shikanai T (2006) CHLORORESPIRATORY REDUCTION 6 Is a Novel Factor Required for Accumulation of the Chloroplast NAD(P)H Dehydrogenase Complex in Arabidopsis. Plant Physiology 141: 737-744

Pilon-Smits EAH, Garifullina GF, Abdel-Ghany S, Kato S-I (2002) Characterization of a NifS-like chloroplastic protein from A*rabidopsis.* Implications for its role in sulfur and selenium metabolism. Plant Physiology 130: 1309-1318

Stockel J, Oelmuller R (2004) A novel protein for photosystem I biogenesis. Journal of Biological Chemistry 279: 10243-10251

Vert G, Grotz N, Dedaldechamp F, Gaymard F, Guerinot ML, Briat J-F, Curie C (2002) IRT1, an A*rabidopsis* transporter essential for iron uptake from the soil and for plant growth. The Plant Cell 14: 1223-1233

Ye H, Abdel-Ghany SE, Anderson TD, Pilon-Smits EAH, Pilon M (2006) CpSufE activates the cysteine desulfurase CpNifS for chloroplastic Fe-S cluster formation. Journal of Biological Chemistry 281: 8958-8969

Yonekura-Sakakibara K, Onda Y, Ashikari T, Tanaka Y, Kusumi T, Hase T (2000) Analysis of reductant supply systems for ferredoxin-dependent sulfite reductase in

photosynthetic and nonphotosynthetic organs of maize. Plant Physiology 122: 887-894